

UNCLASSIFIED

AD NUMBER
ADB262142
NEW LIMITATION CHANGE
TO Approved for public release, distribution unlimited
FROM Distribution: Further dissemination only as directed by Dept. of the Navy, Washington, DC 20350, Jun 64; or higher DoD authority.
AUTHORITY
DoDD 5230.24

THIS PAGE IS UNCLASSIFIED

NOTICE

This copy may not be further
reproduced or distributed in
any way without specific
authorization in each instance,
procured through the
Director of Libraries
Massachusetts Institute of Technology

DTIC QUALITY INSPECTED 4

20001207 027

NOTICE: THIS MATERIAL MAY BE
PROTECTED BY COPYRIGHT LAW
(TITLE 17 U.S. CODE)



LARGE PAYLOAD NUCLEAR ROCKETS

by

JOHN DONALD CHRISTIE

S. B. Massachusetts Institute of Technology (1959)

S. M. Massachusetts Institute of Technology (1960)

Mech. E., Massachusetts Institute of Technology (1963)

SUBMITTED IN PARTIAL FULFILLMENT
OF THE REQUIREMENTS FOR THE
DEGREE OF DOCTOR OF SCIENCE

at the

MASSACHUSETTS INSTITUTE OF TECHNOLOGY

June, 1964

Signature of Author.....*John D. Christie*.....
Department of Mechanical Engineering May 15, 1964
Certified by.....*George A. Brown*.....
Thesis Supervisor
Accepted by.....*Walter M. Robinson*.....
Chairman, Departmental Committee on Graduate Students

DISTRIBUTION STATEMENT F:

Further dissemination only as directed by

Jun 64
Dept. of the Navy,
or higher DoD authority.

Wash., DC 20350

AGM 01-03-0474

LARGE PAYLOAD NUCLEAR ROCKETS

by

JOHN DONALD CHRISTIE

Submitted to the Department of Mechanical Engineering in partial fulfillment of the requirements for the degree of Doctor of Science.

ABSTRACT

A nuclear rocket power plant system consisting of a solid core reactor, pressure shell, turbopump, and nozzle in which hydrogen is used as the propellant was investigated analytically over a wide range of conditions. The reactors considered were cylindrical graphite cores impregnated with U-235 reflected both radially and on the inlet end. Temperature and stress limitations were defined and possible ranges of operating conditions within these limitations were determined. Complete rocket systems with corresponding payload weights were determined for a sample earth orbit mission. The range of parameters considered included:

- (1) Hydrogen temperatures at the reactor exit up to 4800°R
- (2) Hydrogen pressures at the reactor exit up to 1000 psia
- (3) Reactor void fractions for hydrogen flow from 0.2 to 0.4
- (4) Reactor power levels up to 30,000 megawatts

The major results of this study are:

- (1) A range of maximum possible reactor operating conditions limited by stresses and surface temperatures is determined. This results in a plot of maximum possible propellant exit temperature vs. hydrogen flow through the reactor which is independent of the fluid pressure as long as the pressure never exceeds a specific value determined from the stress limitation.

- (2) A simplified analysis which permits rapid hand calculations of the maximum possible ranges of operation to within 10% of the results from detailed machine calculations.
- (3) A method for optimizing the payload or ratio of payload to gross weight for a particular nuclear rocket mission.

Additional results possibly of more general interest are:

- (1) A procedure and Fortran coded program for calculating heat transfer and pressure drop characteristics for the subsonic flow of a compressible chemically reacting gas in a heated tube with friction.
- (2) A procedure and Fortran coded program for calculating the thermodynamic and transport properties of hydrogen over a temperature range from 1500 to 4000° Kelvin and for pressures from 0.01 to 100.0 atmospheres. The effects of compressibility factor unequal to one and of dissociation are taken into account where necessary.

Thesis Supervisor: Professor George A. Brown

Title: Associate Professor of Mechanical Engineering

ACKNOWLEDGEMENTS

The author acknowledges the advice and help of his Thesis Committee which consists of Professor George A. Brown, Kent Hansen, and Warren M. Rohsenow. He is particularly grateful for the encouragement and support of George A. Brown, his thesis supervisor.

Informative discussions with Dr. Arthur C. Herrington and his encouragement at different stages of the investigation were quite valuable to the author in the preparation of this thesis.

Additional knowledge of value for the investigation was obtained by working and talking with Richard K. Plebuch.

The financial support of the Applied Science Division of the Operations Evaluation Group and the Institute of Naval Studies of the Center of Naval Analyses is gratefully acknowledged.

This work was done in part at the M.I.T. Computation Center and the time made available by them is appreciated.

For the many hours of assistance in the preparation of the final document, the author is indebted to Miss Elaine Audet, Mr. Waldron Cluett, Jr., and Miss Deborah Pike.

TABLE OF CONTENTS

	Page
ABSTRACT.....	ii
ACKNOWLEDGEMENTS.....	iv
TABLE OF CONTENTS.....	v
LIST OF FIGURES.....	viii
LIST OF TABLES.....	xv
NOMENCLATURE.....	xvi
Chapter I: INTRODUCTION.....	1
A. Advantages of Nuclear Rocket Systems.....	1
B. Possible Types of Nuclear Rocket Systems...	3
C. Status of Nuclear Rocket Program.....	6
D. Description of System.....	7
Chapter II: OBJECTIVES AND LIMITATIONS.....	12
A. Objectives.....	12
B. Limitations.....	14
C. Assumptions.....	15
Chapter III: OVERALL APPROACH.....	17
A. General.....	17
B. Powerplant.....	17
C. Total Rocket System.....	19
D. Choice of Independent Variables.....	20
Chapter IV: REACTOR CALCULATIONS.....	25
A. Critical Sizes.....	25
B. Heat Transfer and Pressure Drop Characteris- tics.....	35
C. Stress Analysis.....	54
D. Limiting Performance of Reactor.....	69

	Page
Chapter V: SIMPLIFIED REACTOR ANALYSIS.....	79
A. Objective.....	79
B. Wall Temperature Limitation.....	80
C. Stress Limitation.....	85
Chapter VI: POWERPLANT PERFORMANCE.....	93
A. Calculation of Component Characteristics..	93
B. Powerplant Characteristics.....	96
Chapter VII: SAMPLE MISSION.....	106
A. Mission Calculations.....	106
B. Rocket System Characteristics.....	108
C. Mission Results.....	109
Chapter VIII: SUMMARY OF RESULTS AND CONCLUSIONS.....	115
A. Results.....	115
B. Conclusions.....	119
Chapter IX: RECOMMENDATIONS	120
BIBLIOGRAPHY.....	122
Appendix A: HYDROGEN PROPERTIES.....	A-1
1. Summary.....	A-1
2. General Method.....	A-1
3. Thermodynamic Properties.....	A-2
4. Thermodynamic Property Derivatives.....	A-16
5. Transport Properties.....	A-28
a. Transport Properties Below 1000°K....	A-28
b. Transport Properties Above 1000°K....	A-34
6. Hydrogen Property Results.....	A-38
7. Description of Computer Subroutine.....	A-73
Appendix B: HEAT TRANSFER AND PRESSURE-DROP CHARACTERIS- TICS FOR THE FLOW OF A COMPRESSIBLE GAS IN A CONSTANT AREA CHANNEL.....	B-1

	Page
1. Summary.....	B-1
2. Development of Fluid Flow Equations.....	B-1
3. Choice of Initial Independent Variables...	B-13
4. Starting Procedure.....	B-14
5. Stepwise Trial and Error Procedure.....	B-18
6. Calculation of Fluid Stagnation Properties from the Static Properties and Fluid Velocity.....	B-19
7. Pressure and Temperature Corrections for.. the Stepwise Trial and Error Procedure....	B-20
Appendix C: STRESS CALCULATIONS.....	C-1
1. General.....	C-1
2. Stress Equations when $\sigma_r = 0$ at $r = r_0$..	C-4
3. Stress Equations when $(d\sigma_r/dr) = 0$ at $r = r_0$	C-7
4. Failure Criteria.....	C-10
Appendix D: COMPUTER PROGRAM AND SAMPLE SOLUTION.....	D-1
1. Description of Program.....	D-1
2. Description of Input and Output Variables.	D-8
3. Fortran Listing of the Computer Program...	D-17
4. Sample Problem.....	D-53
BIOGRAPHICAL NOTE.....	E-1

LIST OF FIGURES

FIG. NO.	TITLE	PAGE
1-1	Nuclear Rocket Schematic	8
1-2	Powerplant Schematic	10
4-1	Reactor Weight vs. Flow Area	27
4-2	Reactor Radius vs. Flow Area	28
4-3	Reactor Length vs. Flow Area	29
4-4	Reactor Core Radius and Length vs. Void Fraction for Minimum Reactor Weight per Unit Flow Area	30
4-5	Effect of Radial Reflector Thickness on Reactor Weight per Unit Flow Area for C/U-235 = 500	32
4-6	Effect of Beryllium Reflector Thickness on Radial Power Peaking for C/U-235 = 500	34
4-7	Effect of Beryllium Axial Reflector Thickness on Axial Power Profile	36
4-8	Hydrogen Stagnation Temperature and Relative Power Density vs. Non-Dimensional Length for a Constant Coolant Channel Surface Temperature	41
4-9	Hydrogen Stagnation Temperature, Static Temperature Stagnation Pressure, Static Pressure, and Mach Num- ber vs. Non-Dimensional Reactor Length for Chopped	

	PAGE
Sine Power Distribution	50
4-10 Relative Power Density vs. Non-Dimensional Reactor Length for Chopped Sine Power Distributions and Actual Power Distribution in a Reflected Reactor	51
4-11 Distribution of Principal Stresses in an Annular Element with Uniform Heat Generation	61
4-12 Distribution of Principal Stresses in an Annular Element with Uniform Heat Generation	62
4-13 Hydrogen Temperature, Coolant Channel Surface Temperature, Solid Centerline Temperature, Shear Stress at Coolant Channel Surface, and Local Power Density in Reactor vs. Non-Dimensional Reactor Length for Chopped Sine Power Distribution	65
4-14 Hydrogen Stagnation Temperature, Static Temperature, Stagnation Pressure, Static Pressure, and Mach Number vs. Non-Dimensional Reactor Length for Constant Wall Temperature	67
4-15 Hydrogen Temperature, Coolant Channel Surface Temperature, Solid Centerline Temperature, Shear Stress at Coolant Channel Surface, and Local	

	Power Density in Reactor vs. Non-Dimensional Reactor Length for Constant Wall Temperature	68
4-16	Maximum Shear Stress vs. Hydrogen Flow per Unit Area in Reactor Core with Chopped Sine Power Distribution	73
4-17	Maximum Hydrogen Temperature at Reactor Exit vs. Flow per Unit Area as Determined by Different Material Limitations	74
4-18	Maximum Hydrogen Temperature at Reactor Exit vs. Flow Rate per Unit Area Through Core with Chopped Sine Power Distribution as Determined by Material Limitations	76
4-19	Maximum Hydrogen Temperature at Reactor Exit vs. Flow Rate per Unit Area Through Core with Chopped Sine Power Distribution as Determined by Material Limitations	77
5-1	Maximum Hydrogen Temperature at Reactor Exit vs. Flow Rate per Unit Area Through Core with Chopped Sine Power Distribution as Determined by Material Limitations	84
6-1	Power Plant Component Weights and Power Plant System Weight vs. Hydrogen Flow per Unit Area	

	in Reactor for Systems on Limiting Performance Envelope Shown in Fig. 4-17	98
6-2	Maximum Power Developed and Ratio of Maximum Power to Powerplant System Weight vs. Hydrogen F Flow per Unit Area in Reactor for Systems on Limiting Performance Envelope	99
6-3	Ratio of Maximum Possible Power Developed to Powerplant System Weight vs. Hydrogen Flow per Unit Area in Reactor for Systems on Limit- ing Performance Envelopes	101
6-4	Ratio of Maximum Possible Power Developed to Powerplant System Weight vs. Hydrogen Flow Rate in Reactor for Systems on Limiting Performance Envelopes	103
6-5	Ratio of Maximum Possible Power Developed to Powerplant System Weight vs. Hydrogen Flow per Unit Area in Reactor for Systems on Limiting Performance Envelopes: $v = 0.3$	104
7-1	Maximum Payload Weight vs. Hydrogen Flow per Unit Area in Reactor for Earth Orbital Mission Using Powerplant Systems on Limiting Performance Envelopes	110

7-2	Maximum Ratio of Payload to Gross Weight vs. Hydrogen Flow per Unit Area in Reactor for Earth Orbital Mission Using Powerplant Systems on Limiting Performance Envelopes	111
7-3	Ratio of Payload to Gross Weight vs. Hydrogen Pressure at Reactor Exit for Earth Orbital Mis- sion	114
A-1	Compressibility Factor for Normal Hydrogen for Temperatures from 150° to 4000°K	A-54
A-2	Molecular Weight of Normal Hydrogen Assuming Equilibrium Composition for Temperatures from 150° to 4000°K	A-55
A-3	Density of Normal Hydrogen Assuming Equilibrium Composition for Temperatures from 150° to 4000°K	A-56
A-4	Enthalpy of Normal Hydrogen Assuming Equilibrium Composition for Temperatures from 150° to 4000°K	A-57
A-5	Entropy of Normal Hydrogen Assuming Equilibrium Composition for Temperatures from 150° to 4000°K	A-58
A-6	Specific Heat of Normal Hydrogen Assuming Equili- brium Composition for Temperatures from 150° to 4000°K	A-59
A-7	$(\partial H / \partial p)_T$ for Normal Hydrogen Assuming Equilibrium Composition for Temperatures from 150° to 4000°K	A-60

A-8	$(\partial S / \partial T)_P$ for Normal Hydrogen Assuming Equilibrium Composition for Temperatures from 150° to 4000°K	A-61
A-9	$(\partial S / \partial p)_T$ for Normal Hydrogen Assuming Equilibrium Composition for Temperatures from 150° to 4000°K	A-62
A-10	ω_T for Normal Hydrogen Assuming Equilibrium Composition for Temperatures from 150° to 4000°K	A-63
A-11	ω_P for Normal Hydrogen Assuming Equilibrium Composition for Temperatures from 150° to 4000°K	A-64
A-12	σ_T for Normal Hydrogen Assuming Equilibrium Composition for Temperatures from 150° to 4000°K	A-65
A-13	σ_P for Normal Hydrogen Assuming Equilibrium Composition for Temperatures from 150° to 4000°K	A-66
A-14	ξ_T for Normal Hydrogen Assuming Equilibrium Composition for Temperatures from 150° to 4000°K	A-67
A-15	ξ_P for Normal Hydrogen Assuming Equilibrium Composition for Temperatures from 150° to 4000°K	A-68
A-16	γ for Normal Hydrogen Assuming Equilibrium Composition for Temperatures from 150° to 4000°K	A-69
A-17	Viscosity of Normal Hydrogen Assuming Equilibrium Composition for Temperatures from 150° to 4000°K	A-70

A-18 Thermal Conductivity of Normal Hydrogen Assuming Equilibrium Composition for Temperatures from 150° to 4000°K

A-71

A-19 Prandtl Number for Normal Hydrogen Assuming Equilibrium Composition for Temperatures from 150° to 4000°K

A-72

LIST OF TABLES

Table No.	Title	Page
3-1	Independent Variables and Fixed Quantities Required to Determine Nuclear Rocket Characteristics.....	24
A-1	Hydrogen Properties - Equilibrium Composition p = 1.0 atm.....	A-39
A-2	Hydrogen Properties - Equilibrium Composition p = 10.0 atm.....	A-44
A-3	Hydrogen Properties - Equilibrium Composition p = 100.0 atm.....	A-49

NOMENCLATURE

A	matrix of coefficients for atomic hydrogen property equations
A^*	area for choked compressible flow
A^*	collision integral function
A_E	cross sectional area at nozzle exit plane
A_f	cross sectional area for flow
A_S	surface area
A_T	cross sectional area of nozzle throat
B	matrix of coefficients for molecular hydrogen property equations
B'	first modified verial coefficient
B^*	collision integral function
c	local speed of sound
C'	second modified verial coefficient
c_p	specific heat at constant pressure
\bar{c}_p	average specific heat at constant pressure
CQ_1	constant for chopped sine power distribution
D	diffusion coefficient
d	diameter of coolant channel
D_R	diameter of pressure shell
D_T	diameter of nozzle throat
E	Young's modulus

F	free energy
f	friction factor
g	acceleration of gravity
g_o	acceleration given to unit mass by unit force
H	enthalpy per unit mass
ΔH_{TP}	enthalpy change per unit mass across turbine
h	heat transfer coefficient
h_p	height at the end of burning
HP_p	horsepower required by pump
I_{sp}	specific impulse
k	thermal conductivity
K_p	equilibrium constant for chemical reaction
L	reactor length
M	Mach number
n	molar density
Nu	Nuselt number
P_{sys}	power developed by powerplant
p	pressure
P_i	partial pressure of species i
P_{SE}	stagnation pressure at exit of reactor
P_{SRI}	stagnation pressure at inlet of reactor
P_T	pressure in hydrogen storage tank
P_{TP}	pump discharge pressure
PD	power density

Pr	Prandtl number
Q	heat addition per unit mass
Q_T	total heat addition per unit mass
q	heat flux per unit time
$QDIST$	normalized axial power distribution in reactor
R	reactor radius
R	Universal gas constant
r	radius
Re	Reynolds number
S	entropy per unit mass
s_E	solid fraction of end reflector
s_R	solid fraction of radial reflector
St	Stanton number
T	temperature
T^*	reduced temperature
T_C	temperature at centerline between coolant channels
T_{SE}	stagnation temperature at reactor exit
T_{SRI}	stagnation temperature at reactor inlet
T_W	surface (wall) temperature of coolant channel
T_{WM}	maximum wall temperature along coolant channel
t_E	thickness of end reflector
t_P	operating (burning) time of rocket powerplant
t_R	thickness of radial reflector

t_w	web thickness between coolant channels
V	velocity
ΔV_p	velocity increment required for mission
v	specific volume
v	void fraction
W	molecular weight
w	mass flow rate
W_c	weight of reactor core
W_E	weight of end reflector
W_E	empty weight of rocket
W_{ET}	total weight of reflected reactor
W_G	gross weight of rocket
W_{H_2}	weight of hydrogen propellant
W_i	heat generation rate per unit volume
W_N	total nozzle weight
W_{NC}	weight of convergent section of nozzle
W_{ND}	weight of divergent section of nozzle
W_{PL}	payload weight
W_{PS}	weight of pressure shell
W_R	weight of radial reflector
W_S	structure weight
W_{SYS}	weight of powerplant system
W_T	weight of propellant tank

W_{TP}	weight of turbopump
W_x	shaft work
x	axial distance
x_M	location of T_{WM}
x_α	mole fraction of atomic species
x_β	mole fraction of molecular species
y	axial distance
y_W	bleed rate for turbopump
Z	compressibility factor
$Z^{(ij)}$	collision integral function

GREEK

α	coefficient of thermal expansion
ρ	isentropic exponent (defined by Eq. A-42)
Δ	finite increment
ζ_p	$(p/\gamma)(\partial\gamma/\partial p)_T$
ζ_T	$(T/\gamma)(\partial\gamma/\partial T)_p$
η	R/Wcp
η_p	pump efficiency
η_T	turbine efficiency
θ	temperature difference ($T-T_w$)
λ	thermal conductivity
λ	ratio of gross to empty weight of rocket

μ	viscosity
ν	Poisson's ratio
ρ	mass density
ρ_C	density of core material
ρ_E	density of end reflector material
ρ_L	density of liquid hydrogen in propellant tank
ρ_N	density of nozzle material
ρ_{PS}	density of pressure shell material
ρ_R	density of radial reflector material
σ	stress
σ_N	design stress for nozzle material
σ_P	$(p/Z) (\partial Z / \partial p)_T$
σ_{PS}	design stress for pressure shell material
σ_{SH}	shear stress
σ_T	$(T/Z) (\partial Z / \partial T)_p$
σ_{YP}	yield point stress
τ_W	wall shear stress
ω_P	$(p/W) (\partial W / \partial p)_T$
ω_T	$(T/W) (\partial W / \partial T)_p$
Ω	collision integral
$\langle \Omega \rangle$	collision integral

SUBSCRIPTS

AV	average
B	bulk properties

f	film properties
i	chemical species
i	inside radius of annulus
int	internal portion of transport property
j	chemical species
max	maximum
o	outside radius of annulus
R	portion of transport property due to chemical reaction
r	radial direction
r	real gas
S	stagnation conditions
Z	axial direction
α	atomic species
β	molecular species
θ	tangential direction

SUPERSCRIPTS

o	standard state
o	translational portion of transport property
-	molar property

CHAPTER I

INTRODUCTION

A. Advantages of Nuclear Rocket Systems

As rockets move by virtue of the principle of conservation of momentum, it is desirable to exhaust the propellant from the vehicle at as high a velocity as is possible. This exhaust velocity depends upon the propellant temperature and molecular weight. The interest in nuclear rocket systems stems from the vast amount of energy available from the fission reactions in a nuclear reactor of relatively small mass and volume. This energy can be used in a nuclear rocket system to heat a propellant with a low molecular weight to a high temperature. Very large propellant exhaust velocities can be obtained in this manner.

A commonly used measure of performance of rocket systems is the specific impulse that they can develop. Specific impulse is defined as the ratio of the thrust developed to the mass rate of flow of propellant exhausted from the rocket. For ideal operating conditions when the nozzle exhaust pressure is the same as the ambient pressure, the specific impulse is equal to the exhaust velocity divided by g_0 , the acceleration given to a unit mass by a unit force. This exhaust velocity and consequently the specific impulse are directly proportional to the square root of the propellant stagnation temperature at the nozzle entrance and inversely proportional to the square root of the molecular weight.

In chemical systems the molecular weight of the exhaust gases is determined by the fuel and oxidizer employed. The average molecular weight of exhaust gases in chemical systems is around 18 while diatomic hydrogen with a molecular weight of 2 can be used in nuclear systems. For the same stagnation temperature the use of hydrogen would provide a factor of three increase in specific impulse over a chemical system.

In reality the propellant stagnation temperatures that can be obtained in nuclear systems are presently lower than those that can be reached in chemical systems. In chemical systems the exhaust gases are generated by combustion, and the gases can be at a considerably higher temperature than the combustion chamber walls which are regeneratively cooled in a liquid propellant system. Exhaust gas stagnation temperatures in the vicinity of 6000°F can be obtained in this manner. In a nuclear system with a solid reactor core the energy must be transferred from the core material to the propellant. Consequently the propellant stagnation temperature cannot exceed the maximum possible temperature in the core which is determined by structural or chemical limits of the core material. This temperature is less than 6000°F because suitable core materials have little or no strength at this temperature. For solid cores which are heat transfer limited, the maximum propellant stagnation temperatures attainable are nearer to 4500°F .

As a result of this temperature limitation, values of specific impulse for solid core nuclear systems are in the range of 700 to 800 $\text{lb}_f - \text{sec}/\text{lb}_m$. This is a factor of two over the maximum specific impulse for chemical systems which is about 350 $\text{lb}_f - \text{sec}/\text{lb}_m$ for liquid oxygen - liquid hydrogen (1)*.

Bussard and DeLauer (2) have made a comparison of performance conditions for nuclear and chemical rocket systems. For a set of assumed propellant conditions they show that the nuclear rocket systems are superior to chemical systems for missions requiring high vehicle burnout velocities. This type of study indicates the region of interest for nuclear rockets where further study and work should be profitable.

B. Possible Types of Nuclear Rocket Systems

A number of different types of propulsion systems for nuclear rockets have been proposed. They range from different core concepts as solid and gaseous cores to other more indirect systems involving shock tubes or electric arc heaters. The most highly developed type of system is the solid core reactor employing conventional convective heat transfer to increase the energy of the propellant. The other more advanced or exotic systems have been proposed as methods of increasing performance primarily by circumventing the inherent temperature limitations of the solid core heat transfer reactors.

*Numbers in parentheses refer to items in the bibliography.

In a gaseous core reactor, where the fissionable fuel would be mixed with the propellant, the exhaust gases could be heated to a higher temperature than the containing walls of the reactor. Consequently, specific impulses greater than those obtainable in a solid core heat transfer device could be obtained. The difficulty with this type of system lies in containing the fissionable fuel, or at least a large fraction of it in the reactor and not exhausting it with the propellant.

Systems employing shock tubes or electric arc heaters can in principle obtain propellant temperatures as high as 10^5 °R (2). They are generally considered for low acceleration, low thrust missions as the weight of the powerplant is large relative to the thrust it can produce.

Another exotic proposal is a nuclear pulse system in which energy is generated in a series of short pulses by small nuclear explosions. Effective exhaust velocities corresponding to exceedingly high temperatures are possible in principle as there is no fundamental temperature limitation (3). If the adverse effects of the explosions can be tolerated, the system could be used to propel large payloads in space.

Although the solid core heat transfer reactor is temperature limited it is the most highly developed nuclear propulsion system and the only one that is being tested at the present time. There are three basic types of solid core reactors that can be

considered: the homogeneous thermal or intermediate reactor, the heterogeneous thermal or intermediate reactor, and the fast reactor. In the homogeneous reactor the fuel is intimately mixed with a moderator which slows down the neutrons and provides a heat transfer surface for the propellant. This type of system requires a moderator that can withstand high temperatures. In the heterogeneous reactor the fuel is separated from the moderator and the moderator does not have to provide the heat transfer surface. Consequently, moderator materials that cannot withstand high temperatures can be used if they are cooled independently of the fuel elements. This adds to the complexity of the system but gives more freedom in the choice of materials. In a fast reactor no moderator is used to slow down the neutrons. The reactor can be made very small in size and the best high-temperature materials can be used to contain the fuel. The neutron economy of fast reactors is less than that of moderated systems and more fissionable material is required. This leads to difficult material problems as fissionable materials are not good structural materials (4). The small size of fast reactors is not necessarily an advantage because the solid core reactors are heat transfer limited and a reasonably large amount of heat transfer surface area is required to obtain high propellant exhaust temperatures.

The most promising reactor designs to date are the homogeneous solid core reactors. The choice of suitable moderator

materials for the core is quite limited because of the 4000°R or greater operating temperature required. In addition to having mechanical strength at high temperature the material must not be a neutron absorber and must not react with the propellant. Ceramics have the necessary temperature stability but are poor mechanically and have low thermal conductivities. Refractory metals that have reasonable strength at high temperatures are not good moderators for thermal neutrons. The best material that is presently available is graphite although it reacts with hydrogen at high temperatures. This deficiency can be corrected by coating the heat transfer surfaces of the graphite with a material which is resistant to chemical reactions with hydrogen. Some carbides have been suggested for this use.

C. Status of Nuclear Rocket Program

The United States effort in the nuclear rocket field began in 1955 with "Project Rover." This program is a joint effort of the Atomic Energy Commission and the National Aeronautics and Space Administration. The purpose of this program is to prove the feasibility of solid-core nuclear reactors for heating hydrogen to the temperatures required for rocket propulsion and to develop a flyable nuclear rocket propulsion system.

The initial stages of the program involved the testing of three KIWI-A reactors to learn about the practical limitations of high temperature reactor operation. The KIWI-B reactor

tests began in 1961 and are still in progress. The objectives of these tests are to demonstrate start-up and full power operation using liquid hydrogen as a coolant and to select a basic core design to be used in the NERVA (Nuclear Engine for Rocket Vehicle Application) system (5). The final stage of the Rover Program is RIFT (Reactor in Flight Test) and work has commenced into the development of this system.

The Rover Program includes all of the nuclear rocket reactor and propulsion system hardware development done to date in the United States. A number of analytical studies and designs for specific missions have been completed. A partial list of some of the earlier studies, both unclassified and classified, is given in reference (6).

D. Description of System

A nuclear rocket system is similar to a liquid fueled chemical rocket system in most respects. The principle difference between the two is that the nuclear rocket has a nuclear reactor rather than a combustion chamber to energize the exhaust gases, and it only requires a single propellant rather than a fuel and an oxidizer. A schematic diagram of a nuclear rocket is shown in Fig. 1-1. The power plant is defined to consist of the nuclear reactor and reflector, the pressure shell, turbopump, and the nozzle. The complete rocket then consists of the power-

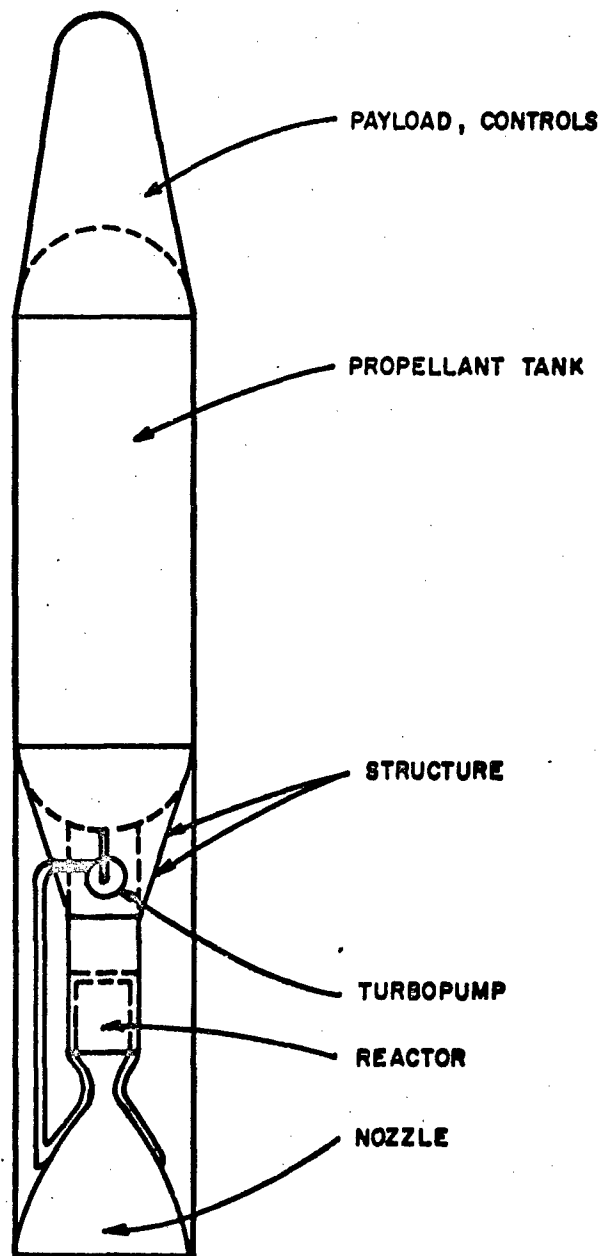


FIG. I-1: NUCLEAR ROCKET SCHEMATIC

plant, propellant, propellant tank, structure, controls, and payload.

The hydrogen propellant is stored in liquid form. It first flows through the pump where its pressure is increased to a value considerably above the critical pressure which is 12.77 atmospheres (7). This avoids any possible problems that might arise with two-phase flow. The hydrogen is then used to regeneratively cool the nozzle and reflector before it is heated to its maximum temperature in the reactor and exhausted through the convergent-divergent nozzle. A small fraction of the hot hydrogen is removed from the main flow before it is exhausted through the nozzle to drive the turbine which is connected to the pump. Fig. 1-2 is a schematic diagram of the powerplant showing the path of the propellant flow through the system.

An alternate way of driving the pump would be to use a topping turbine in which all of the hydrogen flows through the turbine before entering the reactor. In this system only a small amount of work is derived from each pound of a large mass flow while in the bleed system ten to twenty times as much work per pound is taken from the hotter and smaller mass flow. The topping system can be more efficient as all of the propellant is used to generate thrust but the control problems

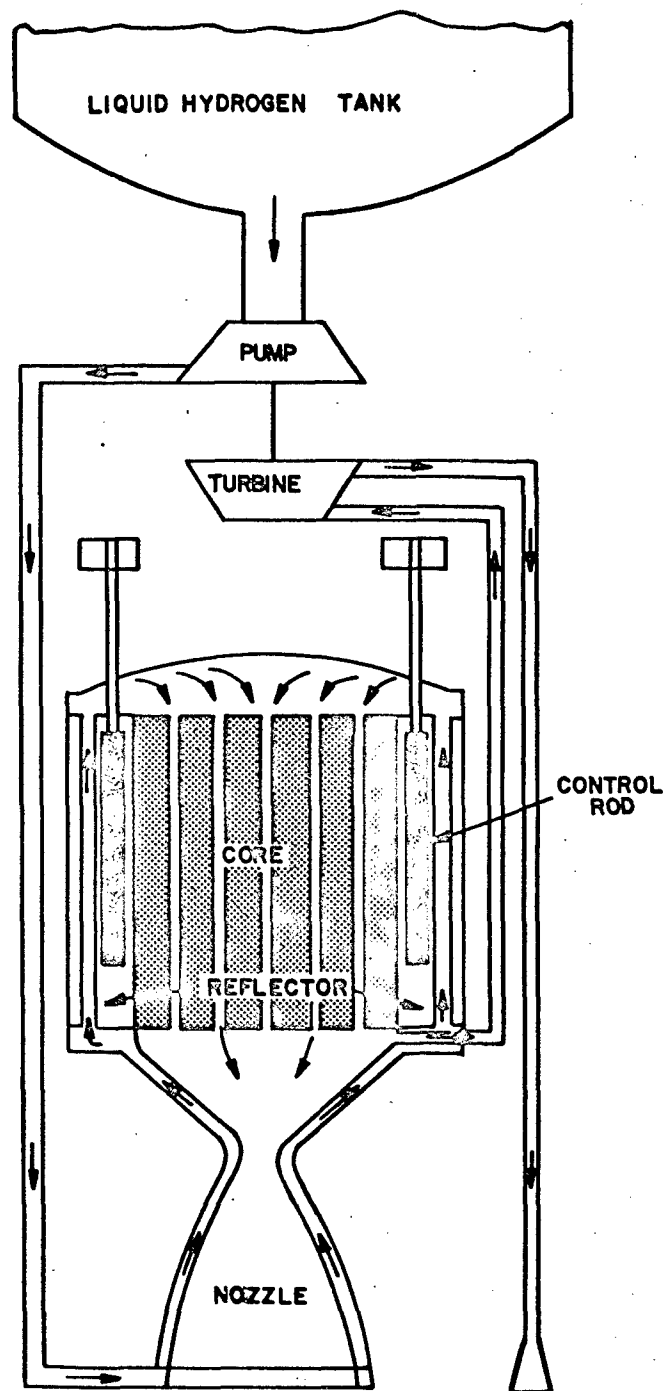


FIG. 1-2: POWER PLANT SCHEMATIC

associated with it make it less favorable than the bleed system.

In Fig. 1-2 the control rods are located in the reflector rather than in the core. This type of control system will perturb the shape of the power distribution in the core less radically than control rods in the core. Control rods in the core would not be able to withstand the high temperatures developed and would have to be cooled separately. The positioning of the control rods in the reflector avoids this cooling problem.

CHAPTER II

OBJECTIVES AND LIMITATIONS

A. Objectives

The objectives of this study are to obtain a method of characterizing the nuclear rocket system with a minimum amount of complexity, determine limiting values of performance, and obtain a method for optimizing the total rocket for a given mission.

To characterize the system with a minimum amount of complexity requires the use of the minimum number of independent variables that is possible. It is also desirable to break up the system where possible so that the different parts or subsystems that are independent of the whole can be investigated separately. The analysis used to describe the system is less detailed than a final design study for a particular rocket would be, yet it is detailed enough to make generalizations about desirable characteristics and choice of independent variables.

The characteristics to be determined include those for the complete system and for the powerplant alone where possible.

The important characteristics of the powerplant include the size and weight of the individual components, the power, thrust, and specific impulse developed, and the amount of propellant flow required to obtain this power. The powerplant was defined

previously to consist of the reactor and reflector, pressure shell, nozzle, and turbopump. The weights of the components including the powerplant, the total system weight, and the payload are among the most important characteristics of the complete rocket system.

In order to determine limiting values of performance, the causes of component failure or restrictions on the manufacturing of items must be determined and then related by the analysis to the performance characteristics of the system. Values of system characteristics can then be determined for conditions that reach but do not exceed these limitations.

Once a method and analytical procedure are developed to characterize the nuclear rocket it is desirable to find a method to optimize the system for a particular mission. For most rocket systems the best configuration for a given mission is considered to be the one which has the minimum weight. This implies that the payload weight or the ratio of payload to gross weight should be maximized at a fixed gross weight. An alternative would be to minimize the gross weight for a fixed payload weight.

For all the above objectives a particular detailed model of the nuclear rocket is used in the analysis. A further objective of this study is to find more rapid simplified methods to

get approximate answers to the above problems where possible. This is only possible after the detailed calculations are completed to give a basis for comparison.

B. Limitations

A number of limitations are set on the range of variables in this study. The reactors considered are limited to cores of graphite impregnated with U-235 with a carbon to uranium atom ratio of 500, which means that the reactor is intermediate. For larger carbon to uranium ratios the average neutron energy would approach the thermal range and the reactor sizes would increase. Carbon to uranium ratios less than 500 may not be obtainable with-in present technology. The core geometry for all cases is a right circular cylinder with uniformly spaced coolant channel holes. The core is reflected radially and on the inlet end where the hydrogen propellant enters the core.

The radial reflector is 8 centimeters of beryllium for all reactors. This value is close to the optimum for minimum reactor weight per unit flow area for the range of reactors considered (8). The variation of reactor size and the local power peaking caused by changing the radial reflector thickness is also shown in reference 8. The end reflector for all reactors is 3 centimeters of beryllium. This thickness was used on the basis of its effect on the axial power profile. It shapes the power

distribution in a desirable way and does not cause excessive local power peaking at the core reflector interface.

The propellant is restricted to hydrogen although some consideration has been given to other fluids as ammonia and water (9, 10). The hydrogen is considered to be stored in liquid form in the propellant tank. Only one tank pressure of 20 psia is used in the study. The value of 20 psia was considered to be high enough to avoid cavitation problems at the pump inlet but not so high as to add considerable additional weight to the tankage.

The turbopump system is limited to a bleed turbine rather than a topping turbine as it is presently the type being used in the first nuclear rocket engines and does not involve additional control problems. The nozzles are restricted to the convergent-divergent regeneratively cooled type with an area ratio of 50 to one.

C. Assumptions

The following assumptions are made throughout the analysis unless it is specifically stated otherwise for a particular case.

1. The reactor is considered to be homogeneous so that all solid parts of the core are generating power. This is equivalent to assuming that any structural elements which are not loaded with fuel and may be present in a particular core design

have a negligible effect on the average core power density and do not cause local power peaking problems.

2. The radial power profile in the reactor core is flat so the ratio of the maximum to average power is one at any axial position in the core.

3. The coolant channel holes are uniformly spaced in the core. Together with the above two assumptions this implies that an equal amount of heat is removed from each coolant channel.

4. The thermal conductivity and structural properties of graphite are independent of temperature over the range of reactor core temperatures considered. In the analysis average properties of graphite taken from design curves are used.

5. The temperature of the hydrogen propellant at the entrance to the reactor core is 400°R . This implies that there is sufficient heating of the hydrogen in the regeneratively cooled nozzle and reflector to raise its temperature from below the critical temperature of 60°R to 400°R which is an increase in enthalpy of approximately 1300 BTU/lb.

CHAPTER III

OVERALL APPROACH

A. General

In order to characterize the nuclear rocket system with a minimum amount of complexity, it is desirable to separate the different independent parts where possible. The characteristics of the powerplant as defined to include the reactor, reflectors, pressure shell, turbopump, and nozzle can be determined independently of any mission. Consequently, the powerplant is investigated first and then tied into the complete system when additional parameters are required.

B. Powerplant

The reactor is the one component in a nuclear rocket that differentiates it from liquid chemical systems and is limiting in the sense that it is the power producing element. The restrictions on the reactor arise from nuclear physics and from mechanical and chemical considerations.

The primary requirement that determines the reactor size is that it be just critical. For a given set of reactor materials any number of critical right circular cylinders could be constructed. These would range from long thin cylinders to short ones resembling a pancake shape. The critical dimensions of the core also depend on the reflector material, reflector thickness, and on the core and reflector void fractions. The void fraction is the ratio of the core cross sectional area which is free for

coolant flow to the total area. The effect of these parameters on the critical dimensions of reactor cores has been studied in some detail by Plebuch (8). His results for critical sizes of rocket reactors are used in this study.

The further possible restrictions that may limit the reactor performance are mechanical strength, erosion, and/or a chemical reaction between the core material and the propellant. To determine which if any of these factors is limiting performance the heat transfer and pressure drop characteristics of the coolant and the temperature and stress distributions in the core must be calculated. Maximum permissible values of temperatures and stresses must be set for the reactor materials and compared with the maximum values calculated for given coolant conditions in a particular reactor. If any of the limitations are exceeded, the coolant conditions which are independent variables must be changed and the process repeated until no limitations are exceeded. In this manner a range of allowable coolant conditions can be obtained for a given reactor. The whole process can be repeated for a number of different reactors.

The characteristics of the whole powerplant can be determined after the heat transfer and pressure drop characteristics in the core are determined. The pressure shell size and weight can be obtained after the maximum pressure in the reactor core is calculated. This pressure and the reactor size are sufficient to determine the dimensions of the pressure shell.

The nozzle size and weight are calculated for a given ratio

of the exit area to throat area of 50. The nozzle size also depends upon the mass flow rate of propellant through it and the stagnation conditions of this propellant. The stagnation properties of the fluid are known independent variables and the mass rate of flow of propellant is determined from the reactor size and the fluid conditions at the reactor exit.

The turbopump size and weight depend on the volume flow rate of propellant and the pressure rise required across the pump. The hydrogen storage pressure is fixed at 20 psia, and the pump outlet pressure can be related to the pressure of the propellant at the inlet to the reactor. The volume rate of flow is simply related to the mass flow rate as the hydrogen is liquid at the inlet to the pump. The bleed flow rate of hydrogen required to run the turbine is determined by the pump work. The amount of work developed per pound of hydrogen flowing through the turbine is fixed so the bleed rate is just the pump work divided by this value.

C. Total Rocket System

The complete powerplant characteristics can be determined as outlined above without considering a mission or an operating time for the rocket. To determine the characteristics of the whole rocket the "burning" or operating time must be known.

Once the burning time is assumed or calculated for a particular mission the propellant weight is easily determined. Knowing the weight and volume of propellant the amount of tankage required

can be determined. The thickness of the tank walls is calculated such that the stresses are below a specified value for the material.

The weight of the structural members to tie the different components together and make a solid frame is assumed to be proportional to the gross weight of the rocket. The mission calculations yield the ratio of the gross to empty weight as well as the burning time. With these values and the flow rate of propellant through the powerplant the gross weight is easily determined.

The payload weight for the mission is then the difference between the gross weight and the weights of all the other components. Using this method of calculation it is possible to obtain negative numerical values for the payload weight. When this occurs, it implies that the particular configuration contains a powerplant that does not develop enough power per unit weight to do the mission.

D. Choice of Independent Variables

The foregoing method implies a choice of certain independent variables yet leaves the choice of others quite free. A number of quantities which could be varied but would only have a small effect on the system are fixed for all calculations in the study.

The critical size of a reactor can be determined if the void fraction v and the length L are specified because the core and reflector materials are fixed and the reflector thicknesses are not varied. It will be shown in the next chapter that

only the void fraction need be independent to determine the critical length L and radius R if in addition it is specified that the reactor is to have the minimum possible weight for a given flow area. The flow area is defined as the part of the reactor cross sectional area which is free for coolant flow.

In order to calculate the heat transfer and pressure drop characteristics of the coolant in the core it is necessary to specify the shape of the axial power distribution in the core, the diameter of a coolant channel or the magnitude of the power distribution as a function of axial position, the inlet and outlet temperatures of the coolant, the pressure of the coolant at one end of the core, and either the flow per unit area or the Mach number of the coolant at the same end of the core where the pressure is specified. The conditions at the exit of the reactor were chosen as independent variables where possible as it is easier to anticipate the effects of their changes and approach the desirable range of operation than it is when using the conditions at the inlet end of the reactor. The coolant flow rate per unit area w/A_f was chosen as independent rather than the Mach number at the reactor exit because it turned out to be more significant to the overall performance. It is relatively easy to insure that the Mach number is not limiting when w/A_f is independent but the inverse is not true. The other independent coolant conditions are the temperature and

pressure at the reactor exit, T_{SE} and p_{SE} respectively, and the temperature at the reactor inlet T_{SRI} . Unless it is otherwise specified for a particular case, the diameter of a coolant channel is specified and not the magnitude of the power distribution.

To determine the interior temperatures and the stresses in the core, it is necessary to know the coolant channel diameter and the local pressure and power density. If the coolant channel diameter is not specified as independent, it can be determined before any stress calculations are started as the magnitude of the power distribution would then be known. Similarly if the channel diameter is independent, the local power density is determined before the interior temperatures and stresses are calculated.

The parameters which are necessary for the calculation of the other powerplant components are either fixed or determined from the above variables. The fixed quantities as mentioned in Chapter II are the nozzle area ratio and the type of turbopump. The amount of work obtained from each pound of hot hydrogen in the turbine is also fixed rather than varied with pressure level or other flow conditions. The propellant pressure required at the pump outlet is calculated back from the pressure at the reactor inlet. The inlet pressure to the pump or tank storage pressure is fixed at 20 psia.

The additional independent variables required for the cal-

culatation of the complete rocket system involve the mission characteristics. The sample mission used in this study is for a single stage rocket which lifts off a stationary earth and takes a payload into a 300 mile high earth orbit. The two independent quantities which are specified are the altitude of the orbit h_p and the velocity increment required ΔV_p . With these quantities and the characteristics of the powerplant all the component sizes and weights can be calculated. The ability of the rocket to carry a payload on the given mission and the magnitude of the payload is then determined.

Table 3-1 is a summary of the independent variables and of the other fixed quantities required to determine the characteristics of the nuclear rocket system as described here and in the previous chapter.

TABLE 3-1

INDEPENDENT VARIABLES USED TO DETERMINE
NUCLEAR ROCKET CHARACTERISTICS

v	- reactor void fraction
d	- diameter of coolant channel in reactor
T_{SE}	- temperature of propellant at reactor exit
T_{SRI}	- temperature of propellant at reactor entrance
P_{SE}	- pressure of propellant at reactor exit
w/A_f	- propellant flow rate per unit area in reactor
$QDIST$	- normalized axial power distribution in reactor
ΔV_p	- velocity increment required for mission
h_p	- change in altitude required in gravity field

FIXED QUANTITIES REQUIRED TO DETERMINE
NUCLEAR ROCKET CHARACTERISTICS

t_R	- thickness of radial reflector around reactor
t_E	- thickness of end reflector on reactor
A_E/A_T	- ratio of exit to throat area of convergent devergent nozzle
P_T	- pressure of hydrogen propellant in storage tank
ΔH_{TP}	- enthalpy drop per pound of hydrogen in turbine for bleed turbopump system

CHAPTER IV

REACTOR CALCULATIONS

A. Critical Sizes

The reactors considered in this thesis are limited to solid graphite moderated cores impregnated with U-235 with a carbon to uranium atom ratio of 500. The cores are right circular cylinders reflected radially and on one end where the coolant enters the reactor.

This type of reactor has been studied in considerable detail by Plebuch (8). His study of the nuclear physics of rocket reactors was undertaken in conjunction with this study to tie together the reactor physics with the overall system analysis. The numerical results from his study are used in this thesis rather than using less sophisticated and less accurate analytical calculations.

Plebuch has considered the effect of different variations in core and reflector properties on the critical sizes and weights of the reactors and on the power distributions which they generate. The variables taken into account in his study include fuel to moderator ratio, solid fraction of the core, reflector material, reflector thickness, reflector solid fraction, and reflector position. The solid fraction s is just 1 minus the void fraction v . Results are presented for both analytical "modified" three group and numerical two dimensional multigroup calculations.

For a given fuel to moderator ratio, reflector material, and reflector thicknesses a series of reactor sizes can be determined for a given core void fraction. Fig. 4-1 is a plot of reactor weights versus the cross sectional area free for coolant flow. Four different curves are shown for core void fractions from 0.1 to 0.4. The radial reflector is 8 centimeters thick and the end reflector 3 centimeters, the material being beryllium in both cases. The curve which is tangent to the constant void fraction curves defines the locus of minimum reactor weights for given flow areas. It is interesting to note that the minimum reactor weight for a given void fraction does not coincide with the minimum reactor weight for a given flow area.

The corresponding plots of the reactor radius and length versus flow area are shown in Figs. 4-2 and 4-3 respectively. The dashed lines show how the radius and length vary along the minimum weight per unit flow area curve. By cross plotting, the reactor radius and height corresponding to the minimum weight curve are obtained versus the reactor void fraction. This is shown in Fig. 4-4. The core length to diameter ratio decreases along the minimum weight curve as the void fraction and flow area increase. This can be seen from Fig. 4-4 or from Figs. 4-2 and 4-3 in combination. For a void fraction of 0.1 the reactor length to diameter ratio is 1.14 while for $v = 0.4$ the ratio is reduced to 0.725.

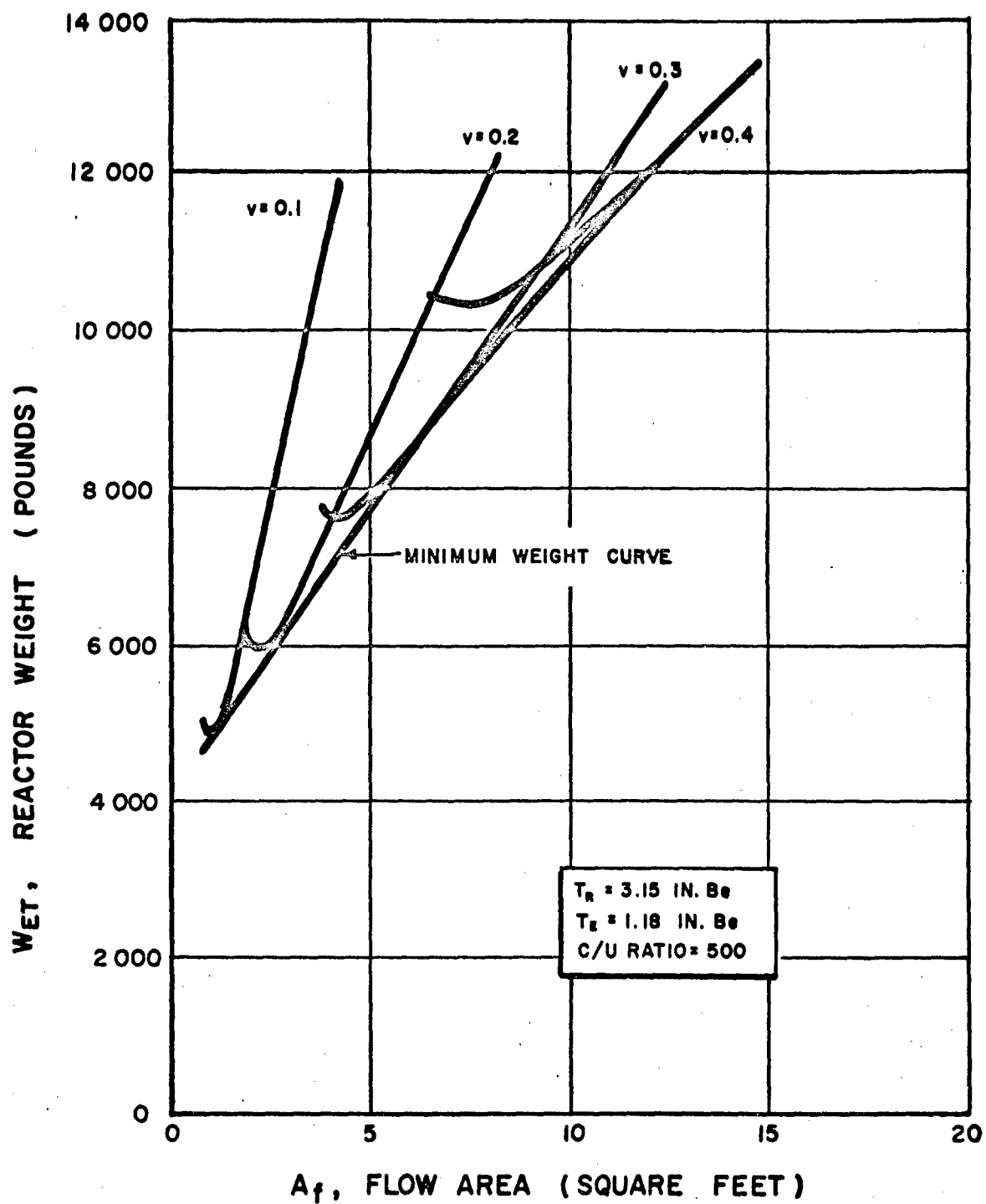


FIG. 4-1: REACTOR WEIGHT VS FLOW AREA

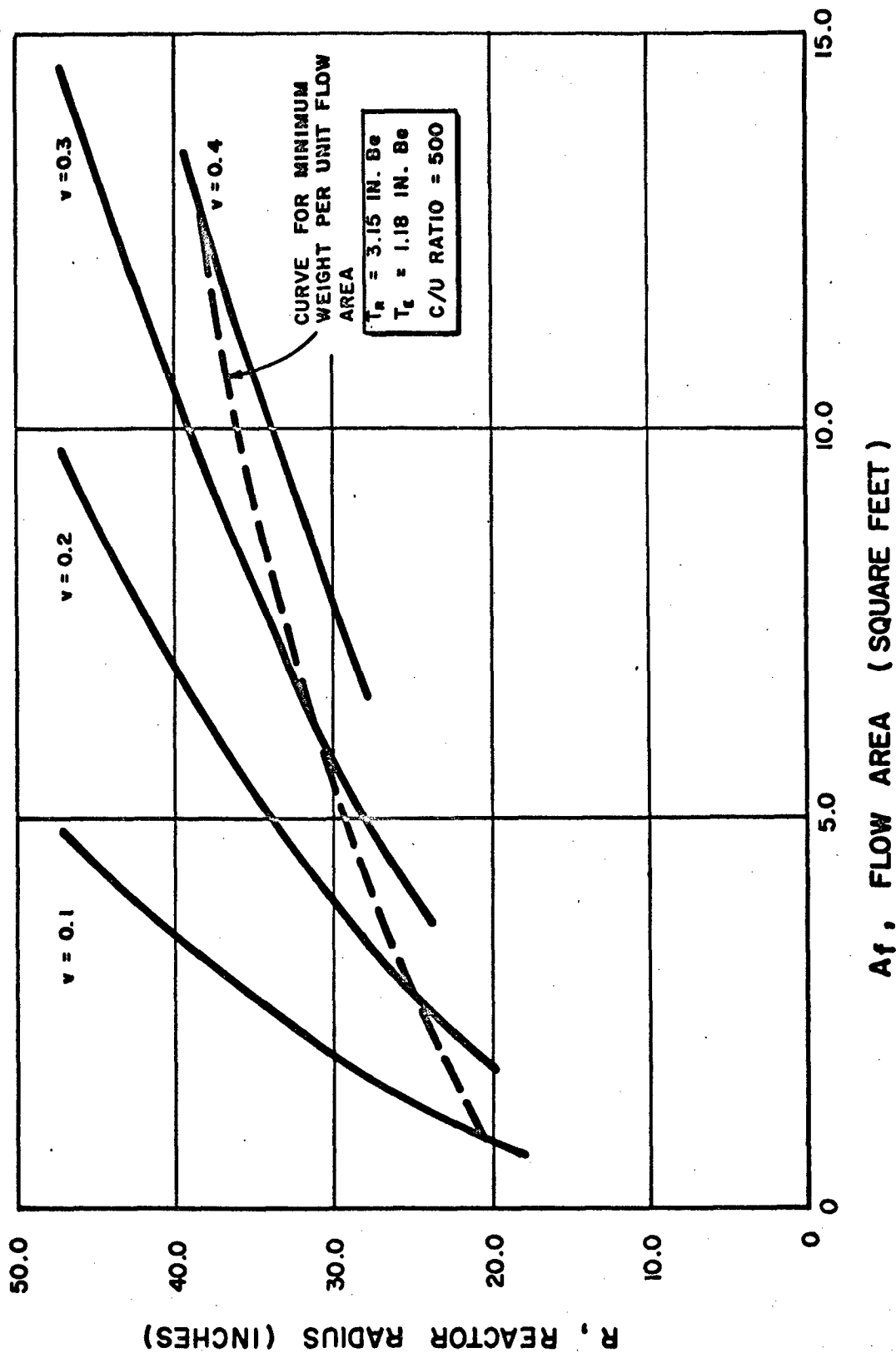


FIG. 4-2: REACTOR RADIUS VS FLOW AREA

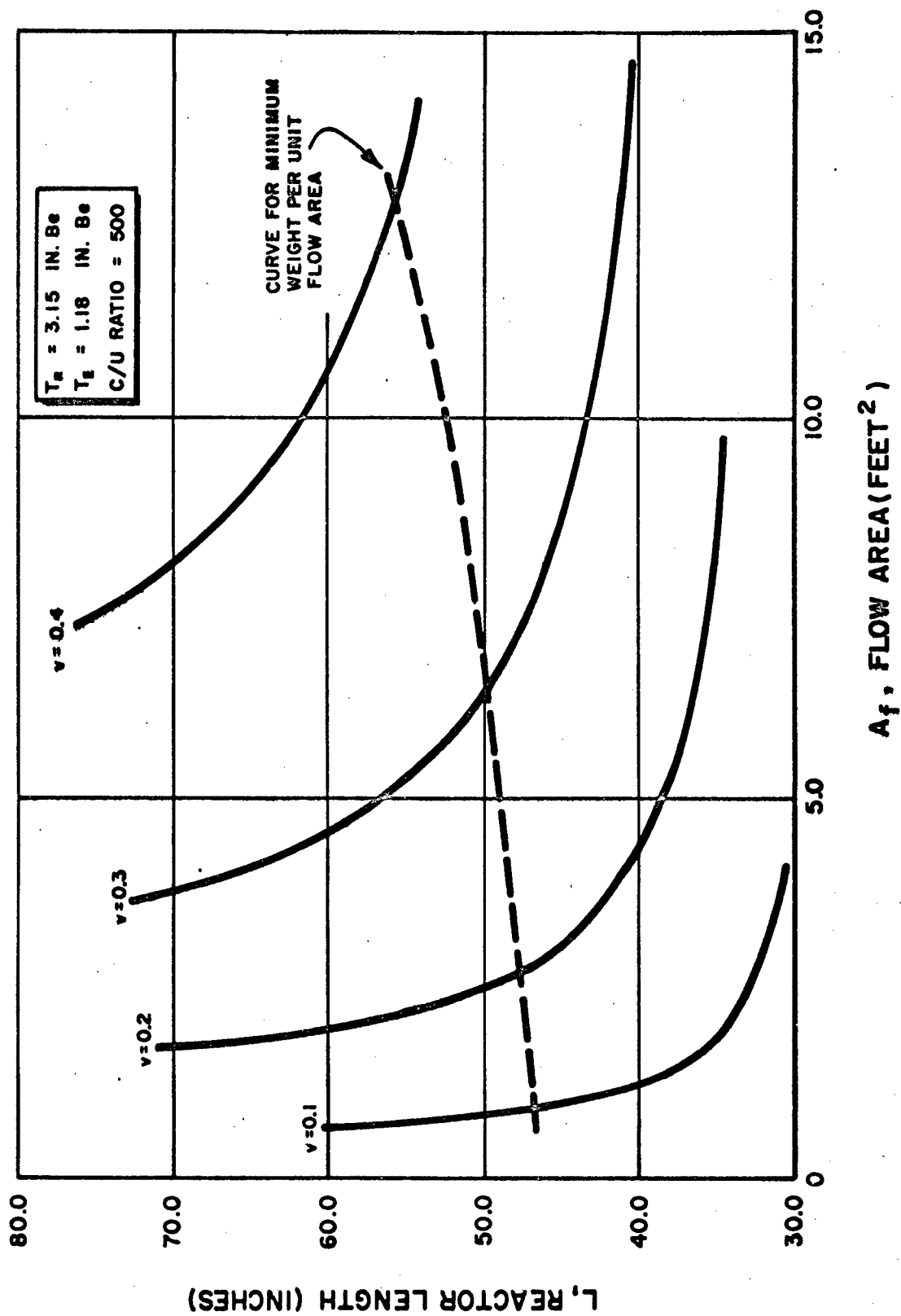


FIG.4-3: REACTOR LENGTH VS FLOW AREA

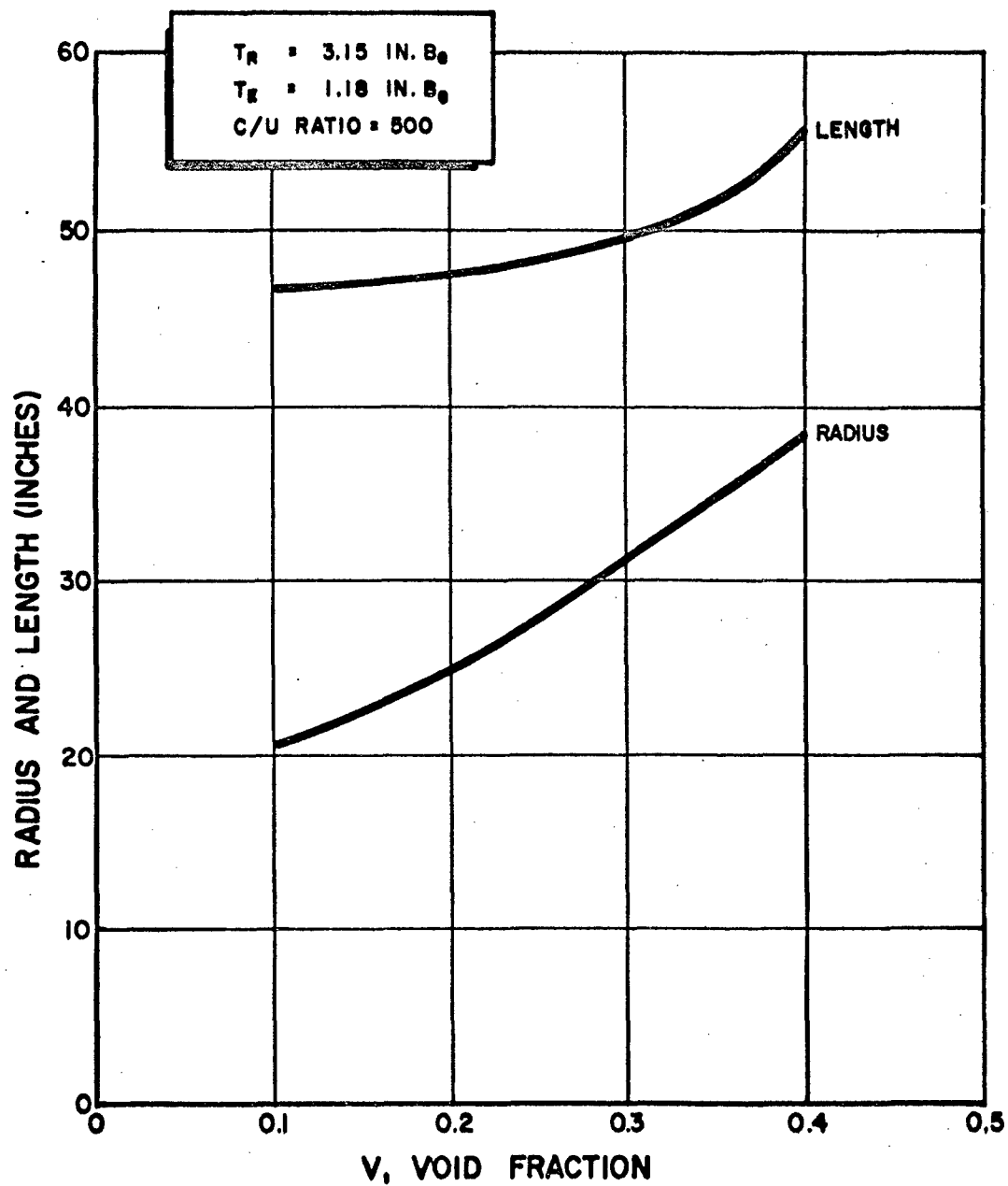


FIG. 4-4 : REACTOR CORE RADIUS AND LENGTH VS VOID FRACTION FOR MINIMUM REACTOR WEIGHT PER UNIT FLOW AREA

The use of the reactor with the minimum weight for a given flow area was suggested earlier by Herrington and this author (11, 12) and the idea has also been used independently for reactor weight studies of different types of reactors (13). This makes it possible to determine the critical size and weight of the reactor with only one independent variable rather than two. The independent variable chosen for this study is the core void fraction. Both the critical radius and height can be determined from Fig. 4-4 and then the area and weight are easily calculated.

The radial reflector thickness of 8 centimeters is used for all reactors rather than including the reflector thickness as a variable. The variation of reactor weight per unit flow area with radial reflector thickness has been determined by Plebuch and is shown in Fig. 4-5 (reproduced from reference 8). The core radii of interest at void fractions of 0.2 or greater are greater than 25 inches or 63.5 centimeters as is shown in Fig. 4-4. Fig. 4-5 shows that the 8 centimeter reflector gives close to the minimum weight per unit flow area for core radii greater than 75 centimeters and that it is a reasonable compromise if one value is to be chosen for all radii from 63.5 to 100 centimeters.

The second reason for using the 8 centimeter reflector thickness is to avoid extreme local power peaking problems at the core reflector interface. For uniform uranium loading in

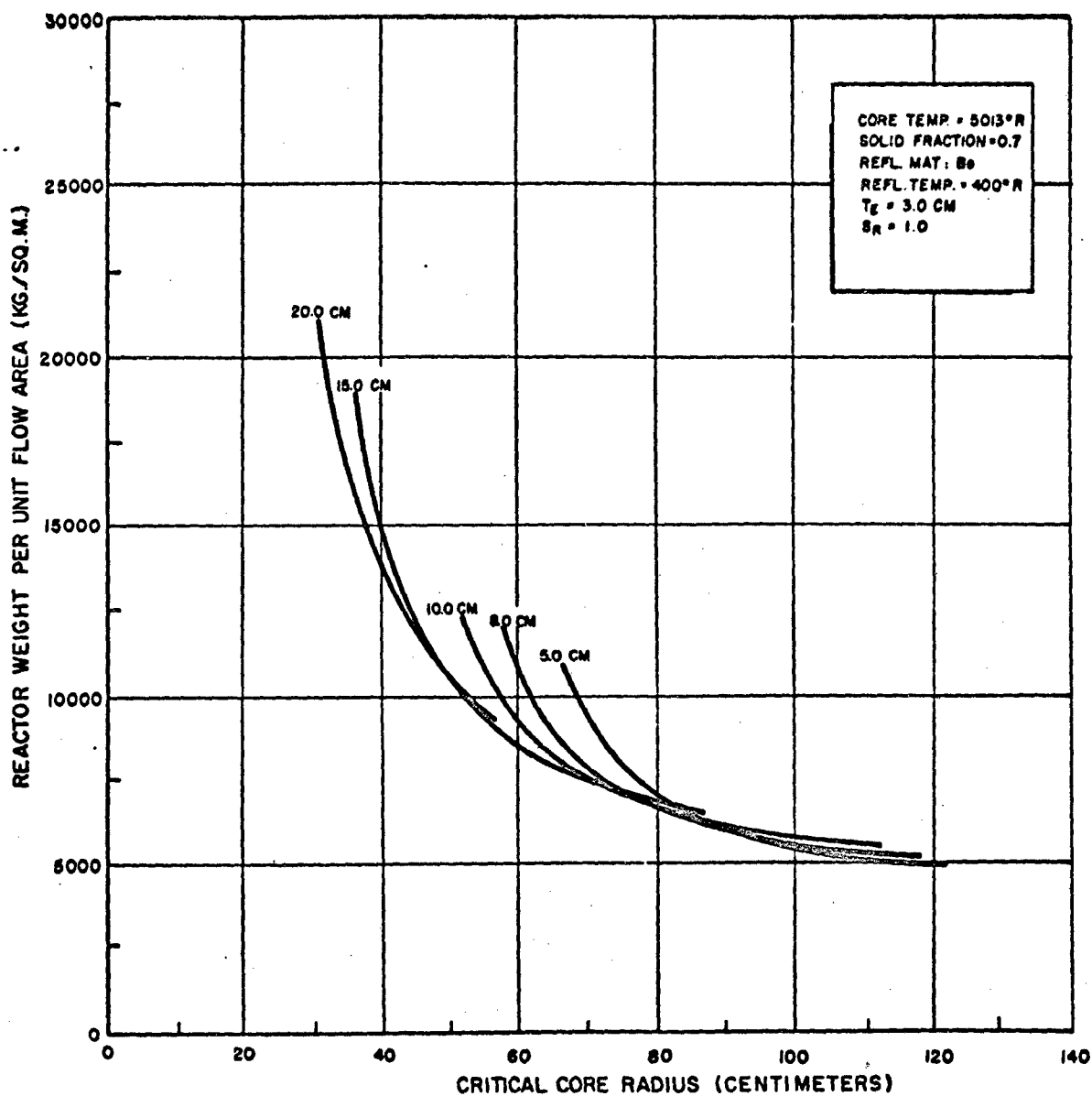


FIG. 4-5: EFFECT OF RADIAL REFLECTOR THICKNESS ON REACTOR WEIGHT PER UNIT FLOW AREA FOR C/U-235 = 500

the radial direction there is a local power peak at the core reflector interface due to relatively slow neutrons being reflected back into the core. The power peaking is defined to be the ratio of the power at the core reflector interface to the power at the center of the core. The dependence of this power peaking on the radial reflector thickness is shown in Fig. 4-6 (reproduced from reference 8). For a reflector thickness of 8 centimeters the peaking goes from 1.6 at a radius of 60 centimeters down to slightly less than 1.0 at a radius of 100 centimeters. This is quite reasonable compared to the peaking problems associated with the thicker reflectors. The power peaking associated with the 8 centimeter radial reflector can be reduced and the radial power profile flattened with nonuniform fuel loading and possibly by distributing absorbing materials in the reactor. The amount of nonuniform loading required is discussed by Plebuch (8).

The 3 centimeter end reflector was chosen for its power shaping capabilities. It is desirable to increase the power density of rocket reactors as much as possible so that either more power is transferred to the propellant for a given reactor or a smaller reactor can be used to get the same propellant conditions at the reactor exit. A reflector on the inlet end of the reactor increases the average power density in the reactor by increasing the power level near the inlet. To the first ap-

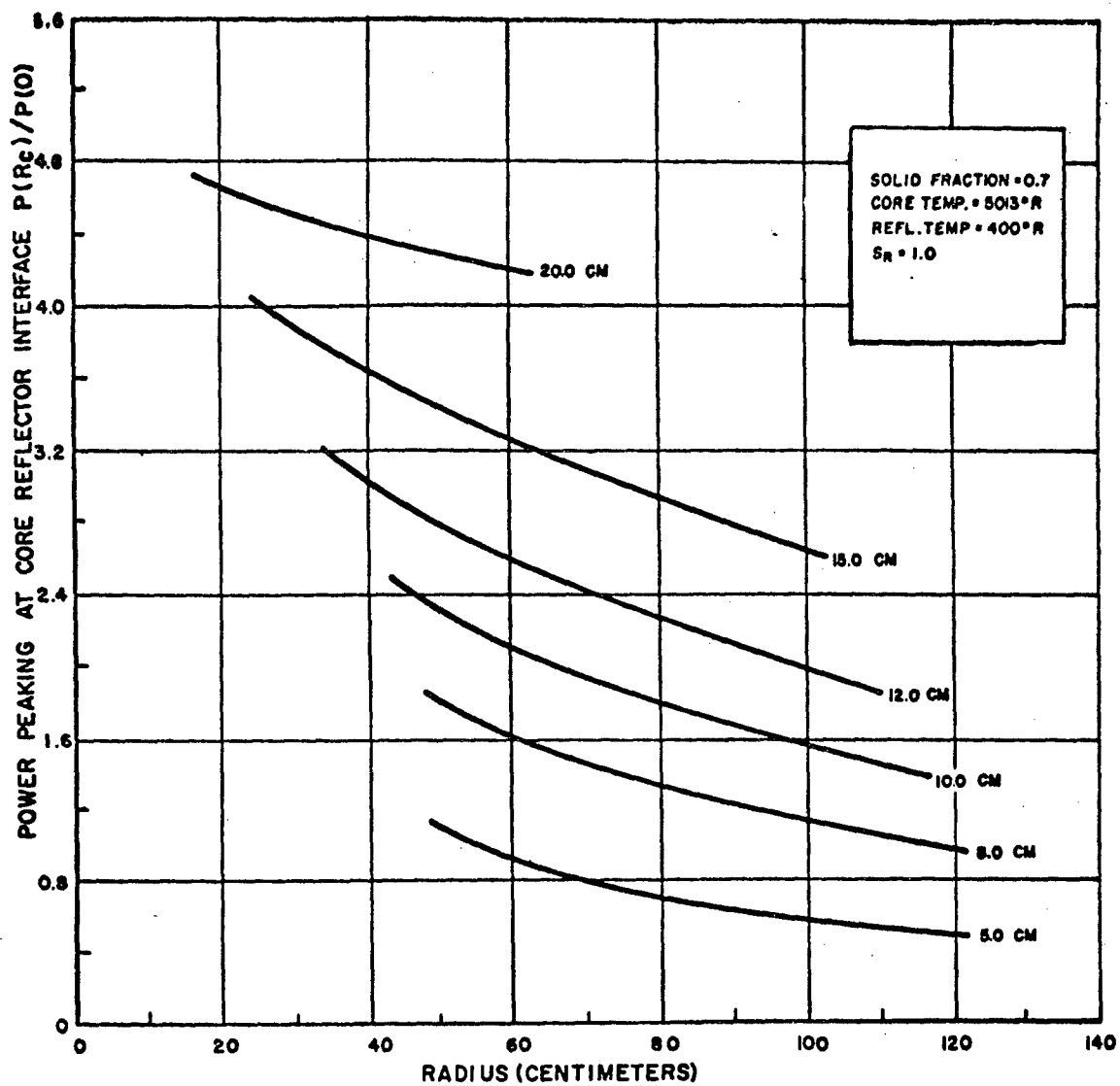


FIG.4-6: EFFECT OF BERYLLIUM REFLECTOR THICKNESS ON RADIAL POWER PEAKING FOR C/U-235 = 500

proximation the axial power profile in an unreflected reactor is a sine wave whereas in a reactor reflected on one end it is a chopped sine wave. In reality there is a local power peaking at the core reflector interface which is caused by the absorption of neutrons which have been slowed down and reflected back into the core. The power shaping and power peaking effects of the reflector are shown in Fig. 4-7. It can be seen that an 8 centimeter reflector causes a power peak almost twice as large as the 3 centimeter reflector. High power peaking at the inlet end of the reactor could cause extremely high temperatures to occur in the core material which would be undesirable. The 3 centimeter end reflector is used for all reactors in this study unless otherwise specified as it shapes the power profile in a desirable way but does not cause excessive peaking.

B. Heat Transfer and Pressure Drop Characteristics

In order to determine when conditions in the reactor are such that temperatures or stresses will limit the performance the local values of these parameters must be calculated. The local fluid properties, surface temperature of the coolant channel, and power density can be determined before the interior temperatures and stresses in the core are calculated. The independent variables required for these heat transfer calculations are the coolant stagnation temperature and pressure at the reactor exit, T_{SE} and p_{SE} respectively, the coolant temperature

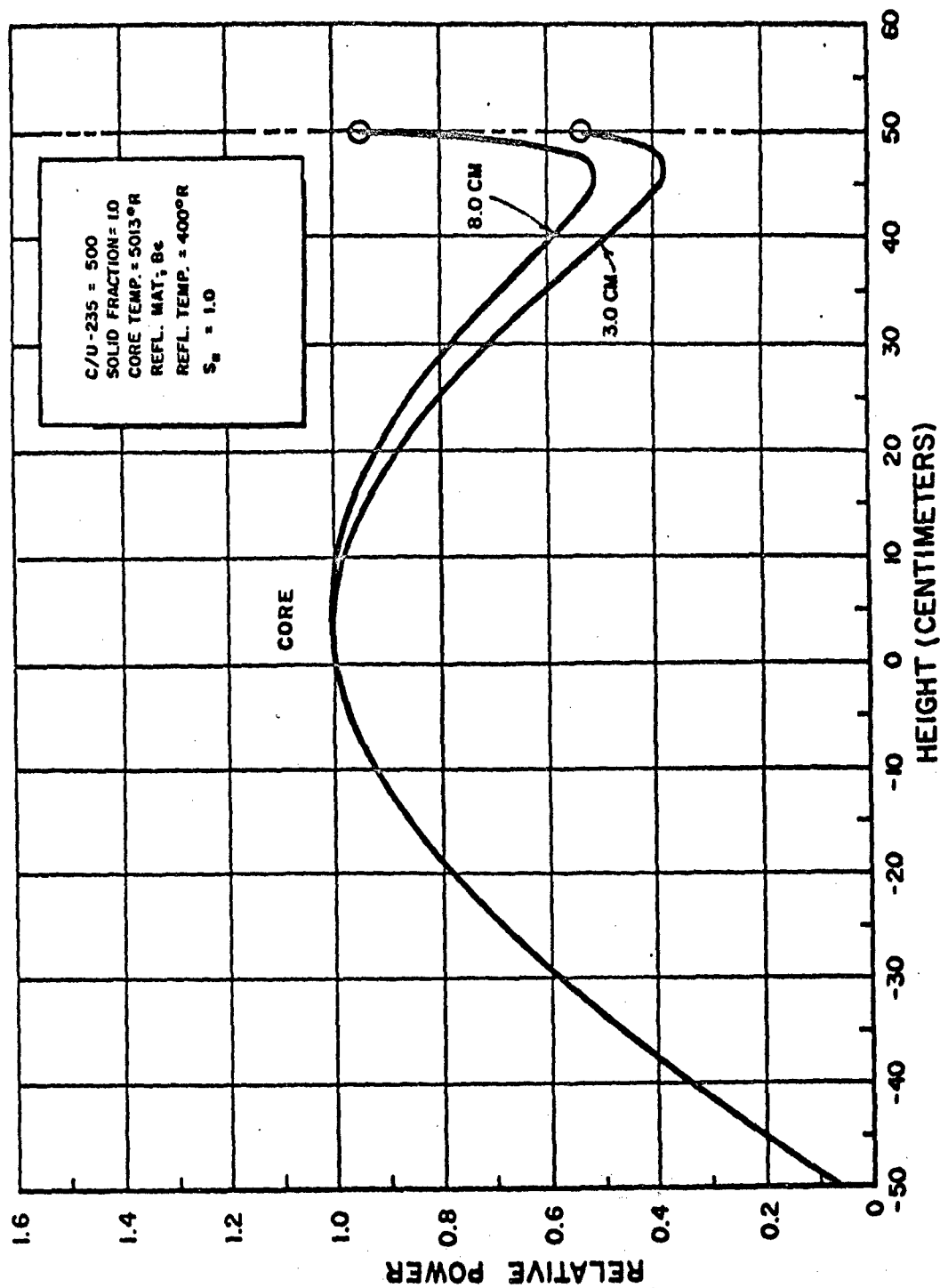


FIG. 4-7: EFFECT OF BERYLLIUM AXIAL REFLECTOR THICKNESS ON AXIAL POWER PROFILE

at the reactor inlet T_{SRI} , the coolant flow rate per unit area w/A_f , the channel diameter d and length L , and the shape of the power distribution. An alternative is to specify the magnitude of the power distribution at each position and calculate the diameter of coolant channel required. In addition to these variables it is also necessary to have relations for the heat transfer coefficient and friction factor in terms of the properties of the flow. The most simple relations involve assuming average values for these coefficients which are good over the length of the coolant channel. This would be correct only if the fluid properties did not change with temperature which is not true for a compressible gas. Empirical correlations for heat transfer coefficients that are functions of the heat transfer surface temperature as well as the fluid properties have been developed for flow conditions similar to those occurring in nuclear reactors (14, 15). These conditions include the effects of large temperature differences between the heat transfer surface and the fluid which occur near the inlet end of rocket reactors. The correlations are in general complex in the sense that they employ an artificial film temperature at which the fluid properties should be evaluated. This film temperature is usually defined as the arithmetic average of the local fluid temperature and the surface temperature of the coolant channel wall. Some of the correlations also

are functions of the distance traversed along the tube measured from the inlet end. The correlation used in most of this work is one by Taylor and Kirchgessner (14) developed for heat transfer to helium flowing in a tube. Tests have been made that indicate that hydrogen heat transfer results are correlated equally well with the same expression (14). The correlation is presented and discussed further in Appendix B where all the heat transfer and pressure drop equations are developed.

The friction factor correlation used in the calculations is

$$f = 0.046 / (Re_B)^{0.2} \quad (4-1)$$

rather than the more complicated Karman-Nikuradse relation which must be solved by trial and error. Over the range of Reynolds numbers from 5000 to 200,000 Eq. 4-1 fits the data quite well (14,16). This range of Reynolds numbers includes the values occurring in the coolant channels of nuclear rocket reactors.

To do the necessary detailed calculations the thermodynamic and transport properties of hydrogen gas are required. The equations for these properties have been obtained or developed and translated into Fortran language for use in machine computations. The subroutine will produce the properties of normal hydrogen for temperatures between 150° and 4000° Kelvin and over a range of pressures from 0.01 to 100.0 atmospheres. The effects of dissociation and compressibility factor unequal to one are taken into account where necessary.

The enthalpy, entropy, and specific heat of the ideal gas are calculated using empirical equations taken from reference 17. The compressibility factor is calculated using an empirical equation obtained from curve fitting published data (18) and from second virial coefficient calculations. The equations for calculating the thermodynamic properties and their partial derivatives including dissociation and compressibility effects were derived from basic thermodynamic relations.

The transport properties are calculated using a modified Buckingham potential for temperatures up to 1000°K (19). Above 1000°K these properties are calculated using equations and collision integrals developed by Vanderslice et al (20). High pressure corrections for the transport properties are determined using equations from NBS RP 1932 (21).

The development of these relations and the Fortran subroutine is presented in Appendix A. Since this subroutine was developed other programs for calculating hydrogen properties have become available in the literature (22, 23).

The actual heat transfer and pressure drop characteristics can be calculated with different degrees of accuracy and sophistication. The first calculations were done using an average heat transfer coefficient and averaged properties for hydrogen. Other calculations done using a local heat transfer coefficient dependent on the local hydrogen properties and the solid surface temperature show the inadequacy of the first calculations. An example of the errors that can be caused by using an average

heat transfer coefficient is shown in Fig. 4-8. The curves are for a run where the wall temperature was specified as constant rather than specifying the shape of the power distribution. The shape of the power profile required to give the constant wall temperature is then calculated along with the distribution of the coolant temperature. The power density curve which looks like a negative exponential was calculated using an average heat transfer coefficient, while the second curve was obtained using the heat transfer coefficient based on film properties and dependent on the local surface temperature as well as the fluid properties. The second more accurate power profile does not rise sharply at the inlet because the heat transfer at high ratios of surface to bulk fluid temperature is not simply proportional to the temperature differences as one might expect. These results clearly show the necessity of detailed calculations rather than simple analytical solutions for the determination of the local properties in the reactor.

The detailed calculations for the temperature, pressure, and power density distributions involve trial and error solutions at each iteration along the channel length. The calculation procedure was developed for digital machine calculations as a large number of these solutions are required to find the limiting performance characteristics of the reactor. The analysis used for this flow is similar to the generalized one-dimensional continuous flow analysis using influence coefficients as developed by Shapiro (24).

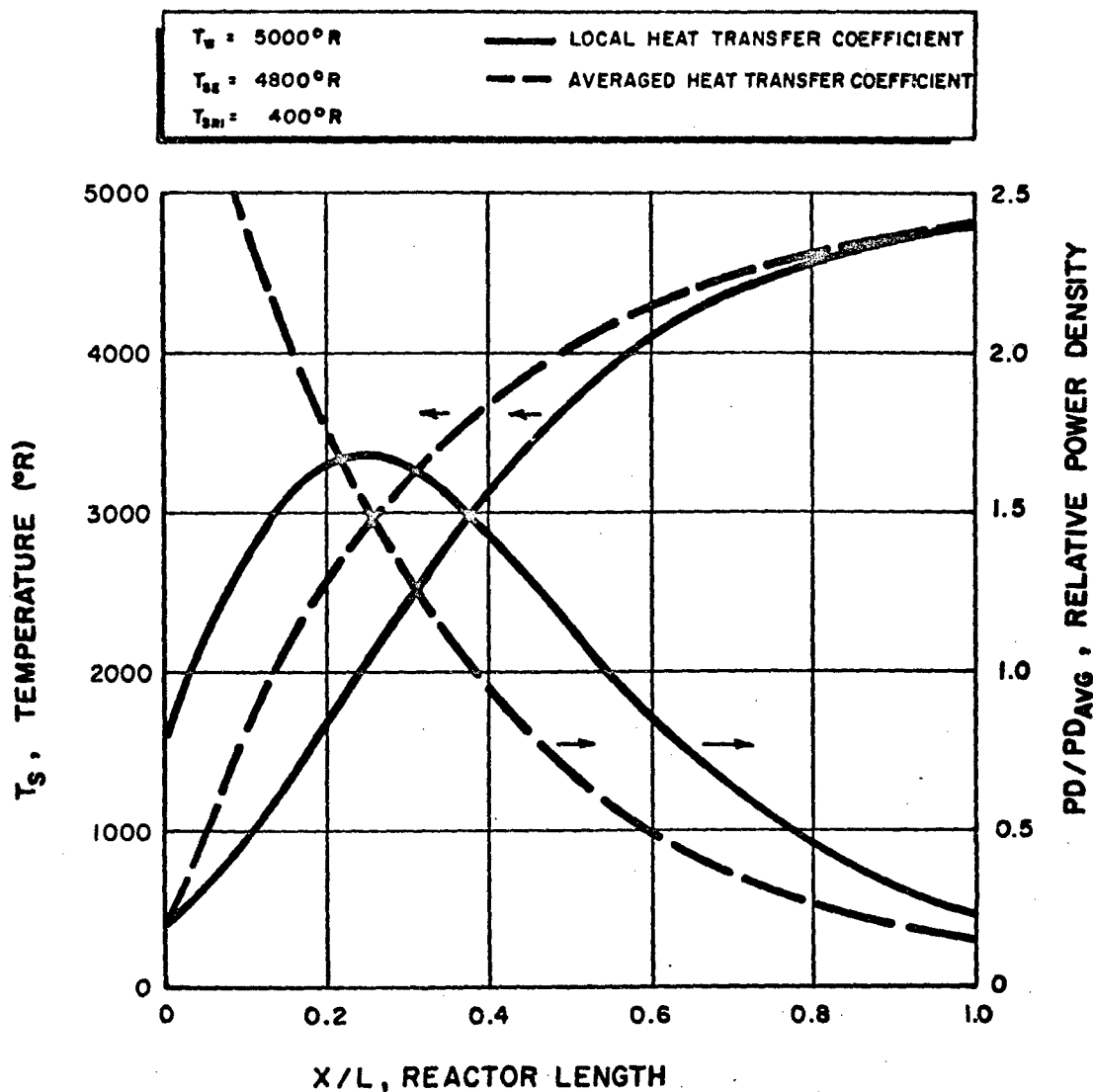


FIG. 4-8: HYDROGEN STAGNATION TEMPERATURE AND RELATIVE POWER DENSITY VS NON-DIMENSIONAL REACTOR LENGTH FOR A CONSTANT COOLANT CHANNEL SURFACE TEMPERATURE

The analysis is restricted to the simultaneous external effects of heat transfer and wall friction, but it is generalized in that it includes the internal effects of chemical reactions and changes in molecular weight and specific heat due to dissociation. The basic assumptions are as follows:

- (1) The flow is one-dimensional and steady.
- (2) Changes in stream properties are continuous.
- (3) The cross sectional area for flow is constant.
- (4) The mass flow rate is constant.
- (5) The gas mixture is in thermodynamic equilibrium.

The five basic equations governing the flow and the condition of the fluid are expressed for a differential length of the coolant channel as the control volume. The equation of state of the fluid can be expressed as

$$p = Z\rho RT/W \quad (4-2)$$

The continuity equation is

$$w = \rho VA_f \quad (4-3)$$

The Mach number is the ratio of the local velocity to the speed of sound. Employing the relation between the temperature and the speed of sound the expression for Mach number is

$$M^2 = V^2 / (\gamma RT/W) \quad (4-4)$$

The energy equation for a differential element is

$$w dQ - w dW_x = w(dH + d\frac{V^2}{2}) \quad (4-5)$$

The momentum equation is

$$-A_f dp - \tau_w dA_s = w dV \quad (4-6)$$

The wall shear stress can be expressed in terms of the friction factor as

$$\tau_w = f \frac{\rho V^2}{2} \quad (4-7)$$

The cross sectional area A_f and the heat transfer area dA_s are related to the hydraulic diameter so that

$$d = \frac{4A_f}{(dA_s/dx)} \quad (4-8)$$

Using Eqs. 4-3, 4-7 and 4-8 the momentum equation can be written as

$$-dp - f \frac{\rho V^2}{2} 4 \frac{dx}{d} = \rho V dV \quad (4-9)$$

Noting with the use of Eqs. 4-2 and 4-3 that

$$\frac{\rho V^2}{2} = \frac{p \gamma M^2}{Z} \quad (4-10)$$

Eq. 4-9 can be rewritten as

$$\frac{dp}{p} + \frac{\gamma M^2}{2Z} 4f \frac{dx}{d} + \frac{\gamma M^2}{2Z} \frac{dV^2}{V^2} = 0 \quad (4-11)$$

The enthalpy change in the energy equation can be expressed in terms of pressure and temperature changes as

$$dH = \left(\frac{\partial H}{\partial T} \right)_p dT + \left(\frac{\partial H}{\partial p} \right)_T dp \quad (4-12)$$

The partial derivative with respect to temperature is just the specific heat, and the derivative with respect to pressure, as shown in Appendix A, is

$$\left(\frac{\partial H}{\partial p} \right)_T = \frac{ZRT}{pW} \left[1 - \frac{T}{V} \left(\frac{\partial V}{\partial T} \right)_p \right] \quad (4-13)$$

Using these expressions for the enthalpy derivatives and noting that the work term dW_x is zero for the case under consideration the energy equation can be written

$$\frac{dQ}{c_p T} = \frac{dT}{T} + \frac{ZR}{c_p W} \left[1 - \frac{T}{v} \left(\frac{\partial v}{\partial T} \right)_p \right] \frac{dp}{p} + \frac{v^2}{2c_p T} \frac{dv^2}{v^2} \quad (4-14)$$

Taking logarithms of the equation of state (4-2) gives

$$\ln p = \ln Z + \ln \rho + \ln R + \ln T - \ln W \quad (4-15)$$

Then taking the differential of each side of Eq. 4-15

$$\frac{dp}{p} = \frac{dZ}{Z} + \frac{d\rho}{\rho} + \frac{dT}{T} - \frac{dW}{W} \quad (4-16)$$

Similar operations on Eqs. (4-3) and (4-4) result in

$$0 = \frac{d\rho}{\rho} + \frac{dv}{v} \quad (4-17)$$

and

$$\frac{dM^2}{M^2} = \frac{dv^2}{v^2} + \frac{dW}{W} - \frac{d\gamma}{\gamma} - \frac{dT}{T} \quad (4-18)$$

Considering W , γ , and Z as functions of temperature and pressure it can be shown that

$$\frac{dW}{W} = \frac{T}{W} \left(\frac{\partial W}{\partial T} \right)_p \frac{dT}{T} + \frac{p}{W} \left(\frac{\partial W}{\partial p} \right)_T \frac{dp}{p} \quad (4-19)$$

$$\frac{d\gamma}{\gamma} = \frac{T}{\gamma} \left(\frac{\partial \gamma}{\partial T} \right)_p \frac{dT}{T} + \frac{p}{\gamma} \left(\frac{\partial \gamma}{\partial p} \right)_T \frac{dp}{p} \quad (4-20)$$

and

$$\frac{dZ}{Z} = \frac{T}{Z} \left(\frac{\partial Z}{\partial T} \right)_p \frac{dT}{T} + \frac{p}{Z} \left(\frac{\partial Z}{\partial p} \right)_T \frac{dp}{p} \quad (4-21)$$

The value of $\frac{T}{W} \left(\frac{\partial W}{\partial T} \right)_p$ and the other partial derivatives with respect to temperature and pressure can be determined in the hydrogen properties subroutine.

Eqs. 4-11, 4-14 and 4-16 through 4-21 are eight algebraic equations with ten variables which are differentials. They are $\frac{dp}{p}$, $\frac{d\rho}{\rho}$, $\frac{dT}{T}$, $\frac{dW}{W}$, $\frac{dZ}{Z}$, $\frac{dM^2}{M^2}$, $\frac{dv^2}{v^2}$, $\frac{d\gamma}{\gamma}$, $\frac{dQ}{c_p T}$, and $4f \frac{dx}{d}$. Eight of the variables can be taken as dependent and two as independent. The variables taken as being independent are $\frac{dQ}{c_p T}$ and $4f \frac{dx}{d}$. After a considerable amount of algebra, the following expression can be obtained for $\frac{dM^2}{M^2}$:

$$\frac{dM^2}{M^2} = J \frac{dQ}{c_p T} + \frac{1}{2D} \left[-B + (1 + \eta \gamma M^2 D) J \right] 4f \frac{dx}{d} \quad (4-22)$$

where the quantities B, D, J, and η , presented in Appendix B, involve the derivatives of the fluid properties.

The two quantities $\frac{dQ}{c_p T}$ and $4f \frac{dx}{d}$ can be related to each other through the correlations for the heat transfer coefficient and the friction factor. The heat transfer correlation is

$$\frac{hd}{k_f} = 0.021 \left(\frac{\rho_f v d}{\mu_f} \right)^{0.8} \left(\frac{c_{pf} \mu_f}{k_f} \right)^{0.4} \quad (4-23)$$

The correlation for the friction factor, Eq. 4-1, can be written

$$f = 0.046 \left(\frac{\mu_B}{\rho v d} \right)^{0.2} \quad (4-24)$$

The local heat transfer rate divided by the cross sectional area is

$$\frac{dq}{A_f} = h \frac{dA_s}{A_f} (T_W - T_B) = \frac{w}{A_f} dQ \quad (4-25)$$

Eqs. 4-23 through 4-25 can be combined and with the use of Eqs. 4-3 and 4-8 the following expression results:

$$4f \frac{dx}{d} = \frac{0.046}{0.021} \frac{T_{AV}}{T_W - T_B} \left(\frac{\rho_{AV}}{\rho_f} \right)^{0.8} \left(\frac{\mu_B}{\mu_f} \right)^{0.2} \frac{c_{pAV}}{c_{pf}} \left(Pr_f \right)^{0.6} \frac{dQ}{c_p T_{AV}} \quad (4-26)$$

where the subscript AV implies evaluation at the static temperature averaged along the direction of flow. For a differential element T_{AV} would equal T , but for a finite element as used in the calculations the temperature is averaged. Then the dx and dQ become finite differences Δx and ΔQ .

With the relation between $4f \frac{dx}{d}$ and $\frac{dQ}{c_p T}$ it is now possible to find the change in Mach number and the other fluid properties with the specification of only one independent variable if the wall temperature is specified in Eq. 4-26. For the case of a constant wall temperature along the channel this is the procedure which is used. In the program as it was developed a temperature change is specified to fix the value of dQ . The value of $4f \frac{dx}{d}$ is then computed and the change in Mach number determined from Eq. 4-22.

If the local wall temperature is not specified the shape of the power distribution must be and the value of $4f \frac{dx}{d}$ is deter-

mined in another manner. Eq. 4-26 is then used to determine the local wall temperature. When the shape of the power distribution is specified, either in analytical or tabular form, the ratio of the heat transferred to the propellant from the end of the reactor to a given point along the length to the total heat transferred Q/Q_T is solely a function of the nondimensional length x/L . The total amount of heat transferred to the propellant is determined from the fluid temperatures at the reactor inlet and exit. The heat transferred up to any local value is determined from that local fluid temperature and the temperature at the end of the reactor. The ratio Q/Q_T is then used to find the local value of x/L . The difference between this value of x/L and that of the last step is then $\Delta x/L$. The local friction factor f can be determined from Eq. 4-24. The channel diameter d and length L are specified so the value of $4f \frac{\Delta x}{d}$ is then the product of these known quantities.

$$4f \frac{\Delta x}{d} = \left(\frac{\Delta x}{L} \right) 4f \left(\frac{L}{d} \right) \quad (4-27)$$

With this value and the ΔQ calculated from the specified temperature change the change of Mach number is calculated using Eq. 4-22. As soon as $\frac{dM^2}{M^2}$ is determined less complicated expressions can be obtained for the changes in pressure and temperature.

$$\frac{dp}{p} = \frac{D \frac{dM^2}{M^2} + \frac{B}{2} 4f \frac{dx}{d}}{-A - B \frac{Z}{\gamma M^2}} \quad (4-28)$$

and

$$\frac{dT}{T} = \frac{\frac{dM^2}{M^2} + F \frac{dp}{p}}{B} \quad (4-29)$$

The quantities A and F are similar to B and D in Eq. 4-22 in that they contain thermodynamic property derivatives. These coefficients are therefore dependent on the fluid temperature and pressure. The method of solution involves a trial and error procedure because estimates of the local temperature must be made to calculate the coefficients. When the pressure and temperature changes are calculated from Eqs. 4-28 and 4-29 the initial estimates must be checked and corrected if they were in error.

The local coolant channel surface temperature is determined by trial and error from Eq. 4-26 when the power distribution is specified. The solution is a trial and error procedure because the fluid properties are functions of the film temperature which depends on the wall temperature. The entire procedure is presented in detail in Appendix D. The description given above presents the main ideas but does not include all the trial and error loops which are necessary. The fluid enthalpy is dependent on the static pressure as well as the temperature which means the amount of heat transferred is a function of the pressure. This results in a trial and error calculation for the calculation of ΔQ for each step. Another trial and error solution

is necessary for the calculation of the static fluid properties.

The results of these calculations are tabular values of the axial distributions of the fluid static and stagnation temperatures, fluid static and stagnation pressures, Mach number, coolant channel surface temperature, and other conditions of the flow which may be of interest. The complete list is given in Appendix D with the sample solution. A typical plot of the most significant parameters is shown in Fig. 4-9. The hydrogen stagnation temperature at the reactor exit is 4668°R and the stagnation pressure is 800 psia while the temperature at the reactor inlet is 400°R . The mass flow rate per unit area is $0.858 \text{ lb/sec-in}^2$. These results are for a chopped sine power distribution where the local heat flux is of the form:

$$\frac{dq}{dx} = A_1 \sin \left[CQ_1 \left(1 - \frac{x}{L} \right) \right] \quad (4-30)$$

and CQ_1 is equal to 2.5.

The value of the constant CQ_1 determines where the sine wave is chopped off at the inlet end of the reactor. If CQ_1 is equal to π the sine wave would not be chopped at all while if CQ_1 is equal to $\pi/2$ the maximum heat flux would occur at the reactor inlet. Fig. 4-10 shows power distribution for two values of CQ_1 along with the power distribution determined from reactor physics calculations for a core reflected on one end with 3 centimeters of beryllium. Values of CQ_1 in the range

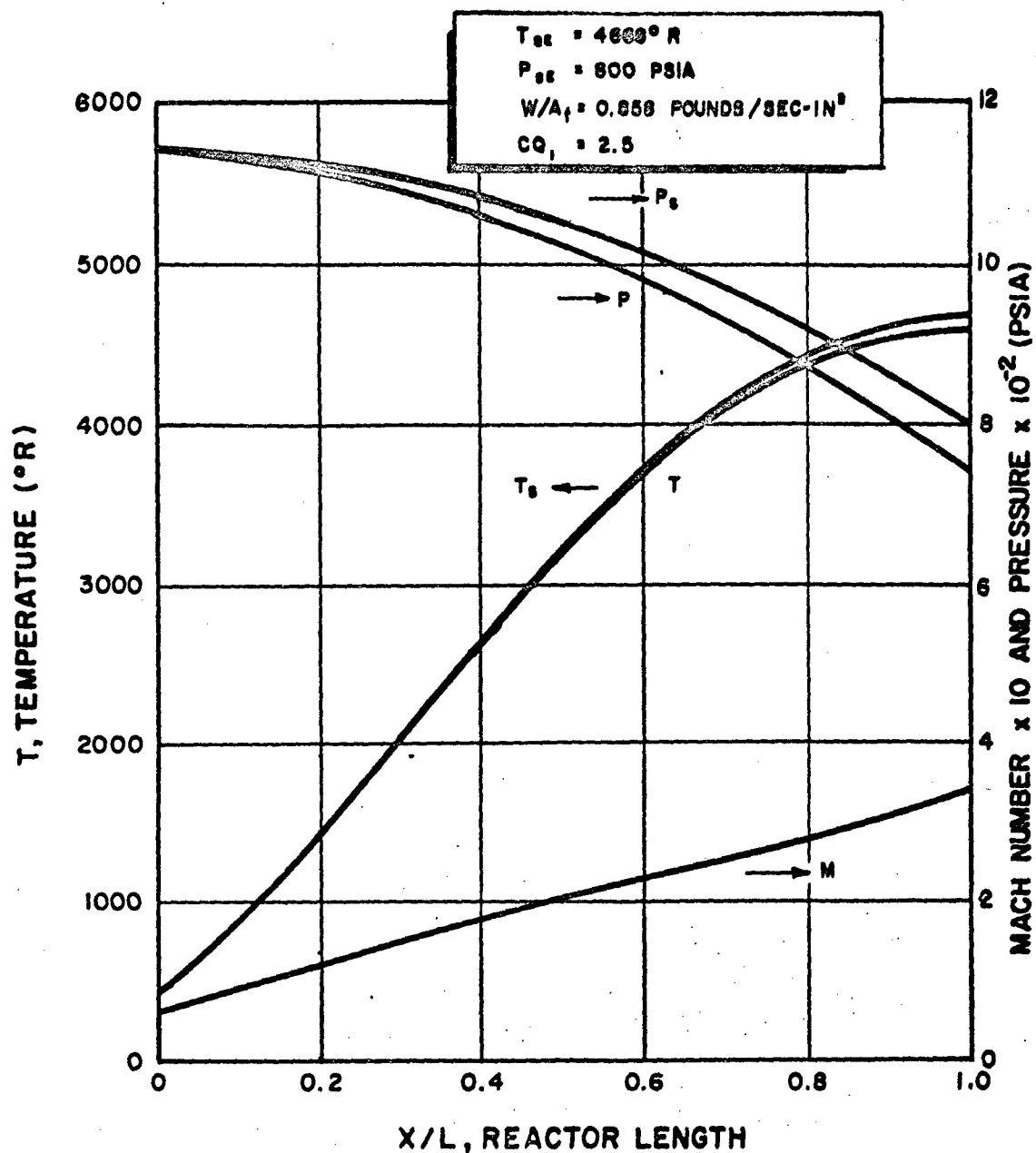


FIG.4-9: HYDROGEN STAGNATION TEMPERATURE, STATIC TEMPERATURE, STAGNATION PRESSURE, STATIC PRESSURE, AND MACH NUMBER VS NON-DIMENSIONAL REACTOR LENGTH FOR CHOPPED SINE POWER DISTRIBUTION

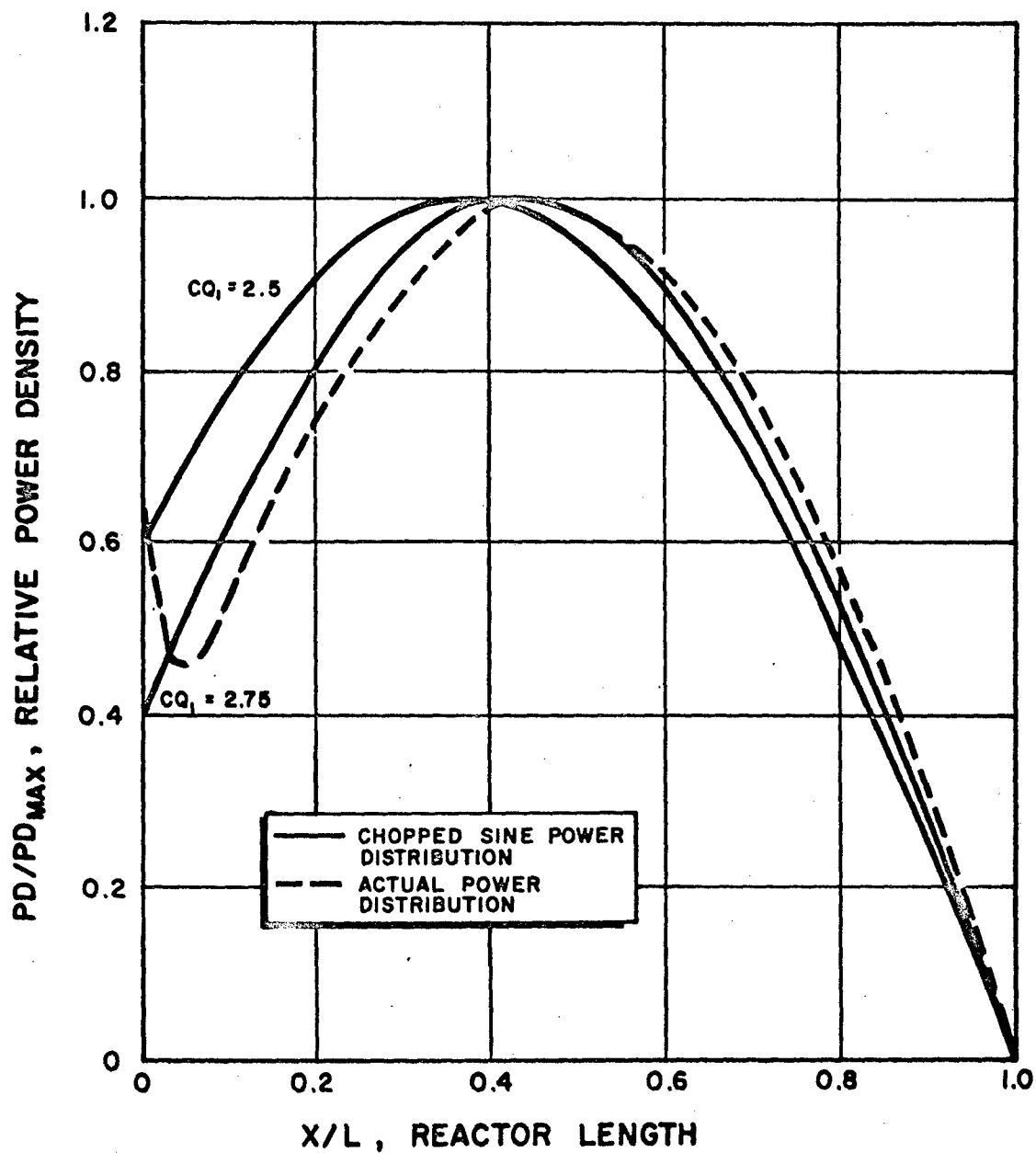


FIG. 4-10: RELATIVE POWER DENSITY VS NON-DIMENSIONAL REACTOR LENGTH FOR CHOPPED SINE POWER DISTRIBUTIONS AND ACTUAL POWER DISTRIBUTION IN A REFLECTED REACTOR

of 2.5 to 2.75 produce chopped sine profiles which are reasonable approximations to the real distributions.

The results in Fig. 4-9 were calculated using the program presented in Appendix D. The number of steps between the reactor inlet and exit where calculations are performed was varied for a typical set of data. The effect on the results in going from 50 to 200 calculational steps was less than one per cent. A run was also made using 100 steps and a plot of any result versus the number of steps does not produce an asymptotic value that one would reach by going to an infinite number of steps. This is because the accuracy demanded of the trial and error loops in the program allows a small random variation in the results that is as large as the difference that is obtained in going from 50 to 200 steps. The conclusion reached from this is that 50 calculation steps are sufficient and that using more would be a waste of time as the time required for a run is almost directly proportional to the number of steps.

It is also possible to use different hydrogen properties with the program. The hydrogen properties can be calculated excluding the effects of dissociation and/or compressibility factor unequal to one. This is explained in detail in Appendix A where the equations are developed. If both the effects of dissociation and compressibility factor unequal to one are excluded

the difference in the heat transfer and pressure drop results may be a few per cent. The change in the calculated stagnation pressure at the reactor inlet for a sample run was 25 psia out of 1100 or a change of 2.3⁰/o . The use of the more accurate hydrogen properties does not require a noticeable increase in the length of time required for a run, consequently these properties were used for all further runs.

Along with the above results for the heat flux and temperature distributions the specification of the void fraction of the reactor and the geometry of the coolant channel distribution is sufficient to make the calculation of the local power density and maximum temperature in reactor core possible. At any axial position the power generation is assumed to be uniform in the solid fraction of the core. The local power density is then the local heat flux per unit length divided by the area over which it is generated:

$$PD = \frac{dq}{dx} \frac{1}{A_T} \quad (4-31)$$

Expressed in terms of known quantities this is

$$PD = \frac{V}{L} \frac{W}{A_f} \frac{\Delta Q}{(\Delta x/L)} \quad (4-32)$$

The geometry used to calculate the maximum core temperature is a spacing of coolant channels on the vertices of equilateral triangles. An approximate solution for this shape with uniform heat generation has been found and is available in the literature

(25). No exact solution can be found as the boundary conditions cannot be simultaneously satisfied in both circular and rectangular coordinates. The temperature difference between the maximum in the solid and that at the surface of the coolant channel is proportional to the local power density and the square of the coolant channel diameter. The exact form of the equation showing the dependence on the reactor void fraction is presented in Appendix D.

C. Stress Analysis

The actual design of fuel elements for the reactor core should be related to temperature and stress considerations, the method of supporting the core, possible vibration problems, and to manufacturing tolerances. It is impossible to determine analytically the best design taking all the above considerations into effect. As it is not the purpose of this work to design fuel elements or reactor cores, a fairly simple model was used to make stress calculations. If it becomes desirable a different model or models could be used. This would only affect the numerical values used in the rest of the analysis and not the general method.

The model used to make stress calculations is an annular element with uniform heat generation in the solid. The combination of thermal stresses and stresses due to applied loads

can be solved analytically for this case. Some work has been done on the calculation of stresses due to applied loads in plates or cylinders with a number of circular holes (26, 27). The temperature distribution has been obtained for a heat generating cylinder with a ring of holes for coolant flow (28). The extension of the stress calculations to include the thermal stresses for these geometries is a formidable task which should be accomplished but is not undertaken in this study.

In the annular element used as a model for stress calculations the inside diameter is the same as the coolant channel diameter in the core. The void fraction free for coolant flow is also the same for the annulus as it is for the core. If the actual geometry in the core is a spacing of coolant channel holes on the vertices of equilateral triangles, the distance between holes or the web thickness is of the same order of magnitude as the hole diameter. For a void fraction of 0.3 and a channel diameter of 0.1 inches the web thickness is 0.074 inches. The outside diameter of an annulus with a void fraction of 0.3 and an inside diameter of 0.1 inches is 0.183 inches. This means the distance between holes for stacked annuli is 0.083 inches which is about 10% greater than it is for the holes spaced on the vertices of equilateral triangles.

In order to determine when the reactor or the model used

is stress limited a failure criterion must be employed and a limiting condition set for the material. Graphite is a brittle material and ideally the failure criterion applied should be valid for brittle fracture. Unfortunately, the understanding of the fundamentals of brittle fracture is not so highly developed that the theory is easily applicable to engineering problems. There are two theories for the propagation of cracks causing failure in brittle materials. One theory first formulated by Griffith is deterministic while the second proposed by Weibull is probabilistic in nature (29). Both theories can account for some but not all of the aspects of brittle fracture. They both involve arbitrary constants which must be determined empirically for the material under consideration. The probabilistic theory has been applied to some engineering problems and related to a factor of safety with regard to a single stress value like a yield stress (30, 31).

The failure criterion used in this analysis is the maximum shear criterion. The maximum principal stress would be the failure criterion for an ideal brittle material (32). For the model used in this analysis the maximum shear criterion is used because it is more conservative than the maximum principal stress criterion.

For the annular model the stresses were calculated for two different sets of boundary conditions. In both cases the radial

stress at the inner radius was assumed to be equal to the negative value of the local coolant pressure, and the whole element is considered to be free to expand in the axial direction so the problem is one of plain strain. The principal stresses are then in the radial, tangential, and axial directions. The two different boundary conditions considered are those on the outer radius of the annulus. If the annulus is considered as a unit cell in the core so that it is like all other cells at the same axial position, the outer boundary must be considered adiabatic to insure that the temperature gradient be zero at the outside radius. Similarly there is no reason to have a discontinuity in the gradient of the radial stress at this position, in which case the second boundary condition on the stress should be that the derivative of the radial stress with respect to radius is zero at the outer boundary. The other possibility is that the radial stress be set equal to zero or the negative of the fluid pressure at this boundary. The latter condition would result in a discontinuity in the gradient of the radial stress if two annuli were placed side by side.

The basic equations for the stresses in a circular cylinder with a nonuniform temperature distribution and no axial displacement are (33)

$$\sigma_{\theta_r} = \frac{\alpha E}{1 - \nu} \frac{1}{r^2} \int_{r_i}^r \theta r dr + \frac{E}{1 + \nu} \left(\frac{C_1}{1 - 2\nu} - \frac{C_2}{r^2} \right) \quad (4-33)$$

$$\sigma_{\theta} = \frac{\alpha E}{1-\nu} \frac{1}{r^2} \int_{r_i}^r \theta r dr - \frac{\alpha E \theta}{1-\nu} + \frac{E}{1+\nu} \left(\frac{C_1}{1-2\nu} + \frac{C_2}{r} \right) \quad (4-34)$$

$$\sigma_z = -\frac{\alpha E \theta}{1-\nu} + \frac{2\nu E C_1}{(1+\nu)(1-2\nu)} \quad (4-35)$$

If a uniform axial stress $\sigma_z = C_3$ is superposed, C_3 can be chosen such that the resultant force on the ends is zero.

This means that the axial displacement will be uniform but unequal to zero. The equations for the radial and tangential stresses remain unchanged.

The temperature distribution in an annular element with uniform heat generation and an adiabatic outside surface is

$$\theta = T - T_w = \frac{W_i}{2k} \left(r_0^2 \ln \frac{r}{r_i} - \frac{r^2 - r_i^2}{2} \right) \quad (4-36)$$

where T_w is the temperature at r_i and W_i is the heat generation rate. This expression is developed in Appendix B along with all the expressions for the stresses. With this temperature distribution and a set of boundary conditions for the radial stress, the constants in Eqs. 4-33 through 4-35 can be evaluated and the equations for the stresses obtained in terms of known quantities.

For the boundary conditions

$$\sigma_r = -p \text{ at } r = r_i \quad (4-37)$$

and

$$\sigma_r = 0 \text{ at } r = r_0$$

*4-38)

the results are

$$\sigma_r = - \frac{v}{(r/r_0)^2} \left[\frac{1 - \left(\frac{r}{r_0}\right)^2}{1 - v} \right] p + \frac{\alpha E}{1-v} \frac{W_i}{4k} \frac{r_i^2}{v} \left\{ \frac{\left(\frac{r}{r_0}\right)^2 - v}{1 - v} - \frac{1}{\left(\frac{r}{r_0}\right)^2} \ln \frac{1}{\sqrt{v}} \right. \\ \left. - \ln \left[\frac{r}{r_0} \sqrt{\frac{1}{v}} \right] - \frac{\left(\frac{r}{r_0}\right)^2 - v}{4 \left(\frac{r}{r_0}\right)^2} \left[1 - \left(\frac{r}{r_0}\right)^2 \right] \right\} \quad (4-39)$$

$$\sigma_\theta = \frac{v \left[1 + \left(\frac{r}{r_0}\right)^2 \right]}{\left(\frac{r}{r_0}\right)^2 (1 - v)} p + \frac{\alpha E}{1-v} \frac{W_i}{4k} \frac{r_i^2}{v} \left\{ \frac{\left(\frac{r}{r_0}\right)^2 + v}{1 - v} - \frac{1}{\left(\frac{r}{r_0}\right)^2} \ln \frac{1}{\sqrt{v}} \right. \\ \left. - \ln \left[\frac{r}{r_0} \sqrt{\frac{1}{v}} \right] + \frac{1}{4 \left(\frac{r}{r_0}\right)^2} \left[-5 \left(\frac{r}{r_0}\right)^2 - v + \left(\frac{r}{r_0}\right)^2 \left\{ 3 \left(\frac{r}{r_0}\right)^2 - v \right\} \right] \right\} \quad (4-40)$$

$$\sigma_z = \frac{\alpha E}{1-v} \frac{W_i}{4k} \frac{r_i^2}{v} \left\{ 2 \left[\frac{1}{1-v} \ln \frac{1}{\sqrt{v}} - \ln \left(\frac{r}{r_0} \sqrt{\frac{1}{v}} \right) \right] - \frac{3-v}{2} + \left[\left(\frac{r}{r_0}\right)^2 - v \right] \right\} \quad (4-41)$$

In the above expressions the void fraction v has been inserted for $(r_i/r_0)^2$. The value of σ_z was determined using C_3 such that the resultant force on the ends of the element is zero.

Similar equations result for the other set of boundary conditions

where

$$\sigma_r = -p \quad \text{at} \quad r = r_i \quad (4-42)$$

$$\frac{d\sigma_r}{dr} = 0 \quad \text{at} \quad r = r_o \quad (4-43)$$

They are

$$\sigma_r = -p + \frac{E\alpha}{1-\nu} \frac{W_i}{4k} \frac{r_i^2}{v} \left\{ -\ln \left[\frac{r}{r_o} \sqrt{\frac{1}{v}} \right] + \frac{\left(\frac{r}{r_o}\right)^2 - v}{4} \left[\frac{1}{v \left(\frac{r}{r_o}\right)^2} + 1 \right] \right\} \quad (4-44)$$

$$\sigma_\theta = -p - \frac{E\alpha}{1-\nu} \frac{W_i}{4k} \frac{r_i^2}{v} \left\{ \ln \left[\frac{r}{r_o} \sqrt{\frac{1}{v}} \right] - \frac{\left[\left(\frac{r}{r_o}\right)^2 + v\right](1 - v^2)}{4v \left(\frac{r}{r_o}\right)^2} + \frac{\left(\frac{r}{r_o}\right)^2 - v}{4 \left(\frac{r}{r_o}\right)^2} \left[2 - 3 \left(\frac{r}{r_o}\right)^2 - v \right] \right\} \quad (4-45)$$

The value of σ_z is given by Eq. 4-41 as it is for the other set of boundary conditions.

The radial distribution of the three principal stresses is shown in Figs. 4-11 and 4-12 for the two different sets of boundary conditions. The power density is 100 megawatts per cubic foot, and the coolant pressure is 500 psia for both cases. The inner diameter is 0.100 inches and the outer diameter is 0.182 inches corresponding to a void fraction of 0.3. The shapes of these curves are typical for the range of pressures and power densities of interest although the absolute values of the stresses will change.

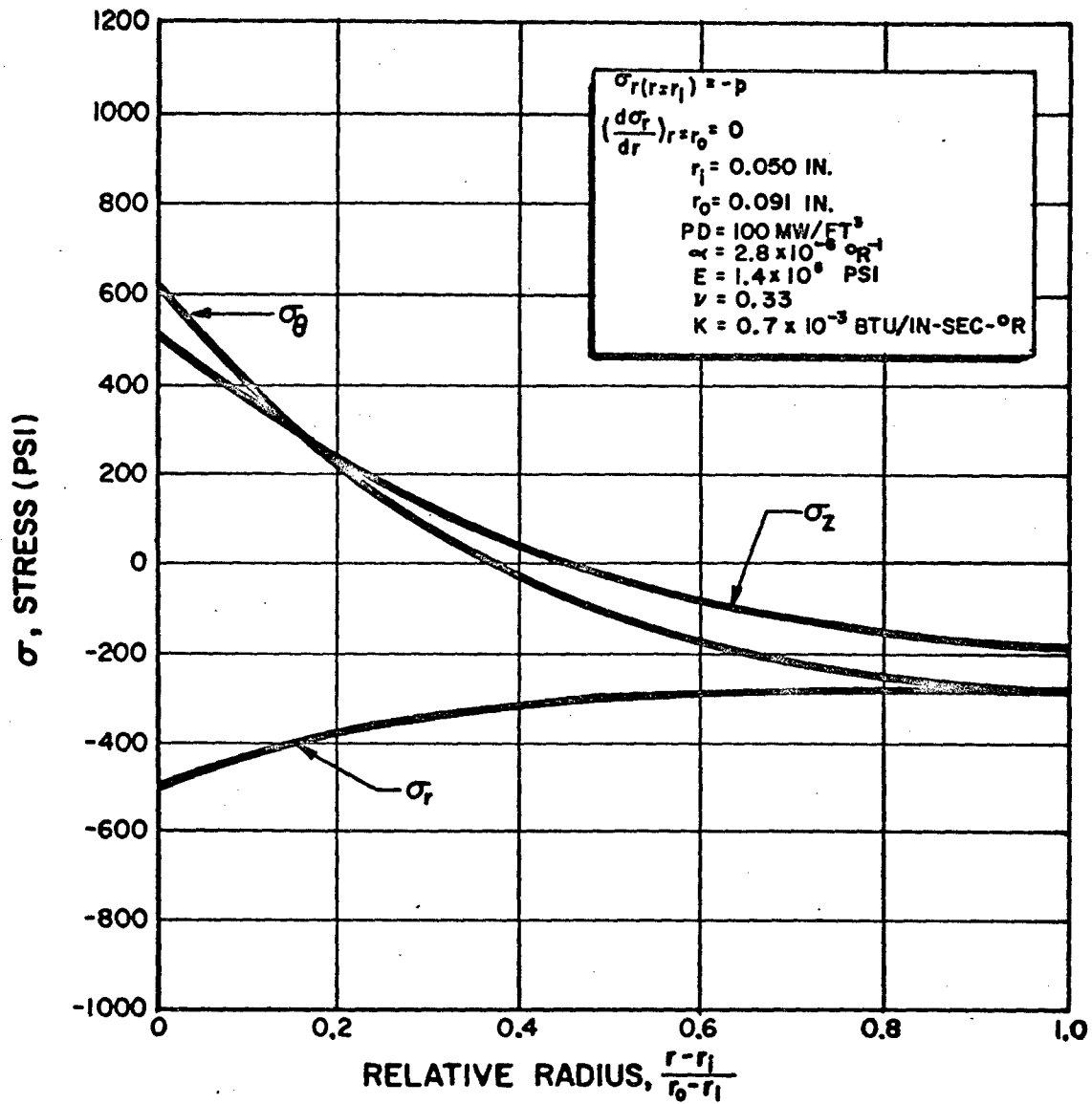


FIG. 4-11: DISTRIBUTION OF PRINCIPAL STRESSES IN AN ANNULAR ELEMENT WITH UNIFORM HEAT GENERATION

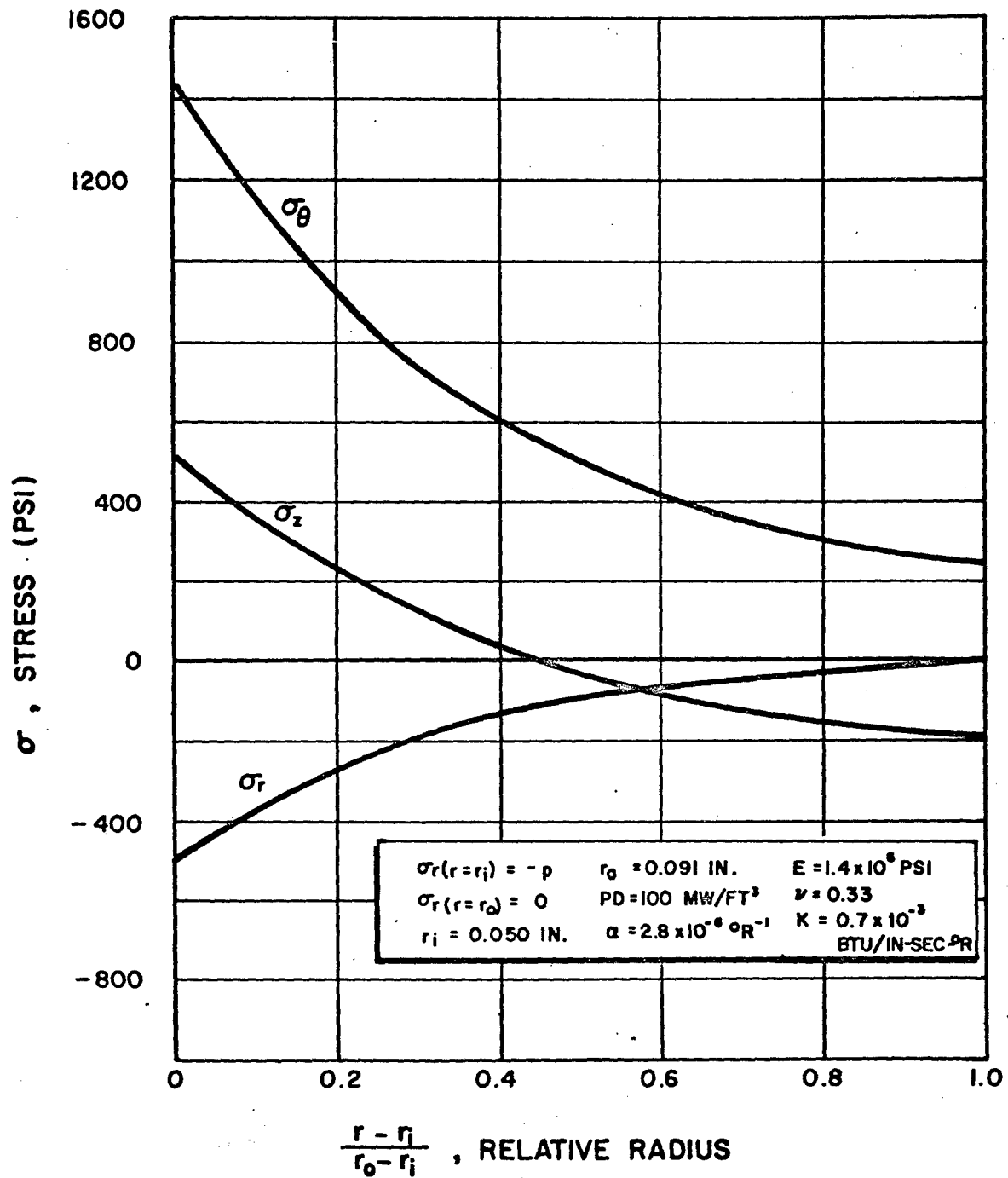


FIG. 4-12: DISTRIBUTION OF PRINCIPAL STRESSES IN AN ANNULAR ELEMENT WITH UNIFORM HEAT GENERATION

It can really be seen that the worst stress conditions occur at the inside radius of the element. This is true for the maximum shear stress, maximum stress, or any other common failure criterion. It is also true for different values of power density and pressure. This simplifies the determination of the maximum stress in an element as the stresses need only to be calculated at the inside radius rather than at a number of different radii. It also means that the equations for calculating the stresses can be simplified as is shown in Appendix C where they are developed. For the case where the gradient of the radial stress is zero at the outer boundary the equations for the stresses at the inner radius are

$$\sigma_r = -p \quad (4-46)$$

$$\sigma_\theta = -p + \frac{\alpha E}{1-\nu} \frac{W_i}{4k} \frac{r_i^2}{\nu} \left[\frac{(1-\nu)^2}{2\nu} \right] \quad (4-47)$$

$$\sigma_z = \frac{\alpha E}{1-\nu} \frac{W_i}{4k} \frac{r_i^2}{\nu} \left[\frac{2}{1-\nu} \ln \frac{1}{\sqrt{\nu}} - \frac{3-\nu}{2} \right] \quad (4-48)$$

The equations for σ_r and σ_θ with the other set of boundary conditions can be reduced in a similar fashion. The expression for σ_z is given by Eq. 4-48. The heat generation rate is equal to the local power density PD divided by the solid frac-

tion of the core and appropriate conversion factors.

In all further calculations the stresses are calculated for the case where the gradient of the radial stress is equal to zero at the outer boundary of the annulus. This set of boundary conditions is considered to be more realistic for the model as it is considered a unit cell of the reactor core. The form of the equations used in the computer program is presented in Appendix D. The stresses are calculated at each step along the core along with the temperatures and other fluid properties. The difference between the maximum and minimum principle stresses yields the maximum shear stress at that point.

The distribution of the maximum shear stress is shown in Fig 4-13 along with the distributions of the wall temperature, maximum core temperature, coolant stagnation temperature, and power density. The independent parameters used to calculate these results are the same as those used to obtain the coolant property distributions presented in Fig. 4-9. For the case shown the maximum shear stress occurs where the local power density is maximum. This will be true as long as the maximum shear stress is obtained from the tangential and radial stresses. The difference between these two stresses is independent of the fluid pressure and proportional to the local heat generation rate as can be seen from Eqs. 4-46 and 4-47.

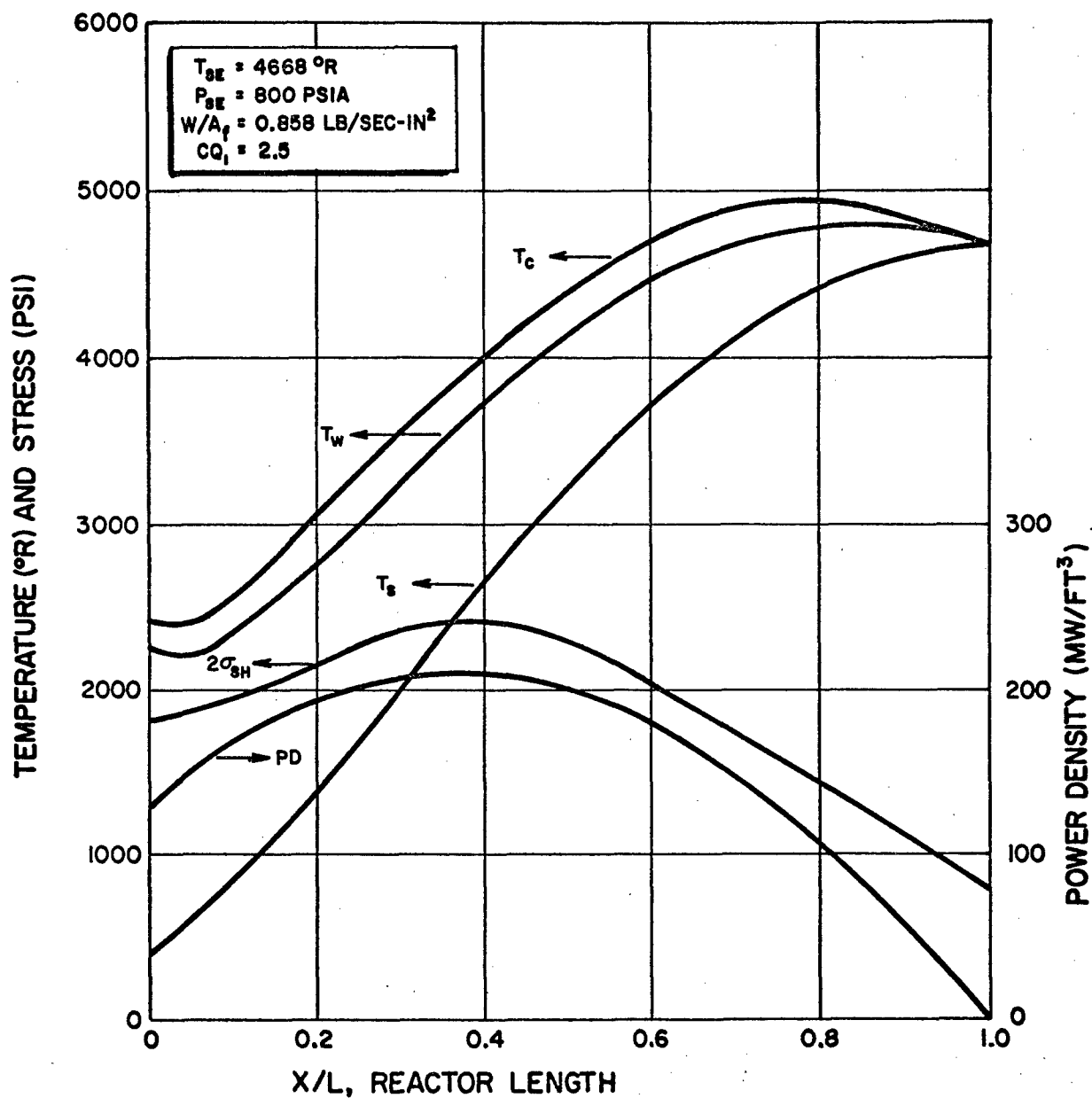


FIG. 4-13: HYDROGEN TEMPERATURE, COOLANT CHANNEL SURFACE TEMPERATURE, SOLID CENTERLINE TEMPERATURE, SHEAR STRESS AT COOLANT CHANNEL SURFACE, AND LOCAL POWER DENSITY IN REACTOR VS NON-DIMENSIONAL REACTOR LENGTH FOR CHOPPED SINE POWER DISTRIBUTION.

It was initially thought that a power density distribution corresponding to a constant wall temperature would be desirable. This would be particularly true if the reactor was surface temperature limited. A number of constant wall temperature runs were calculated and the distributions of maximum solid temperature and stress determined. An example of the results is shown in Figs. 4-14 and 4-15. The coolant properties are shown in the first figure while the maximum solid temperature and the stress distributions are shown in the second. The hydrogen stagnation temperature at the reactor exit is 4600°R and the stagnation pressure is 800 psia. The flow rate per unit area is $0.800 \text{ lb/sec-in}^2$ and the wall temperature is constant at 4611°R . The maximum shear stress for these conditions is higher than the graphite material can tolerate. If the results in Fig. 4-15 are compared with those in Fig. 4-13 one can see that both the maximum stress and the maximum solid temperature are higher for the constant wall temperature case even though the hydrogen stagnation temperature at the exit and the flow rate per unit area are less than they are for the case with a chopped sine power distribution. This occurs primarily because the shape of the power distribution required to obtain a constant wall temperature is such that a higher local power density exists even though the total power represented by the area under the curve is less than for the other case. The coolant channel

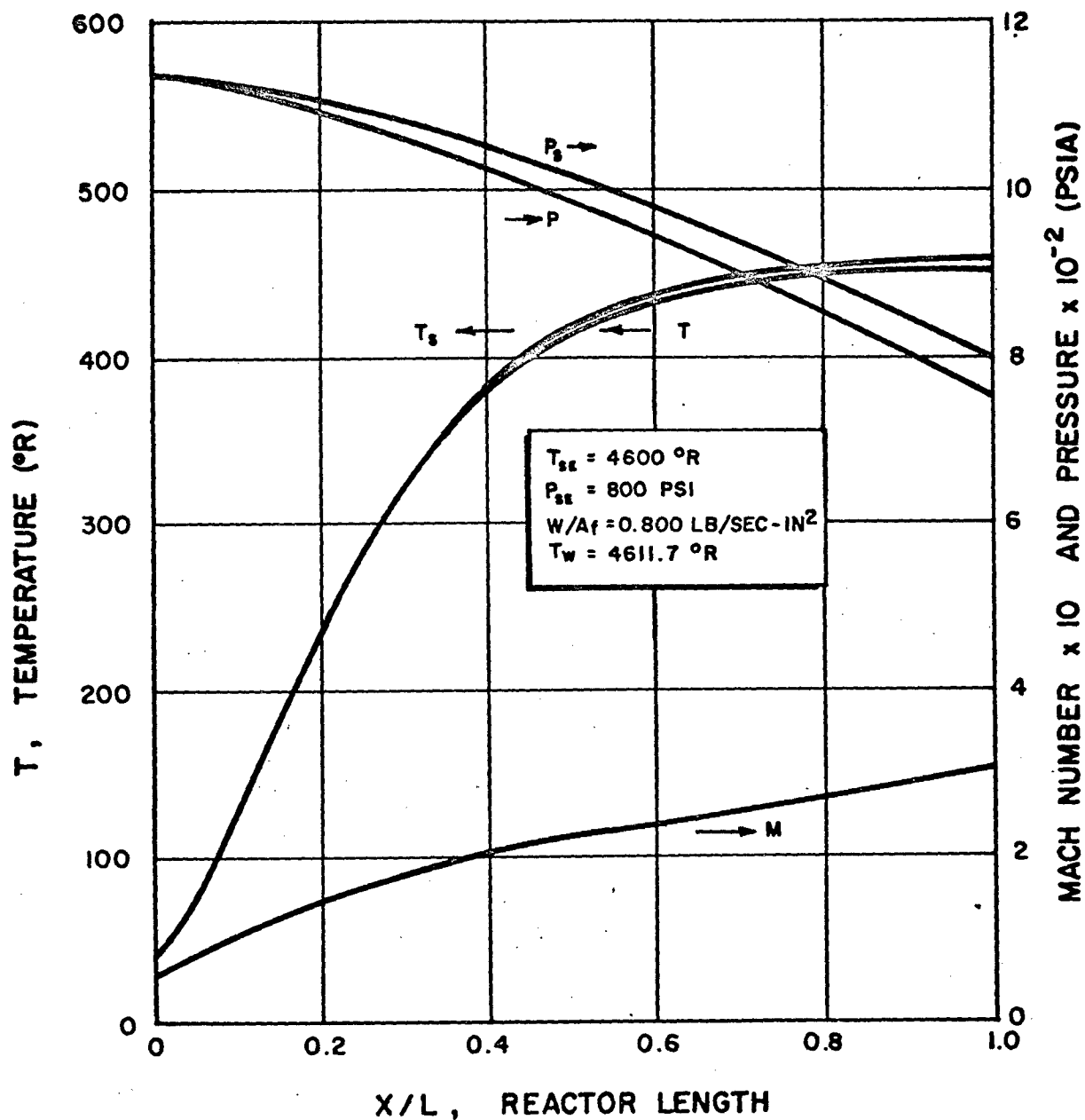


FIG. 4-14: HYDROGEN STAGNATION TEMPERATURE, STATIC TEMPERATURE, STAGNATION PRESSURE, STATIC PRESSURE, AND MACH NUMBER VS NON-DIMENSIONAL REACTOR LENGTH FOR CONSTANT WALL TEMPERATURE

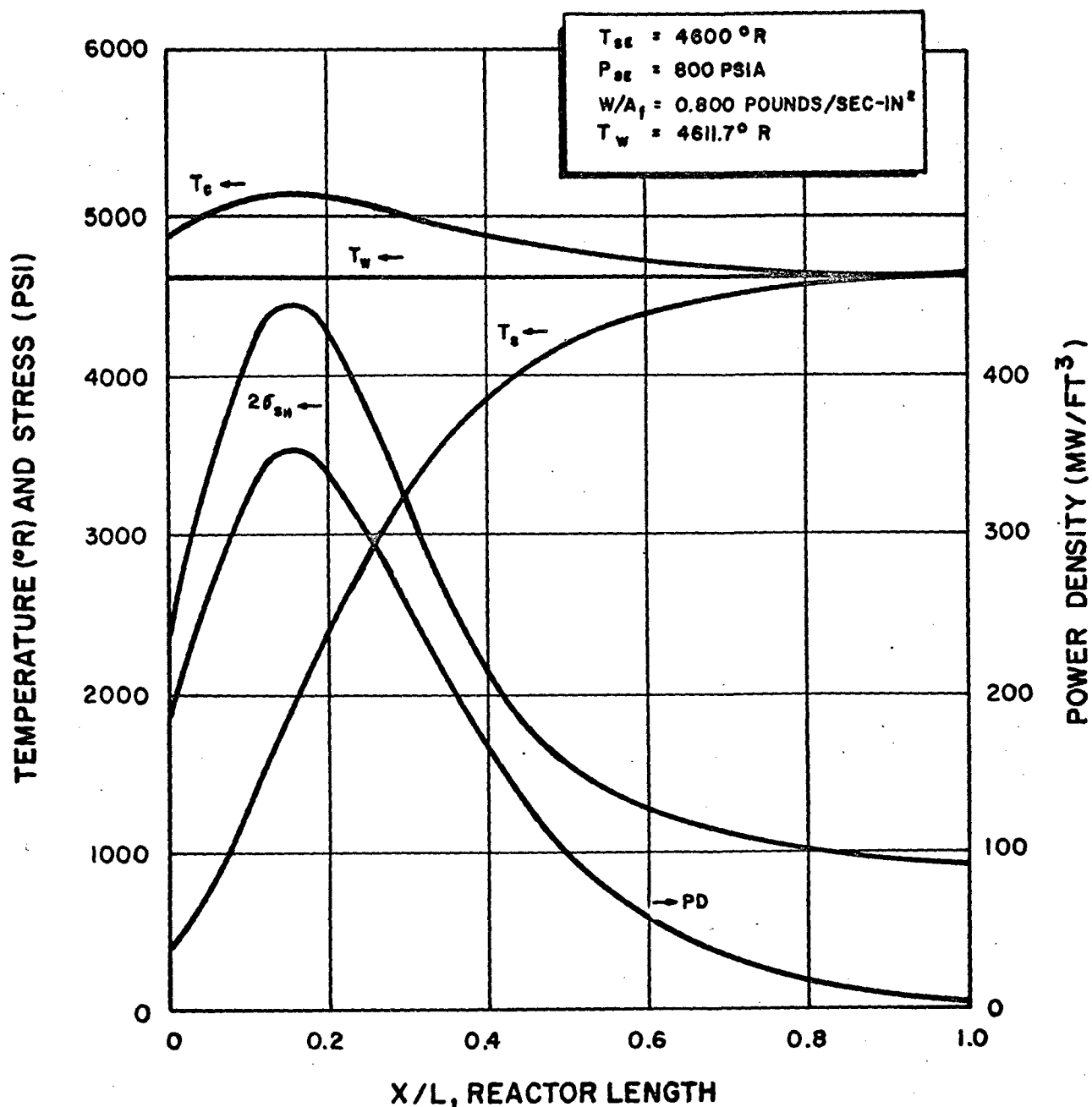


FIG. 4-15: HYDROGEN TEMPERATURE, COOLANT CHANNEL SURFACE TEMPERATURE, SOLID CENTERLINE TEMPERATURE, SHEAR STRESS AT COOLANT CHANNEL SURFACE, AND LOCAL POWER DENSITY IN REACTOR VS NON-DIMENSIONAL REACTOR LENGTH FOR CONSTANT WALL TEMPERATURE

diameter for the constant wall temperature case is 0.106 inches rather than 0.100 inches as for the chopped sine power distribution case but this has a relatively minor effect on the stress compared to the local power density effect mentioned above. These results show that the power distribution corresponding to a constant wall temperature is not as desirable as the chopped sine power distribution. This was found to be true for any of a large number of constant wall temperature cases that were run. It may be desirable to shape the power distribution in some other way so that a higher exit gas temperature of higher flow rate per unit area can be obtained without increasing the maximum temperatures or stresses in the core. This has not been done in this study but could be the subject of some further work.

D. Limiting Performance of Reactor

The procedure outlined in the last two sections of this chapter permits the determination of the coolant properties, reactor surface and maximum solid temperatures, power density, and maximum stress distributions along the axis of the core. The rate of local power generation in the core may be fixed by one of a number of possible factors. These include:

1. A surface temperature above which excessive chemical reaction between the coolant and the channel surface material may take place.

2. A temperature in the solid part of the core above which the reactor material does not have satisfactory mechanical strength.

3. Stresses in the core material that may cause fracture or excessive strains and dimensional changes. Graphite will react with hydrogen at high temperatures, but this deficiency can be overcome by coating the coolant channels (34,35). The mechanical strength of graphite increases with temperature up to values near 5000°R and then drops off rapidly (36). The actual values of the tensile strength for graphite have some variation because it is a brittle material and does not have a well defined yield point as ductile materials do. The maximum allowable stress for graphite that is used in this study is taken from a curve developed at Los Alamos for design purposes (36). The other graphite properties required for the stress calculations are taken from this same source. The limiting values used for the three factors mentioned above are:

1. Coolant channel surface temperature no greater than 4800°R.

2. Temperature in the solid fraction of the reactor core no greater than 5000°R.

3. Maximum shear stress no greater than 1200 psi.

With these limitations set on the core material and the

procedure developed to calculate the conditions in the reactor for a given set of independent parameters, it is possible to determine the upper bounds on reactor performance. For each run with a given set of variables it is possible to determine the distributions of wall temperature, maximum solid temperature, and stress as was shown in Fig. 4-13. If any one of the three limitations is exceeded at any point in the reactor the operating conditions are unsatisfactory and at least one of the independent parameters must be changed to obtain a workable system. The procedure used to determine the upper performance bounds is as follows.

1. A particular void fraction is chosen to set the reactor length and radius.
2. A particular coolant channel diameter is chosen.
3. The shape of the power distribution is fixed for the reactor.
4. The hydrogen stagnation pressure at the reactor exit is chosen.
5. The hydrogen stagnation temperature at the reactor exit is set at a specific value.
6. The flow rate per unit area through the reactor is varied in finite steps and the reactor characteristics determined for each different condition.

7. The hydrogen stagnation temperature is changed and step 6 is repeated.

When these results are obtained the maximum stress, wall temperature, and solid temperature are plotted versus the flow rate per unit area for given hydrogen temperatures. A typical plot for the maximum stress is shown in Fig. 4-16. Only the highest stress at the worst axial location is used to make this plot. Using Fig. 4-16 it is possible to determine the highest possible flow rate per unit area that can be passed through the reactor and still obtain a specific hydrogen stagnation temperature without exceeding a specified stress value. If at the points where the $2\sigma_{SH} = 2400$ psi the hydrogen stagnation temperature is plotted versus the corresponding flow per unit area, the solid line in Fig. 4-17 is obtained. The same procedure using plots of maximum wall temperature and maximum centerline temperature similar to Fig. 4-16 yields the other two curves in Fig. 4-17.

For the graphite material considered and the limitations imposed the maximum solid temperature is not an important limitation because either of the other two limitations is reached first. The limiting performance of the reactor occurs along the envelope defined by the wall temperature limitation and the stress limitation. The envelope in Fig. 4-17 is for one reactor size

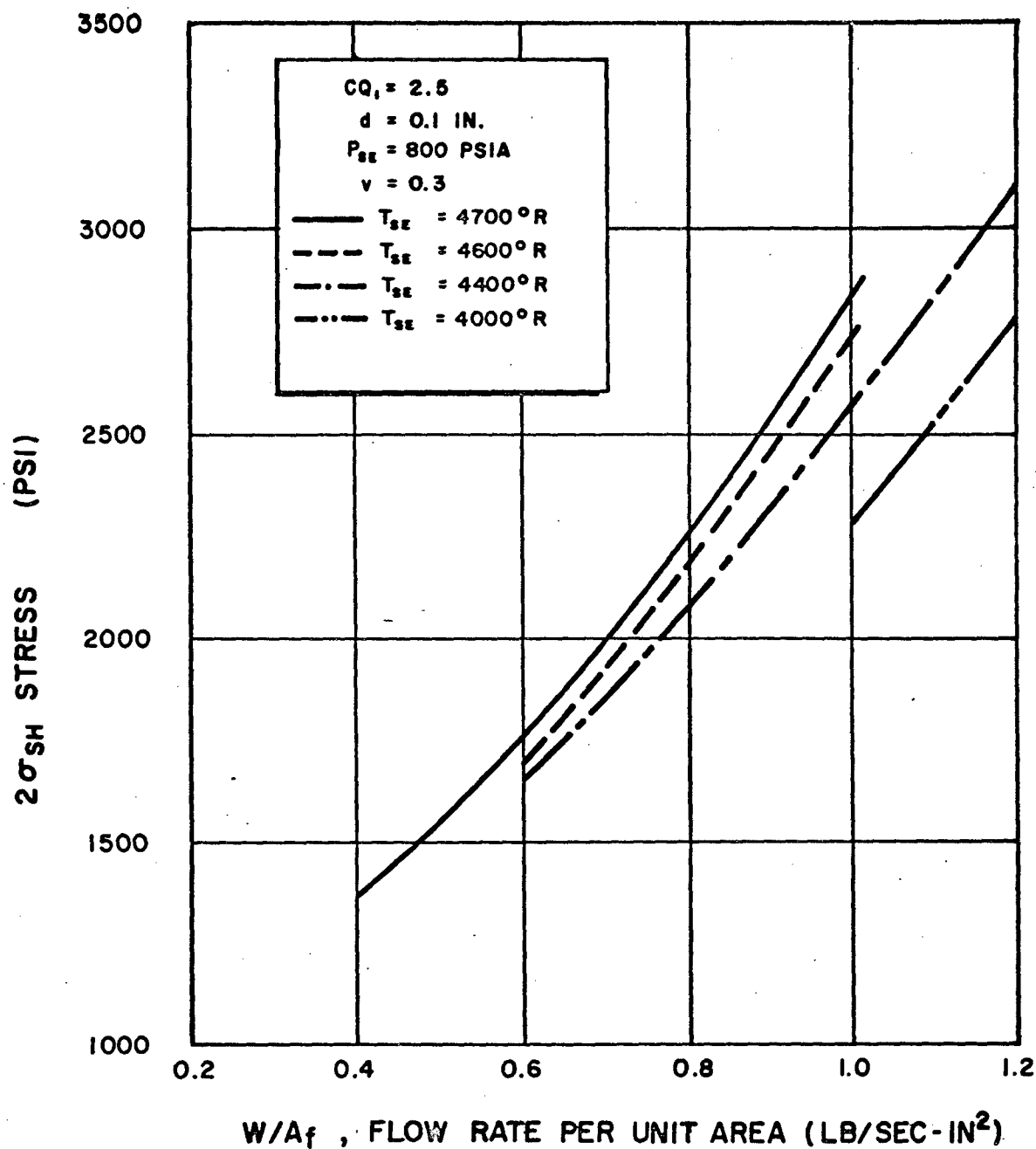


FIG. 4-16: MAXIMUM SHEAR STRESS VS HYDROGEN FLOW PER UNIT AREA IN REACTOR CORE WITH CHOPPED SINE POWER DISTRIBUTION

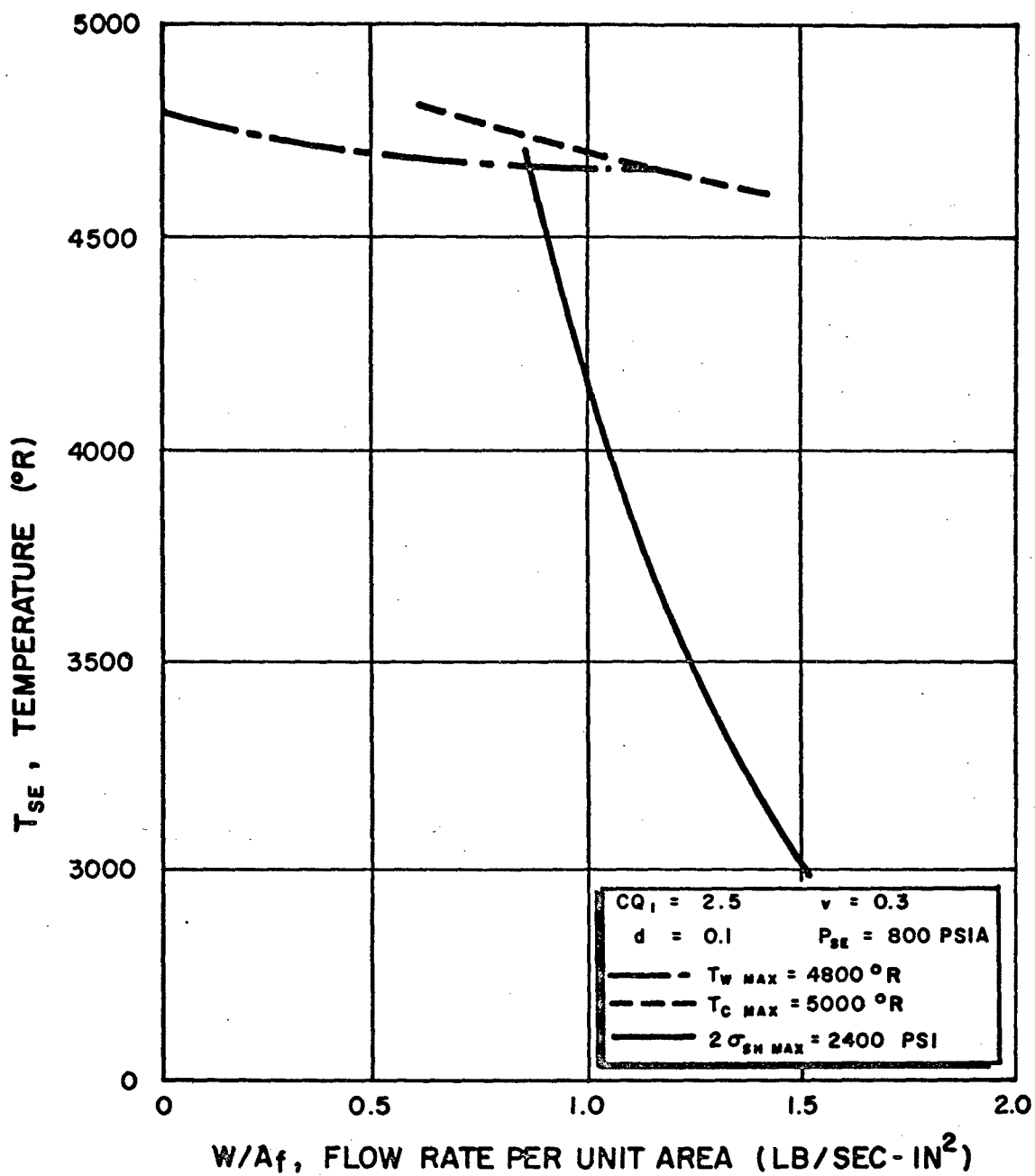


FIG.4-17: MAXIMUM HYDROGEN TEMPERATURE AT REACTOR EXIT VS FLOW PER UNIT AREA AS DETERMINED BY DIFFERENT MATERIAL LIMITATIONS

with one coolant channel size and one shape of the power distribution. The position of the envelope is insensitive to pressure in that its position does not change when the hydrogen pressure at the reactor exit is changed to either 600 or 1000 psia.

The effect of a variation in coolant channel diameter with other conditions held constant can be seen in Fig. 4-18. For an increase in coolant channel diameter from 0.100 inches to 0.125 inches the most significant change is in the location of the stress limiting curve. The flow rate per unit area must be reduced by 30% or more in order to obtain the same hydrogen stagnation temperature at the reactor exit. The effect of changing the reactor power distribution is also shown in Fig. 4-18. The change in the shape of the chopped sine profile when CQ_1 is changed from 2.5 to 2.75 was shown in Fig. 4-10. It can be seen that this change in the power profile has only a small effect on the position of the limiting performance envelope for the reactor. The small shift of the point of maximum power toward the exit of the reactor causes the stress limitation to occur at slightly lower flow rates.

The effect of a change in the reactor void fraction and consequently the reactor size is shown in Fig. 4-19. A reduction in the void fraction from 0.3 to 0.2 has approximately the same effect as increasing the coolant channel diameter from

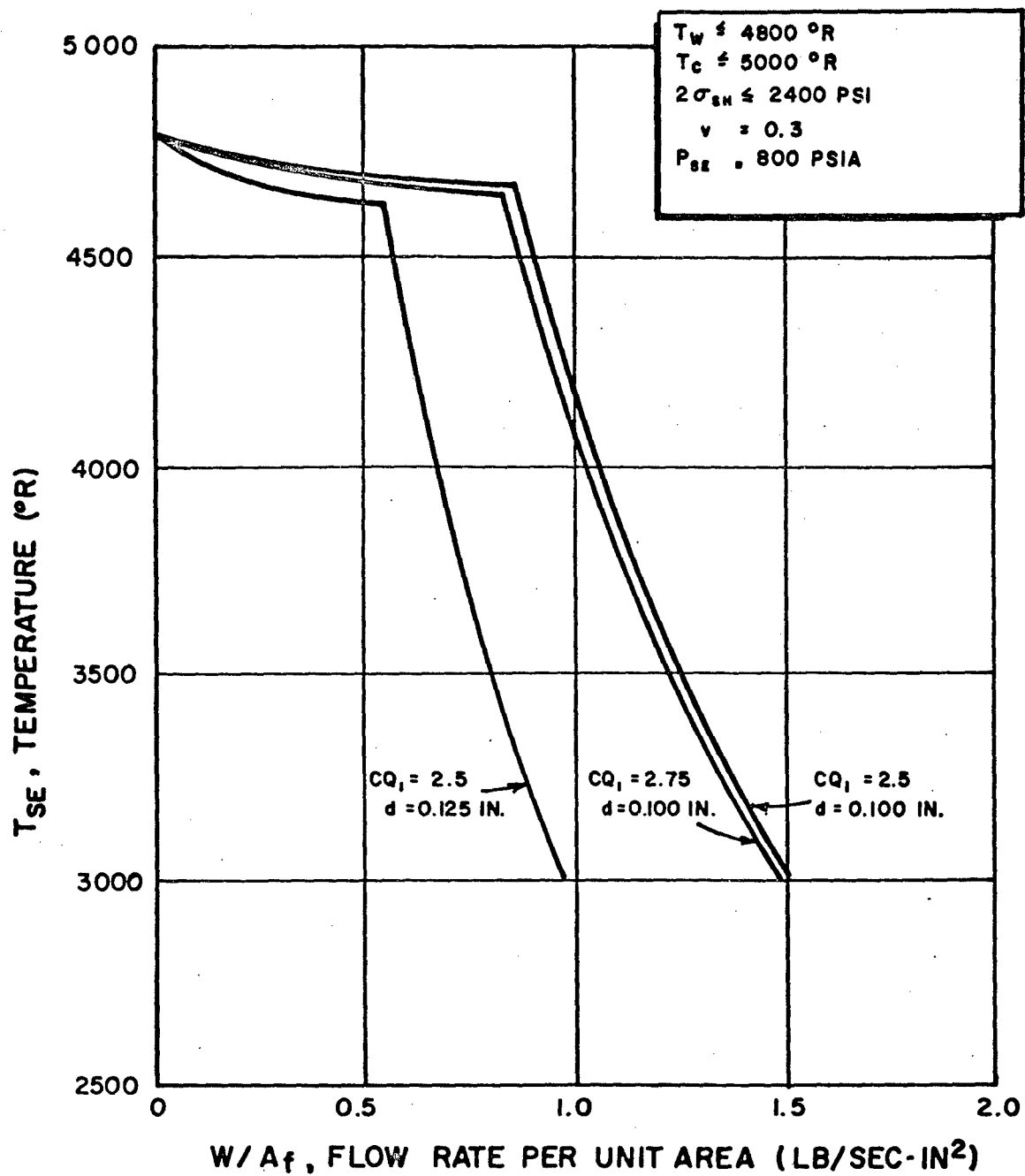


FIG. 4-18: MAXIMUM HYDROGEN TEMPERATURE AT REACTOR EXIT VS FLOW RATE PER UNIT AREA THROUGH CORE WITH CHOPPED SINE POWER DISTRIBUTION AS DETERMINED BY MATERIAL LIMITATIONS

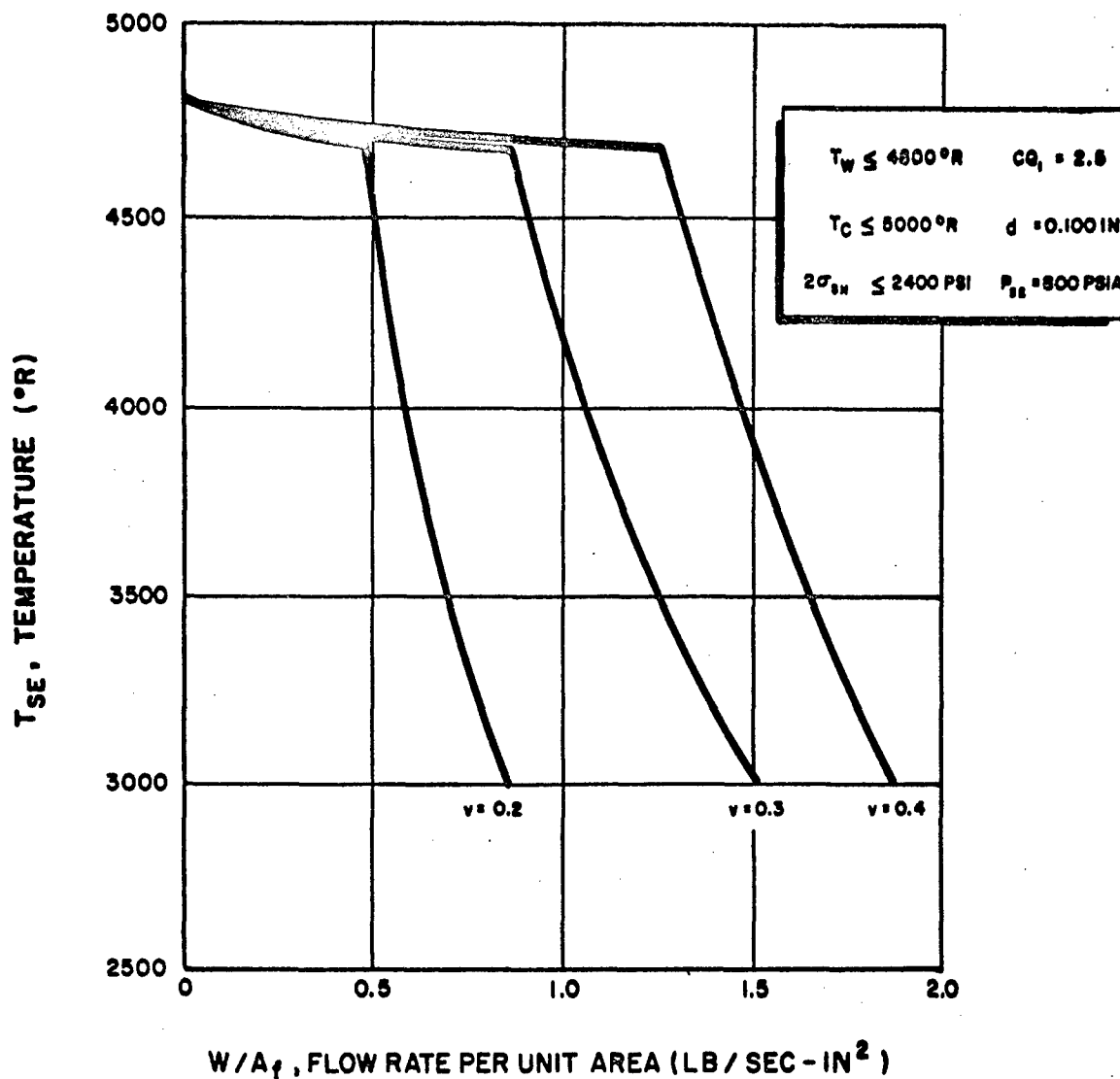


FIG. 4-19: MAXIMUM HYDROGEN TEMPERATURE AT REACTOR
 EXIT VS FLOW RATE PER UNIT AREA THROUGH CORE
 WITH CHOPPED SINE POWER DISTRIBUTION AS
 DETERMINED BY MATERIAL LIMITATIONS

0.100 to 0.125 while holding the void fraction constant at 0.3. Increasing the reactor void fraction to 0.4, which is probably near the upper limit from a structural point of view, increases the possible flow rate per unit area that can be passed through a reactor and consequently increases the maximum power level. As the reactor void fraction is increased the reactor radius and flow area increase as was shown in Figs. 4-1 and 4-4. Consequently if the hydrogen stagnation temperature was plotted versus the actual mass flow rate rather than the flow per unit area, the envelopes would be spread further apart exaggerating this effect. As a rough approximation the reactor power is the product of the mass flow rate, the hydrogen stagnation temperature at the exit and some average specific heat, if the inlet temperature is neglected with respect to the exit temperature. Consequently any increase in mass flow rate or flow per unit area for a given reactor at a given exit temperature causes a proportional increase in the power developed by the reactor.

CHAPTER V

SIMPLIFIED REACTOR ANALYSIS

A. Objective

The detailed machine calculations presented in the last section of Chapter IV show that over a certain range of flow rates the wall temperature is the limiting condition. At higher flow rates the stresses in the graphite restrict the range of possible operation. In order to obtain a limiting envelope of hydrogen exit temperature versus flow per unit area a large number of runs must be calculated and the results cross plotted to find the independent conditions where the limiting performance line is. It is then desirable to calculate a number of runs for conditions along this line to check the accuracy of the cross plotting procedures. Making calculations for the conditions on the envelope also eliminates the requirement of cross plotting other results of interest to determine their values.

It is desirable to obtain a simple approximate analytic method for predicting the conditions where the reactor is wall temperature or stress limited. This procedure can serve two purposes. For the initial calculations on a particular system the accuracy required on limiting performance calculations may be such that approximate analytic calculations will be sufficient. In the event that more accurate calculations are required the

approximate results can be used to define the region where further calculations are to be carried out. This can cut down the amount of work and machine calculations by a considerable amount. The amount of cross plotting required to determine the conditions of limiting performance can be reduced significantly and in some cases none will be necessary. The analysis developed here was used for this latter purpose in completing the results of the detailed machine calculations presented in the last chapter. More specifically the objective of the simplified analysis is to obtain two analytic expressions, one to relate the wall temperature to the independent variables (T_{SE} and w/A_f) and the second to relate the maximum stress to the same variables.

B. Wall Temperature Limitation

For a power distribution which is a chopped sine wave the local heat flux per unit length is given by Eq. 4-30 which is repeated here

$$\frac{dq}{dx} = A_1 \sin \left[CQ_1 \left(1 - \frac{x}{L} \right) \right] \quad (5-1)$$

By integrating over the coolant channel length and noting that

$$\int_0^L dq = wQ_T \quad (5-2)$$

where Q_T is the total enthalpy rise of the hydrogen, the constant A_1 can be evaluated. The resulting expression for the local heat

flux is

$$\frac{dq}{dx} = \frac{wQ_T}{L} \frac{CQ_1}{1 - \cos CQ_1} \sin \left[CQ_1 \left(1 - \frac{x}{L} \right) \right] \quad (5-3)$$

The local heat flux can also be expressed in terms of the wall temperature and a heat transfer coefficient.

$$\frac{dq}{dx} = h \frac{dA_s}{dx} (T_W - T) = h\pi d (T_W - T) \quad (5-4)$$

Eqs. 5-3 and 5-4 could be combined to obtain an expression for the wall temperature if the local fluid temperature T was known. This temperature can be evaluated approximately by ignoring the dependence of the enthalpy on pressure and assuming an average specific heat for the fluid. Then

$$Q_T = \bar{c}_p (T_{SE} - T_{SRI}) \quad (5-5)$$

and

$$\frac{dq}{dx} = w \bar{c}_p \frac{dT}{dx} \quad (5-6)$$

Combining this with Eq. 5-3 and integrating results in the following expression:

$$T = T_{SRI} + \frac{T_{SE} - T_{SRI}}{1 - \cos CQ_1} \left\{ \cos \left[CQ_1 \left(1 - \frac{x}{L} \right) \right] - \cos CQ_1 \right\} \quad (5-7)$$

Eqs. 5-3, 5-4, and 5-7 can now be combined to produce the following expression for the wall temperature.

$$T_W = T_{SRI} = \frac{T_{SE} - T_{SRI}}{1 - \cos CQ_1} \left\{ \cos \left[CQ_1 \left(1 - \frac{x}{L} \right) \right] - \cos CQ_1 + \frac{CQ_1}{St} \frac{d}{4L} \sin \left[CQ_1 \left(1 - \frac{x}{L} \right) \right] \right\} \quad (5-8)$$

The Stanton number

$$St = \frac{h}{\rho V c_p} \quad (5-9)$$

is an average value incorporating an averaged heat transfer coefficient.

If Eq. 5-8 is differentiated with respect to x and the differential set equal to zero, the following relation is obtained for the position where the wall temperature is a maximum.

$$CQ_1 \left(1 - \frac{x_M}{L} \right) = \tan^{-1} \left(\frac{CQ_1}{St} \frac{d}{4L} \right) \quad (5-10)$$

When this is inserted back into Eq. 5-8 and the inverse tangent is related to the corresponding inverse sine and cosine functions, an equation relating the maximum wall temperature to the exit coolant temperature and the average Stanton number results. After some simplification it can be reduced to the following expression:

$$\frac{T_{WM} - T_{SRI}}{T_{SE} - T_{SRI}} = \frac{\sqrt{1 + \frac{CQ_1^2}{St} \frac{d}{4L}} - \cos CQ_1}{1 - \cos CQ_1} \quad (5-11)$$

If the Reynolds analogy is used to relate the Stanton number to the friction factor and Eq. 4-1 is employed to relate the friction factor to the flow per unit area, the desired relation between the maximum wall temperature, the hydrogen exit temperature, and the flow per unit area is obtained.

$$\frac{T_{SE} - T_{SRI}}{T_{WM} - T_{SRI}} = \frac{1 - \cos CQ_1}{\sqrt{1 + \left[\frac{CQ_1 \left(\frac{w}{A} \frac{d}{\mu} \right)^{0.2}}{2(0.046)L/d} \right]^2} - \cos CQ_1} \quad (5-12)$$

For a particular reactor and a given shape of the power distribution numerical values can be inserted for L , d , and CQ_1 . A representative value can be used for the viscosity of the hydrogen coolant. For the results shown in this chapter a value of 375 micropoise corresponding to a hydrogen temperature of $4500^\circ R$ was used. The hydrogen temperature at the reactor inlet is fixed at $400^\circ R$.

The results of the calculations for three different void fractions are shown by the dashed lines in Fig. 5-1. As with the more detailed calculations shown by the solid lines, only the parts of the curves which are nearly horizontal are for the

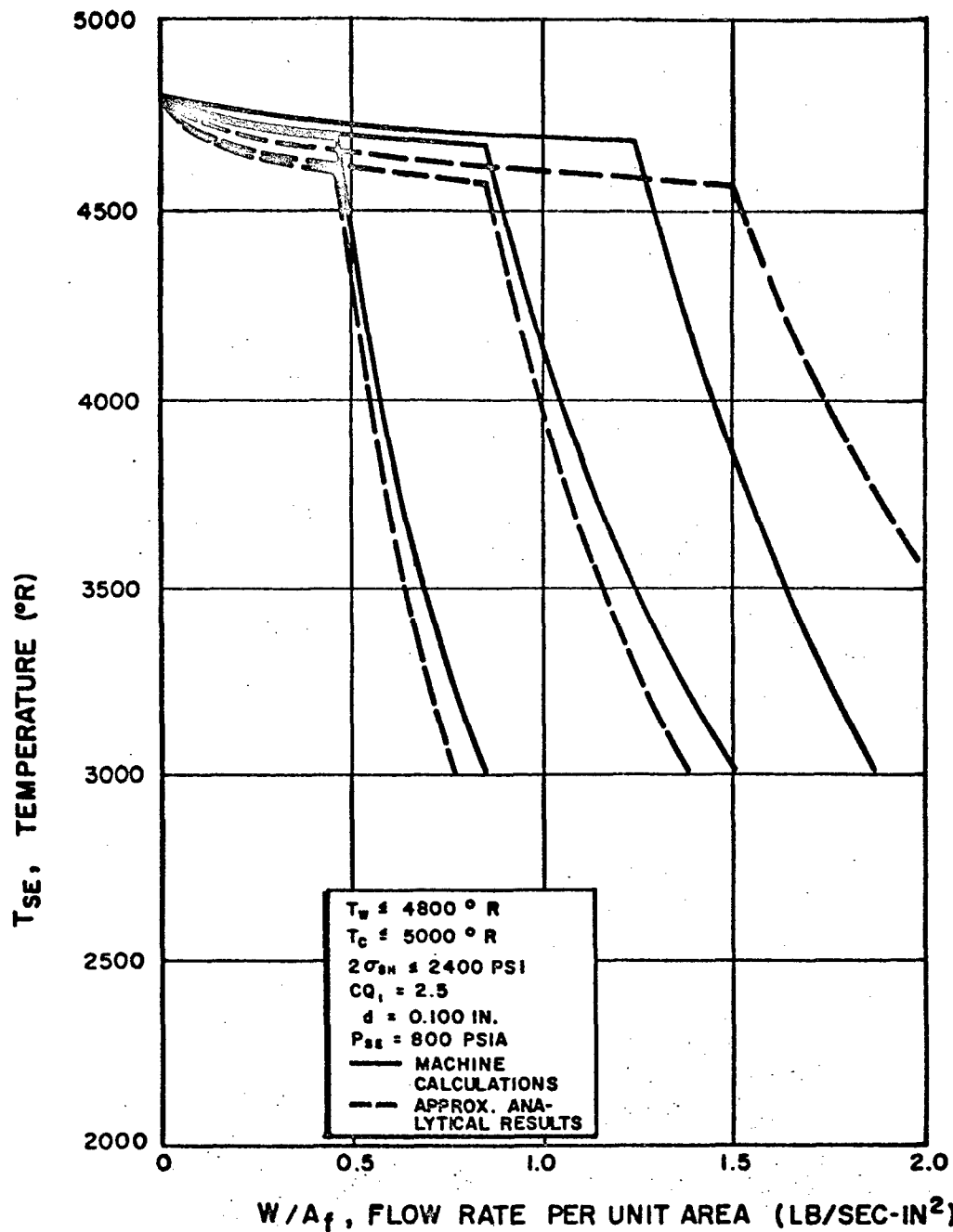


FIG. 5-1: MAXIMUM HYDROGEN TEMPERATURE AT REACTOR EXIT VS FLOW RATE PER UNIT AREA THROUGH CORE WITH CHOPPED SINE POWER DISTRIBUTION AS DETERMINED BY MATERIAL LIMITATIONS

wall temperature limitation. The second part of the curve after the discontinuity in slope defines the stress limited region. The analysis for this is shown in the next section of this chapter. The simplified analysis for the wall temperature limitation predicts the hydrogen exit temperature at a given flow rate per unit area within 100°R of the more accurate machine calculations. It is on the conservative side in that it predicts lower values of T_{SE} at a given flow per unit area than it should. If one does these simple calculations before doing detailed machine calculations, the range of hydrogen exit temperatures can be limited to the region between these answers and the maximum allowable wall temperature. In this way the number of calculations required to obtain the detailed solution can be reduced significantly.

C. Stress Limitation

For the annular stress model and the boundary conditions used in the detailed calculations the three principal stresses at the inner radius are given by Eqs. 4-46, 4-47, and 4-48. These can be rewritten using the local power density as follows.

$$\sigma_r = -p \quad (5-13)$$

$$\sigma_{\theta} = -p + \frac{PD\alpha E r_i^2}{4(1-\nu)k} \frac{(1-\nu)}{2\nu^2} \quad (5-14)$$

$$\sigma_z = \frac{PD\alpha E r_i^2}{4(1-\nu)k} \frac{1}{\nu(1-\nu)} \left[\frac{2}{(1-\nu)} (-\ln\sqrt{\nu}) - \frac{3-\nu}{2} \right] \quad (5-15)$$

The maximum shear stress is determined from the difference of the maximum and minimum principal stresses. The minimum principal stress at the inner radius is always the radial stress which is compressive. The maximum stress can be either the tangential or the axial stress.

First consider the case where the maximum principal stress is σ_θ .

Then

$$2\sigma_{SH_{max}} = \frac{\alpha E r_i^2}{4(1-\nu)k} \frac{1-\nu}{2\nu^2} PD \quad (5-16)$$

and it is independent of the fluid pressure. To find the maximum stress in the element the maximum local power density must be obtained.

From the expression for the local heat flux dq/dx given by Eq. 5-3, it can be determined that the maximum heat flux occurs at

$$\frac{x}{L} = 1 - \frac{\pi}{2CQ_1} \quad (5-17)$$

and its value is

$$\left(\frac{dq}{dx}\right)_{\max} = \frac{wQ_T}{L} \frac{CQ_1}{1 - \cos CQ_1} \quad (5-18)$$

The ratio of the maximum power density to the average is also the ratio of the maximum to average heat flux which is

$$\frac{\left(\frac{dq}{dx}\right)_{\max}}{\left(\frac{dq}{dx}\right)_{\text{avg}}} = \frac{CQ_1}{1 - \cos CQ_1} = \frac{PD_{\max}}{PD_{\text{avg}}} \quad (5-19)$$

The average power density is

$$PD_{\text{avg}} = \frac{wQ_T}{A_T L} = \frac{wQ_T}{A_f L} v \quad (5-20)$$

and

$$PD_{\max} = \frac{w}{A_f} Q_T \frac{v}{L} \frac{CQ_1}{1 - \cos CQ_1} \quad (5-21)$$

Using the approximate expression for Q_T given by Eq. 5-5 and inserting Eq. 5-21 into 5-16 an expression relating the maximum shear stress, the hydrogen temperature at the reactor exit, and the flow rate per unit area is obtained.

$$2\sigma_{SH_{\max}} = \frac{\alpha E r_i^2}{8(1-v)k} \frac{(1-v)}{vL} \frac{CQ_1}{1 - \cos CQ_1} \frac{w}{A_f} \bar{c}_p (T_{SE} - T_{SRI}) \quad (5-22)$$

Solving for T_{SE}

$$T_{SE} = T_{SRI} + 2\sigma_{SH_{max}} \frac{32(1-\nu)k}{E} \frac{\nu L}{(1-\nu)dZ} \frac{1 - \cos CQ_1}{CQ_1} \frac{1}{\bar{c}_p} \frac{1}{w/A_f} \quad (5-23)$$

By inserting the known variables and a limiting stress in this equation, one obtains limiting values of T_{SE} for given values of w/A_f .

If the axial stress is greater than the tangential stress the maximum shear stress is determined from the difference between σ_z and σ_r .

$$2\sigma_{SH_{max}} = \frac{\alpha E r_i^2}{4(1-\nu)k} \frac{1}{\nu(1-\nu)} \left[\frac{-2 \ln \sqrt{\nu}}{1-\nu} - \frac{3-\nu}{2} \right] PD + P \quad (5-24)$$

This expression is not independent of the fluid pressure and the maximum value of the stress does not necessarily occur where the power density is a maximum. However, to obtain a conservative estimate the maximum power can be used. The resulting expression is of the form

$$2\sigma_{SH_{max}} = B_Z \frac{w}{A_f} \bar{c}_p (T_{SE} - T_{SRI}) + P \quad (5-25)$$

where

$$B_Z = \frac{\alpha E r_i^2}{4(1-\nu)k} \frac{CQ_1}{1 - \cos CQ_1} \frac{1}{Lv} \left[\frac{-2 \ln \sqrt{\nu}}{1-\nu} - \frac{3-\nu}{2} \right] \quad (5-26)$$

For the case when $\sigma_\theta > \sigma_z$ the equation for the maximum stress can be put in a similar form

$$2\sigma_{SH_{max}} = B_\theta \frac{w}{\theta A_f} \bar{c}_p (T_{SE} - T_{SRI}) \quad (5-27)$$

where

$$B_\theta = \frac{\alpha E r_i^2}{4(1-\nu)k} \frac{CQ_1}{1 - \cos CQ_1} \left(\frac{1-\nu}{2L\nu} \right) \quad (5-28)$$

Numerical calculations show that B_θ is always greater than B_z for void fractions between 0.2 and 0.4. Consequently, as long as the fluid pressure in the reactor is such that

$$p < 2\sigma_{SH_{max}} \left(1 - \frac{B_z}{B_\theta} \right) \quad (5-29)$$

The maximum shear stress is determined from σ_θ and σ_r and is independent of the pressure. For example, with a void fraction of 0.4, $T_{SE} = 4600^\circ R$ and $2\sigma_{SH_{max}} = 2400$ psi this limiting pressure is approximately 1200 psia.

The maximum hydrogen temperature that can be achieved in a given reactor with a given flow rate when it is stress limited is then given by Eq. 5-23. This same equation could be rearranged to determine the maximum allowable flow rate if the hydrogen temperature is the specified quantity. If the fluid pressure at any point in the reactor does not satisfy Eq. 5-29

a lower exit temperature or a lower flow rate must be used and the maximum performance will not be achieved.

The stress limited portions of the dashed curves shown in Fig. 5-1 were calculated using Eq. 5-23. For void fractions of 0.2 and 0.3 the agreement with the detailed calculations is quite good. At a given value of T_{SE} the maximum flow rate per unit area is predicted within 7% for all temperatures down to 3000°R. The curve for a void fraction of 0.4 does not agree with the detailed calculations because Eq. 5-29 is not satisfied when the hydrogen pressure at the reactor exit is 800 psia. The detailed calculations show that the pressure near the inlet end of the reactor is near 1500 psia for the specified conditions. The results also show that the maximum principal stress is in the axial and not in the tangential direction. This is expected because Eq. 5-29 is not satisfied. If the pressures in the reactor could be reduced sufficiently by changing the value of p_{SE} the solid curve in Fig. 5-1 would be shifted to the right of the dashed curve.

There is a lower limit on the value of the exit pressure that can be obtained for a given flow rate per unit area and exit temperature. This limit is reached when the Mach number at the exit of the reactor is 1. An approximate value for this lower limit can be obtained by using relationships which are valid for the one-dimensional flow of a perfect gas. When

the Mach number is unity (24):

$$\frac{w}{A_f} \frac{\sqrt{T_{SE}}}{P_{SE}} = \sqrt{\frac{\gamma w}{R} \left(\frac{2}{\gamma + 1} \right)^{\frac{\gamma+1}{\gamma-1}}} \quad (5-30)$$

If a value of 1.32 is inserted for γ , being representative for hydrogen at high temperatures, and the right hand side of the equation evaluated, the following relation is obtained:

$$\frac{w}{A_f} \frac{\sqrt{T_{SE}}}{P_{SE}} = 0.137 \quad (5-31)$$

where w/A_f is in lb/sec - in², T_{SE} is in °R, and P_{SE} is in psia. If the flow per unit area and the temperature are fixed, Eq. 5-31 can be solved for the pressure. The value of pressure would be the minimum possible exit pressure as a lower value would imply that the flow was supersonic and that is impossible in a constant area channel. For an exit temperature of 4680°R and a flow rate per unit area of 1.5 lb/sec - in², this minimum exit pressure is approximately 740 psia. This value is not sufficient to reduce the maximum pressure in the reactor to a value of 1200 psia which would satisfy Eq. 5-29. Consequently the maximum performance for the reactor with a void fraction of 0.4 is less than that predicted by Eq. 5-23. To get a closer approximation to the limiting value of flow per unit area in this case Eq. 5-25 would have to be used. This would involve

obtaining a value for the maximum pressure in the reactor. This can only be done by calculating the pressure drop in the coolant channel. To do this the detailed machine calculations must be carried out or an additional approximate analysis must be developed.

The effect of changes in the coolant channel diameter and changes in the chopped sine power profile on the stress limiting curve can be seen by examining Eq. 5-23. The flow rate per unit area and the temperature rise across the reactor are inversely proportional to the square of the coolant channel diameter. This explains the relatively large shift of the curve in Fig. 4-18 for a change in diameter from 0.100 inches to 0.125 inches. The approximate curve for a diameter of 0.125 inches, which is not shown, has a deviation of 8% or less from the accurate results for all temperatures down to 3000°R. The deviation for all runs that are not pressure limited is within this same range.

CHAPTER VI

POWERPLANT PERFORMANCE

A. Calculation of Component Characteristics

The powerplant was defined to consist of four components; the reactor including the reflector, the pressure shell, the turbopump, and the nozzle. The performance characteristics of the reactor have been covered in detail in the last two chapters. The sizes and weights of the other components can now be determined and combined to get the characteristics of the whole powerplant.

The reactor size is determined from the void fraction as shown in Chapter IV. The weight of the reactor core is then

$$W_C = \rho_C \pi R^2 L (1 - v) \quad (6-1)$$

where the density of the core material ρ_C is 1.659 gm/cm³. The weight of the end reflector is

$$W_E = \rho_E \pi R^2 t_E (1 - v_E) \quad (6-2)$$

The radial reflector weight is

$$W_R = \rho_R \pi \left[(R + t_R)^2 - R^2 \right] (L + t_E) (1 - v_R) \quad (6-3)$$

The density of both the radial and end reflectors is that for beryllium, 1.85 gm/cm^3 . The weight of the reflected reactor is just the sum of the above three weights.

The pressure shell which contains the reactor and reflector consists of a cylindrical portion and a hemispherical end. It must withstand the maximum pressure in it which is the hydrogen pressure at the reactor inlet. The wall thickness is based on the hoop stress so that

$$t_w = \frac{P_{SRI} D_R}{2\sigma_{PS}} \quad (6-4)$$

where D_R is the diameter of the pressure shell. The weight of the pressure shell is then

$$W_{PS} = \frac{\rho_{PS} \pi D_R^2 L P_{SRI}}{2\sigma_{PS}} \left(1 - \frac{D_R}{4L} \right) \quad (6-5)$$

A material with an allowable stress of 60,000 psi and a density of 484 lb/ft^3 was assumed for the pressure shell.

The turbopump system is a bleed system where a small fraction of the hot hydrogen is removed from the main flow to drive the turbine. The power required for the pump is

$$HP_P = \frac{w(p_{TP} - p_T)}{\eta_P \rho_L} \quad (6-6)$$

where $p_{TP} = 1.33 p_{SRI}$ is the pump discharge pressure, η_P is the pump efficiency, and ρ_L is the density of the liquid hydrogen. The pump discharge pressure is greater than the reactor inlet pressure to take care of pressure losses in the nozzle, reflector,

and piping. The amount of work done per pound of hydrogen in the turbine is fixed at 1775 Btu/lb. This corresponds to a turbine inlet temperature of approximately 1860°R and a pressure ratio of 3.1 across the turbine. The bleed rate is the fraction of the propellant flow which must be removed to run the turbine

$$y_W = \frac{HP_P}{w \eta_T \Delta H_{TP}} \quad (6-7)$$

The efficiency of the pump and turbine are both 0.707 so that the overall efficiency of the turbopump system is 0.5. The weight of the turbopump is assumed to be proportional to the flow rate through the pump and the pump discharge pressure (42, 43). The equation for the turbopump weight (44) is

$$W_{TP} = 0.00251 P_{TP} w \quad (6-8)$$

where P_{TP} is in psia and w is in lb/sec.

The regeneratively cooled nozzle is assumed to have a ratio of exit area to throat area of 50. The half-angle is 30° for the convergent section and 15° for the divergent section. The nozzle wall is assumed to consist of longitudinal tubes for regenerative cooling surrounded by an outer shell to sustain the hoop stress. The nozzle weight is based on equations in references 43 and 44. The weight of the convergent section is

$$W_{NC} = \frac{1.5 \pi \rho_{NR}^D P_{SE}}{8 \sigma_N \sin 30^\circ} (D_R^2 - D_T^2) \quad (6-9)$$

where ρ_N and σ_N are the density and strength of the nozzle material, 484 lb/ft³ and 60,000 psi respectively, and D_T is the diameter of the nozzle throat. The diameter of the nozzle throat is obtained by considering an isentropic expansion of the hydrogen from the conditions at the exit of the reactor to a Mach number of unity. This process which is shown in detail in Appendix D yields the throat area A_T from which the diameter is easily obtained. The weight of the divergent section is

$$W_{ND} = C_1 D_T^2 P_{SE}^{1/3} \left[\frac{A_E}{A_T} - 1 \right] + C_2 P_{SE} D_T^3 \left[\left(\frac{A_E}{A_T} \right)^{1/6} - 1 \right] + C_3 P_{SE} D_T^3 \quad (6-10)$$

where $C_1 = 0.147$, $C_2 = 0.000268$, $C_3 = 0.0000117$, and A_E is the exit area of the nozzle. The pressure must be in pounds per square foot absolute and the throat diameter in feet for Eq. 6-10. The lengths of the convergent and divergent sections and the design exit pressure for the nozzle are also calculated using equations presented in Appendix D. The total nozzle weight is just the sum of the two weights determined from Eqs. 6-9 and 6-10.

B. Powerplant Characteristics

The total weight of the powerplant system is just the sum of the component weights developed in the previous section.

$$W_{\text{SYS}} = W_{\text{ET}} + W_{\text{PS}} + W_{\text{TP}} + W_{\text{N}} \quad (6-11)$$

where W_{ET} is the total weight of the end reflected reactor and W_{N} is the total weight of the nozzle. Fig. 6-1 shows how the weights of the components and the powerplant vary for a particular system with a fixed reactor size. The weights at any given flow per unit area are calculated for the conditions defined by the limiting performance envelope shown in Fig. 4-17.

The net power developed by the powerplant is the power transferred to the hydrogen in the reactor minus the power required by the turbopump. This net power is

$$P_{\text{sys}} = w Q_{\text{T}} (1 - y_{\text{W}}) \quad (6-12)$$

This power and the power per unit weight of the system are shown in Fig. 6-2 for the same conditions as curves in Figs. 4-17 and 6-1. The discontinuities in the slopes of the curves occur where the limitation on the reactor performance changes from wall temperature to stress. The reactor power increases almost linearly with flow rate when the reactor is wall temperature limited because there is only a small decrease in the exit gas temperature. When the reactor is stress limited, the power remains approximately constant independent of the flow rate. This occurs because any increase in flow rate is accom-

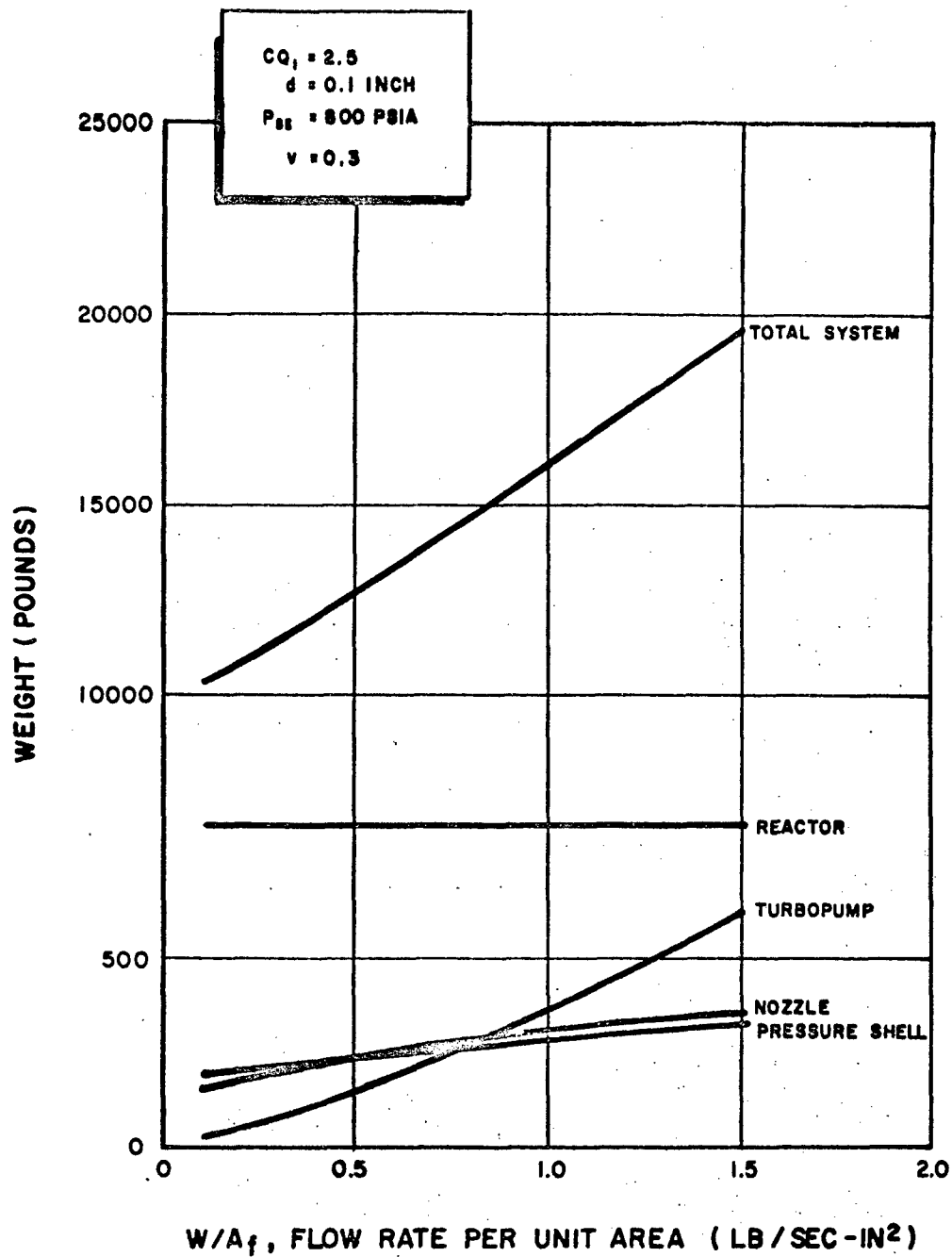


FIG. 6-1: POWER PLANT COMPONENT WEIGHTS AND POWER PLANT SYSTEM WEIGHT VS HYDROGEN FLOW PER UNIT AREA IN REACTOR FOR SYSTEMS ON LIMITING PERFORMANCE ENVELOPE SHOWN IN FIG. 4-17

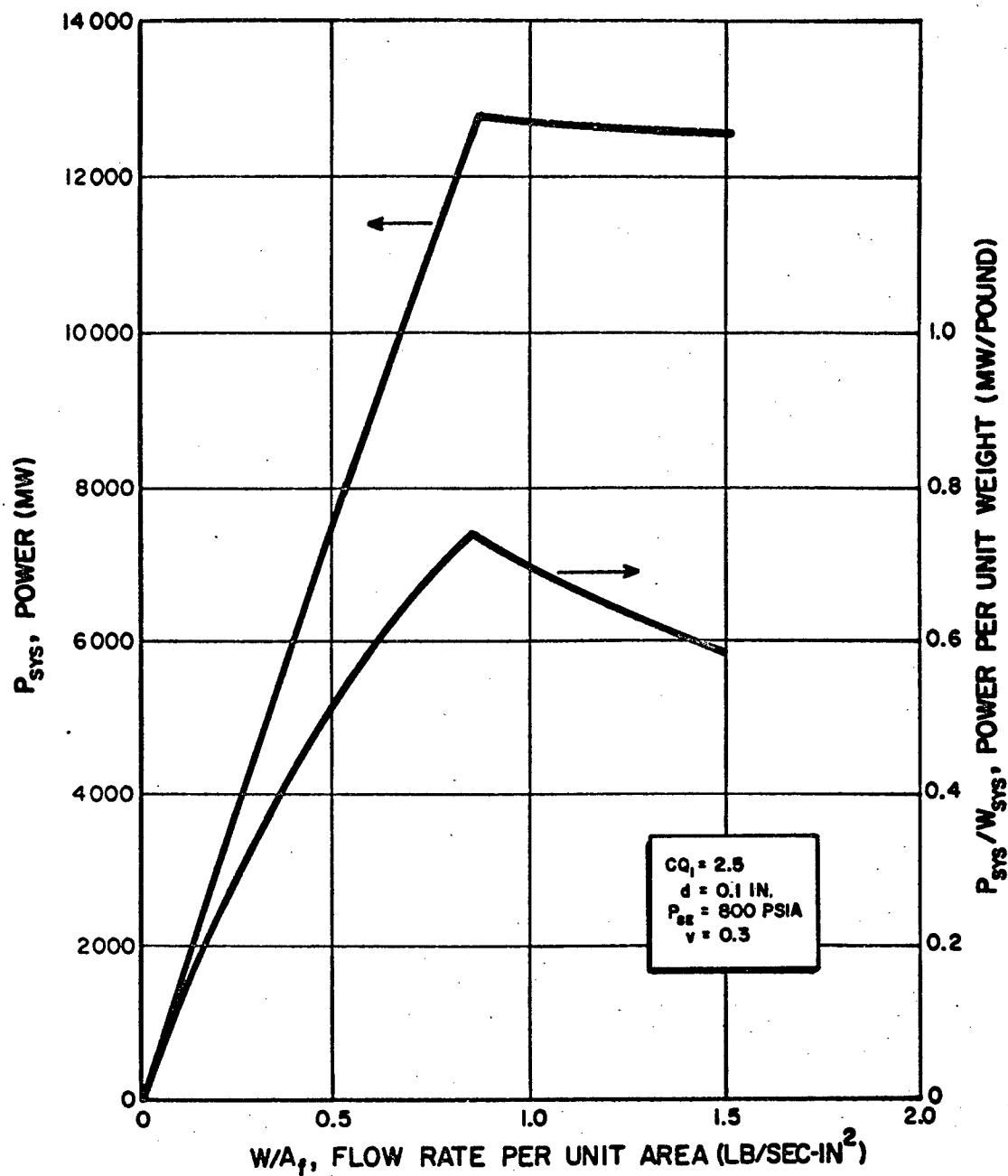


FIG. 6-2: MAXIMUM POWER DEVELOPED AND RATIO OF MAXIMUM POWER TO POWER PLANT SYSTEM WEIGHT VS HYDROGEN FLOW PER UNIT AREA IN REACTOR FOR SYSTEMS ON LIMITING PERFORMANCE ENVELOPE

anied by a corresponding decrease in the exit gas temperature. From Eq. 5-16 it can be seen that the maximum power density in the reactor is fixed once the reactor is stress limited. For a given reactor the shape of the power distribution is a constant. Consequently the total power is fixed at a specific value along with the maximum power density. The slight decrease in net power accompanying an increase in flow rate in Fig. 6-2 is due to the larger amount of power that is required to run the turbopump. The actual power developed by the reactor does remain constant for this sytem when it is stress limited.

The net power per unit weight of the power-plant decreases once the reactor is stress limited because the system weight continues to increase even though the power does not. There are no discontinuities in the slopes of the curves for the component weights as can be seen in Fig. 6-1.

The effect of changes in void fraction and consequently reactor size on the power per unit weight can be seen in Fig. 6-3. All three curves are for the conditions determined by the limiting performance curves shown in Fig. 4-19. The maximum possible power per unit weight increases as the reactor void fraction and size increase. It appears at first that it would always be advantageous to use a reactor with the maximum void fraction. However, the reactor with a void fraction of 0.2 has a flow area of 2.72 ft^2 while the reactor with a void fraction

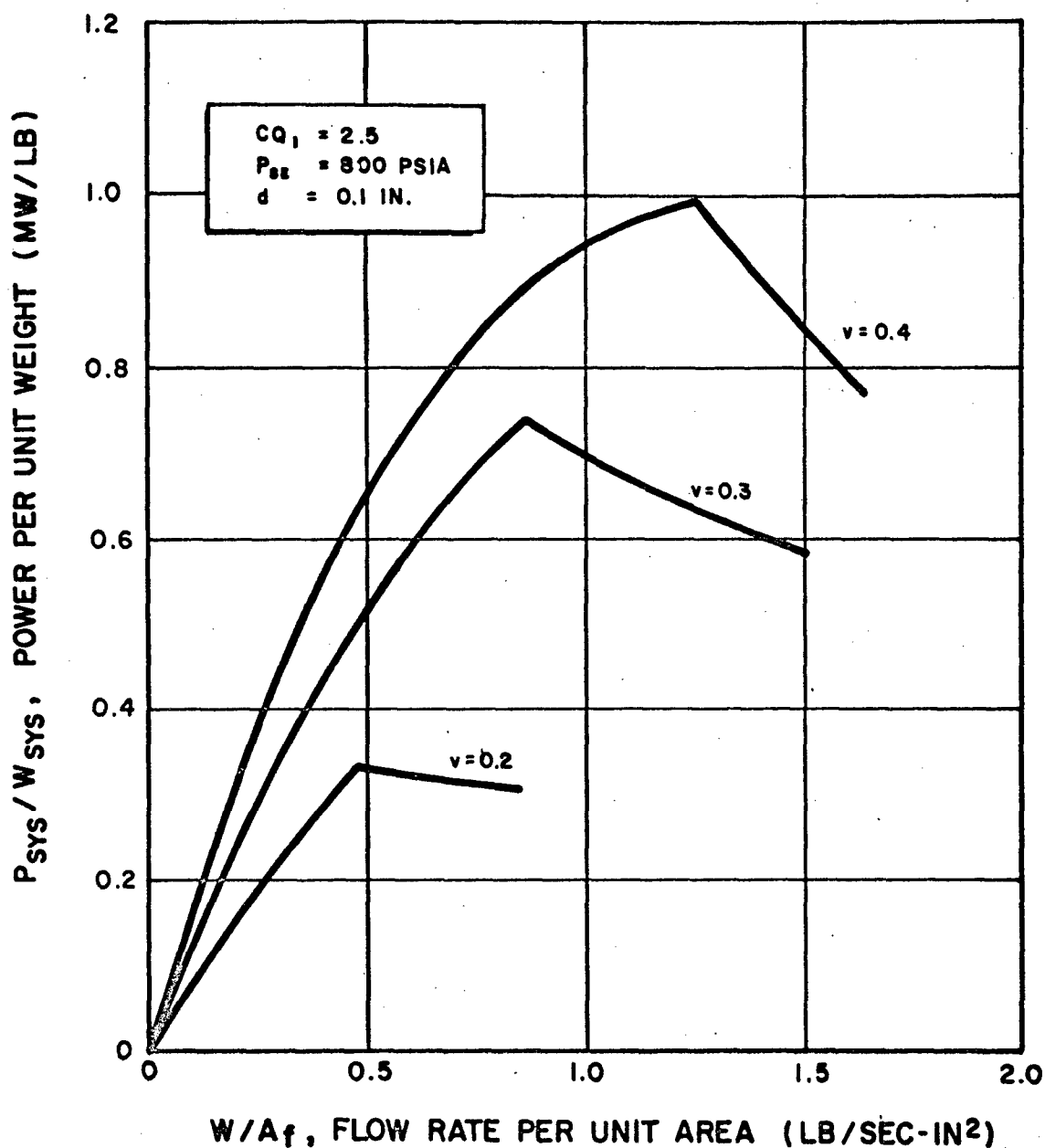


FIG.6-3: RATIO OF MAXIMUM POSSIBLE POWER DEVELOPED
 TO POWER PLANT SYSTEM WEIGHT VS HYDROGEN
 FLOW PER UNIT AREA IN REACTOR FOR SYSTEMS
 ON LIMITING PERFORMANCE ENVELOPES

of 0.4 has a flow area of 12.87 ft². Consequently, if the ratio of power to weight is plotted versus the hydrogen flow rate rather than the flow per unit area the relative position of the curves is changed. This is shown in Fig. 6-4. For a particular mass flow rate of hydrogen the maximum power per unit system weight can be obtained when the reactor which would be both wall temperature and stress limited at that flow rate is used. For example, at a flow rate of 790 lb/sec a reactor with a void fraction of 0.3 should be used to obtain the maximum power per unit weight. The curves in Fig. 6-4 or a similar set with the net power plotted versus the hydrogen flow rate could also be used to determine what reactor and what flow rate should be used to obtain a specific amount of power.

The effect of a change in the shape of the power profile on the power per unit system weight is shown in Fig. 6-5. For a change in CQ_1 from 2.5 to 2.75 there is only a slight decrease in the maximum power per unit weight that can be developed. An increase in the hydrogen pressure at the reactor exit causes a small decrease in the power per unit weight. This is primarily due to an increase in the system weight and not a decrease in the reactor power as the limiting performance of the reactor is insensitive to changes in pressure as was stated in Chapter IV. The effect of a change in the coolant channel diameter is also

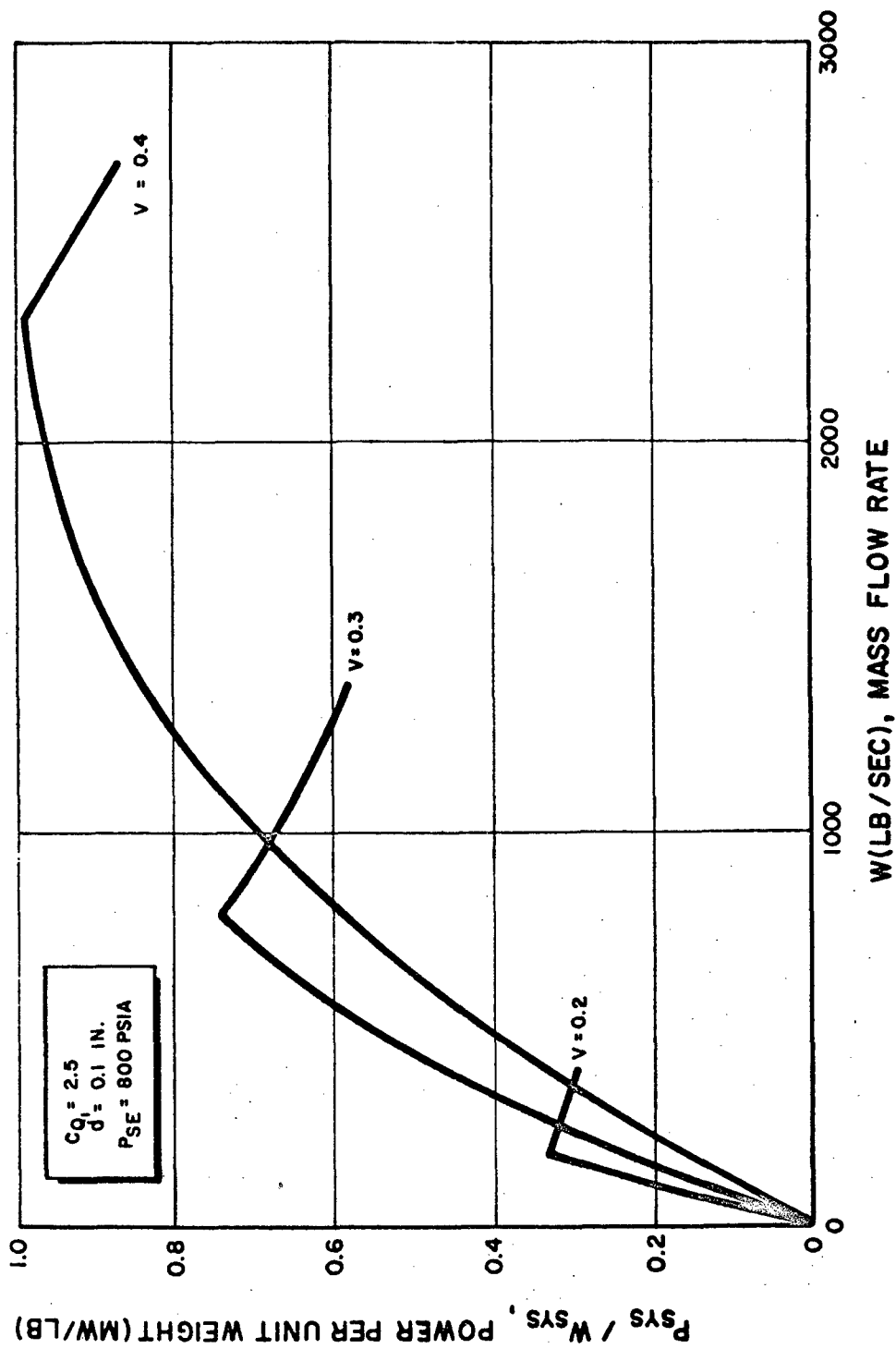


FIG. 6-4: RATIO OF MAXIMUM POSSIBLE POWER DEVELOPED TO POWERPLANT
 SYSTEM WEIGHT VS HYDROGEN FLOW RATE IN REACTOR FOR SYSTEMS
 ON LIMITING PERFORMANCE ENVELOPES.

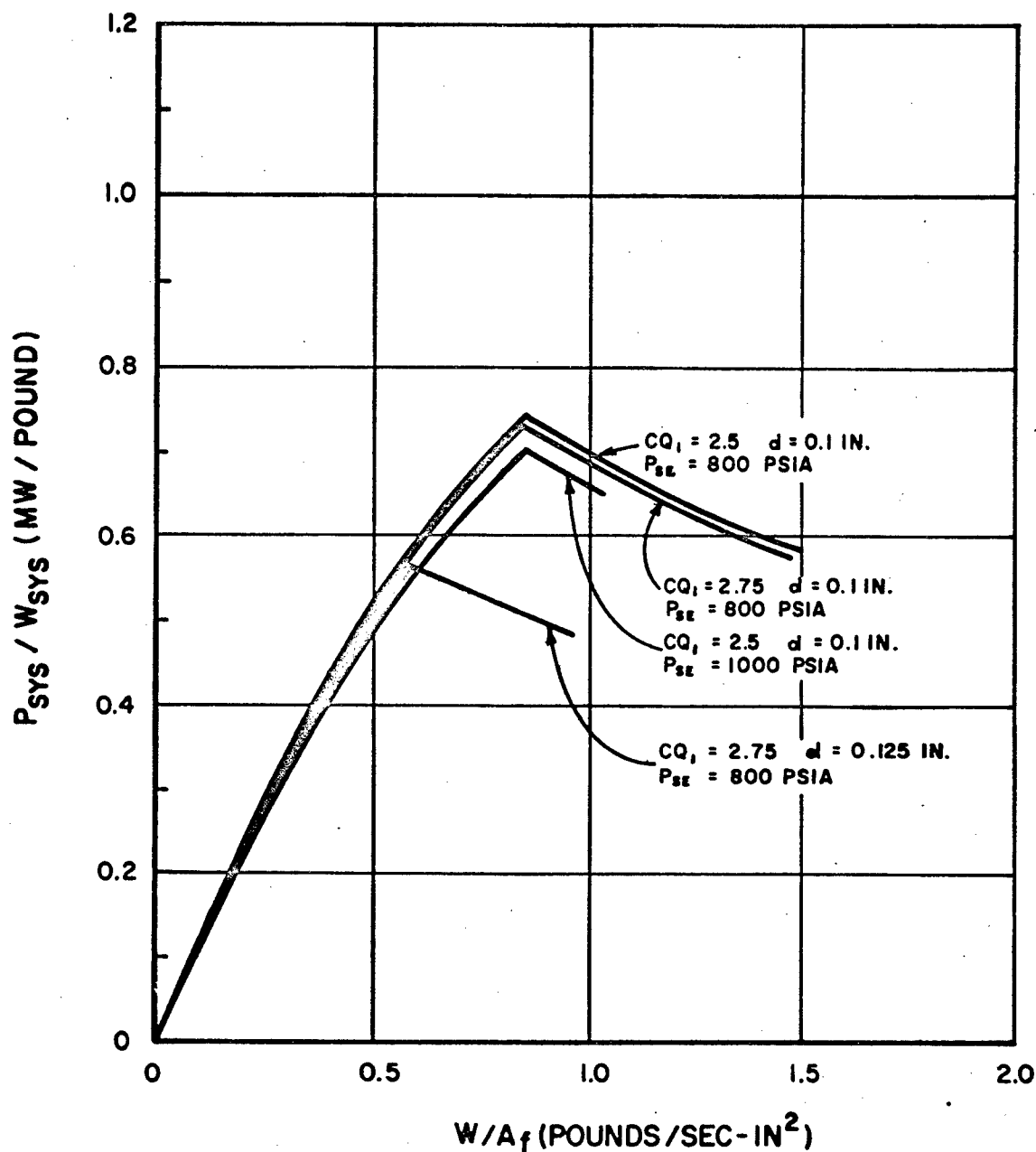


FIG.6-5: RATIO OF MAXIMUM POSSIBLE POWER DEVELOPED TO POWER PLANT SYSTEM WEIGHT VS HYDROGEN FLOW PER UNIT AREA IN REACTOR FOR SYSTEMS ON LIMITING PERFORMANCE ENVELOPES: $V=0.3$

shown in Fig. 6-5. An increase in diameter results in a decrease in the power per unit weight that can be achieved. This effect is more significant when the reactor is stress limited and the reactor becomes stress limited at lower flow rates per unit area as the coolant channel diameter is increased.

CHAPTER VII

SAMPLE MISSION

A. Mission Calculations

To determine the characteristics of the complete rocket system an operating or "burning" time must be known. This permits the calculation of the total amount of propellant and tankage that is required. In order to compare different rocket systems a particular mission was chosen. The payload weights that can be carried on the mission by the different systems then provide a good basis for comparison.

In order to show the method of calculation and comparison a sample 300 mile earth orbital mission was chosen. The velocity increment required for this mission is 26,000 ft/sec (43). This value is based on a vertical flight in a constant gravity field with no atmospheric drag. The burnout velocity for a single stage vehicle starting from rest (1) is

$$V_p = I_{sp} g_o \ln \lambda - g t_p \quad (7-1)$$

where λ is the ratio of the initial gross weight to the empty weight at the end of burning.

$$\lambda = \frac{W_G}{W_E} \quad (7-2)$$

This burnout velocity is equal to the velocity increment ΔV_p required for the mission as the initial velocity of the vehicle is zero. The altitude at the end of burning (1) is

$$h_p = I_{sp} g_o t_p \left[1 + \frac{1}{\lambda - 1} \ln \frac{1}{\lambda} \right] - \frac{1}{2} g t_p^2 \quad (7-3)$$

The burnout velocity and altitude are specified by the mission and the specific impulse is a known quantity for a particular powerplant. Consequently, Eqs. 7-1 and 7-3 are two equations in two unknowns. Due to the nature of the equations the easiest way to obtain a solution is by using a trial and error method. Eq. 7-1 solved for λ is

$$\lambda = \exp \left(\frac{V_p + g t_p}{I_{sp} g_o} \right) \quad (7-4)$$

Eq. 7-3 can be solved for t_p to give

$$t_p = \frac{1}{g} \left[I_{sp} g_o \left(1 - \frac{\ln \lambda}{\lambda - 1} \right) - \sqrt{(I_{sp} g_o)^2 \left(1 - \frac{\ln \lambda}{\lambda - 1} \right)^2 - 2gh_p} \right] \quad (7-5)$$

If t_p is initially set to zero, Eq. 7-4 solved for λ , and this value of λ is used in Eq. 7-5, a positive value of t_p is obtained. If this value of t_p is inserted in Eq. 7-4 and the process is repeated, another value of t_p is obtained. Each successive value of t_p is closer to the preceeding one. When the desired accuracy on t_p is obtained, the process is stopped and the final values are used for further computations.

B. Rocket System Characteristics

Once the burning time is determined the total mass of hydrogen required for the mission is

$$W_{H_2} = w t_p \quad (7-6)$$

The propellant tank is assumed to be cylindrical with hemispherical ends. The equations for the length to diameter ratio of the tank and the tank weight are taken from reference 44.

The tank weight is

$$W_T = \frac{6.88 \times 10^7}{P_T^2} (1.131 \times 10^{-11} W_{H_2} P_T^3 + 0.00407) \quad (7-7)$$

where the tank pressure is in psia and the weight of propellant is in pounds.

The empty weight is determined from λ and the weight of the hydrogen.

$$W_E = \frac{W_{H_2}}{\lambda - 1} \quad (7-8)$$

The gross weight is just the sum of the empty weight and the weight of the hydrogen. The weight of the controls and structure required to tie the components together is assumed to be equal to two percent of the gross weight of the system. This value

is representative for large rockets (44). To obtain more accurate estimates specific design studies would be required.

The payload weight that can be carried on the mission is the gross weight minus the weights of all the other components and the propellant.

$$W_{PL} = W_G - W_{SYS} - W_{H2} - W_T - W_S \quad (7-9)$$

C. Mission Results

The payload weights for the sample mission are shown in Fig. 7-1 for the powerplant systems containing reactors with void fractions of 0.3 and 0.4. The independent parameters are those determined by the limiting performance envelopes shown in Fig. 4-19. The powerplant system with a reactor whose void fraction is 0.2 is incapable of getting into a 300 mile earth orbit with no payload. The same payloads divided by the corresponding gross weights of the rocket systems are shown in Fig. 7-2. Both sets of curves have sharp maxima that correspond to the transition from a wall temperature to a stress limitation in the reactor. Using both figures it is possible to determine which rocket system has the minimum gross weight for a given payload. For example, for a payload of 10,000 pounds it can be seen in Fig. 7-1 that the system with a reactor void fraction of 0.4 requires a

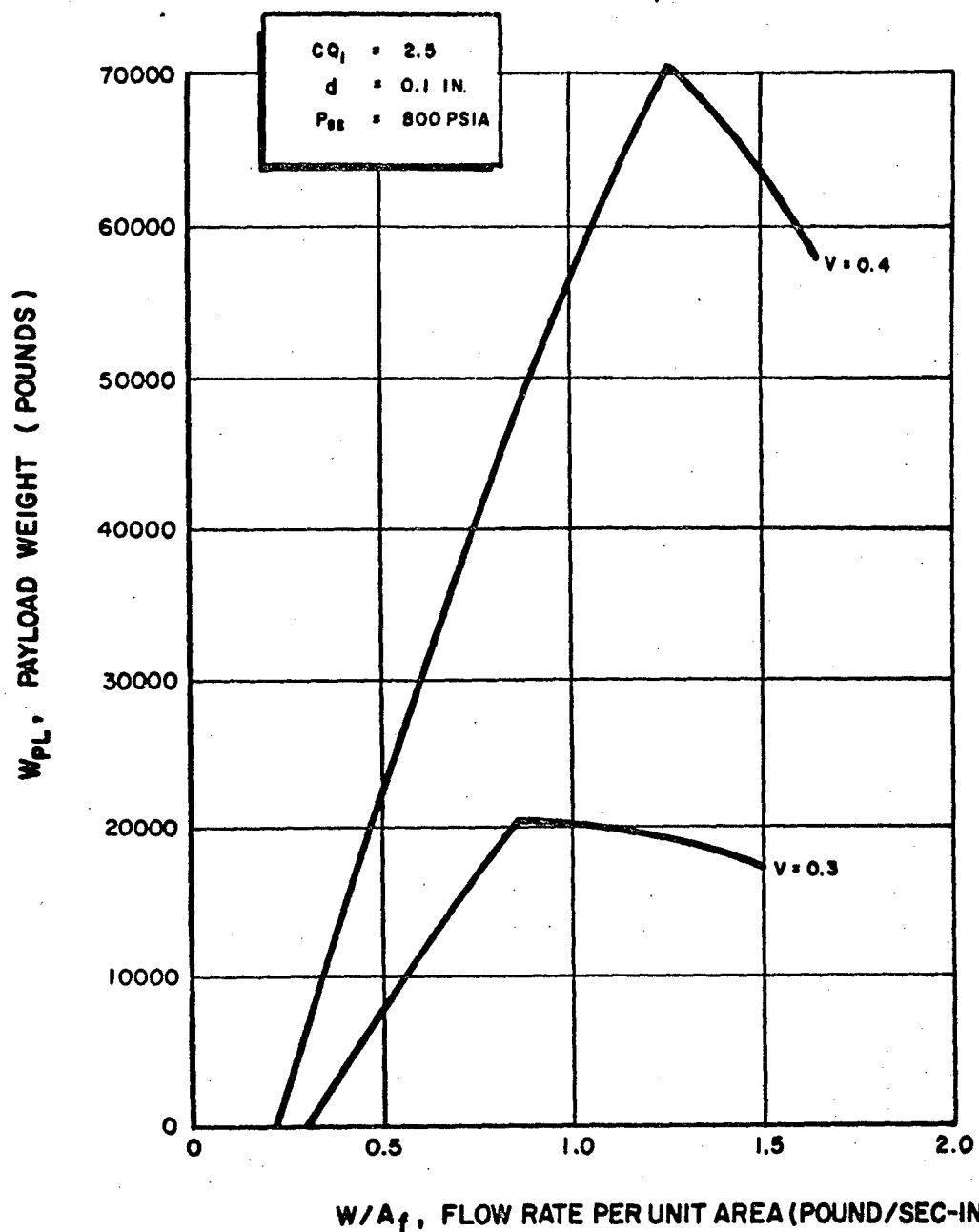
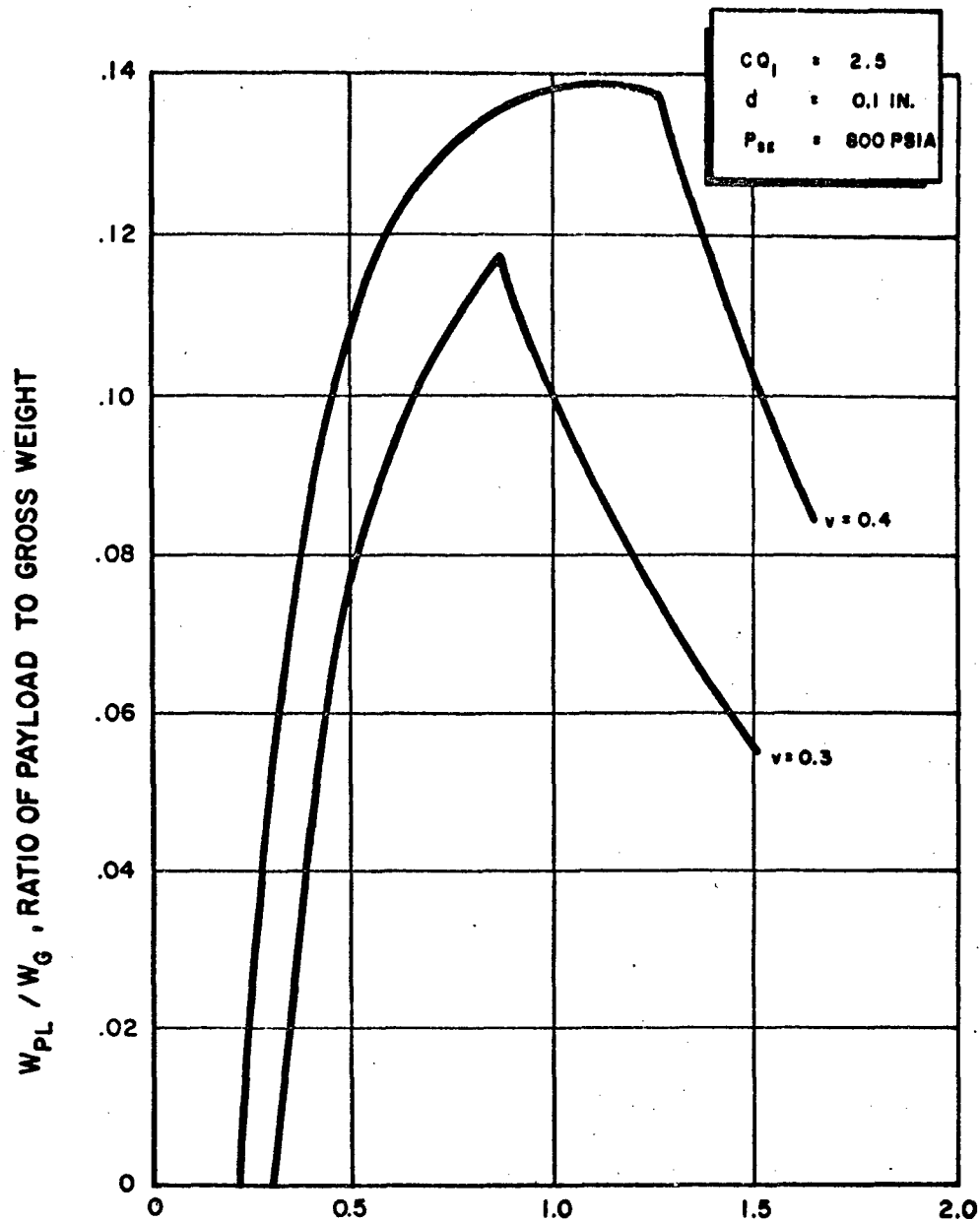


FIG. 7-1: MAXIMUM PAYLOAD WEIGHT VS HYDROGEN
 FLOW PER UNIT AREA IN REACTOR FOR
 EARTH ORBITAL MISSION USING POWER-
 PLANT SYSTEMS ON LIMITING PERFORMANCE
 ENVELOPES



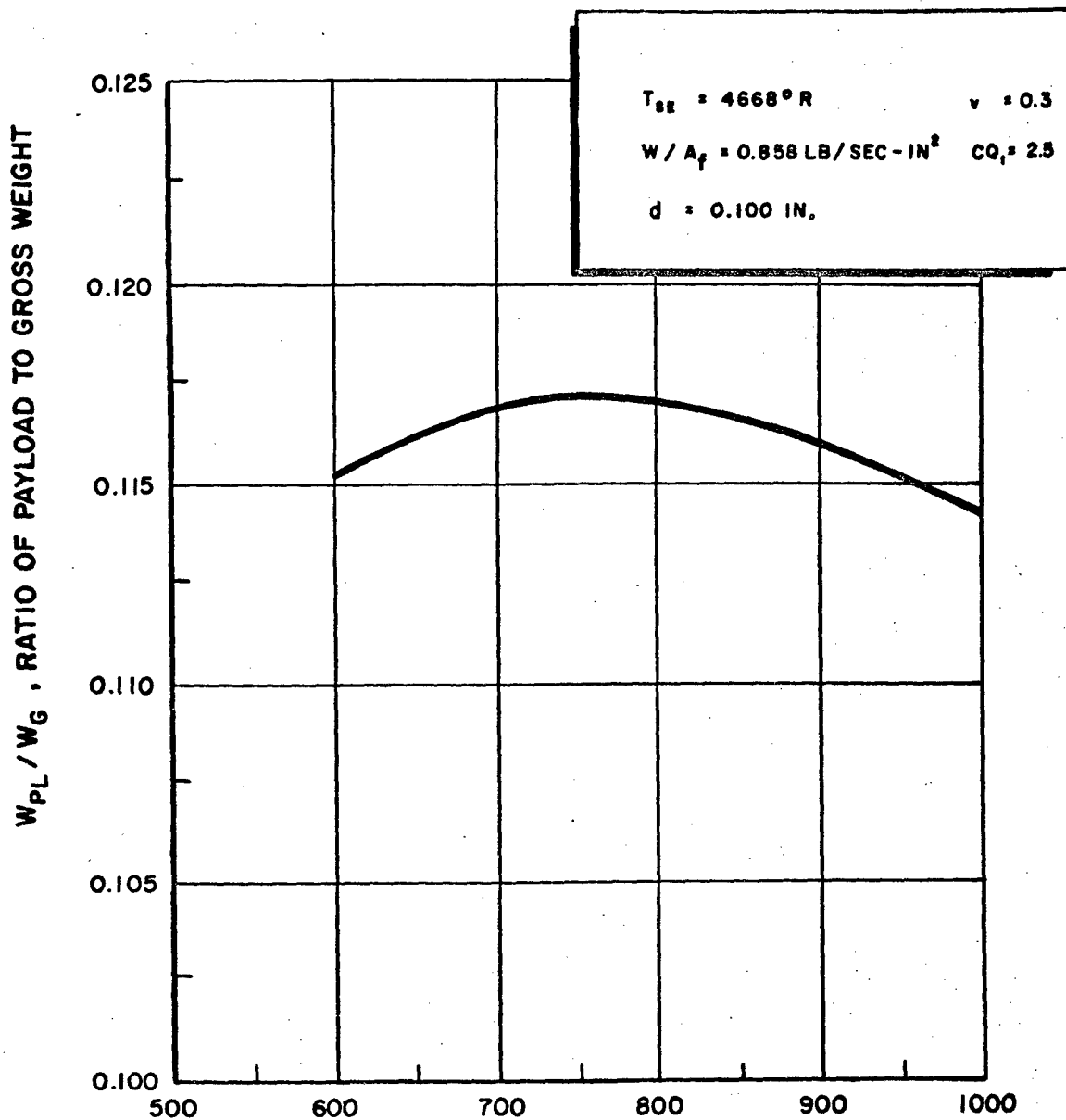
W/A_f, FLOW RATE PER UNIT AREA (POUNDS/SEC-IN²)

FIG. 7-2: MAXIMUM RATIO OF PAYLOAD TO GROSS WEIGHT VS HYDROGEN FLOW PER UNIT AREA IN REACTOR FOR EARTH ORBITAL MISSION USING POWERPLANT SYSTEMS ON LIMITING PERFORMANCE ENVELOPES

flow rate per unit area of 0.34 lb/sec-in^2 while the system with a reactor void fraction of 0.3 requires a w/A_f of 0.56 lb/sec-in^2 . From Fig. 7-2 the former system is seen to have a ratio of payload to gross weight of 0.071 while the same ratio for the latter system is 0.089. The result is that the system with a reactor having a void fraction of 0.3 is better on a weight basis because its gross weight is less than that of the system with $v=0.4$. Further inspection of the curves shows that the system with $v=0.3$ is superior on a weight basis for values of payload up to 20,500 pounds. For larger payloads another system must be used. The comparison was made here for only two systems. For a payload of 10,000 pounds there is probably a better system, which has a reactor with a void fraction less than 0.3 but obviously greater than 0.2. In order to determine the best rocket configuration the characteristics of more systems with different intermediate reactor sizes would have to be calculated.

The pressure of the hydrogen in the reactor was shown to have little effect of the performance characteristics of the powerplant as long as it is less than the limiting value specified for stress purposes by Eq. 5-29. The effect of the operating pressure on the complete system and particularly on its payload carrying capacity is also small. The ratio of the payload

to gross weight of a system is plotted versus the hydrogen pressure at the reactor exit in Fig. 7-3. The hydrogen temperature at the reactor exit and the flow rate per unit area are fixed at 4668°R and $0.858 \text{ lb/sec-in}^2$ respectively so the reactor is both wall temperature and stress limited for all cases. The reactor has a void fraction of 0.3 and coolant channels with a diameter of 0.100 inches. There is a fairly flat maximum in the ratio of payload to gross weight even as shown on the expanded scale. The gross weight of the system increases with pressure for values of p_{SE} up to 1000 psia while the payload weight alone also has a relatively flat maximum. For five runs calculated at equal intervals of 100 psi the minimum payload is 20,150 pounds when $p_{\text{SE}} = 1000 \text{ psia}$ and the maximum is 20,460 pounds when $p_{\text{SE}} = 800 \text{ psia}$. This is a variation in payload weight of only 2%. However, these calculations do show the desirable range of operating pressures and indicate the penalty incurred for operating off of the optimum point.



P_{SE} (PSIA), HYDROGEN PRESSURE AT REACTOR EXIT

FIG.7-3: RATIO OF PAYLOAD TO GROSS WEIGHT VS
HYDROGEN PRESSURE AT REACTOR EXIT
FOR EARTH ORBITAL MISSION.

CHAPTER VIII

SUMMARY OF RESULTS AND CONCLUSIONS

A. Results

For a given set of temperature and stress limits on the reactor core material the maximum possible operating conditions of the reactor have been determined. These maximum operating conditions are expressed in terms the hydrogen propellant temperature at the reactor exit and the flow rate per unit area through the reactor. At low values of flow rate per unit area the reactors are wall temperature limited while at higher values stresses are limiting. These limiting values are shown on plots of maximum hydrogen temperature at the reactor exit versus propellant flow rate per unit area through the reactor. Separate curves for different reactors show the effect of changes in reactor power distribution, void fraction, and the diameter of the coolant channels. A decrease in the reactor void fraction or an increase in the diameter of the coolant channels causes the reactor to become stress limited at lower values of flow per unit area. The limiting performance curves of hydrogen exit temperature versus flow per unit area are insensitive to changes in the operating pressure as long as it is below a specific value determined from the stress limitation.

The amount of power that can be removed from the reactor increases with the flow rate of propellant through it as long as

the reactor is wall temperature limited. At higher values of flow when the stresses are limiting, any increase in flow rate must be accompanied by a decrease in the hydrogen temperature at the reactor exit. The result is that the power cannot be increased above the value which is obtained when both the wall temperature and stress limits occur at the same time. For the complete powerplant which includes the pumping equipment required for its operation, the net power produced decreases as the flow rate of propellant is increased once the reactor is stress limited. However, the weight of the powerplant always increases with the flow rate of propellant through it. Consequently, there is a sharp maximum in the power per unit weight of the powerplant that occurs at the point where the reactor is both wall temperature and stress limited.

If the power per unit weight is plotted versus the mass flow rate of hydrogen rather than flow per unit area, the curves for different reactor sizes intersect. For a given flow rate of hydrogen it is then possible to determine which reactor will provide the maximum power per unit weight. For larger flow rates and larger power requirements it is desirable to use reactors with larger void fractions. The limiting performance conditions of hydrogen temperature at the reactor exit and flow rate per unit area can be determined within 10% by a simplified analysis. Two analytic expressions were developed to predict the position of

the limiting performance envelope for the reactor. One expression covers the wall temperature limitation while the second covers the stress limited region. This simplified analysis can be used to obtain initial approximate answers and to reduce the amount of computation time required to get detailed results. These analytic expressions also show the effect of changes in reactor void fraction, coolant channel diameter, and reactor power distribution on the limiting performance envelopes. It is also possible to obtain a value for the operating pressure in a reactor below which the stress limit is independent of pressure. Only when the pressure is above this specified value is the maximum shear stress dependent on pressure. When this occurs, the reactor must operate at less than its maximum possible power level.

After the limiting performance envelopes are obtained for a number of different reactors, they can be used to determine the optimum system configuration for a particular mission. The results obtained in this study are based on the assumption that the minimum gross system weight to do a given job is the best measure of performance for determining an optimum system. Values of payload weight and the ratio of payload to gross weight for a given mission are calculated for all the powerplant systems on the limiting performance envelopes. Plots of these parameters versus the flow rate per unit area through the reactors show that maxima do exist. For the particular sample mission chosen

for this analysis, a 300 mile earth orbital mission, these maxima occur at the same values of flow per unit area that the maxima in power per unit powerplant weight occur. This same method can be used to find the optimum system configuration for any similar mission. To make any generalization with regard to the position of the maxima in payload and in the power per unit powerplant weight more missions would have to be investigated or some approximate analytical analysis would have to be developed.

The above results are restricted to powerplants with solid core gas cooled reactors and to nuclear rocket systems. In addition, some further results which may be of more general interest were obtained. A procedure for calculating the heat transfer and pressure drop characteristics for the subsonic flow of a compressible chemically reacting gas in a tube with heat addition and wall friction was developed. This procedure is presented in detail in the appendices along with a Fortran coded program for machine calculations.

Equations for calculating the thermodynamic and transport properties of normal hydrogen over a temperature range from 150° to 4000° Kelvin and for pressures from 0.01 to 100.0 atmospheres were compiled and developed where necessary. The effects of dissociation and of compressibility factor unequal to one are taken into account where necessary. A Fortran coded program of these equations is available and is presented in Appendix A.

B. Conclusions

The results that were obtained in this study can be used to reach a number of conclusions. For a given set of limitations on the core material the maximum power that can be developed by the powerplant is obtained when the reactor is both wall temperature and stress limited.

The maximum power that can be developed by the powerplant is independent of the fluid operating pressure as long as the pressure in the reactor is less than a specified value determined by stress limitations.

The significance of the amount of coolant flow per unit area through the reactor on the powerplant performance indicates the desirability of using the reactor configuration which provides maximum flow area per unit weight of the reflected reactor.

The operating pressure of the coolant in the reactor should be determined from mission calculations as the powerplant performance is not sensitive to the fluid pressure.

Shaping the axial power profile in the reactor such that the coolant channel surface temperature would be constant is not desirable. This particular form of power profile would cause a reduction in the maximum possible power obtainable from the reactor. Other variations on shaping the axial power profile may be advantageous.

CHAPTER IX

RECOMMENDATIONS

A. As result of this investigation it has become evident that a number of areas could be studied further to obtain a better insight and better answers in the field of nuclear rocket propulsion. Specific recommendations are listed below.

1. Stress calculations for actual fuel element geometries should be completed. The results of these calculations could then be compared to those from the simpler model used here and the probable error determined. The degree of complexity required for a stress model could then be determined.

2. The use of the maximum shear failure criterion should be checked with the other failure criteria against experimental tests on fuel element geometries where possible. In this manner the best failure criterion for use in design calculations could be determined. Even if experimental data are unavailable the different failure criteria should be applied to the accurate stress calculations on more realistic fuel element geometries.

3. The simplified analysis for determining the limitations on reactor performance should be extended if possible to include the determination of the pressure drop across the reactor. It would then be possible to predict the maximum stresses in the reactor for any operating pressure rather than just the maximum possible performance for the reactor system.

4. If the work in the above paragraph is carried out it should be possible to extend the approximate analytic analysis so that numerical results could be obtained for payloads and gross weights of systems for different missions.

5. The possible gains that can be obtained in powerplant performance by shaping the axial power distribution should be determined. With nonuniform fuel loading and possibly the insertion of a neutron absorbing material it might be possible to obtain an ideal power distribution that would cause the core material to be either wall temperature or stress limited at every axial position. The effect of such an axial power distribution on the powerplant performance should be determined.

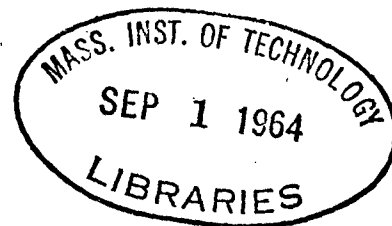
BIBLIOGRAPHY

1. Sutton, G. P., "Rocket Propulsion Elements," John Wiley and Sons, Inc., New York, 1956.
2. Bussard, R. W. and DeLauer, R. D., "Nuclear Rocket Propulsion," McGraw Hill Book Co., Inc., New York, 1958.
3. Rom, F. E., Lietzke, A. F., and Johnson, P. G., "Nuclear Rockets for Unmanned Missions," Nucleonics, Vol. 20, No. 11, 53-57, November, 1962.
4. Taylor, T. B., "Advanced Propulsion Concepts," Proceedings of the International Symposium on Aerospace Nuclear Propulsion, IRE Transactions on Nuclear Science, Vol. NS-9, No. 1, 21-26. October 23-27, 1961.
5. Schreiber, R. E., "A Review of Project Rover," Proceedings of the International Symposium on Aerospace Nuclear Propulsion, IRE Transactions on Nuclear Science, Vol. NS-9, No. 1, 16-20, October 23-27, 1961.
6. Wang, C.J., "Nuclear Propulsion," Astronautics, 42, November, 1959.
7. Roder, H. M. and Goodwin, R.D., "Provisional Thermodynamic Functions for Para-Hydrogen," NBS TN - 130, United States Department of Commerce, National Bureau of Standards, December, 1961.
8. Plebuch, R.K., "Reactor Physics of Nuclear Rocket Reactors," Sc.D. Thesis, Department of Nuclear Engineering, Massachusetts Institute of Technology, September, 1963.
9. Krieger, F. J., "A Parametric Study of Certain Low-Molecular-Weight-Compounds as Nuclear Rocket Propellants II. Ammonia," RM-2401, The Rand Corporation, Santa Monica, California, July, 1959.
10. Krieger, F. J., "A Parametric Study of Certain Low-Molecular-Weight-Compounds as Nuclear Rocket Propellants III. Water," RM-2402, The Rand Corporation, Santa Monica, California, July, 1959.
11. Christie, J. D. and Herrington, A.C., "Nuclear Rockets for Large-Payload Booster Application I. Preliminary Reactor Studies," ASD Technical Memorandum 1, Applied Science Div. Operations Evaluation Group, Office of the Chief of Naval Operations, Cambridge, Massachusetts, September, 1961.

12. Herrington, A. C., "Nuclear Rockets for Large-Payload Booster Application II. Reactor Calculations," ASD Technical Memorandum 5, Applied Science Div., Operations Evaluation Group, Office of the Chief of Naval Operations, Cambridge, Massachusetts, March, 1962.
13. Hyland, R. E., "Reactor-Weight Study of Beryllium Oxide, Beryllium, Lithium-7 Hydride, and Water as Moderators with Tungsten 184 Structural Material and Uranium Dioxide Fuel," NASA TN D-1407, September, 1962.
14. Taylor, M.F. and Kirchgessner, T. A., "Measurements of Heat Transfer and Friction Coefficients for Helium Flowing in a Tube at Surface Temperatures up to 5900 R," NASA TN D-133, October, 1959.
15. Hendricks, R.C., Graham, R. W., Hsu, Y.Y., and Mederios, A.A., "Correlation of Hydrogen Heat Transfer in Boiling and Supercritical Pressure States," ARS 1710-61, presented at American Rocket Society Propellants, Combustion, and Liquid Rockets Conference; Palm Beach, Florida, April 26-28, 1961.
16. McAdams, W. H., "Heat Transmission," McGraw Hill Book Co., Inc., New York, 1954.
17. Gordon, S., Zeleznik, F. J., and Huff, V. N., "A General Method for Automatic Computation of Equilibrium Compositions and Theoretical Rocket Performance of Propellants," NASA TN D-132, October, 1959.
18. Hilsenrath, J. et. al., "Tables of Thermal Properties of Gases," NBS Circular 564, United States Department of Commerce, National Bureau of Standards, November, 1955.
19. Mason, E. A., and Rice, W. E., "The Intermolecular Potentials of Helium and Hydrogen," Journal of Chemical Physics, Vol. 22, No. 3, 522-535, March, 1954.
20. Vanderslice, J. T., Weissman, S., Mason, E. A., and Fallon, R. J., "High Temperature Transport Properties of Dissociating Hydrogen," The Physics of Fluids, Vol. 5. No. 2, 155-164, February, 1962.
21. Woolley, H. W., Scott, R. B., and Brickwedde, F. G., "Compilation of Thermal Properties of Hydrogen in Its Various Isotopic and Ortho-Para Modifications," United States Department of Commerce, National Bureau of Standards Journal of Research, Vol. 41, 379-475, November, 1948.

22. Farmer, O. A., "Digital Programs for Para Hydrogen Properties," LAMS-2762, November, 1962.
23. Harry, D. P. III, "Formulation and Digital Coding of Approximate Hydrogen Properties for Application to Heat-Transfer and Fluid-Flow Computations," NASA TN D-1664, May, 1963.
24. Shapiro, A. H., "The Dynamics and Thermodynamics of Compressible Fluid Flow," The Ronald Press Company, New York, 1953.
25. Schneider, P. J., "Conduction Heat Transfer," Addison-Wesley Publishing Company, Inc. Reading, Massachusetts, 1955.
26. Hulbert, L. E., "The Numerical Solution of Two-Dimensional Problems of the Theory of Elasticity," Ph.D. Thesis, Ohio State University, 1963.
27. White, S. N. Jr., "Difference Equations for Plane Thermal Elasticity, LAMS-2745, October, 1962.
28. Rowley, J. C. and Payne, J. B., "Steady-State Temperature Solution for a Heat-Generating Circular Cylinder Cooled by a Ring of Equal Holes," LA-2486, April, 1961.
29. Weil, N. A., "Studies of the Brittle Behavior of Ceramics Materials," Technical Documentary Report No. ASD-TR-61-628 prepared by Armour Research Foundation of Illinois Institute of Technology, April, 1962.
30. Anthony, F. M. and Mistretta, A. L., "Leading Edge Design with Brittle Materials," IAS Paper No. 61-151-1845 presented at the National IAS-ARS Joint Meeting, Los Angeles, California, June 13-16, 1961.
31. Anthony, F. M. and Pearl, H. A., "Selection of Materials for Hypersonic Leading Edge Applications," IAS Paper No. 59-111, 1959.
32. Seeley, F. B. and Smith, J. O., "Resistance of Materials," John Wiley and Sons, Inc., London, 1956.
33. Timoshenko, S. and Goodier, J. N., "Theory of Elasticity," McGraw Hill Book Company, Inc., New York, 1951.
34. Finger, H. B., "The Case for Nuclear Energy," Nucleonics, Vol. 19, No. 4, 58-63, April, 1961.

35. Yasui, G., "Reactor Heat Removal Limitations of Nuclear Rockets," ARS 1211-60 presented at ARS Semi-Annual Meeting, Los Angeles, California, May 9-12, 1960.
36. Merryman, R. G., Wagner, P., and MacMillan, D. P., "H⁴LM Graphite," LAMS-2725, September, 1962.
37. Rice, W. E., and Hirschfelder, J. O., "Second Virial Coefficients of Gases Obeying a Modified Buckingham (Exp-Six) Potential," Journal of Chemical Physics, Vol. 22, No. 2, 187-192, February, 1954.
38. Hougen, O. A., Watson, K. M., and Ragatz, R. A., "Chemical Process Principles Part II: Thermodynamics," John Wiley and Sons, Inc., New York, 1959.
39. Mason, E. A., "Transport Properties of Gases Obeying a Modified Buckingham (Exp-Six) Potential," Journal of Chemical Physics, Vol. 22, No. 2, 169-186, February, 1954.
40. Hirschfelder, J. O., Curtiss, C. F., and Byrd, R. B., "Molecular Theory of Gases and Liquids," John Wiley and Sons, Inc., New York, 1954.
41. Hirschfelder, J. O., "Heat Conductivity in Polyatomic, Electronically Excited, or Chemically Reacting Mixtures III," Sixth Symposium on Combustion, 351-366, Reinhold Publishing Corporation, New York, 1957.
42. Rohlik, H. E. and Crouse, J. E., "Analytical Investigation of the Effect of Turbopump Design on Gross Weight Characteristics of a Hydrogen-Propelled Nuclear Rocket," NASA MEMO 5-12-59E, June, 1959.
43. Sams, E. W., "Performance of Nuclear Rocket for Large Payload, Earth Satellite Booster," IAS Paper No. 59-94 presented at IAS National Summer Meeting, Los Angeles, California, June 16-19, 1959.
44. Johnson, P. G. and Smith, R. L., "An Optimization of Powerplant Parameters for Orbital Launch Nuclear Rockets," NASA TN D-675, February, 1961.



APPENDIX A HYDROGEN PROPERTIES

1. Summary

One Fortran subroutine has been written to produce the thermodynamic and transport properties of normal hydrogen. The range of temperatures is from 150° to 4000° Kelvin and the range of pressures is from 0.01 to 100.0 atmospheres.

The equations used in the subroutine are a combination of empirical and theoretical equations. The effects of dissociation and compressibility factor being unequal to unity can be included or excluded in the calculation of the properties. A number of thermodynamic property derivatives may also be determined using this subroutine.

2. General Method

The equations for calculating the hydrogen properties are developed in such a manner that either the properties of the molecular species or of an equilibrium mixture of the molecular and atomic species can be computed. When dissociation occurs, both the molecular and atomic species are considered as semi-perfect gases so that the equation for chemical equilibrium can be written in terms of the partial pressures of the two components. At relatively lower temperatures and higher pressures when the dissociation is not important, the effect of the compres-

sibility factor being unequal to one is taken into account for the molecular species. In the intermediate range of temperature and pressure when the effects of both compressibility factor unequal to one and dissociation are small but not zero, the properties of the mixture are calculated including both effects to insure that no discontinuities occur in the calculated properties.

3. Thermodynamic Properties

The enthalpies, entropies, and specific heats of the components considered as ideal gases in the standard state are calculated from empirical equations which are functions of temperature only (17).

$$\frac{\bar{H}^{\circ}_{\alpha}}{RT} = A_1 + \frac{A_2 T}{2} + \frac{A_3 T^2}{3} + \frac{A_4 T^3}{4} + \frac{A_5}{T} \quad (\text{A-1})$$

$$\frac{\bar{S}^{\circ}_{\alpha}}{R} = A_1 \ln T + A_2 T + \frac{A_3 T^2}{2} + \frac{A_4 T^3}{3} + A_6 \quad (\text{A-2})$$

$$\frac{\bar{c}^{\circ}_{p,\alpha}}{R} = A_1 + A_2 T + A_3 T^2 + A_4 T^3 \quad (\text{A-3})$$

A similar set of equations exists for the atomic species with the A_i coefficients replaced with B_i 's. The coefficients A_i and B_i listed in reference 17 were obtained from a least squares fit of tabulated values of the thermodynamic functions for selected temperature intervals with continuity from one interval to

the next. For machine computations the coefficients are read in as data and stored as elements of two matrices A and B.

The equation for equilibrium between the molecular and atomic species can be written as follows.

$$\frac{P_{\beta}^2}{P_{\alpha}} = K_p(T) = \exp \left(- \frac{\Delta F^{\circ}}{RT} \right) = \exp \left(- \frac{\Delta H^{\circ}}{RT} + \frac{\Delta S^{\circ}}{R} \right) \quad (A-4)$$

where ΔF° , ΔH° , and ΔS° are the changes in free energy, enthalpy, and entropy for the dissociation reaction



with both components in their standard states. In terms of the quantities in Eqs. A-1 and A-2 and the corresponding values for atomic hydrogen

$$\frac{\Delta F^{\circ}}{RT} = \left(2 \frac{\bar{H}_{\beta}^{\circ}}{RT} - \frac{\bar{H}_{\alpha}^{\circ}}{RT} \right) - \left(2 \frac{\bar{S}_{\beta}^{\circ}}{R} - \frac{\bar{S}_{\alpha}^{\circ}}{R} \right) \quad (A-6)$$

The mole fraction of the atomic species x_{β} in terms of the partial pressures is

$$x_{\beta} = \frac{P_{\beta}}{P_{\alpha} + P_{\beta}} = \frac{P_{\beta}}{P} \quad (A-7)$$

Similarly

$$x_{\alpha} = \frac{P_{\alpha}}{P} = 1 - x_{\beta} \quad (A-8)$$

Inserting Eqs. A-7 and A-8 into Eq. A-4 and solving for x_β

$$x_\beta = \frac{-1 + \sqrt{1 + 4 p \exp \left(\frac{\Delta F^\circ}{RT} \right)}}{2 p \exp \left(\frac{\Delta F^\circ}{RT} \right)} \quad (\text{A-9})$$

The molecular weight of the mixture is

$$W = \frac{n_\alpha W_\alpha + n_\beta W_\beta}{n} = x_\alpha W_\alpha + x_\beta W_\beta \quad (\text{A-10})$$

Noting that W_α is just twice W_β and using Eq. A-8 the expression for W reduces to

$$W = W_\beta (2 - x_\beta) \quad (\text{A-11})$$

In order to take into account the effect of the compressibility factor being unequal to one for molecular hydrogen, it is necessary to know how Z_α varies with temperature and pressure. For the purpose of these calculations the functional relationship for Z_α is approximated as the first two terms of the modified virial form of the equation of state. The virial equation in standard form is

$$Z = \frac{p\bar{v}}{RT} = 1 + \frac{B(T)}{\bar{v}} + \frac{C(T)}{\bar{v}^2} - \frac{D(T)}{\bar{v}^3} + \dots \quad (\text{A-12})$$

The modified form is a series in p rather \bar{v} such that

$$Z = \frac{P\bar{V}}{RT} = 1 + B'(T) p + C'(T) p^2 + \dots \quad (A-13)$$

where

$$B'(T) = \frac{B(T)}{RT} \quad (A-14)$$

and

$$C'(T) = \frac{C(T) - \frac{B(T)^2}{RT}}{(RT)^2} \quad (A-15)$$

The approximation

$$Z = 1 + B'(T) p_{\alpha} \quad (A-16)$$

used in these calculations is quite accurate above 300°K but obviously is in considerable error as the temperature approaches the critical temperature.

The value of $B'(T)$ is calculated from an empirical equation of the form

$$B' = 0.01 \exp \left[- (B_0 + B_1 T + B_2 T^2 + B_3 T^3 + B_4 T^4) \right] \quad (A-17)$$

where the coefficients B_0 through B_4 were obtained by a least squares polynomial fit to the log of tabulated and calculated values of B' . The values of B' for temperatures less than 600°K

were calculated from values of Z_α tabulated for a pressure of 100 atmospheres (18). The values of B' for temperatures above 600°K were calculated using Eq. A-14 where the values of $B(T)$ were calculated from tabulated values of the integral for the second virial coefficient using the Buckingham potential (37). Eq. A-4 governing chemical equilibrium for the dissociation reaction was written for the two components being considered ideal gases. The equation for Z_α does not necessarily give $Z_\alpha = 1.00$ when equation A-4 gives $x_\beta = 0$. In the interest of preventing any discontinuities in the properties the equation of state for the mixture is written of the following form:

$$P \bar{v} = ZRT \quad (A-18)$$

or

$$Pv = Z \frac{R}{W} T \quad (A-19)$$

where

$$Z = \frac{Z_\alpha}{x_\alpha + x_\beta Z_\alpha} = \frac{Z_\alpha}{1 + x_\beta (Z_\alpha - 1)} \quad (A-20)$$

This equation for Z results from the assumption that the molar densities are additive as they are for a Gibbs Dalton mixture even though Z_α may be unequal to 1.0. From Eq. A-20 it can be seen that when $x_\beta = 0$ and the effect of the compres-

sibility factor becomes significant, $Z = Z_\alpha$ and the equation of state (A-19) reduces to that for pure molecular hydrogen.

When $Z_\alpha = 1$, $Z = 1$ and the equation of state for the mixture reduces to that for a mixture of ideal gases.

The calculation of the deviations of the thermodynamic properties of molecular hydrogen from the ideal gas properties at the same temperature requires the integration of compressibility factor derivatives from zero pressure to the pressure level p (38). The enthalpy departure is

$$\bar{H}_{\alpha r} - \bar{H}_\alpha = -RT^2 \int_0^p \left(-\frac{\partial Z_\alpha}{\partial T} \right)_p \frac{dp}{p_\alpha}$$

Using Eq. A-16 and carrying out the integration yields

$$\bar{H}_{\alpha r} = \bar{H}_\alpha - RT^2 \frac{dB'}{dT} p_\alpha$$

or

$$\frac{\bar{H}_{\alpha r}}{RT} = \frac{\bar{H}_\alpha}{RT} - T p_\alpha \frac{dB'}{dT} \quad (A-21)$$

The entropy of the ideal molecular hydrogen gas at its partial pressure is

$$\bar{S}_\alpha = R \left(\frac{\bar{S}_\alpha^0}{R} - \ln p_\alpha \right) \quad (A-22)$$

The departure of the entropy of the real gas from that of the ideal gas at the same pressure is

$$\bar{S}_\alpha - \bar{S}_{\alpha r} = -R \int_0^{p_\alpha} \frac{1 - Z_\alpha}{p_\alpha} dp_\alpha + \frac{\bar{H}_\alpha - \bar{H}_{\alpha r}}{T}$$

Again using equation A-16 and carrying out the integration

$$\bar{S}_{\alpha r} = \bar{S}_\alpha - R \left[B' p_\alpha + T \frac{dB'}{dT} p_\alpha \right]$$

or

$$\frac{\bar{S}_{\alpha r}}{R} = \frac{\bar{S}_\alpha}{R} - p_\alpha \left(B' + T \frac{dB'}{dT} \right) \quad (\text{A-23})$$

The departure of the molar heat capacity is obtained by taking the derivative of the molal enthalpy departure. From Eq. A-22

$$\bar{c}_{p\alpha r} = \bar{c}_{p\alpha} - RT p_\alpha \left(2 \frac{dB'}{dT} + T \frac{d^2 B'}{dT^2} \right) \quad (\text{A-24})$$

or

$$\frac{\bar{c}_{p\alpha r}}{R} = \frac{\bar{c}_{p\alpha}}{R} - T p_\alpha \left(2 \frac{dB'}{dT} + T \frac{d^2 B'}{dT^2} \right) \quad (\text{A-25})$$

The enthalpy and entropy per unit mass of the mixture of the two species is just

$$H = \frac{RT}{W} \left(x_{\alpha} \frac{\bar{H}_{\alpha r}}{RT} + x_{\beta} \frac{\bar{H}_{\beta}}{RT} \right) \quad (A-26)$$

and

$$S = \frac{R}{W} \left(x_{\alpha} \frac{\bar{S}_{\alpha r}}{R} + x_{\beta} \frac{\bar{S}_{\beta}}{R} \right) \quad (A-27)$$

The specific heat of the mixture can be obtained by differentiating the expression for enthalpy.

$$c_p = \left(\frac{\partial H}{\partial T} \right)_p = \left\{ \frac{\partial}{\partial T} \left[\frac{RT}{W} \left(x_{\alpha} \frac{\bar{H}_{\alpha r}}{RT} + x_{\beta} \frac{\bar{H}_{\beta}}{RT} \right) \right] \right\}_T \quad (A-28)$$

$$c_p = \frac{1}{W} \left(x_{\alpha} \bar{c}_{p\alpha r} + x_{\beta} \bar{c}_{p\beta} \right) + \frac{1}{W} \left[\bar{H}_{\alpha r} \left(\frac{\partial x_{\alpha}}{\partial T} \right)_p + \bar{H}_{\beta} \left(\frac{\partial x_{\beta}}{\partial T} \right)_p \right] + (x_{\alpha} \bar{H}_{\alpha r} + x_{\beta} \bar{H}_{\beta}) \left[\frac{-1}{W^2} \left(\frac{\partial W}{\partial T} \right)_p \right] \quad (A-29)$$

Using Eq. A-11 and noting that $x_{\alpha} + x_{\beta} = 1$ Eq. A-29 can be simplified to

$$c_p = \frac{R}{W} \left(x_{\alpha} \frac{\bar{c}_{p\alpha r}}{R} + x_{\beta} \frac{\bar{c}_{p\beta}}{R} \right) + \frac{1}{W} \left(\frac{\partial x_{\beta}}{\partial T} \right)_p \left[\frac{2\bar{H}_{\beta} - \bar{H}_{\alpha r}}{2 - x_{\beta}} \right] \quad (A-30)$$

The value of $\left(\frac{\partial x_{\beta}}{\partial T} \right)_p$ can be determined by rewriting Eq. A-4 and differentiating. Eq. A-4 in terms of mole fractions is

$$\frac{x_{\beta}^2}{1 - x_{\beta}} p = \exp \left(-\frac{\Delta \bar{F}^0}{RT} \right) \quad (A-31)$$

or

$$p x_{\beta}^2 + x_{\beta} \exp \left(-\frac{\Delta \bar{F}^0}{RT} \right) - \exp \left(-\frac{\Delta \bar{F}^0}{RT} \right) = 0 \quad (A-32)$$

Then

$$2 p x_{\beta} \left(\frac{\partial x_{\beta}}{\partial T} \right)_p + \exp \left(- \frac{\Delta \bar{F}^0}{RT} \right) \left(\frac{\partial x_{\beta}}{\partial T} \right)_p + x_{\beta} \exp \left(- \frac{\Delta F^0}{RT} \right) \left[\frac{\partial \left(- \frac{\Delta \bar{F}^0}{RT} \right)}{\partial T} \right]_p - \exp \left(- \frac{\Delta F}{RT} \right) \left[\frac{\partial \left(- \frac{\Delta F^0}{RT} \right)}{\partial T} \right]_p = 0 \quad (A-33)$$

To get the last term

$$\left[\frac{\partial \left(- \frac{\bar{F}^0}{RT} \right)}{\partial T} \right]_p = \left[\frac{\partial}{\partial T} \left(- \frac{\bar{H}^0}{RT} + \frac{\bar{S}^0}{R} \right) \right]_p = - \frac{\bar{C}_{p^0}}{RT} + \frac{\bar{H}^0}{RT^2} + \frac{\bar{C}_{p^0}}{RT} = \frac{\bar{H}^0}{RT^2} \quad (A-34)$$

Therefore

$$\left[\frac{\partial \left(- \frac{\Delta \bar{F}^0}{RT} \right)}{\partial T} \right]_p = \frac{\Delta \bar{H}^0}{RT^2} \quad (A-35)$$

Using Eq.s A-31 and A-35, Eq. A-33 can be solved for $\left(\frac{\partial x_{\beta}}{\partial T} \right)_p$

to give

$$\left(\frac{\partial x_{\beta}}{\partial T} \right)_p = \frac{x_{\beta}(1-x_{\beta})}{2 - x_{\beta}} \left(\frac{\Delta \bar{H}^0}{RT^2} \right) \quad (A-36)$$

From Eq. A-11 it can be seen that

$$\left(\frac{\partial W}{\partial T} \right)_p = -W_{\beta} \left(\frac{\partial x_{\beta}}{\partial T} \right)_p \quad (A-37)$$

Defining

$$\omega_T = \frac{T}{W} \left(\frac{\partial W}{\partial T} \right)_P \quad (A-38)$$

results in

$$\omega_T = \frac{-T}{(2-x_\beta)} \left(\frac{\partial x_\beta}{\partial T} \right)_P = \frac{-x_\beta(1-x_\beta)}{(2-x_\beta)^2} \left(\frac{\Delta \bar{H}^0}{RT} \right) \quad (A-39)$$

Using Eq. A-39 in Eq. A-30 the expression for c_p can be written

$$c_p = \frac{R}{W} \left[x_\alpha \frac{c_{p\alpha r}}{R} + x_\beta \frac{c_{p\beta}}{R} - \omega_T \left(\frac{2\bar{H}_\beta - \bar{H}_{\alpha r}}{RT} \right) \right] \quad (A-40)$$

In order to calculate the speed of sound in the hydrogen it is necessary to calculate the value of $\left(\frac{\partial p}{\partial \rho} \right)_S$. For a perfect gas:

$$\left(\frac{\partial p}{\partial \rho} \right)_S = \frac{\gamma RT}{W} \quad (A-41)$$

where γ is the ratio of specific heats. For the purposes of these calculations γ is defined as

$$\gamma \equiv \frac{W}{RT} \left(\frac{\partial p}{\partial \rho} \right)_S \quad (A-42)$$

For an equilibrium mixture of the atomic and molecular species of a gas γ , as defined by Eq. A-42, is not the ratio of specific heats but is related to this ratio in a fairly simple manner as will be shown later.

Starting with Eq. A-42 an expression for γ will be developed which will permit its calculation from other known quantities.

$$\text{As } v = \frac{1}{p}$$

$$\gamma = \frac{W}{RT} \left(\frac{\partial p}{\partial p} \right)_S = -\frac{Wv^2}{RT} \left(\frac{\partial p}{\partial v} \right)_S \quad (\text{A-43})$$

An expression for $\left(\frac{\partial p}{\partial v} \right)_S$ in terms of the partial derivatives $\left(\frac{\partial v}{\partial T} \right)_p$ and $\left(\frac{\partial v}{\partial p} \right)_T$ can be derived from basic thermodynamic relations. The result from a table compiled by Bridgeman is (38)

$$\left(\frac{\partial p}{\partial v} \right)_S = \frac{c_p/T}{\frac{1}{T} \left[c_p \left(\frac{\partial v}{\partial p} \right)_T + T \left(\frac{\partial v}{\partial T} \right)_p^2 \right]} \quad (\text{A-44})$$

Then in Eq. A-43

$$\gamma = \frac{-v^2}{\frac{RT}{W} \left[\left(\frac{\partial v}{\partial p} \right)_T + \frac{T}{c_p} \left(\frac{\partial v}{\partial T} \right)_p^2 \right]} \quad (\text{A-45})$$

The two derivatives of the specific volume must be evaluated to obtain γ . From Eq. A-19

$$v = \frac{ZRT}{pW} \quad (A-46)$$

Taking the partial derivative with respect to pressure

$$\left(\frac{\partial v}{\partial p}\right)_T = -\frac{ZRT}{p^2 W} + \frac{RT}{pW} \left(\frac{\partial Z}{\partial p}\right)_T - \frac{ZRT}{pW^2} \left(\frac{\partial W}{\partial p}\right)_T \quad (A-47)$$

Define

$$\sigma_p = \frac{p}{Z} \left(\frac{\partial Z}{\partial p}\right)_T \quad (A-48)$$

$$\omega_p = \frac{p}{W} \left(\frac{\partial W}{\partial p}\right)_T \quad (A-49)$$

Using these definitions and Eq. A-46

$$\left(\frac{\partial v}{\partial p}\right)_T = -\frac{v}{p} (1 + \omega_p - \sigma_p) \quad (A-50)$$

In a similar fashion it can be shown that

$$\left(\frac{\partial v}{\partial T}\right)_p = \frac{v}{T} (1 - \omega_T + \sigma_T) \quad (A-51)$$

where

$$\sigma_T = \frac{T}{Z} \left(\frac{\partial Z}{\partial T}\right)_p \quad (A-52)$$

and ω_T was defined by Eq. A-38.

From Eq. A-11

$$\left(\frac{\partial W}{\partial p}\right)_T = -W_\beta \left(\frac{\partial x_\beta}{\partial p}\right)_T \quad (\text{A-53})$$

Then

$$\omega_p = \frac{p}{W} \left(\frac{\partial W}{\partial p}\right)_T = -\frac{p}{(2-x_\beta)} \left(\frac{\partial x_\beta}{\partial p}\right)_T \quad (\text{A-54})$$

The value of $\left(\frac{\partial x_\beta}{\partial p}\right)_T$ can be determined in the same manner that $\left(\frac{\partial x_\beta}{\partial T}\right)_p$ was starting with Eq. A-32. In this case the derivative of the change in free energy $\left(\frac{\Delta \bar{F}^0}{RT}\right)$ is zero because the free energy is a function of temperature only.

The result is

$$\left(\frac{\partial x_\beta}{\partial p}\right)_T = -\frac{x_\beta(1-x_\beta)}{p(2-x_\beta)} \quad (\text{A-55})$$

Then in Eq. A-54

$$\omega_p = \frac{x_\beta(1-x_\beta)}{(2-x_\beta)^2} \quad (\text{A-56})$$

Comparing Eqs. A-56 and A-39 one can see that

$$\omega_T = -\omega_p \left(\frac{\Delta \bar{H}^0}{RT}\right) \quad (\text{A-57})$$

The other two quantities that must be evaluated to determine γ are σ_p and σ_T . Differentiation of Eq. A-20 results in

$$\left(\frac{\partial Z}{\partial T}\right)_p = \frac{Z}{Z_\alpha} \left[(1 - Zx_\beta) \left(\frac{\partial Z_\alpha}{\partial T}\right)_p - Z (Z_\alpha - 1) \left(\frac{\partial x_\beta}{\partial T}\right)_p \right] \quad (A-58)$$

Then

$$\sigma_T = \frac{T}{Z_\alpha} \left[(1 - Zx_\beta) \left(\frac{\partial Z_\alpha}{\partial T}\right)_p - Z (Z_\alpha - 1) \left(\frac{\partial x_\beta}{\partial T}\right)_p \right] \quad (A-59)$$

Similarly

$$\sigma_p = \frac{p}{Z_\alpha} \left[(1 - Zx_\beta) \left(\frac{\partial Z_\alpha}{\partial p}\right)_T - Z (Z_\alpha - 1) \left(\frac{\partial x_\beta}{\partial p}\right)_T \right] \quad (A-60)$$

The values of the derivatives of x_β have been determined as expressed by Eqs. A-36 and A-55. The values of the derivatives of Z_α can be determined by differentiating Eq. A-16. Eq. A-16 can be rewritten

$$Z_\alpha = 1 + B' (T) p (1 - x_\beta) \quad (A-61)$$

Then differentiation gives

$$\left(\frac{\partial Z_\alpha}{\partial T}\right)_p = p (1 - x_\beta) \frac{dB'}{dT} - B' p \left(\frac{\partial x_\beta}{\partial T}\right)_p \quad (A-62)$$

and

$$\left(\frac{\partial Z}{\partial p}\right)_T = B' (1 - x_\beta) - B' p \left(\frac{\partial x_\beta}{\partial p}\right)_T \quad (\text{A-63})$$

The value of $\frac{dB'}{dT}$ is easily determined from Eq. A-17 and will not be worked out here.

It was mentioned previously that γ as defined here is not just the ratio of specific heats. In terms of quantities defined above the relationship between γ and this ratio is

$$\frac{\gamma}{c_p/c_v} = \frac{-Z \frac{v}{p}}{\left(\frac{\partial v}{\partial p}\right)_T} = \frac{Z}{1 + \omega_p - \sigma_p} \quad (\text{A-64})$$

From this relation the effects dissociation and compressibility can easily be determined. It is obvious that if the gas is considered a perfect gas the ratio goes to unity and γ is then equal to the ratio of specific heats.

The above equations are sufficient to calculate W , Z , ρ , H , S , c_p , and γ . In the next section expressions for derivatives of these properties will be developed.

4. Thermodynamic Property Derivatives

As well as the property derivatives calculated above to get γ , expressions for $\left(\frac{\partial H}{\partial p}\right)_T$, $\left(\frac{\partial S}{\partial T}\right)_p$, $\left(\frac{\partial S}{\partial p}\right)_T$, $\frac{T}{\gamma} \left(\frac{\partial \gamma}{\partial T}\right)_p$, and $\frac{p}{\gamma} \left(\frac{\partial \gamma}{\partial p}\right)_T$ will be developed in this section.

From the basic relation

$$Tds = dH - v dp \quad (A-65)$$

$$T \left(\frac{\partial S}{\partial p} \right)_T = \left(\frac{\partial H}{\partial p} \right)_T - v \quad (A-66)$$

From Maxwells' relations

$$\left(\frac{\partial S}{\partial p} \right)_T = - \left(\frac{\partial v}{\partial T} \right)_p \quad (A-67)$$

Therefore

$$\left(\frac{\partial H}{\partial p} \right)_T = - T \left(\frac{\partial v}{\partial T} \right)_p + v \quad (A-68)$$

Using Eq. A-51 in Eq. A-68 and simplifying results in

$$\left(\frac{\partial H}{\partial p} \right)_T = v (\omega_T - \sigma_T) \quad (A-69)$$

The value of $\left(\frac{\partial S}{\partial p} \right)_T$ can be determined from either Eq. A-66 or A-67. Using Eq. A-65 to get $\left(\frac{\partial S}{\partial T} \right)_p$

$$T \left(\frac{\partial S}{\partial T} \right)_p = \left(\frac{\partial H}{\partial T} \right)_p - 0 = c_p \quad (A-70)$$

or

$$\left(\frac{\partial S}{\partial T} \right)_p = \frac{c_p}{T} \quad (A-71)$$

To obtain the two partial derivatives of γ requires the evaluation of a number of second derivatives. The dimensionless variables ζ_T and ζ_p are defined

$$\zeta_T = \frac{T}{\gamma} \left(\frac{\partial \gamma}{\partial T} \right)_p \quad (A-72)$$

and

$$\zeta_p = \frac{p}{\gamma} \left(\frac{\partial \gamma}{\partial p} \right)_T \quad (A-73)$$

Using Eq. A-45 to obtain the derivatives one gets

$$\zeta_T = \frac{T}{\gamma} \left[\frac{\partial}{\partial T} \left\{ - \frac{Wv^2}{RT} \left[\frac{1}{\left(\frac{\partial v}{\partial p} \right)_T + \frac{T}{c_p} \left(\frac{\partial v}{\partial T} \right)_p^2} \right] \right\} \right]_p \quad (A-74)$$

or

$$\zeta_T = \frac{T}{\gamma} \left\{ - \frac{\gamma}{T} + \frac{\gamma}{W} \left(\frac{\partial W}{\partial T} \right)_p + \frac{2\gamma}{v} \left(\frac{\partial v}{\partial T} \right)_p \frac{\gamma}{\left(\frac{\partial v}{\partial p} \right)_T + \frac{T}{c_p} \left(\frac{\partial v}{\partial T} \right)_p^2} \right. \\ \left. \left[\frac{\partial^2 v}{\partial T \partial p} + \frac{1}{c_p} \left(\frac{\partial v}{\partial T} \right)_p^2 - \frac{T}{c_p^2} \left(\frac{\partial v}{\partial T} \right)_p^2 \left(\frac{\partial c_p}{\partial T} \right)_p + \frac{2T}{c_p} \left(\frac{\partial v}{\partial T} \right)_p \right. \right. \\ \left. \left. \left(\frac{\partial^2 v}{\partial T^2} \right)_p \right] \right\} \quad (A-75)$$

Then simplifying and using the definition of ω_T

$$\zeta_T = -1 + \omega_T + 2 \frac{T}{v} \left(\frac{\partial v}{\partial T} \right)_p - \frac{T}{\left(\frac{\partial v}{\partial p} \right)_T + \frac{T}{c_p} \left(\frac{\partial v}{\partial T} \right)_p^2} \left[\frac{\partial^2 v}{\partial T \partial p} + \frac{1}{c_p} \left(\frac{\partial v}{\partial T} \right)_p \left\{ \left(\frac{\partial v}{\partial T} \right)_p \left[1 - \frac{T}{c_p} \left(\frac{\partial c_p}{\partial T} \right)_p + 2 T \left(\frac{\partial^2 v}{\partial T^2} \right)_p \right] \right\} \right] \quad (A-76)$$

In a similar fashion

$$\zeta_p = \omega_p + \frac{2p}{v} \left(\frac{\partial v}{\partial p} \right)_T - \frac{p}{\left(\frac{\partial v}{\partial p} \right)_T + \frac{T}{c_p} \left(\frac{\partial v}{\partial T} \right)_p^2} \left\{ \left(\frac{\partial^2 v}{\partial p^2} \right)_T + \frac{T}{c_p} \left(\frac{\partial v}{\partial T} \right)_p \left[2 \left(\frac{\partial^2 v}{\partial T \partial p} \right) - \frac{1}{c_p} \left(\frac{\partial v}{\partial T} \right)_p \left(\frac{\partial c_p}{\partial p} \right)_T \right] \right\} \quad (A-77)$$

In these expressions for ζ_T and ζ_p the five quantities which have not yet been determined are the three second derivatives of the specific volume and the two partial derivatives of the specific heat.

To obtain an expression for $\left(\frac{\partial c_p}{\partial T} \right)_p$ starting with Eq. A-40

$$\begin{aligned} \left(\frac{\partial c_p}{\partial T} \right)_p &= - \frac{c_p}{w} \left(\frac{\partial w}{\partial T} \right)_p + \frac{R}{w} \left[x_\alpha \left(\frac{\partial \bar{c}_{p\alpha r}}{\partial T} \right)_p + x_\beta \left(\frac{\partial \bar{c}_{p\beta}}{\partial T} \right)_p + \right. \\ &\quad \left(\frac{\bar{c}_{p\beta}}{R} - \frac{\bar{c}_{p\alpha}}{R} \right) \left(\frac{\partial x_\beta}{\partial T} \right)_p - \omega_T \left(\frac{2\bar{c}_{p\beta}}{RT} - \frac{\bar{c}_{p\alpha}}{RT} - \frac{2\bar{H}_\beta - \bar{H}_\alpha}{RT^2} \right) \\ &\quad \left. - \left(\frac{2\bar{H}_\beta - \bar{H}_\alpha}{RT} \right) \left(\frac{\partial \omega_T}{\partial T} \right)_p \right] \quad (A-78) \end{aligned}$$

or simplifying and using the definition of ω_T

$$\begin{aligned} \left(\frac{\partial c_p}{\partial T} \right)_p &= - \frac{c_p \omega_T}{T} + \frac{R}{W} \left[x_\alpha \left(\frac{\partial \bar{c}_{p\alpha r}}{\partial T} \right)_p + x_\beta \left(\frac{\partial \bar{c}_{p\beta}}{\partial T} \right)_p + \right. \\ &\quad \left(\frac{\bar{c}_{p\beta}}{R} - \frac{\bar{c}_{p\alpha}}{R} \right) \left(\frac{\partial x_\beta}{\partial T} \right)_p - \frac{\omega_T}{T} \left(\frac{2\bar{c}_{p\beta}}{R} - \frac{\bar{c}_{p\alpha}}{R} - \frac{\Delta \bar{H}}{RT} \right) - \frac{\Delta \bar{H}}{RT} \\ &\quad \left. \left(\frac{\partial \omega_T}{\partial T} \right)_p \right] \end{aligned} \quad (A-79)$$

From equation A-25 and noting that $p_\alpha = x_\alpha p$

$$\begin{aligned} \left(\frac{\partial \bar{c}_{p\alpha r}}{\partial T} \right)_p &= \frac{d\bar{c}_{p\alpha}}{dT} - \left[x_\alpha p - p T \left(\frac{\partial x_\alpha}{\partial T} \right)_p \right] \left[2 \frac{dB'}{dT} + \right. \\ &\quad \left. T \frac{d^2 B'}{dT^2} \right] - T x_\alpha p \left[2 \frac{d^2 B'}{dT^2} + \frac{d^2 B'}{dT^2} + T \frac{d^3 B'}{dT^3} \right] \end{aligned} \quad (A-80)$$

Then in more compact form

$$\begin{aligned} \left(\frac{\partial \bar{c}_{p\alpha r}}{\partial T} \right)_p &= \frac{d\bar{c}_{p\alpha}}{dT} - \left(\frac{\bar{c}_{p\alpha r}}{R} - \frac{\bar{c}_{p\alpha}}{R} \right) \left(\frac{\partial x_\beta}{\partial T} \right)_p \frac{1}{x_\alpha} - p_\alpha \\ &\quad \left[2 \frac{dB'}{dT} + 4 T \frac{d^2 B'}{dT^2} + T^2 \frac{d^3 B'}{dT^3} \right] \end{aligned} \quad (A-81)$$

The values of the derivatives of $\frac{\bar{c}_{P\alpha}}{R}$, $\frac{\bar{c}_{P\beta}}{R}$, and the derivatives of B' are obtained by straightforward differentiation of Eq. A-3, the corresponding equation for $\frac{\bar{c}_{P\beta}}{R}$, and Eq. A-17.

The only term in Eq. A-79 which has not been evaluated is

$\left(\frac{\partial \omega_T}{\partial T}\right)_P$. Starting with Eqs. A-56 and A-57 expressions for the

two derivatives of ω_P and of ω_T are developed as follows.

From Eq. A-56.

$$\left(\frac{\partial \omega_P}{\partial p}\right)_T = \left(\frac{\partial x_\beta}{\partial p_T}\right) \left[\frac{1-x_\beta}{(2-x_\beta)^2} - \frac{x_\beta}{(2-x_\beta)^2} + \frac{2x_\beta(1-x_\beta)}{(2-x_\beta)^3} \right] \quad (A-82)$$

Noting from Eqs. A-55 and A-56 that

$$\left(\frac{\partial x_\beta}{\partial p}\right)_T = \frac{-(2-x_\beta)}{p} \omega_P \quad (A-83)$$

Then

$$\left(\frac{\partial \omega_P}{\partial p}\right)_T = \frac{-(2-x_\beta) \omega_P}{p(2-x_\beta)^2} \left[\frac{(1-2x_\beta)(2-x_\beta) + 2x_\beta(1-x_\beta)}{(2-x_\beta)} \right] \quad (A-84)$$

which simplifies to

$$\left(\frac{\partial \omega_P}{\partial p}\right)_T = - \frac{\omega_P (2-3x_\beta)}{p(2-x_\beta)^2} \quad (A-85)$$

In a similar fashion but using Eq. A-39 rather than A-83 one obtains

$$\left(\frac{\partial \omega}{\partial T}\right)_P = - \frac{\omega_T}{T} \frac{(2-3x_\beta)}{(2-x_\beta)} \quad (\text{A-86})$$

or using Eq. A-85

$$\left(\frac{\partial \omega}{\partial T}\right)_P = - \frac{P}{\omega_P} \frac{\omega_T}{T} \left(\frac{\partial \omega}{\partial P}\right)_T \quad (\text{A-87})$$

From Eq. A-57 and noting that $\frac{\Delta \bar{H}^0}{RT}$ is independent of pressure

$$\left(\frac{\partial \omega_T}{\partial P}\right)_T = - \frac{\Delta \bar{H}^0}{RT} \left(\frac{\partial \omega}{\partial P}\right)_T \quad (\text{A-88})$$

Or

$$\left(\frac{\partial \omega_T}{\partial P}\right)_T = \frac{\omega_T}{\omega_P} \left(\frac{\partial \omega}{\partial P}\right)_T \quad (\text{A-89})$$

Using Eq. A-89 in combination with A-87 results in

$$\left(\frac{\partial \omega}{\partial T}\right)_P = \frac{P}{T} \left(\frac{\partial \omega_T}{\partial P}\right)_T \quad (\text{A-90})$$

Starting with Eq. A-57

$$\left(\frac{\partial \omega_T}{\partial T}\right)_P = - \frac{\Delta \bar{H}^0}{RT} \left(\frac{\partial \omega}{\partial T}\right)_P - \omega_P \left(\frac{\Delta \bar{C}_P^0}{RT}\right) - \frac{\Delta \bar{H}^0}{RT^2} \quad (\text{A-91})$$

or using Eq. A-57 again

$$\left(\frac{\partial \omega_T}{\partial T}\right)_p = - \frac{\Delta \bar{H}^0}{RT} \left(\frac{\partial \omega}{\partial T}\right)_p - \frac{1}{T} \left(\omega_T + \omega_p \frac{\Delta \bar{c}^0}{R}\right) \quad (A-92)$$

Expressions for the second derivatives of the specific volume can be determined by differentiating Eqs. A-50 and A-51.

From Eq. A-51

$$\left(\frac{\partial^2 v}{\partial T^2}\right)_p = \frac{1}{v} \left(\frac{\partial v}{\partial T}\right)_p^2 - \frac{1}{T} \left(\frac{\partial v}{\partial T}\right)_p + \frac{v}{T} \left[\left(\frac{\partial \sigma_T}{\partial T}\right)_p - \left(\frac{\partial \omega_T}{\partial T}\right)_p \right] \quad (A-93)$$

Differentiation of Eq. A-52 gives

$$\left(\frac{\partial \sigma_T}{\partial T}\right)_p = \frac{\sigma_T}{T} - \frac{\sigma_T}{Z} \left(\frac{\partial Z}{\partial T}\right)_p + \frac{T}{Z} \left(\frac{\partial^2 Z}{\partial T^2}\right)_p \quad (A-94)$$

or

$$\left(\frac{\partial \sigma_T}{\partial T}\right)_p = \frac{\sigma_T}{T} (1 - \sigma_T) + \frac{T}{Z} \left(\frac{\partial^2 Z}{\partial T^2}\right)_p \quad (A-95)$$

Inserting Eq. A-95 into A-93 and simplifying yields

$$\begin{aligned} \left(\frac{\partial^2 v}{\partial T^2}\right)_p &= \left(\frac{\partial v}{\partial T}\right)_p \left[\frac{1}{v} \left(\frac{\partial v}{\partial T}\right)_p - \frac{1}{T} \right] + \frac{v}{T} \left[\frac{\sigma_T}{T} (1 - \sigma_T) + \frac{T}{Z} \right. \\ &\quad \left. \left(\frac{\partial^2 Z}{\partial T^2}\right)_p - \left(\frac{\partial \omega_T}{\partial T}\right)_p \right] \end{aligned} \quad (A-96)$$

Similar differentiation of Eqs A-48 and A-50 with respect to pressure results in a similar expression for $(\frac{\partial^2 v}{\partial p^2})_T$ which is

$$\left(\frac{\partial^2 v}{\partial p^2}\right)_T = \left(\frac{\partial v}{\partial p}\right)_T \left[\frac{1}{v} \left(\frac{\partial v}{\partial p}\right)_T - \frac{1}{p} \right] + \frac{v}{p} \left[\frac{\sigma_p}{p} (1 - \sigma_p) + \frac{p}{Z} \left(\frac{\partial^2 Z}{\partial p^2}\right)_T - \left(\frac{\partial \omega}{\partial p}\right)_T \right] \quad (A-97)$$

Differentiating Eq. A-51 with respect to pressure one obtains

$$\frac{\partial^2 v}{\partial p \partial T} = \frac{1}{v} \left(\frac{\partial v}{\partial T}\right)_p \left(\frac{\partial v}{\partial p}\right)_T + \frac{v}{T} \left[\left(\frac{\partial \sigma_T}{\partial p}\right)_T - \left(\frac{\partial \omega_T}{\partial p}\right)_T \right] \quad (A-98)$$

Using the definition of σ_T

$$\left(\frac{\partial \sigma_T}{\partial p}\right)_T = - \frac{\sigma_T}{Z} \left(\frac{\partial Z}{\partial p}\right)_T + \frac{T}{Z} \left(\frac{\partial^2 Z}{\partial T \partial p}\right) \quad (A-99)$$

or

$$\left(\frac{\partial \sigma_T}{\partial p}\right)_T = - \frac{\sigma_T \sigma_p}{p} + \frac{T}{Z} \left(\frac{\partial^2 Z}{\partial T \partial p}\right) \quad (A-100)$$

Then Eq. A-98 can be written as

$$\frac{\partial^2 v}{\partial p \partial T} = \frac{1}{v} \left(\frac{\partial v}{\partial T} \right)_p \left(\frac{\partial v}{\partial p} \right)_T + \frac{v}{T} \left[\frac{T}{Z} \left(\frac{\partial^2 Z}{\partial T \partial p} \right) - \frac{\sigma_T \sigma_p}{p} - \left(\frac{\partial \omega_T}{\partial p} \right)_T \right] \quad (A-101)$$

In developing the expressions for the second derivatives of the specific volume the yet undetermined quantities are the second derivatives of the compressibility factor Z . The first derivative of Z with respect to temperature is given by Eq. A-58. Further differentiation gives

$$\begin{aligned} \left(\frac{\partial^2 Z}{\partial T^2} \right)_p &= \frac{1}{Z} \left(\frac{\partial Z}{\partial T} \right)_p^2 + \frac{1}{Z_\alpha} \left(\frac{\partial Z_\alpha}{\partial T} \right)_p \left(\frac{\partial Z}{\partial T} \right)_p + \frac{Z}{Z_\alpha} \left[(1-Zx_\beta) \left(\frac{\partial^2 Z_\alpha}{\partial T^2} \right)_p - Z \right. \\ &\quad \left(\frac{\partial Z_\alpha}{\partial T} \right)_p \left(\frac{\partial x_\beta}{\partial T} \right)_p - x_\beta \left(\frac{\partial Z_\alpha}{\partial T} \right)_p \left(\frac{\partial Z}{\partial T} \right)_p - Z (Z_\alpha - 1) \left(\frac{\partial^2 x_\beta}{\partial T^2} \right)_p - (Z_\alpha - 1) \\ &\quad \left. \left(\frac{\partial x_\beta}{\partial T} \right)_p \left(\frac{\partial Z}{\partial T} \right)_p - Z \left(\frac{\partial x_\beta}{\partial T} \right)_p \left(\frac{\partial Z_\alpha}{\partial T} \right)_p \right] \quad (A-102) \end{aligned}$$

Using Eqs. A-52 and A-58 in A-102 and simplifying results in

$$\begin{aligned} \left(\frac{\partial^2 Z}{\partial T^2} \right)_p &= \frac{Z}{Z_\alpha} \left\{ - \frac{2Z\sigma_T}{T} \left[x_\beta \left(\frac{\partial Z_\alpha}{\partial T} \right)_p + (Z_\alpha - 1) \left(\frac{\partial x_\beta}{\partial T} \right)_p \right] + (1-Zx_\beta) \right. \\ &\quad \left. \left(\frac{\partial^2 Z_\alpha}{\partial T^2} \right)_p - Z \left[2 \left(\frac{\partial Z_\alpha}{\partial T} \right)_p \left(\frac{\partial x_\beta}{\partial T} \right)_p + (Z_\alpha - 1) \left(\frac{\partial^2 x_\beta}{\partial T^2} \right)_p \right] \right\} \quad (A-103) \end{aligned}$$

In exactly the same manner, the second derivative with respect to pressure can be found and it is equivalent to Eq. A-103 with T replaced by p .

$$\begin{aligned} \left(\frac{\partial^2 Z}{\partial p^2} \right)_T &= \frac{Z}{Z_\alpha} \left\{ \frac{-2Z\sigma_p}{p} \left[x_\beta \left(\frac{\partial Z_\alpha}{\partial p} \right)_T + (Z_\alpha - 1) \left(\frac{\partial x_\beta}{\partial p} \right)_T \right] + (1-Zx_\beta) \left(\frac{\partial^2 Z_\alpha}{\partial p^2} \right)_T \right. \\ &\quad \left. - Z \left[2 \left(\frac{\partial Z_\alpha}{\partial p} \right)_T \left(\frac{\partial x_\beta}{\partial p} \right)_T + (Z_\alpha - 1) \left(\frac{\partial^2 x_\beta}{\partial p^2} \right)_T \right] \right\} \quad (A-104) \end{aligned}$$

Differentiating Eq. A-58 with respect to pressure gives

$$\begin{aligned}
 \frac{\partial^2 Z}{\partial T \partial p} &= \frac{1}{Z} \left(\frac{\partial Z}{\partial T} \right)_p \left(\frac{\partial Z}{\partial p} \right)_T - \frac{1}{Z_\alpha} \left(\frac{\partial Z}{\partial T} \right)_p \left(\frac{\partial Z_\alpha}{\partial p} \right)_T + \frac{Z}{Z_\alpha} \left[(1 - Z x_\beta) \right. \\
 &\left(\frac{\partial^2 Z_\alpha}{\partial T \partial p} \right) - Z \left(\frac{\partial Z_\alpha}{\partial T} \right)_p \left(\frac{\partial x_\beta}{\partial p} \right)_T - x_\beta \left(\frac{\partial Z}{\partial p} \right)_T \left(\frac{\partial Z_\alpha}{\partial T} \right)_p - Z (Z_\alpha - 1) \\
 &\left. \left(\frac{\partial^2 x_\beta}{\partial T \partial p} \right) - (Z_\alpha - 1) \left(\frac{\partial x_\beta}{\partial T} \right)_p \left(\frac{\partial Z}{\partial p} \right)_T - Z \left(\frac{\partial Z_\alpha}{\partial p} \right)_T \left(\frac{\partial x_\beta}{\partial T} \right)_p \right] \quad (A-105)
 \end{aligned}$$

Using the definition of σ_T and σ_p and rearranging Eq. A-105 results in the following expression

$$\begin{aligned}
 \frac{\partial^2 Z}{\partial T \partial p} &= \frac{Z \sigma_p}{p} \left\{ \frac{\sigma_T}{T} - \frac{Z}{Z_\alpha} \left[x_\beta \left(\frac{\partial Z_\alpha}{\partial T} \right)_p - (Z_\alpha - 1) \left(\frac{\partial x_\beta}{\partial T} \right)_p \right] \right\} - \frac{1}{Z_\alpha} \\
 &\left(\frac{\partial Z_\alpha}{\partial p} \right)_T \left[\frac{Z \sigma_T}{T} + Z^2 \left(\frac{\partial x_\beta}{\partial T} \right)_p \right] + \frac{Z}{Z_\alpha} \left\{ (1 - Z x_\beta) \left(\frac{\partial^2 Z_\alpha}{\partial T \partial p} \right) - Z \left[\left(\frac{\partial Z_\alpha}{\partial T} \right)_p \right. \right. \\
 &\left. \left. \left(\frac{\partial x_\beta}{\partial p} \right)_T + (Z_\alpha - 1) \left(\frac{\partial^2 x_\beta}{\partial T \partial p} \right) \right] \right\} \quad (A-106)
 \end{aligned}$$

The expressions for the second derivatives of Z_α can be obtained from Eqs. A-62 and A-63. Differentiating Eq. A-62 with respect to T

$$\left(\frac{\partial^2 Z_\alpha}{\partial T^2}\right)_P = P \left[(1-x_\beta) \frac{d^2 B'}{dT^2} - \frac{dB'}{dT} \left(\frac{\partial x_\beta}{\partial T}\right)_P B' \left(\frac{\partial^2 x_\beta}{\partial T^2}\right)_P - \frac{\partial B'}{\partial T} \left(\frac{\partial x_\beta}{\partial T}\right)_P \right] \quad (A-107)$$

or

$$\left(\frac{\partial^2 Z_\alpha}{\partial T^2}\right)_P = P \left[x_\alpha \frac{d^2 B'}{dT^2} - 2 \frac{dB'}{dT} \left(\frac{\partial x_\beta}{\partial T}\right)_P - B' \left(\frac{\partial^2 x_\beta}{\partial T^2}\right)_P \right] \quad (A-108)$$

From Eq. A-63

$$\left(\frac{\partial^2 Z_\alpha}{\partial p^2}\right)_T = -B' \left(\frac{\partial x_\beta}{\partial p}\right)_T - B' \left(\frac{\partial x_\beta}{\partial p}\right)_T - B' P \left(\frac{\partial^2 x_\beta}{\partial p^2}\right)_T \quad (A-109)$$

or

$$\left(\frac{\partial^2 Z_\alpha}{\partial p^2}\right)_T = -B' \left[2 \left(\frac{\partial x_\beta}{\partial p}\right)_T - P \left(\frac{\partial^2 x_\beta}{\partial p^2}\right)_T \right] \quad (A-110)$$

Differentiating Eq. A-63 with respect to T.

$$\frac{\partial^2 Z_\alpha}{\partial T \partial p} = (1-x_\beta) \frac{dB'}{dT} - B' \left(\frac{\partial x_\beta}{\partial T}\right)_P - P \left[\left(\frac{\partial x_\beta}{\partial p}\right)_T \frac{dB'}{dT} + B' \left(\frac{\partial^2 x_\beta}{\partial T \partial p}\right) \right] \quad (A-111)$$

or using Eq. A-62

$$\frac{\partial^2 Z_\alpha}{\partial T \partial p} = \frac{1}{p} \left(\frac{\partial Z_\alpha}{\partial T} \right)_p - p \left[\left(\frac{\partial x_\beta}{\partial p} \right)_T \frac{dB'}{dT} + B' \left(\frac{\partial^2 x_\beta}{\partial T \partial p} \right) \right] \quad (A-112)$$

5. Transport Properties

The transport properties are calculated using a modified Buckingham potential for temperatures up to 1000°K (19,39). In this region dissociation is not taken into consideration. For pressures above 0.01 atmospheres and temperatures less than 1000°K the gas is essentially pure molecular hydrogen and this is a good assumption. Above 1000°K the transport properties are for an equilibrium mixture of dissociating hydrogen (20). High pressure corrections are calculated from a theoretical formula due to Enskog (21).

a. Transport Properties Below 1000°K

Tabulated values of the collision integrals based on the modified Buckingham or "exp-six" potential used to calculate the transport properties below 1000°K are available in the literature (39,40). For these calculations the values of suitable functions of the collision integrals were fitted in the

least squares sense to empirical equations which are fourth order polynomials in a reduced temperature. The reduced temperature is

$$T^* = \frac{kT}{\epsilon}$$

where T is the absolute temperature, k is Boltzmann's constant, and ϵ is one of the potential parameters. The three parameters in the exp-six potential

$$\phi(r) = \frac{\epsilon}{1-\frac{6}{\alpha}} \left\{ \frac{6}{\alpha} \exp \left[\left(1 - \frac{r}{r_m}\right) \right] - \left(\frac{r_m}{r}\right)^6 \right\} \quad (\text{A-113})$$

are ϵ , the depth of the potential energy minimum; r_m , the position of the minimum; and α , a measure of the steepness of the repulsion energy. For hydrogen the values of the potential parameters are

$$\frac{k}{\epsilon} = 37.3 \text{ } ^\circ\text{K} \quad (\text{A-114})$$

$$\alpha = 14.0 \quad (\text{A-115})$$

$$r_m = 3.337 \text{ } ^\circ\text{A} \quad (\text{A-116})$$

The actual functions fitted to the empirical equations are

$$Z^{(ij)} = T^* \left(1 - \frac{6}{\alpha}\right) \Omega^{(ij)*} \quad (\text{A-117})$$

rather than the more rapidly varying $\Omega^{(ij)*}$ collision integrals.

The coefficient of viscosity of a pure gas is

$$\mu = \frac{5}{16} \left(\frac{WRT}{\pi}\right)^{1/2} \frac{f_{\mu}}{N_0 r_m^2 \Omega^{(22)*}(T^*)} \quad (\text{A-118})$$

where W is the molecular weight, R is the gas constant per mole, N_0 is Avogadro's number, f_{μ} is an infinite series which is nearly unity and its deviations from unity are corrections for the viscosity above the first approximation, and

$\Omega^{(22)*}(T^*)$ is the appropriate collision integral.

For calculations

$$\mu \times 10^7 = 266.93 \frac{\sqrt{WT} f_{\mu}}{r_m^2 \Omega^{(22)*}(T^*)} \quad (\text{A-119})$$

where μ is in poise, T is in degrees kelvin, and r_m is angstroms.

The third approximation for f_{μ} was used in calculating the viscosity of molecular hydrogen. The tabulated values were

fitted to an equation in the same manner as the collision integrals were fitted.

The formula for viscosity as given by Eq. A-119 is correct if the gas is at low pressure and simultaneous encounters of three or more molecules can be neglected. At high pressures the deviation due to the departure from an ideal gas can be accounted for by an equation of the form (20)

$$\frac{\mu_r}{\mu} = 1 + 0.175 (b_{px}) + 0.7557 (b_{px})^2 - 0.405 (b_{px})^3 \quad (A-120)$$

where μ is the value for an ideal gas as calculated using Eq. A-119 and μ_r is the corrected value. The quantity b_{px} can be shown to be given by

$$b_{px} = Z - 1 + T \left(\frac{\partial Z}{\partial T} \right)_p \quad (A-121)$$

where Z is the compressibility factor. The value of $\left(\frac{\partial Z}{\partial T} \right)_p$

can be determined as follows. Starting with

$$dZ = \left(\frac{\partial Z}{\partial T} \right)_p dT + \left(\frac{\partial Z}{\partial p} \right)_T dp \quad (A-122)$$

and dividing by dT

$$\left(\frac{\partial Z}{\partial T} \right)_p = \left(\frac{\partial Z}{\partial T} \right)_P + \left(\frac{\partial Z}{\partial p} \right)_T \left(\frac{\partial p}{\partial T} \right)_p \quad (A-123)$$

Then as the two derivatives of Z with respect to T and p are known and only $\left(\frac{\partial p}{\partial T}\right)_\rho$ must be determined. Noting that only the molecular species is present the equation of state is

$$p = Z_\alpha \rho \frac{R}{W} \quad T = Z \rho \frac{R}{W} T \quad (\text{A-124})$$

Then

$$\left(\frac{\partial p}{\partial T}\right)_\rho = Z \rho \frac{R}{W} + \rho \frac{R}{W} T \left(\frac{\partial Z}{\partial T}\right)_\rho \quad (\text{A-125})$$

as W is constant or

$$\left(\frac{\partial p}{\partial T}\right)_\rho = \frac{p}{T} + \frac{p}{Z} \left(\frac{\partial Z}{\partial T}\right)_\rho \quad (\text{A-126})$$

Combining Eqs. A-123 and A-126 and simplifying results in the following expression

$$\left(\frac{\partial Z}{\partial T}\right)_\rho = \frac{\left(\frac{\partial Z}{\partial T}\right)_p + \frac{p}{T} \left(\frac{\partial Z}{\partial p}\right)_T}{1 - \frac{p}{Z} \left(\frac{\partial Z}{\partial p}\right)_T} \quad (\text{A-127})$$

Using Eqs. A-62 and A-63 to evaluate the derivatives of Z and remembering that for the case being considered the mole fraction of the atomic species and its derivatives are zero the expression for $\left(\frac{\partial Z}{\partial T}\right)_\rho$ can be reduced to

$$\left(\frac{\partial Z}{\partial T}\right)_p = Z \frac{p}{T} \left[T \frac{dB'}{dT} + B' \right] \quad (\text{A-128})$$

Then Eq. A-121 can be simplified using Eqs. A-61 and A-128

$$b_{px} = p \left\{ B' + Z \left[T \frac{dB'}{dT} + B' \right] \right\} \quad (\text{A-129})$$

The thermal conductivity of a pure gas can be written as the sum of the two parts, λ^0 the translational portion and λ_{int} the internal portion, representing the contributions from translational motion and rotational and vibrational motions of the molecules respectively. The first approximation to the translational portion can be written as

$$\lambda^0 = \frac{15}{4} \frac{R}{W} \mu \quad (\text{A-130})$$

Consequently for higher approximations

$$\lambda^0 = \frac{15}{4} \frac{R}{W} \mu \frac{f_\lambda}{f_\mu} \quad (\text{A-131})$$

where f_λ is a series similar to f_μ but for the thermal conductivity rather than the viscosity.

The internal conductivity can be written as (20,41)

$$\lambda_{int} = \lambda - \lambda^0 = \frac{pD}{RT} \left(C_p - \frac{5}{2} R \right) \quad (\text{A-132})$$

where D the self-diffusion coefficient, is given to the third approximation by

$$D = \frac{2.628 \times 10^{-3} T^{3/2}}{p r_m^2 \Omega^{(11)*}(T^*)} f_D \quad (A-133)$$

The thermal conductivity of the pure gas is then the sum of the translational and internal portions.

$$\lambda = \lambda^0 + \lambda_{int} \quad (A-134)$$

A high pressure correction for the thermal conductivity similar to the one for viscosity is

$$\frac{\lambda}{\lambda_0} = 1 + 0.575 (b_{px}) + 0.5017 (b_{px})^2 - 0.204 (b_{px})^3 \quad (A-135)$$

b. Transport Properties Above 1000°K

The transport properties of dissociating hydrogen gas above 1000°K have been calculated and tabulated by vanderslice, et al (20). The development of the equations and the calculational procedure is explained in considerable detail in the report. Consequently very little explanation will be presented here.

As for the properties below 1000^oK, the collision integrals for the properties here have been fitted to fourth order polynomials: The only difference is that in this case the independent parameter is $T/1000$ rather than T^* .

The viscosity of the pure gas component is given by an equation similar to A-119 where f_μ is assumed to be unity and the collision integral $\langle \bar{\Omega}_{ii} \rangle$ includes the r_m^2 of Eq. A-119 where

$$\mu_i = \frac{2.66.93 \times 10^{-7} \sqrt{W_i T}}{\langle \bar{\Omega}_{ii}^{(22)} \rangle} \quad (\text{A-136})$$

The viscosity of the binary mixture is

$$\mu = \left[\frac{x_\alpha^2}{H_{\alpha\alpha}} + \frac{x_\beta^2}{H_{\beta\beta}} - \frac{2x_\alpha x_\beta H_{\alpha\beta}}{H_{\alpha\alpha} H_{\beta\beta}} \right] \left[1 - \frac{H_{\alpha\beta}^2}{H_{\alpha\alpha} H_{\beta\beta}} \right] \quad (\text{A-137})$$

where

$$H_{\alpha\alpha} = \frac{x_\alpha^2}{\mu_\alpha} + \frac{2x_\alpha x_\beta}{W_\alpha + W_\beta} \frac{RT}{pD_{\alpha\beta}} \left[1 + \frac{3W_\beta \langle A_{12}^* \rangle}{5W_\alpha} \right] \quad (\text{A-138})$$

$$H_{\alpha\beta} = - \frac{2x_\alpha x_\beta}{W_\alpha + W_\beta} \frac{RT}{pD_{\alpha\beta}} \left[1 - \frac{3}{5} \langle A_{12}^* \rangle \right] \quad (\text{A-139})$$

The value of $H_{\beta\beta}$ is found by interchanging subscripts in Eq. A-138. The diffusion coefficient is given by

$$D_{ij} = \frac{(2.628 \times 10^{-3}) T^{3/2}}{p \langle \bar{\Omega}_{ij} \rangle (1,1)} \left(\frac{W_i + W_j}{2W_i W_j} \right)^{1/2} \quad (A-140)$$

If i and j are different species than D_{ij} is the mutual diffusion coefficient, but if $j = i$ then D_{ii} is called the self diffusion coefficient and Eq. A-140 reduces to an expression like that in Eq. A-133.

The thermal conductivity of the mixture can be written as the sum of three parts. As for a single component polyatomic gas or non-reacting mixture, there are the internal and the translational conductivities and there is an additional portion due to the chemical reaction.

The translational thermal conductivity of a pure gas to the first approximation is given by Eq. A-130.

The translational conductivity of a binary mixture is

$$\lambda^0 = -4 \left[\frac{x_\alpha^2}{L_{\alpha\alpha}} + \frac{x_\beta^2}{L_{\beta\beta}} - \frac{2x_\alpha x_\beta L_{\alpha\beta}}{L_{\alpha\alpha} L_{\beta\beta}} \right] \left[1 - \frac{L_{\alpha\beta}^2}{L_{\alpha\alpha} L_{\beta\beta}} \right]^{-1} \quad (A-141)$$

where

$$L_{\alpha\alpha} = - \frac{4x_\alpha^2}{\lambda_\alpha^0} - \frac{16}{25} \frac{x_\alpha x_\beta}{(W_\alpha + W_\beta)^2} \frac{T}{p D_{\alpha\beta}} \left[\frac{15}{2} W_\alpha^2 + \frac{25}{4} W_\beta^2 - 3W_\beta^2 \langle B_{12}^* \rangle + 4W_\alpha W_\beta \langle A_{12}^* \rangle \right] \quad (A-142)$$

$$L_{\alpha\beta} = \frac{16}{25} \frac{x_{\alpha} x_{\beta} w_{\alpha} w_{\beta}}{(w_{\alpha} + w_{\beta})^2} \frac{T}{pD_{\alpha\beta}} \left[\frac{55}{4} - 3 \langle B_{12}^* \rangle - 4 \langle A_{12}^* \rangle \right] \quad (A-143)$$

The value of $L_{\beta\beta}$ is obtained by interchanging subscripts in Eq. A-142. The internal thermal conductivity of the mixture is

$$\lambda_{int} = \frac{\lambda_{\alpha} - \lambda_{\alpha}^0}{1 + (D_{\alpha\alpha}/D_{\alpha\beta})(x_{\beta}/x_{\alpha})} + \frac{\lambda_{\beta} - \lambda_{\beta}^0}{1 + (D_{\beta\beta}/D_{\alpha\beta})(x_{\alpha}/x_{\beta})} \quad (A-144)$$

where for the individual species

$$\lambda_i - \lambda_i^0 = \frac{pD_{ii}}{RT} (c_{pi} - \frac{5}{2} R) \quad (A-145)$$

is expressed in Eq. A-132. It should be noted that for the atomic hydrogen species $\lambda_{\beta} - \lambda_{\beta}^0$ is equal to zero.

The portion of the thermal conductivity due to chemical reaction is

$$\lambda_R = \left[\frac{pD_{\alpha\beta}}{RT} \frac{(\Delta H)^2}{RT^2} \right] \left[\frac{x_{\alpha} x_{\beta}}{(1-x_{\alpha})^2} \right] \quad (A-146)$$

The thermal conductivity of the chemically reacting mix-

ture is then

$$\lambda = \lambda^{\circ} + \lambda_{\text{int}} + \lambda_{\text{R}} \quad (\text{A-147})$$

6. Hydrogen Property Results

Tabulated values of the properties assuming equilibrium composition are presented in Tables A-1, A-2, and A-3 for three different pressure levels. The same properties are plotted versus temperature in Figs. A-1 through A-19.

The property values were checked with tabulated values in reference 18 and with other data in the references in regions where it is available. Except for the thermal conductivity and Prandtl number the differences in the property values calculated with the subroutine and the values tabulated in reference 18 are less than 5 % . For temperatures above 300°K the agreement is within 1 % . The thermal conductivity and consequently the Prandtl number agree within 6 % for values of temperatures up to 700°K as tabulated in reference 18. The values as tabulated there were computed from an empirical formula about which the experimental data deviates by plus or minus about 5 % . Consequently the values calculated using this subroutine are within a reasonable accuracy.

TABLE A-1

HYDROGEN PROPERTIES-EQUILIBRIUM COMPOSITION

P= 1.00 ATM

T DEG K	Z	XB	W GM/GM-MOLE	10000 RHO GM/CM ³
150.0	1.0008	0.	2.01626	1.6366
200.0	1.0008	0.	2.01626	1.2276
300.0	1.0006	0.	2.01626	0.8185
400.0	1.0005	0.	2.01626	0.6140
500.0	1.0004	0.	2.01626	0.4912
600.0	1.0003	0.	2.01626	0.4094
700.0	1.0003	0.0000	2.01626	0.3509
800.0	1.0003	0.0000	2.01626	0.3070
900.0	1.0002	0.0000	2.01626	0.2729
1000.0	1.0002	0.0000	2.01626	0.2457
1100.0	1.0002	0.0000	2.01626	0.2233
1200.0	1.0002	0.0000	2.01626	0.2047
1300.0	1.0001	0.0000	2.01626	0.1890
1400.0	1.0001	0.0000	2.01626	0.1755
1500.0	1.0001	0.0000	2.01624	0.1638
1600.0	1.0001	0.0001	2.01621	0.1535
1700.0	1.0001	0.0001	2.01611	0.1445
1800.0	1.0001	0.0004	2.01590	0.1365
1900.0	1.0001	0.0008	2.01546	0.1293
2000.0	1.0001	0.0016	2.01463	0.1227
2100.0	1.0001	0.0031	2.01314	0.1168
2200.0	1.0001	0.0056	2.01062	0.1114
2300.0	1.0001	0.0096	2.00659	0.1063
2400.0	1.0001	0.0157	2.00042	0.1016
2500.0	1.0001	0.0247	1.99134	0.0971
2600.0	1.0001	0.0375	1.97846	0.0927
2700.0	1.0001	0.0550	1.96082	0.0885
2800.0	1.0001	0.0782	1.93741	0.0843
2900.0	1.0000	0.1081	1.90731	0.0801
3000.0	1.0000	0.1453	1.86975	0.0759
3100.0	1.0000	0.1904	1.82430	0.0717
3200.0	1.0000	0.2433	1.77096	0.0674
3300.0	1.0000	0.3035	1.71032	0.0632
3400.0	1.0000	0.3696	1.64363	0.0589
3500.0	1.0000	0.4399	1.57279	0.0548
3600.0	1.0000	0.5119	1.50021	0.0508
3700.0	1.0000	0.5829	1.42859	0.0471
3800.0	1.0000	0.6504	1.36058	0.0436
3900.0	1.0000	0.7121	1.29838	0.0406
4000.0	1.0000	0.7665	1.24350	0.0379

TABLE A-1 CONT.

HYDROGEN PROPERTIES-EQUILIBRIUM COMPOSITION

P= 1.00 ATM

T DEG K	H CAL/GM	S CAL/GM-K	CP CAL/GM-K	DH/DP CAL/GM-PSI
150.0	33933.6	13.237	3.037	0.3202E-02
200.0	34089.9	14.135	3.214	0.4807E-02
300.0	34424.6	15.489	3.417	0.7834E-02
400.0	34768.7	16.479	3.460	0.1029E-01
500.0	35115.1	17.252	3.460	0.1209E-01
600.0	35462.0	17.884	3.476	0.1332E-01
700.0	35810.1	18.421	3.485	0.1409E-01
800.0	36159.8	18.888	3.511	0.1452E-01
900.0	36512.4	19.303	3.542	0.1469E-01
1000.0	36868.3	19.678	3.577	0.1469E-01
1100.0	37228.2	20.021	3.622	0.1455E-01
1200.0	37592.8	20.338	3.671	0.1423E-01
1300.0	37962.5	20.634	3.723	0.1321E-01
1400.0	38337.5	20.912	3.777	0.9622E-02
1500.0	38717.9	21.174	3.832	-0.2054E-02
1600.0	39104.0	21.423	3.892	-0.3545E-01
1700.0	39496.6	21.661	3.962	-0.1198E-00
1800.0	39897.1	21.890	4.053	-0.3113E-00
1900.0	40308.3	22.113	4.179	-0.7076E 00
2000.0	40734.6	22.331	4.359	-0.1467E 01
2100.0	41182.9	22.550	4.621	-0.2827E 01
2200.0	41662.7	22.773	4.998	-0.5129E 01
2300.0	42187.6	23.006	5.529	-0.8836E 01
2400.0	42775.1	23.256	6.258	-0.1455E 02
2500.0	43447.4	23.530	7.233	-0.2303E 02
2600.0	44231.5	23.838	8.503	-0.3520E 02
2700.0	45159.4	24.188	10.118	-0.5214E 02
2800.0	46268.1	24.591	12.125	-0.7508E 02
2900.0	47598.8	25.057	14.562	-0.1053E 03
3000.0	49195.7	25.599	17.453	-0.1442E 03
3100.0	51104.4	26.224	20.795	-0.1929E 03
3200.0	53368.4	26.943	24.547	-0.2521E 03
3300.0	56024.1	27.760	28.606	-0.3216E 03
3400.0	59093.6	28.676	32.783	-0.3997E 03
3500.0	62575.1	29.684	36.789	-0.4828E 03
3600.0	66432.9	30.771	40.239	-0.5645E 03
3700.0	70590.0	31.910	42.703	-0.6366E 03
3800.0	74927.4	33.067	43.791	-0.6896E 03
3900.0	79294.8	34.201	43.285	-0.7160E 03
4000.0	83532.3	35.274	41.223	-0.7118E 03

TABLE A-1 CONT.

HYDROGEN PROPERTIES-EQUILIBRIUM COMPOSITION

P= 1.00 ATM

T DEG K	DS/DT CAL/GM-K2	DS/DP CAL/GM-K-PSI	OMEGT	OMEGP
150.0	0.2025E-01	-0.6706E-01	-0.	0.
200.0	0.1607E-01	-0.6705E-01	-0.	0.
300.0	0.1139E-01	-0.6704E-01	-0.	0.
400.0	0.8650E-02	-0.6703E-01	-0.	0.
500.0	0.6920E-02	-0.6702E-01	-0.	0.
600.0	0.5794E-02	-0.6702E-01	-0.1014E-14	0.1150E-16
700.0	0.4978E-02	-0.6702E-01	-0.4765E-12	0.6290E-14
800.0	0.4389E-02	-0.6702E-01	-0.4791E-10	0.7207E-12
900.0	0.3935E-02	-0.6702E-01	-0.1723E-08	0.2908E-10
1000.0	0.3577E-02	-0.6702E-01	-0.3018E-07	0.5646E-09
1100.0	0.3293E-02	-0.6702E-01	-0.3134E-06	0.6432E-08
1200.0	0.3059E-02	-0.6702E-01	-0.2198E-05	0.4910E-07
1300.0	0.2864E-02	-0.6702E-01	-0.1140E-04	0.2752E-06
1400.0	0.2698E-02	-0.6702E-01	-0.4665E-04	0.1210E-05
1500.0	0.2555E-02	-0.6703E-01	-0.1579E-03	0.4380E-05
1600.0	0.2432E-02	-0.6705E-01	-0.4582E-03	0.1353E-04
1700.0	0.2330E-02	-0.6710E-01	-0.1171E-02	0.3667E-04
1800.0	0.2251E-02	-0.6721E-01	-0.2693E-02	0.8910E-04
1900.0	0.2199E-02	-0.6743E-01	-0.5662E-02	0.1975E-03
2000.0	0.2180E-02	-0.6782E-01	-0.1104E-01	0.4045E-03
2100.0	0.2201E-02	-0.6848E-01	-0.2016E-01	0.7744E-03
2200.0	0.2272E-02	-0.6955E-01	-0.3479E-01	0.1398E-02
2300.0	0.2404E-02	-0.7119E-01	-0.5715E-01	0.2398E-02
2400.0	0.2608E-02	-0.7362E-01	-0.8985E-01	0.3928E-02
2500.0	0.2893E-02	-0.7708E-01	-0.1359E-00	0.6180E-02
2600.0	0.3270E-02	-0.8185E-01	-0.1983E-00	0.9370E-02
2700.0	0.3747E-02	-0.8823E-01	-0.2804E-00	0.1374E-01
2800.0	0.4330E-02	-0.9657E-01	-0.3846E-00	0.1952E-01
2900.0	0.5021E-02	-0.1072E-00	-0.5128E 00	0.2693E-01
3000.0	0.5818E-02	-0.1203E-00	-0.6653E 00	0.3611E-01
3100.0	0.6708E-02	-0.1363E-00	-0.8402E 00	0.4708E-01
3200.0	0.7671E-02	-0.1551E-00	-0.1032E 01	0.5966E-01
3300.0	0.8669E-02	-0.1765E-00	-0.1233E 01	0.7344E-01
3400.0	0.9642E-02	-0.1998E-00	-0.1430E 01	0.8766E-01
3500.0	0.1051E-01	-0.2239E-00	-0.1606E 01	0.1012E-00
3600.0	0.1118E-01	-0.2469E-00	-0.1741E 01	0.1128E-00
3700.0	0.1154E-01	-0.2666E-00	-0.1819E 01	0.1211E-00
3800.0	0.1152E-01	-0.2808E-00	-0.1827E 01	0.1248E-00
3900.0	0.1110E-01	-0.2877E-00	-0.1764E 01	0.1236E-00
4000.0	0.1031E-01	-0.2866E-00	-0.1638E 01	0.1176E-00

TABLE A-1 CONT.

HYDROGEN PROPERTIES-EQUILIBRIUM COMPOSITION

P= 1.00 ATM

T DEG K	SIGT	SIGP	ZETAT	ZETAP
150.0	-0.3182E-03	0.8483E-03	-0.8244E-01	0.2132E-02
200.0	-0.3583E-03	0.7508E-03	-0.9599E-01	0.1784E-02
300.0	-0.3894E-03	0.5980E-03	-0.2031E-01	0.1317E-02
400.0	-0.3836E-03	0.4863E-03	-0.1314E-01	0.1018E-02
500.0	-0.3608E-03	0.4030E-03	-0.1189E-01	0.8140E-03
600.0	-0.3312E-03	0.3398E-03	-0.9716E-02	0.6699E-03
700.0	-0.3003E-03	0.2911E-03	-0.1960E-01	0.5651E-03
800.0	-0.2707E-03	0.2529E-03	-0.2588E-01	0.4873E-03
900.0	-0.2434E-03	0.2227E-03	-0.3284E-01	0.4280E-03
1000.0	-0.2191E-03	0.1983E-03	-0.4608E-01	0.3818E-03
1100.0	-0.1977E-03	0.1784E-03	-0.5370E-01	0.3453E-03
1200.0	-0.1791E-03	0.1621E-03	-0.6117E-01	0.3185E-03
1300.0	-0.1630E-03	0.1484E-03	-0.6587E-01	0.3076E-03
1400.0	-0.1492E-03	0.1368E-03	-0.7033E-01	0.3343E-03
1500.0	-0.1375E-03	0.1270E-03	-0.7579E-01	0.4491E-03
1600.0	-0.1277E-03	0.1184E-03	-0.8439E-01	0.7484E-03
1700.0	-0.1196E-03	0.1109E-03	-0.1007E-00	0.1387E-02
1800.0	-0.1132E-03	0.1043E-03	-0.1282E-00	0.2569E-02
1900.0	-0.1084E-03	0.9836E-04	-0.1680E-00	0.4503E-02
2000.0	-0.1054E-03	0.9295E-04	-0.2195E-00	0.7296E-02
2100.0	-0.1042E-03	0.8797E-04	-0.2766E-00	0.1083E-01
2200.0	-0.1049E-03	0.8331E-04	-0.3338E-00	0.1466E-01
2300.0	-0.1078E-03	0.7888E-04	-0.3737E-00	0.1809E-01
2400.0	-0.1131E-03	0.7459E-04	-0.3867E-00	0.2048E-01
2500.0	-0.1206E-03	0.7039E-04	-0.3711E-00	0.2145E-01
2600.0	-0.1303E-03	0.6619E-04	-0.3329E-00	0.2105E-01
2700.0	-0.1417E-03	0.6195E-04	-0.2808E-00	0.1960E-01
2800.0	-0.1539E-03	0.5759E-04	-0.2227E-00	0.1751E-01
2900.0	-0.1657E-03	0.5309E-04	-0.1651E-00	0.1514E-01
3000.0	-0.1757E-03	0.4841E-04	-0.1115E-00	0.1276E-01
3100.0	-0.1822E-03	0.4355E-04	-0.6320E-01	0.1048E-01
3200.0	-0.1834E-03	0.3851E-04	-0.2080E-01	0.8351E-02
3300.0	-0.1784E-03	0.3336E-04	0.1817E-01	0.6367E-02
3400.0	-0.1666E-03	0.2820E-04	0.5399E-01	0.4500E-02
3500.0	-0.1489E-03	0.2317E-04	0.8792E-01	0.2693E-02
3600.0	-0.1267E-03	0.1844E-04	0.1213E-00	0.8761E-03
3700.0	-0.1026E-03	0.1418E-04	0.1557E-00	-0.1044E-02
3800.0	-0.7901E-04	0.1053E-04	0.1924E-00	-0.3186E-02
3900.0	-0.5799E-04	0.7556E-05	0.2342E-00	-0.5712E-02
4000.0	-0.4078E-04	0.5261E-05	0.2833E-00	-0.8803E-02

TABLE A-1 CONT.

HYDROGEN PROPERTIES-EQUILIBRIUM COMPOSITION

P= 1.00 ATM

T DEG K	GAMMA	1000 MU GM/CM-SEC	1000 LAMBDA CAL/CM-SEC-K	PR
150.0	1.483	0.0553	0.2470	0.6800
200.0	1.444	0.0679	0.3197	0.6826
300.0	1.407	0.0898	0.4486	0.6843
400.0	1.399	0.1090	0.5518	0.6836
500.0	1.399	0.1265	0.6411	0.6827
600.0	1.396	0.1428	0.7277	0.6823
700.0	1.395	0.1583	0.8089	0.6819
800.0	1.391	0.1731	0.8915	0.6817
900.0	1.386	0.1874	0.9735	0.6817
1000.0	1.381	0.1999	1.0467	0.6833
1100.0	1.374	0.2126	1.1293	0.6819
1200.0	1.367	0.2250	1.2138	0.6805
1300.0	1.360	0.2373	1.3007	0.6792
1400.0	1.353	0.2493	1.3891	0.6779
1500.0	1.346	0.2613	1.4804	0.6763
1600.0	1.340	0.2731	1.5764	0.6743
1700.0	1.332	0.2849	1.6815	0.6712
1800.0	1.324	0.2965	1.8042	0.6661
1900.0	1.313	0.3082	1.9573	0.6579
2000.0	1.300	0.3198	2.1597	0.6456
2100.0	1.285	0.3315	2.4379	0.6284
2200.0	1.266	0.3432	2.8273	0.6067
2300.0	1.247	0.3551	3.3723	0.5822
2400.0	1.226	0.3672	4.1246	0.5571
2500.0	1.207	0.3795	5.1417	0.5339
2600.0	1.191	0.3922	6.4845	0.5143
2700.0	1.177	0.4054	8.2131	0.4994
2800.0	1.166	0.4190	10.3782	0.4895
2900.0	1.158	0.4331	13.0124	0.4847
3000.0	1.153	0.4477	16.1186	0.4847
3100.0	1.150	0.4624	19.6556	0.4892
3200.0	1.148	0.4771	23.5222	0.4978
3300.0	1.148	0.4911	27.5446	0.5100
3400.0	1.149	0.5039	31.4639	0.5250
3500.0	1.152	0.5148	34.9496	0.5419
3600.0	1.155	0.5233	37.6331	0.5595
3700.0	1.160	0.5291	39.1728	0.5768
3800.0	1.165	0.5323	39.3401	0.5925
3900.0	1.171	0.5333	38.0984	0.6060
4000.0	1.179	0.5329	35.6270	0.6166

TABLE A-2

HYDROGEN PROPERTIES-EQUILIBRIUM COMPOSITION

P= 10.00 ATM

T DEG K	Z	XB	W GM/GM-MOLE	10000 RHO GM/CM3
150.0	1.0085	0.	2.01626	16.2421
200.0	1.0075	0.	2.01626	12.1934
300.0	1.0060	0.	2.01626	8.1413
400.0	1.0049	0.	2.01626	6.1128
500.0	1.0040	0.	2.01626	4.8943
600.0	1.0034	0.	2.01626	4.0811
700.0	1.0029	0.0000	2.01626	3.4998
800.0	1.0025	0.0000	2.01626	3.0635
900.0	1.0022	0.0000	2.01626	2.7239
1000.0	1.0020	0.0000	2.01626	2.4521
1100.0	1.0018	0.0000	2.01626	2.2297
1200.0	1.0016	0.0000	2.01626	2.0442
1300.0	1.0015	0.0000	2.01626	1.8872
1400.0	1.0014	0.0000	2.01626	1.7526
1500.0	1.0013	0.0000	2.01625	1.6359
1600.0	1.0012	0.0000	2.01624	1.5338
1700.0	1.0011	0.0000	2.01621	1.4437
1800.0	1.0010	0.0001	2.01615	1.3635
1900.0	1.0010	0.0002	2.01601	1.2917
2000.0	1.0009	0.0005	2.01574	1.2270
2100.0	1.0009	0.0010	2.01527	1.1684
2200.0	1.0008	0.0018	2.01447	1.1149
2300.0	1.0008	0.0030	2.01319	1.0658
2400.0	1.0008	0.0050	2.01122	1.0204
2500.0	1.0007	0.0079	2.00831	0.9782
2600.0	1.0007	0.0120	2.00415	0.9387
2700.0	1.0006	0.0177	1.99839	0.9014
2800.0	1.0006	0.0254	1.99062	0.8658
2900.0	1.0006	0.0355	1.98043	0.8317
3000.0	1.0005	0.0485	1.96738	0.7987
3100.0	1.0005	0.0647	1.95101	0.7666
3200.0	1.0004	0.0846	1.93094	0.7350
3300.0	1.0004	0.1086	1.90681	0.7038
3400.0	1.0004	0.1368	1.87837	0.6730
3500.0	1.0003	0.1694	1.84548	0.6423
3600.0	1.0003	0.2064	1.80818	0.6119
3700.0	1.0003	0.2476	1.76666	0.5817
3800.0	1.0002	0.2926	1.72131	0.5519
3900.0	1.0002	0.3408	1.67274	0.5226
4000.0	1.0002	0.3914	1.62171	0.4940

TABLE A-2 CONT.

HYDROGEN PROPERTIES-EQUILIBRIUM COMPOSITION

P= 10.00 ATM

T DEG K	H CAL/GM	S CAL/GM-K	CP CAL/GM-K	DH/DP CAL/GM-PSI
150.0	33934.1	10.964	3.042	0.3202E-02
200.0	34090.6	11.864	3.219	0.4807E-02
300.0	34425.6	13.219	3.421	0.7834E-02
400.0	34770.0	14.210	3.463	0.1029E-01
500.0	35116.7	14.983	3.462	0.1209E-01
600.0	35463.7	15.616	3.478	0.1332E-01
700.0	35812.0	16.153	3.485	0.1409E-01
800.0	36161.8	16.620	3.511	0.1452E-01
900.0	36514.4	17.035	3.542	0.1469E-01
1000.0	36870.3	17.410	3.577	0.1469E-01
1100.0	37230.1	17.753	3.622	0.1458E-01
1200.0	37594.7	18.070	3.670	0.1440E-01
1300.0	37964.4	18.366	3.723	0.1417E-01
1400.0	38339.3	18.644	3.775	0.1386E-01
1500.0	38719.4	18.906	3.828	0.1332E-01
1600.0	39104.9	19.155	3.881	0.1212E-01
1700.0	39495.7	19.392	3.936	0.9368E-02
1800.0	39892.4	19.619	3.998	0.3289E-02
1900.0	40295.6	19.837	4.069	-0.9200E-02
2000.0	40706.7	20.047	4.156	-0.3308E-01
2100.0	41127.6	20.253	4.267	-0.7589E-01
2200.0	41561.2	20.454	4.412	-0.1484E-00
2300.0	42011.5	20.655	4.605	-0.2652E-00
2400.0	42484.2	20.856	4.860	-0.4454E-00
2500.0	42986.0	21.060	5.191	-0.7131E 00
2600.0	43525.3	21.272	5.614	-0.1098E 01
2700.0	44112.3	21.493	6.146	-0.1634E 01
2800.0	44758.7	21.728	6.805	-0.2361E 01
2900.0	45477.8	21.981	7.603	-0.3326E 01
3000.0	46284.5	22.254	8.556	-0.4578E 01
3100.0	47194.6	22.552	9.675	-0.6171E 01
3200.0	48225.2	22.880	10.968	-0.8159E 01
3300.0	49394.2	23.239	12.444	-0.1060E 02
3400.0	50719.7	23.635	14.098	-0.1355E 02
3500.0	52219.3	24.069	15.923	-0.1704E 02
3600.0	53909.4	24.545	17.903	-0.2111E 02
3700.0	55804.0	25.064	20.008	-0.2576E 02
3800.0	57913.5	25.627	22.193	-0.3097E 02
3900.0	60243.2	26.232	24.400	-0.3666E 02
4000.0	62791.5	26.877	26.548	-0.4268E 02

TABLE A-2 CONT.

HYDROGEN PROPERTIES-EQUILIBRIUM COMPOSITION

P= 10.00 ATM

T DEG K	DS/DT CAL/GM-K2	DS/DP CAL/GM-K-PSI	OMEGT	OMEGP
150.0	0.2028E-01	-0.6738E-02	-0.	0.
200.0	0.1609E-01	-0.6728E-02	-0.	0.
300.0	0.1140E-01	-0.6716E-02	-0.	0.
400.0	0.8657E-02	-0.6709E-02	-0.	0.
500.0	0.6924E-02	-0.6705E-02	-0.	0.
600.0	0.5796E-02	-0.6703E-02	-0.3206E-15	0.3637E-17
700.0	0.4979E-02	-0.6702E-02	-0.1507E-12	0.1989E-14
800.0	0.4389E-02	-0.6701E-02	-0.1515E-10	0.2279E-12
900.0	0.3935E-02	-0.6701E-02	-0.5449E-09	0.9197E-11
1000.0	0.3577E-02	-0.6701E-02	-0.9545E-08	0.1785E-09
1100.0	0.3292E-02	-0.6701E-02	-0.9910E-07	0.2034E-08
1200.0	0.3059E-02	-0.6701E-02	-0.6951E-06	0.1553E-07
1300.0	0.2864E-02	-0.6701E-02	-0.3605E-05	0.8704E-07
1400.0	0.2697E-02	-0.6701E-02	-0.1475E-04	0.3827E-06
1500.0	0.2552E-02	-0.6702E-02	-0.4994E-04	0.1385E-05
1600.0	0.2426E-02	-0.6703E-02	-0.1449E-03	0.4279E-05
1700.0	0.2316E-02	-0.6704E-02	-0.3704E-03	0.1160E-04
1800.0	0.2221E-02	-0.6708E-02	-0.8516E-03	0.2818E-04
1900.0	0.2142E-02	-0.6714E-02	-0.1791E-02	0.6246E-04
2000.0	0.2078E-02	-0.6727E-02	-0.3492E-02	0.1280E-03
2100.0	0.2032E-02	-0.6747E-02	-0.6381E-02	0.2452E-03
2200.0	0.2005E-02	-0.6781E-02	-0.1102E-01	0.4430E-03
2300.0	0.2002E-02	-0.6833E-02	-0.1813E-01	0.7607E-03
2400.0	0.2025E-02	-0.6910E-02	-0.2857E-01	0.1249E-02
2500.0	0.2076E-02	-0.7019E-02	-0.4334E-01	0.1971E-02
2600.0	0.2159E-02	-0.7169E-02	-0.6357E-01	0.3003E-02
2700.0	0.2276E-02	-0.7371E-02	-0.9045E-01	0.4432E-02
2800.0	0.2430E-02	-0.7636E-02	-0.1252E-00	0.6357E-02
2900.0	0.2622E-02	-0.7974E-02	-0.1691E-00	0.8882E-02
3000.0	0.2852E-02	-0.8398E-02	-0.2232E-00	0.1211E-01
3100.0	0.3121E-02	-0.8920E-02	-0.2884E-00	0.1616E-01
3200.0	0.3428E-02	-0.9551E-02	-0.3654E-00	0.2112E-01
3300.0	0.3771E-02	-0.1030E-01	-0.4543E-00	0.2705E-01
3400.0	0.4146E-02	-0.1118E-01	-0.5549E 00	0.3401E-01
3500.0	0.4550E-02	-0.1219E-01	-0.6659E 00	0.4199E-01
3600.0	0.4973E-02	-0.1334E-01	-0.7857E 00	0.5092E-01
3700.0	0.5407E-02	-0.1461E-01	-0.9114E 00	0.6066E-01
3800.0	0.5840E-02	-0.1600E-01	-0.1039E 01	0.7099E-01
3900.0	0.6257E-02	-0.1748E-01	-0.1164E 01	0.8160E-01
4000.0	0.6637E-02	-0.1901E-01	-0.1282E 01	0.9205E-01

TABLE A-2 CONT.

HYDROGEN PROPERTIES-EQUILIBRIUM COMPOSITION

P= 10.00 ATM

T DEG K	SIGT	SIGP	ZETAT	ZETAP
150.0	-0.3158E-02	0.8419E-02	-0.9323E-01	0.2123E-01
200.0	-0.3559E-02	0.7458E-02	-0.1068E-00	0.1775E-01
300.0	-0.3873E-02	0.5948E-02	-0.3007E-01	0.1311E-01
400.0	-0.3819E-02	0.4842E-02	-0.2189E-01	0.1014E-01
500.0	-0.3594E-02	0.4015E-02	-0.1951E-01	0.8113E-02
600.0	-0.3302E-02	0.3387E-02	-0.1628E-01	0.6679E-02
700.0	-0.2995E-02	0.2903E-02	-0.2522E-01	0.5637E-02
800.0	-0.2700E-02	0.2524E-02	-0.3072E-01	0.4863E-02
900.0	-0.2430E-02	0.2222E-02	-0.3705E-01	0.4272E-02
1000.0	-0.2187E-02	0.1979E-02	-0.4977E-01	0.3811E-02
1100.0	-0.1974E-02	0.1782E-02	-0.5697E-01	0.3442E-02
1200.0	-0.1788E-02	0.1618E-02	-0.6403E-01	0.3142E-02
1300.0	-0.1627E-02	0.1482E-02	-0.6813E-01	0.2894E-02
1400.0	-0.1490E-02	0.1367E-02	-0.7134E-01	0.2694E-02
1500.0	-0.1373E-02	0.1268E-02	-0.7397E-01	0.2549E-02
1600.0	-0.1274E-02	0.1183E-02	-0.7666E-01	0.2483E-02
1700.0	-0.1192E-02	0.1108E-02	-0.8196E-01	0.2544E-02
1800.0	-0.1124E-02	0.1042E-02	-0.9117E-01	0.2803E-02
1900.0	-0.1069E-02	0.9832E-03	-0.1044E-00	0.3351E-02
2000.0	-0.1027E-02	0.9298E-03	-0.1227E-00	0.4286E-02
2100.0	-0.9965E-03	0.8809E-03	-0.1456E-00	0.5690E-02
2200.0	-0.9768E-03	0.8357E-03	-0.1783E-00	0.7585E-02
2300.0	-0.9677E-03	0.7934E-03	-0.2132E-00	0.9895E-02
2400.0	-0.9690E-03	0.7536E-03	-0.2461E-00	0.1244E-01
2500.0	-0.9802E-03	0.7158E-03	-0.2723E-00	0.1495E-01
2600.0	-0.1001E-02	0.6795E-03	-0.2889E-00	0.1713E-01
2700.0	-0.1030E-02	0.6444E-03	-0.2937E-00	0.1873E-01
2800.0	-0.1067E-02	0.6103E-03	-0.2847E-00	0.1959E-01
2900.0	-0.1109E-02	0.5770E-03	-0.2639E-00	0.1970E-01
3000.0	-0.1155E-02	0.5443E-03	-0.2344E-00	0.1917E-01
3100.0	-0.1201E-02	0.5120E-03	-0.1995E-00	0.1813E-01
3200.0	-0.1243E-02	0.4801E-03	-0.1641E-00	0.1675E-01
3300.0	-0.1279E-02	0.4485E-03	-0.1264E-00	0.1515E-01
3400.0	-0.1304E-02	0.4171E-03	-0.8973E-01	0.1345E-01
3500.0	-0.1315E-02	0.3860E-03	-0.5491E-01	0.1173E-01
3600.0	-0.1309E-02	0.3552E-03	-0.2213E-01	0.1004E-01
3700.0	-0.1284E-02	0.3247E-03	0.8684E-02	0.8381E-02
3800.0	-0.1239E-02	0.2947E-03	0.3685E-01	0.6769E-02
3900.0	-0.1175E-02	0.2654E-03	0.6419E-01	0.5182E-02
4000.0	-0.1093E-02	0.2369E-03	0.9065E-01	0.3612E-02

TABLE A-2 CONT.

HYDROGEN PROPERTIES-EQUILIBRIUM COMPOSITION

P= 10.00 ATM

T DEG K	GAMMA	1000 MU GM/CM-SEC	1000 LAMBDA CAL/CM-SEC-K	PR
150.0	1.512	0.0554	0.2488	0.6776
200.0	1.468	0.0680	0.3216	0.6807
300.0	1.424	0.0900	0.4505	0.6831
400.0	1.412	0.1091	0.5535	0.6828
500.0	1.409	0.1266	0.6426	0.6820
600.0	1.405	0.1429	0.7290	0.6817
700.0	1.402	0.1584	0.8101	0.6813
800.0	1.397	0.1732	0.8925	0.6812
900.0	1.391	0.1874	0.9745	0.6812
1000.0	1.385	0.2000	1.0476	0.6828
1100.0	1.378	0.2127	1.1302	0.6814
1200.0	1.371	0.2251	1.2147	0.6801
1300.0	1.364	0.2373	1.3014	0.6789
1400.0	1.357	0.2494	1.3894	0.6776
1500.0	1.350	0.2613	1.4790	0.6764
1600.0	1.343	0.2732	1.5707	0.6750
1700.0	1.337	0.2849	1.6656	0.6733
1800.0	1.330	0.2966	1.7668	0.6710
1900.0	1.323	0.3082	1.8781	0.6677
2000.0	1.316	0.3198	2.0052	0.6628
2100.0	1.307	0.3314	2.1563	0.6558
2200.0	1.297	0.3430	2.3428	0.6460
2300.0	1.286	0.3547	2.5795	0.6332
2400.0	1.274	0.3665	2.8832	0.6177
2500.0	1.260	0.3784	3.2734	0.6000
2600.0	1.246	0.3905	3.7718	0.5811
2700.0	1.233	0.4027	4.4025	0.5622
2800.0	1.220	0.4153	5.1897	0.5445
2900.0	1.208	0.4281	6.1565	0.5287
3000.0	1.198	0.4413	7.3240	0.5155
3100.0	1.189	0.4548	8.7093	0.5053
3200.0	1.182	0.4687	10.3238	0.4980
3300.0	1.177	0.4830	12.1727	0.4938
3400.0	1.173	0.4976	14.2463	0.4924
3500.0	1.171	0.5123	16.5231	0.4937
3600.0	1.170	0.5270	18.9655	0.4975
3700.0	1.169	0.5415	21.5175	0.5035
3800.0	1.170	0.5555	24.1033	0.5115
3900.0	1.172	0.5687	26.6302	0.5211
4000.0	1.174	0.5808	28.9857	0.5319

TABLE A-3

HYDROGEN PROPERTIES-EQUILIBRIUM COMPOSITION

P=100.00 ATM

T DEG K	Z	XB	W GM/GM-MOLE	10000 RHO GM/CM3
150.0	1.0849	0.	2.01626	150.9813
200.0	1.0751	0.	2.01626	114.2643
300.0	1.0598	0.	2.01626	77.2759
400.0	1.0487	0.	2.01626	58.5753
500.0	1.0403	0.	2.01626	47.2358
600.0	1.0340	0.	2.01626	39.6039
700.0	1.0291	0.0000	2.01626	34.1070
800.0	1.0253	0.0000	2.01626	29.9547
900.0	1.0223	0.0000	2.01626	26.7053
1000.0	1.0198	0.0000	2.01626	24.0922
1100.0	1.0178	0.0000	2.01626	21.9447
1200.0	1.0162	0.0000	2.01626	20.1484
1300.0	1.0148	0.0000	2.01626	18.6236
1400.0	1.0137	0.0000	2.01626	17.3131
1500.0	1.0127	0.0000	2.01626	16.1746
1600.0	1.0118	0.0000	2.01625	15.1765
1700.0	1.0111	0.0000	2.01625	14.2942
1800.0	1.0104	0.0000	2.01622	13.5088
1900.0	1.0098	0.0001	2.01618	12.8050
2000.0	1.0093	0.0002	2.01610	12.1707
2100.0	1.0088	0.0003	2.01595	11.5959
2200.0	1.0084	0.0006	2.01569	11.0724
2300.0	1.0079	0.0010	2.01529	10.5933
2400.0	1.0076	0.0016	2.01466	10.1527
2500.0	1.0072	0.0025	2.01374	9.7457
2600.0	1.0068	0.0038	2.01241	9.3680
2700.0	1.0065	0.0056	2.01057	9.0158
2800.0	1.0062	0.0081	2.00808	8.6858
2900.0	1.0059	0.0114	2.00479	8.3752
3000.0	1.0056	0.0156	2.00054	8.0813
3100.0	1.0053	0.0209	1.99515	7.8018
3200.0	1.0050	0.0276	1.98845	7.5347
3300.0	1.0047	0.0357	1.98026	7.2783
3400.0	1.0044	0.0455	1.97041	7.0309
3500.0	1.0042	0.0571	1.95872	6.7912
3600.0	1.0040	0.0706	1.94505	6.5580
3700.0	1.0037	0.0863	1.92928	6.3304
3800.0	1.0035	0.1041	1.91130	6.1077
3900.0	1.0033	0.1242	1.89105	5.8892
4000.0	1.0031	0.1466	1.86852	5.6746

TABLE A-3 CONT.

HYDROGEN PROPERTIES-EQUILIBRIUM COMPOSITION

P=100.00 ATM

T DEG K	H CAL/GM	S CAL/GM-K	CP CAL/GM-K	DH/DP CAL/GM-PSI
150.0	33938.3	8.650	3.084	0.3202E-02
200.0	34096.9	9.561	3.261	0.4807E-02
300.0	34436.0	10.933	3.458	0.7834E-02
400.0	34783.6	11.933	3.491	0.1029E-01
500.0	35132.7	12.712	3.482	0.1209E-01
600.0	35481.4	13.347	3.491	0.1332E-01
700.0	35830.6	13.886	3.493	0.1409E-01
800.0	36181.0	14.354	3.515	0.1452E-01
900.0	36533.8	14.769	3.543	0.1469E-01
1000.0	36889.7	15.144	3.576	0.1469E-01
1100.0	37249.4	15.487	3.620	0.1458E-01
1200.0	37613.8	15.804	3.668	0.1440E-01
1300.0	37983.1	16.099	3.720	0.1420E-01
1400.0	38357.7	16.377	3.772	0.1399E-01
1500.0	38737.6	16.639	3.824	0.1380E-01
1600.0	39122.6	16.888	3.876	0.1362E-01
1700.0	39512.8	17.124	3.928	0.1345E-01
1800.0	39908.2	17.350	3.980	0.1322E-01
1900.0	40308.9	17.567	4.035	0.1285E-01
2000.0	40715.3	17.775	4.093	0.1218E-01
2100.0	41127.7	17.976	4.157	0.1098E-01
2200.0	41546.9	18.171	4.229	0.8895E-02
2300.0	41973.9	18.361	4.315	0.5468E-02
2400.0	42410.5	18.547	4.420	0.8654E-04
2500.0	42858.7	18.730	4.547	-0.8020E-02
2600.0	43320.9	18.911	4.702	-0.1979E-01
2700.0	43800.1	19.092	4.890	-0.3633E-01
2800.0	44300.1	19.274	5.118	-0.5894E-01
2900.0	44824.9	19.458	5.389	-0.8908E-01
3000.0	45379.2	19.646	5.708	-0.1284E-00
3100.0	45968.0	19.839	6.080	-0.1786E-00
3200.0	46596.6	20.039	6.506	-0.2415E-00
3300.0	47270.9	20.246	6.995	-0.3193E-00
3400.0	47997.0	20.463	7.543	-0.4140E-00
3500.0	48781.1	20.690	8.154	-0.5276E 00
3600.0	49629.2	20.929	8.827	-0.6624E 00
3700.0	50547.7	21.181	9.560	-0.8202E 00
3800.0	51542.6	21.446	10.353	-0.1003E 01
3900.0	52619.9	21.726	11.206	-0.1213E 01
4000.0	53785.1	22.021	12.111	-0.1450E 01

TABLE A-3 CONT.

HYDROGEN PROPERTIES-EQUILIBRIUM COMPOSITION

P=100.00 ATM

T DEG K	DS/DT CAL/GM-K2	DS/DP CAL/GM-K-PSI	OMEGT	OMEGP
150.0	0.2056E-01	-0.7058E-03	-0.	0.
200.0	0.1631E-01	-0.6965E-03	-0.	0.
300.0	0.1153E-01	-0.6842E-03	-0.	0.
400.0	0.8727E-02	-0.6771E-03	-0.	0.
500.0	0.6963E-02	-0.6730E-03	-0.	0.
600.0	0.5818E-02	-0.6708E-03	-0.1014E-15	0.1150E-17
700.0	0.4990E-02	-0.6696E-03	-0.4765E-13	0.6290E-15
800.0	0.4394E-02	-0.6690E-03	-0.4791E-11	0.7207E-13
900.0	0.3936E-02	-0.6688E-03	-0.1723E-09	0.2908E-11
1000.0	0.3576E-02	-0.6688E-03	-0.3018E-08	0.5646E-10
1100.0	0.3291E-02	-0.6689E-03	-0.3134E-07	0.6432E-09
1200.0	0.3057E-02	-0.6691E-03	-0.2198E-06	0.4910E-08
1300.0	0.2862E-02	-0.6692E-03	-0.1140E-05	0.2752E-07
1400.0	0.2694E-02	-0.6694E-03	-0.4665E-05	0.1210E-06
1500.0	0.2550E-02	-0.6695E-03	-0.1579E-04	0.4380E-06
1600.0	0.2423E-02	-0.6696E-03	-0.4583E-04	0.1353E-05
1700.0	0.2310E-02	-0.6697E-03	-0.1171E-03	0.3667E-05
1800.0	0.2211E-02	-0.6699E-03	-0.2693E-03	0.8912E-05
1900.0	0.2124E-02	-0.6701E-03	-0.5664E-03	0.1975E-04
2000.0	0.2047E-02	-0.6704E-03	-0.1105E-02	0.4048E-04
2100.0	0.1979E-02	-0.6710E-03	-0.2019E-02	0.7755E-04
2200.0	0.1922E-02	-0.6720E-03	-0.3488E-02	0.1402E-03
2300.0	0.1876E-02	-0.6735E-03	-0.5740E-02	0.2408E-03
2400.0	0.1842E-02	-0.6758E-03	-0.9050E-02	0.3957E-03
2500.0	0.1819E-02	-0.6791E-03	-0.1374E-01	0.6251E-03
2600.0	0.1808E-02	-0.6837E-03	-0.2019E-01	0.9536E-03
2700.0	0.1811E-02	-0.6899E-03	-0.2878E-01	0.1410E-02
2800.0	0.1828E-02	-0.6981E-03	-0.3996E-01	0.2028E-02
2900.0	0.1858E-02	-0.7087E-03	-0.5416E-01	0.2844E-02
3000.0	0.1903E-02	-0.7220E-03	-0.7184E-01	0.3899E-02
3100.0	0.1961E-02	-0.7385E-03	-0.9342E-01	0.5234E-02
3200.0	0.2033E-02	-0.7585E-03	-0.1193E-00	0.6895E-02
3300.0	0.2120E-02	-0.7824E-03	-0.1499E-00	0.8924E-02
3400.0	0.2219E-02	-0.8106E-03	-0.1854E-00	0.1136E-01
3500.0	0.2330E-02	-0.8436E-03	-0.2261E-00	0.1426E-01
3600.0	0.2452E-02	-0.8815E-03	-0.2721E-00	0.1763E-01
3700.0	0.2584E-02	-0.9247E-03	-0.3234E-00	0.2153E-01
3800.0	0.2725E-02	-0.9735E-03	-0.3799E-00	0.2595E-01
3900.0	0.2873E-02	-0.1028E-02	-0.4412E-00	0.3091E-01
4000.0	0.3028E-02	-0.1088E-02	-0.5069E 00	0.3641E-01

TABLE A-3 CONT.

HYDROGEN PROPERTIES-EQUILIBRIUM COMPOSITION

P=100.00 ATM

T DEG K	SIGT	SIGP	ZETAT	ZETAP
150.0	-0.2936E-01	0.7826E-01	-0.2008E-00	0.2035E-00
200.0	-0.3335E-01	0.6989E-01	-0.2129E-00	0.1694E-00
300.0	-0.3676E-01	0.5646E-01	-0.1243E-00	0.1252E-00
400.0	-0.3660E-01	0.4639E-01	-0.1063E-00	0.9739E-01
500.0	-0.3469E-01	0.3875E-01	-0.9329E-01	0.7833E-01
600.0	-0.3204E-01	0.3287E-01	-0.7994E-01	0.6479E-01
700.0	-0.2919E-01	0.2829E-01	-0.7997E-01	0.5490E-01
800.0	-0.2640E-01	0.2468E-01	-0.7801E-01	0.4752E-01
900.0	-0.2382E-01	0.2179E-01	-0.7822E-01	0.4186E-01
1000.0	-0.2149E-01	0.1945E-01	-0.8598E-01	0.3742E-01
1100.0	-0.1943E-01	0.1753E-01	-0.8924E-01	0.3386E-01
1200.0	-0.1762E-01	0.1595E-01	-0.9318E-01	0.3094E-01
1300.0	-0.1606E-01	0.1462E-01	-0.9475E-01	0.2850E-01
1400.0	-0.1472E-01	0.1350E-01	-0.9575E-01	0.2640E-01
1500.0	-0.1357E-01	0.1254E-01	-0.9609E-01	0.2459E-01
1600.0	-0.1260E-01	0.1170E-01	-0.9583E-01	0.2300E-01
1700.0	-0.1179E-01	0.1097E-01	-0.9674E-01	0.2160E-01
1800.0	-0.1111E-01	0.1033E-01	-0.9918E-01	0.2039E-01
1900.0	-0.1056E-01	0.9748E-02	-0.1023E-00	0.1937E-01
2000.0	-0.1011E-01	0.9224E-02	-0.1066E-00	0.1857E-01
2100.0	-0.9748E-02	0.8745E-02	-0.1113E-00	0.1802E-01
2200.0	-0.9469E-02	0.8304E-02	-0.1233E-00	0.1775E-01
2300.0	-0.9257E-02	0.7894E-02	-0.1372E-00	0.1778E-01
2400.0	-0.9104E-02	0.7511E-02	-0.1524E-00	0.1812E-01
2500.0	-0.8997E-02	0.7151E-02	-0.1682E-00	0.1874E-01
2600.0	-0.8928E-02	0.6810E-02	-0.1845E-00	0.1960E-01
2700.0	-0.8888E-02	0.6486E-02	-0.2007E-00	0.2060E-01
2800.0	-0.8866E-02	0.6179E-02	-0.2132E-00	0.2163E-01
2900.0	-0.8855E-02	0.5886E-02	-0.2206E-00	0.2259E-01
3000.0	-0.8844E-02	0.5608E-02	-0.2224E-00	0.2337E-01
3100.0	-0.8825E-02	0.5344E-02	-0.2183E-00	0.2391E-01
3200.0	-0.8790E-02	0.5094E-02	-0.2123E-00	0.2417E-01
3300.0	-0.8731E-02	0.4857E-02	-0.1979E-00	0.2411E-01
3400.0	-0.8640E-02	0.4634E-02	-0.1794E-00	0.2378E-01
3500.0	-0.8511E-02	0.4426E-02	-0.1579E-00	0.2322E-01
3600.0	-0.8339E-02	0.4233E-02	-0.1344E-00	0.2247E-01
3700.0	-0.8120E-02	0.4055E-02	-0.1096E-00	0.2158E-01
3800.0	-0.7850E-02	0.3892E-02	-0.8611E-01	0.2062E-01
3900.0	-0.7527E-02	0.3746E-02	-0.6131E-01	0.1959E-01
4000.0	-0.7148E-02	0.3616E-02	-0.3635E-01	0.1856E-01

TABLE A-3 CONT.

HYDROGEN PROPERTIES-EQUILIBRIUM COMPOSITION

P=100.00 ATM

T DEG K	GAMMA	1000 MU GM/CM-SEC	1000 LAMBDA CAL/CM-SEC-K	PR
150.0	1.823	0.0574	0.2694	0.6575
200.0	1.716	0.0699	0.3432	0.6646
300.0	1.598	0.0915	0.4710	0.6721
400.0	1.544	0.1104	0.5714	0.6747
500.0	1.514	0.1277	0.6581	0.6755
600.0	1.490	0.1438	0.7426	0.6760
700.0	1.474	0.1592	0.8222	0.6761
800.0	1.458	0.1739	0.9036	0.6764
900.0	1.445	0.1881	0.9849	0.6766
1000.0	1.433	0.2006	1.0574	0.6784
1100.0	1.421	0.2132	1.1396	0.6773
1200.0	1.410	0.2256	1.2239	0.6762
1300.0	1.399	0.2379	1.3105	0.6752
1400.0	1.389	0.2499	1.3982	0.6742
1500.0	1.380	0.2618	1.4872	0.6733
1600.0	1.372	0.2737	1.5776	0.6724
1700.0	1.364	0.2854	1.6692	0.6715
1800.0	1.356	0.2970	1.7635	0.6704
1900.0	1.349	0.3086	1.8614	0.6690
2000.0	1.342	0.3202	1.9645	0.6672
2100.0	1.335	0.3318	2.0752	0.6646
2200.0	1.327	0.3434	2.1970	0.6610
2300.0	1.320	0.3550	2.3351	0.6560
2400.0	1.312	0.3666	2.4950	0.6495
2500.0	1.303	0.3784	2.6826	0.6414
2600.0	1.294	0.3902	2.9049	0.6315
2700.0	1.285	0.4021	3.1709	0.6202
2800.0	1.275	0.4142	3.4888	0.6076
2900.0	1.265	0.4264	3.8672	0.5942
3000.0	1.256	0.4389	4.3147	0.5806
3100.0	1.247	0.4515	4.8394	0.5672
3200.0	1.238	0.4643	5.4492	0.5544
3300.0	1.231	0.4774	6.1531	0.5427
3400.0	1.224	0.4908	6.9547	0.5323
3500.0	1.218	0.5044	7.8580	0.5234
3600.0	1.213	0.5182	8.8648	0.5159
3700.0	1.209	0.5322	9.9746	0.5101
3800.0	1.205	0.5464	11.1840	0.5058
3900.0	1.203	0.5606	12.4890	0.5030
4000.0	1.202	0.5749	13.8783	0.5017

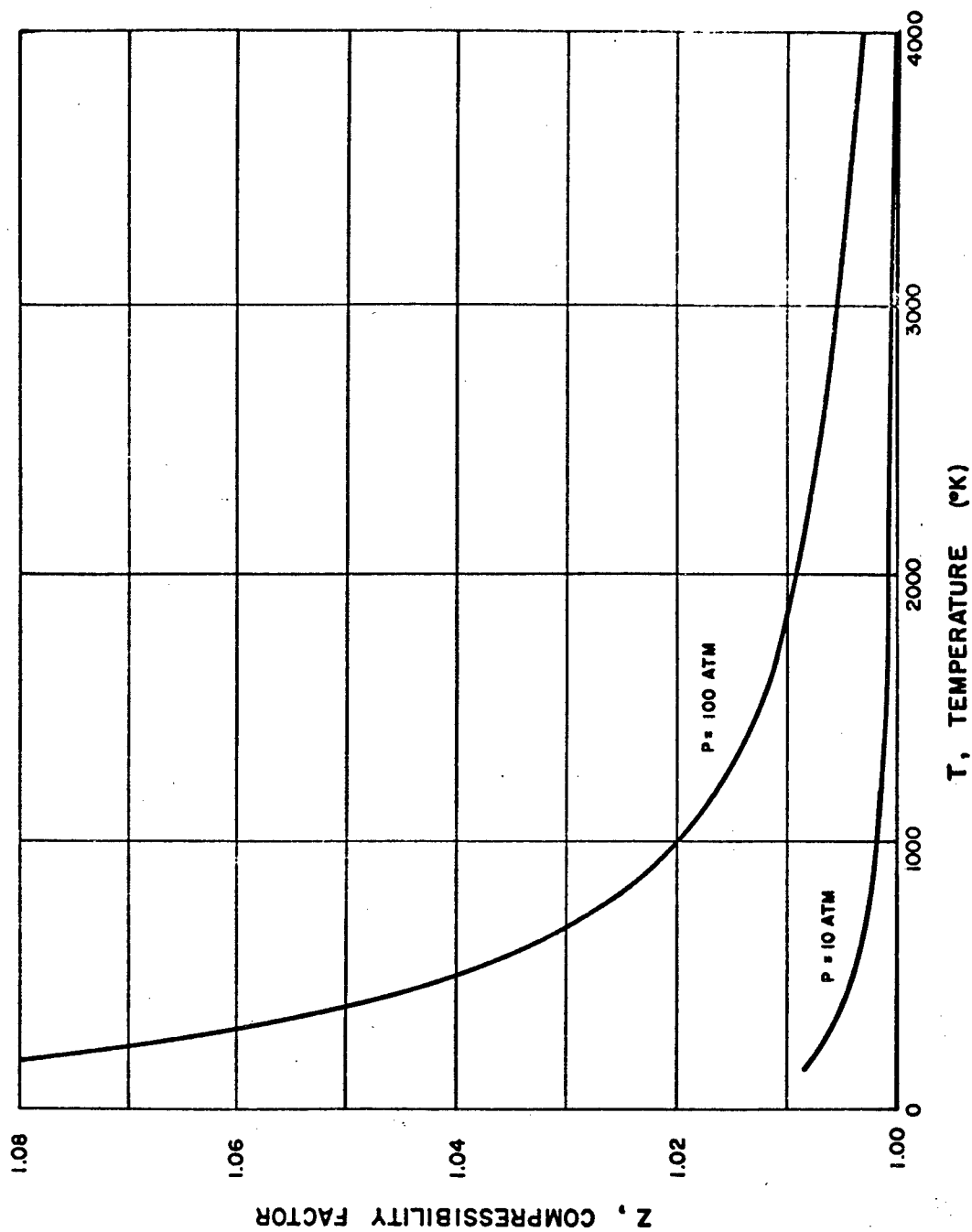


FIG. A-1: COMPRESSIBILITY FACTOR FOR NORMAL HYDROGEN FOR TEMPERATURES FROM 150° TO 4000°K

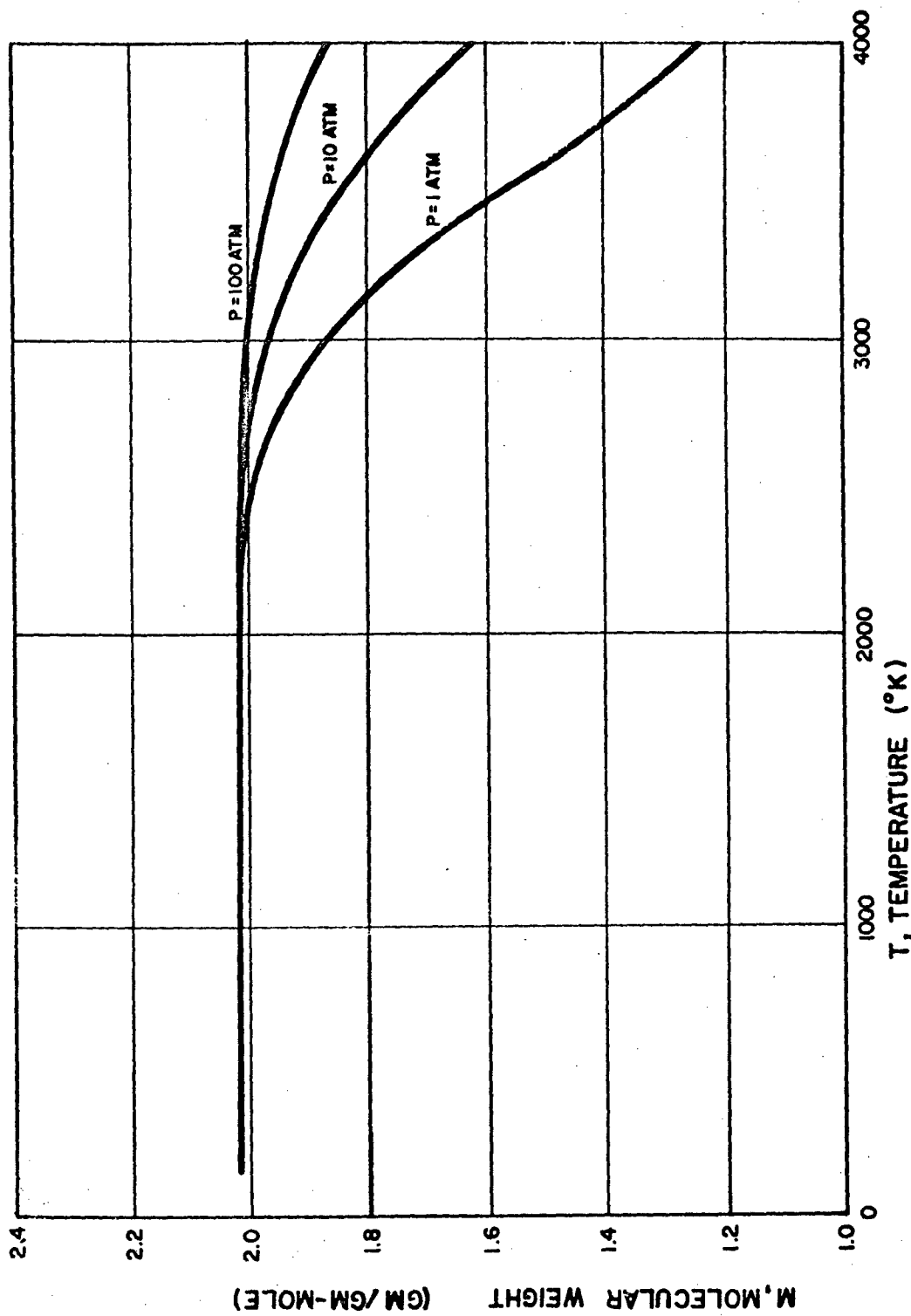


FIG. A-2: MOLECULAR WEIGHT OF NORMAL HYDROGEN ASSUMING EQUILIBRIUM COMPOSITION FOR TEMPERATURES FROM 150° TO 4000° K

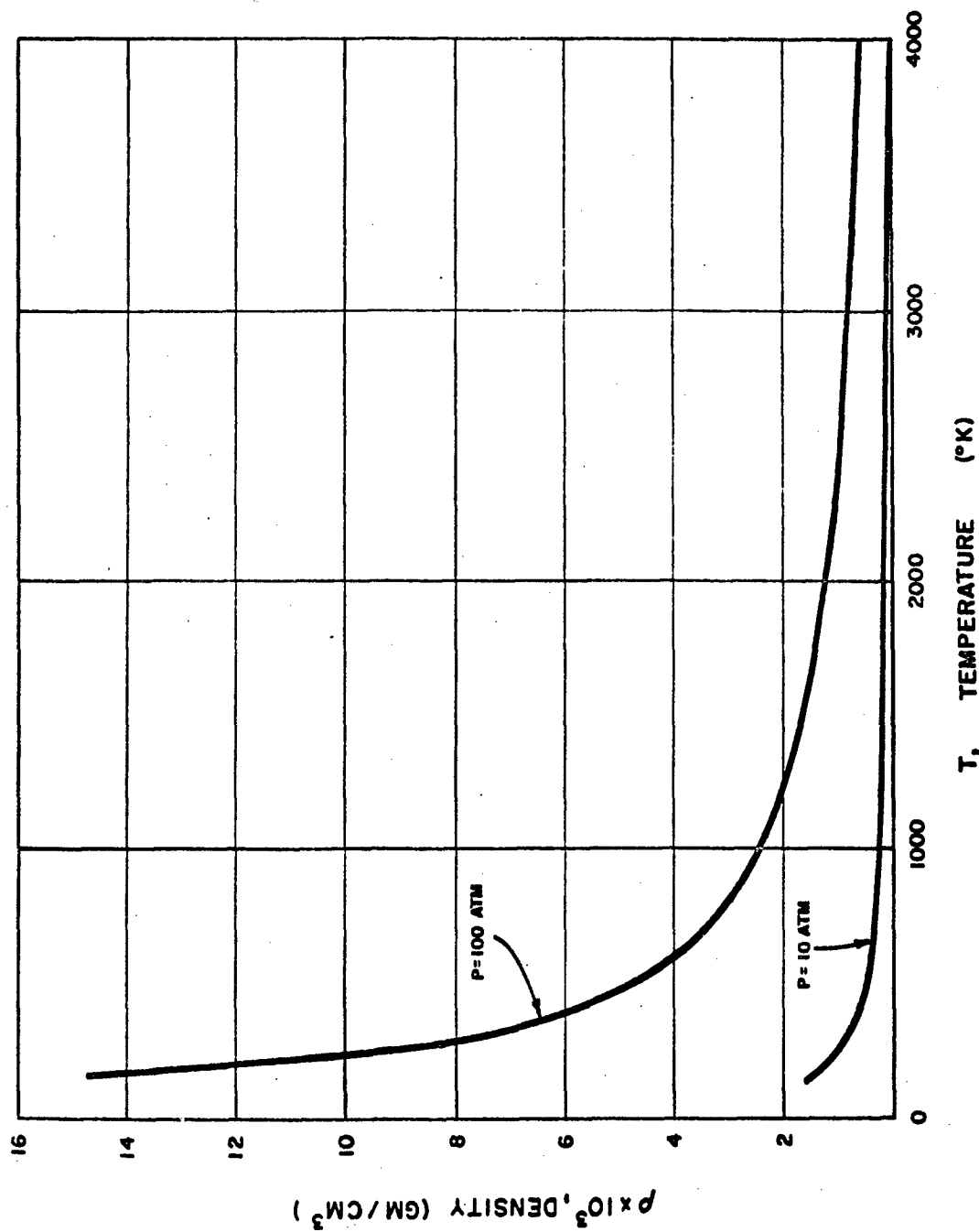


FIG. A-3: DENSITY OF NORMAL HYDROGEN ASSUMING EQUILIBRIUM COMPOSITION FOR TEMPERATURES FROM 150° TO 4000°K

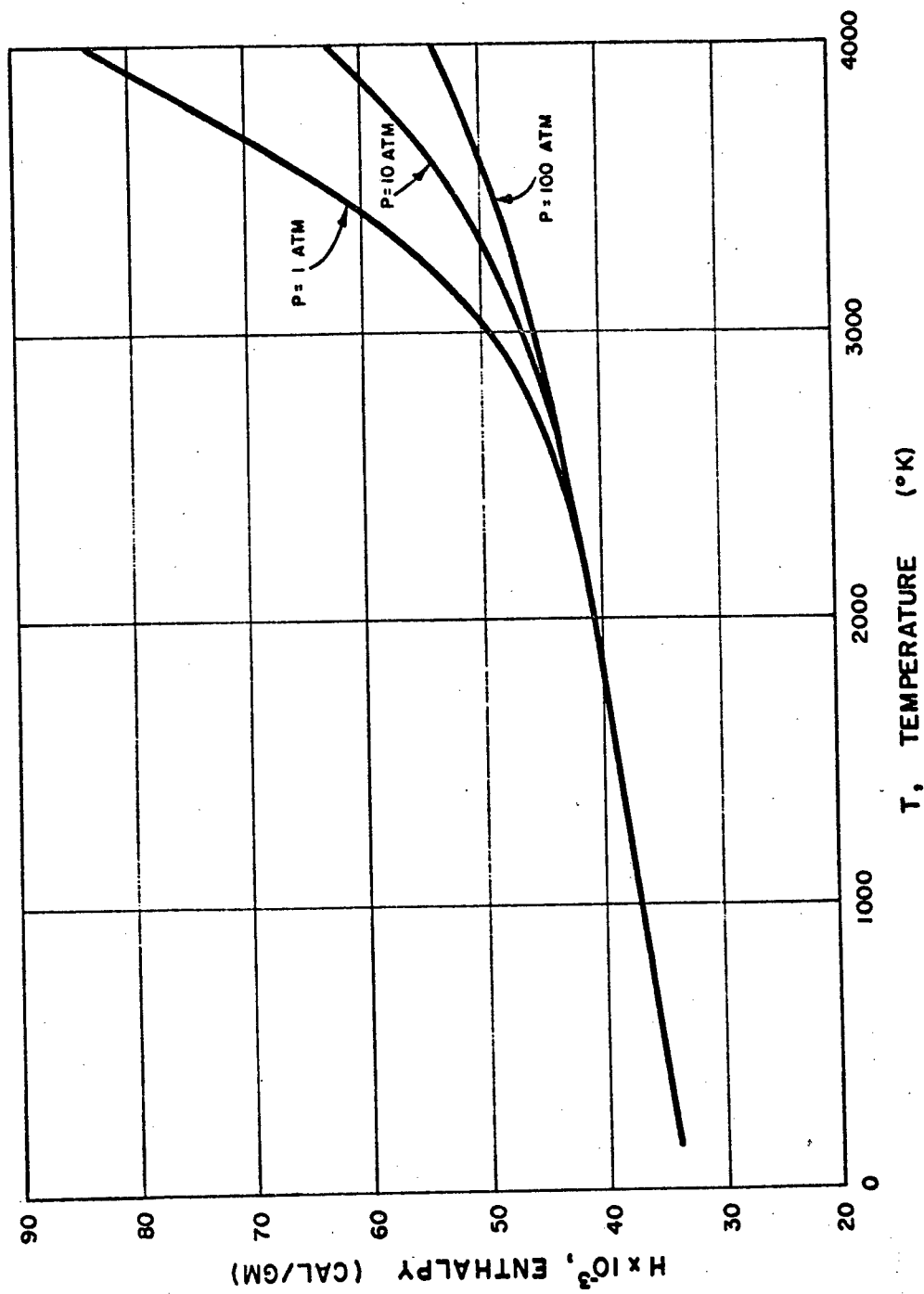


FIG. A-4: ENTHALPY OF NORMAL HYDROGEN ASSUMING EQUILIBRIUM COMPOSITION
FOR TEMPERATURES FROM 150° TO 4000°K

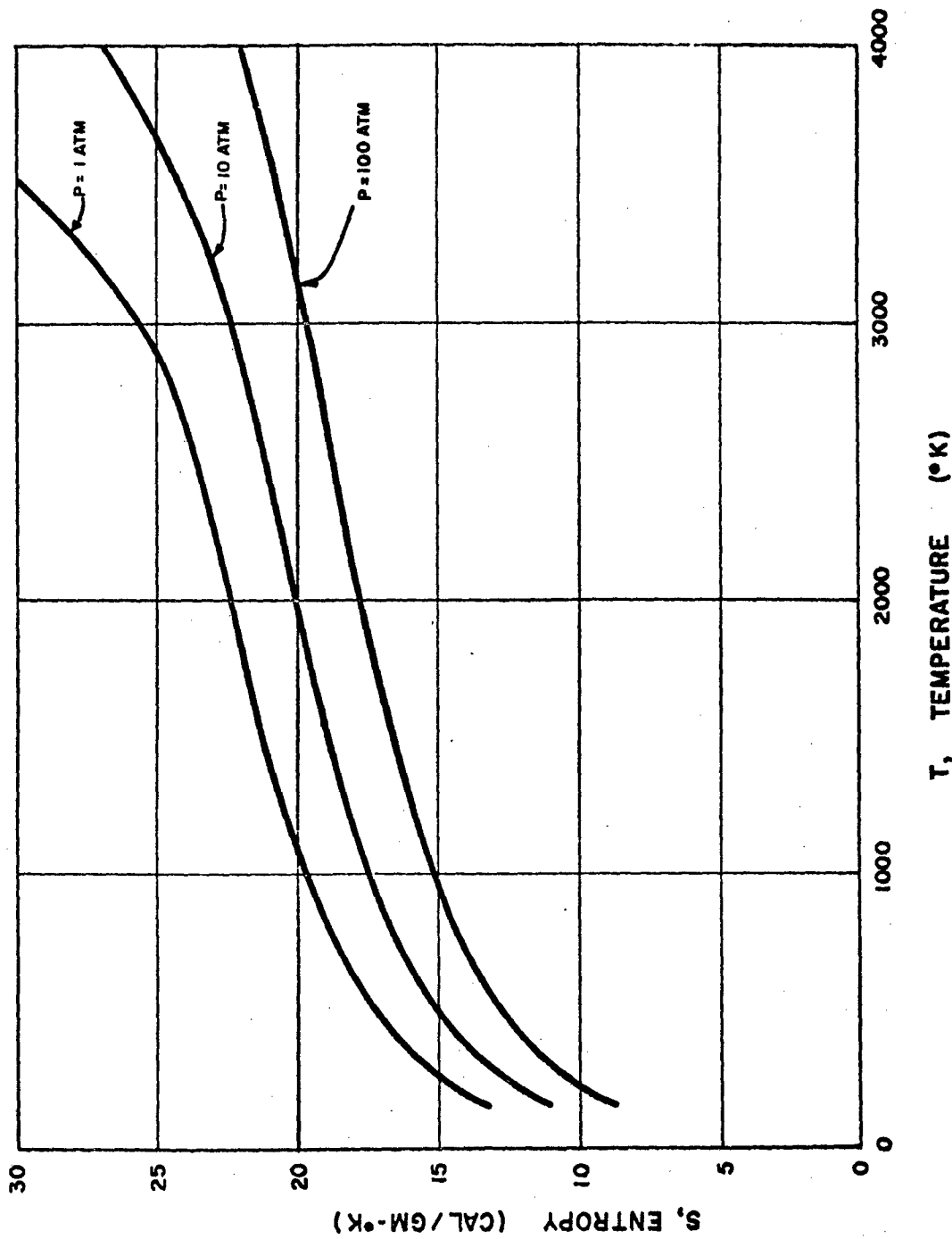


FIG. A-5: ENTROPY OF NORMAL HYDROGEN ASSUMING EQUILIBRIUM COMPOSITION FOR TEMPERATURES FROM 150° TO 4000° K

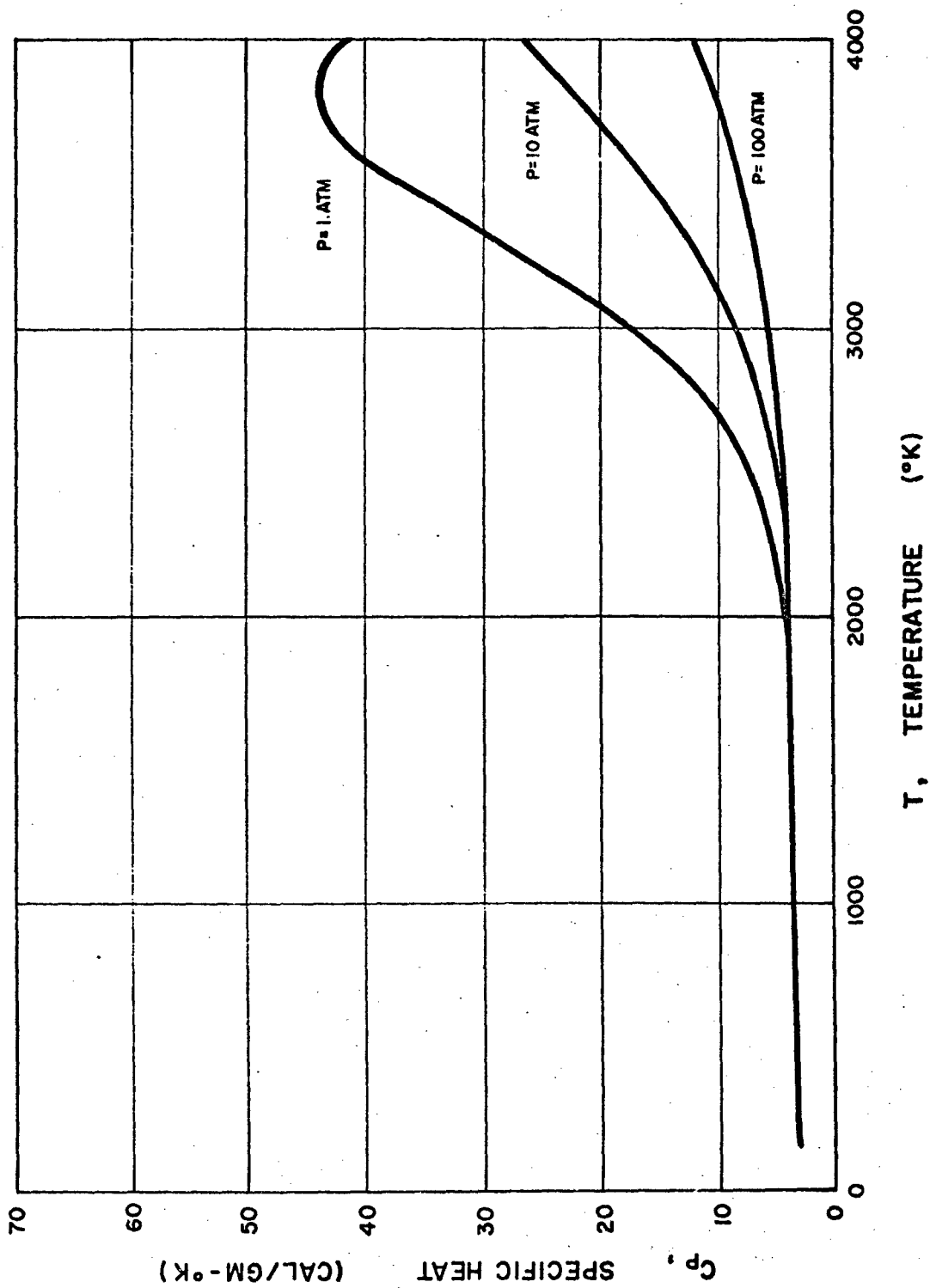


FIG.A-6: SPECIFIC HEAT OF NORMAL HYDROGEN ASSUMING EQUILIBRIUM COMPOSITION FOR TEMPERATURES FROM 150° TO 4000°K

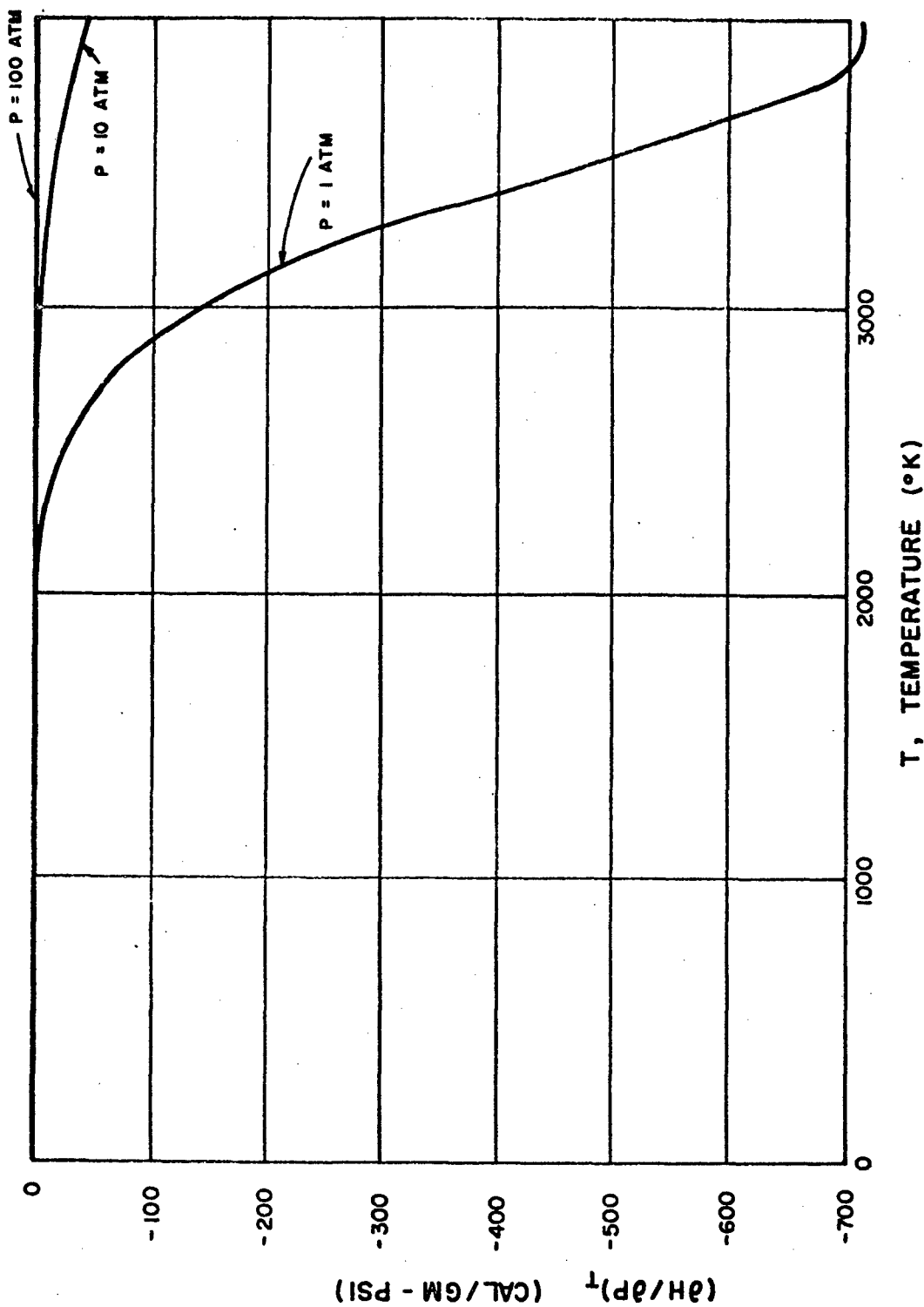


FIG. A-7: $(\partial H / \partial P)_T$ FOR NORMAL HYDROGEN ASSUMING EQUILIBRIUM COMPOSITION
FOR TEMPERATURES FROM 150° TO 4000°K

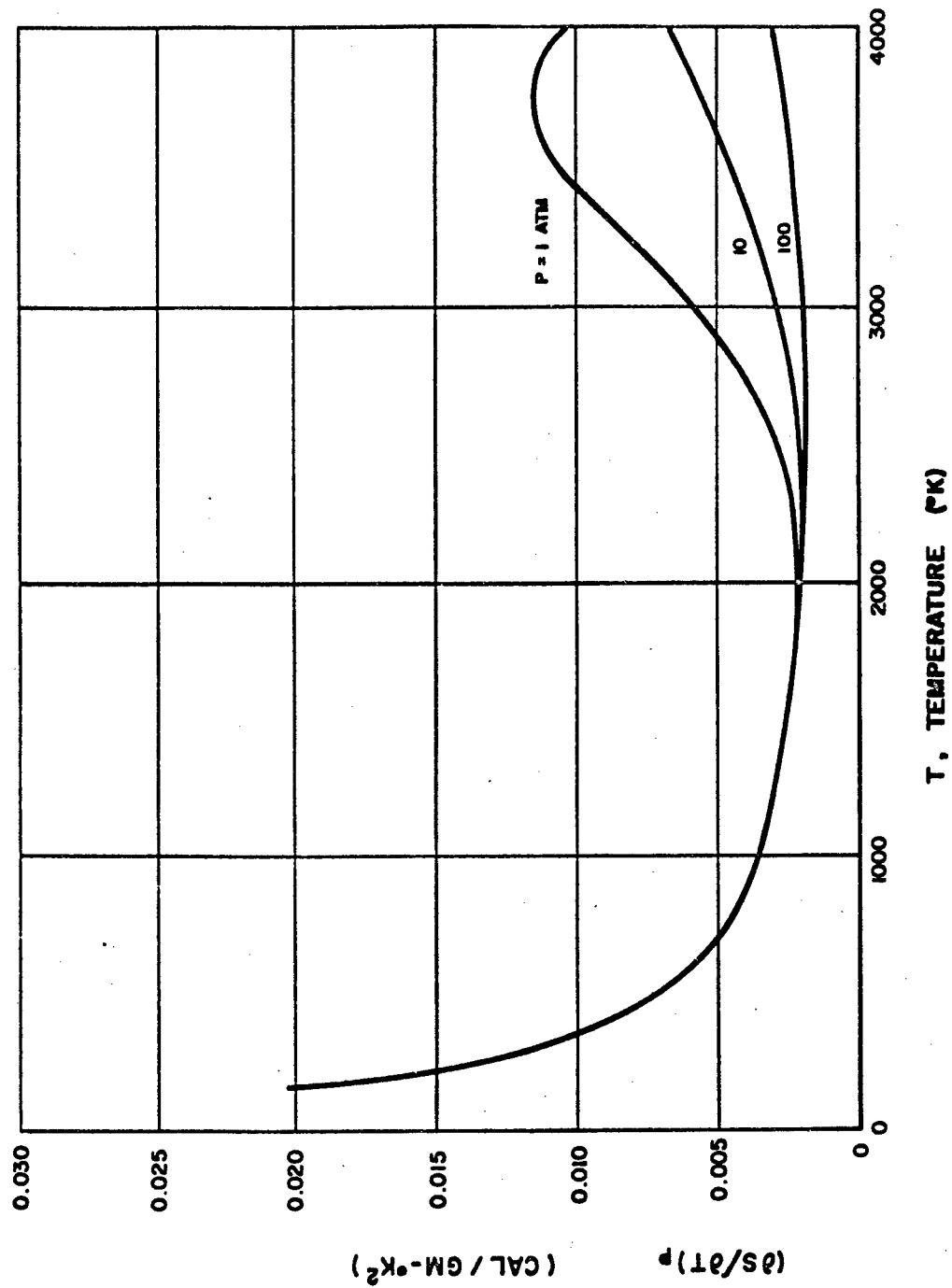


FIG. A-8: $(\partial S / \partial T)_P$ FOR NORMAL HYDROGEN ASSUMING EQUILIBRIUM COMPOSITION FOR TEMPERATURES FROM 150° TO 4000°K

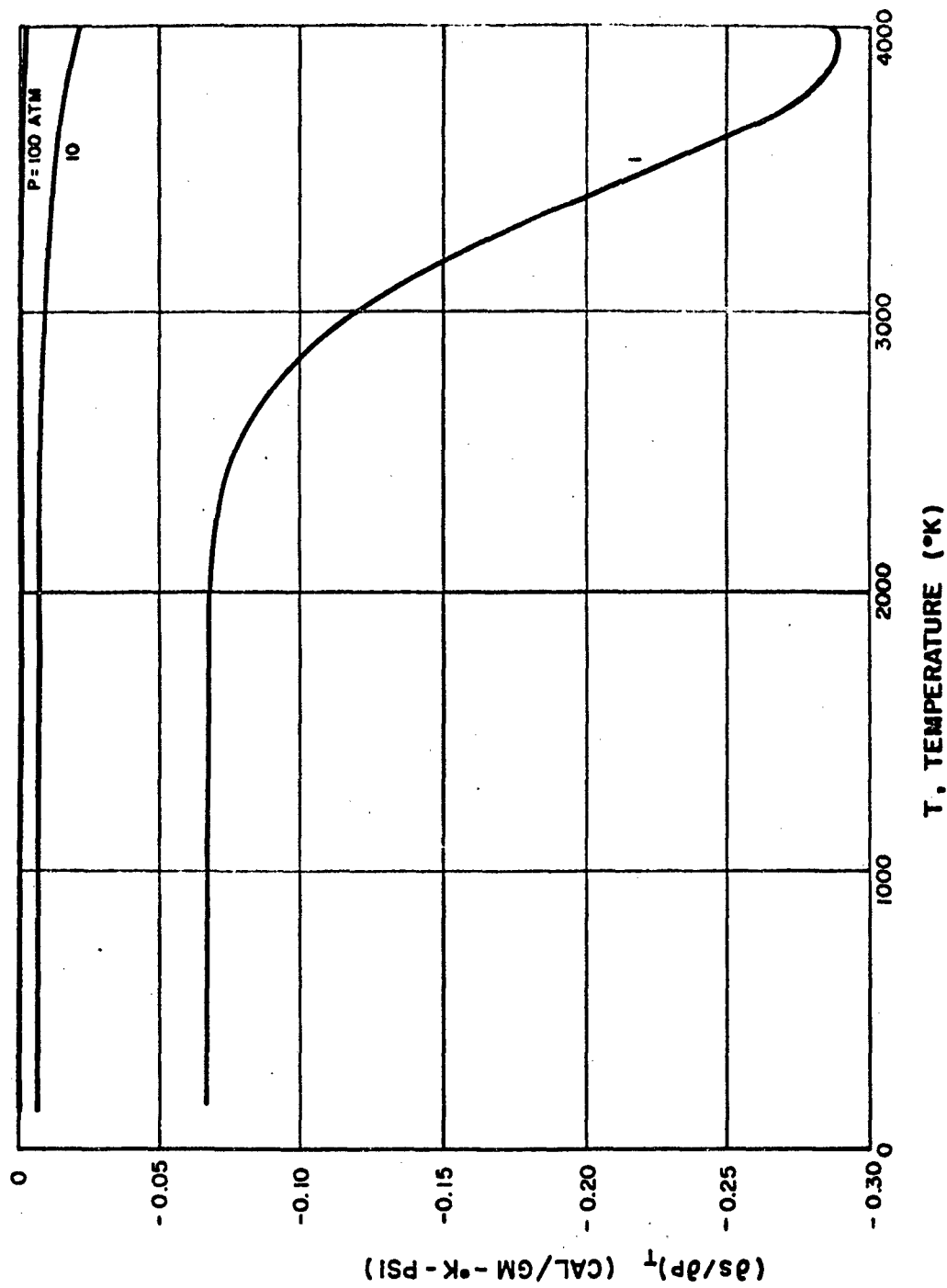


FIG. A-9: $(\partial S / \partial P)_T$ FOR NORMAL HYDROGEN ASSUMING EQUILIBRIUM COMPOSITION FOR TEMPERATURES FROM 150° TO 4000°K

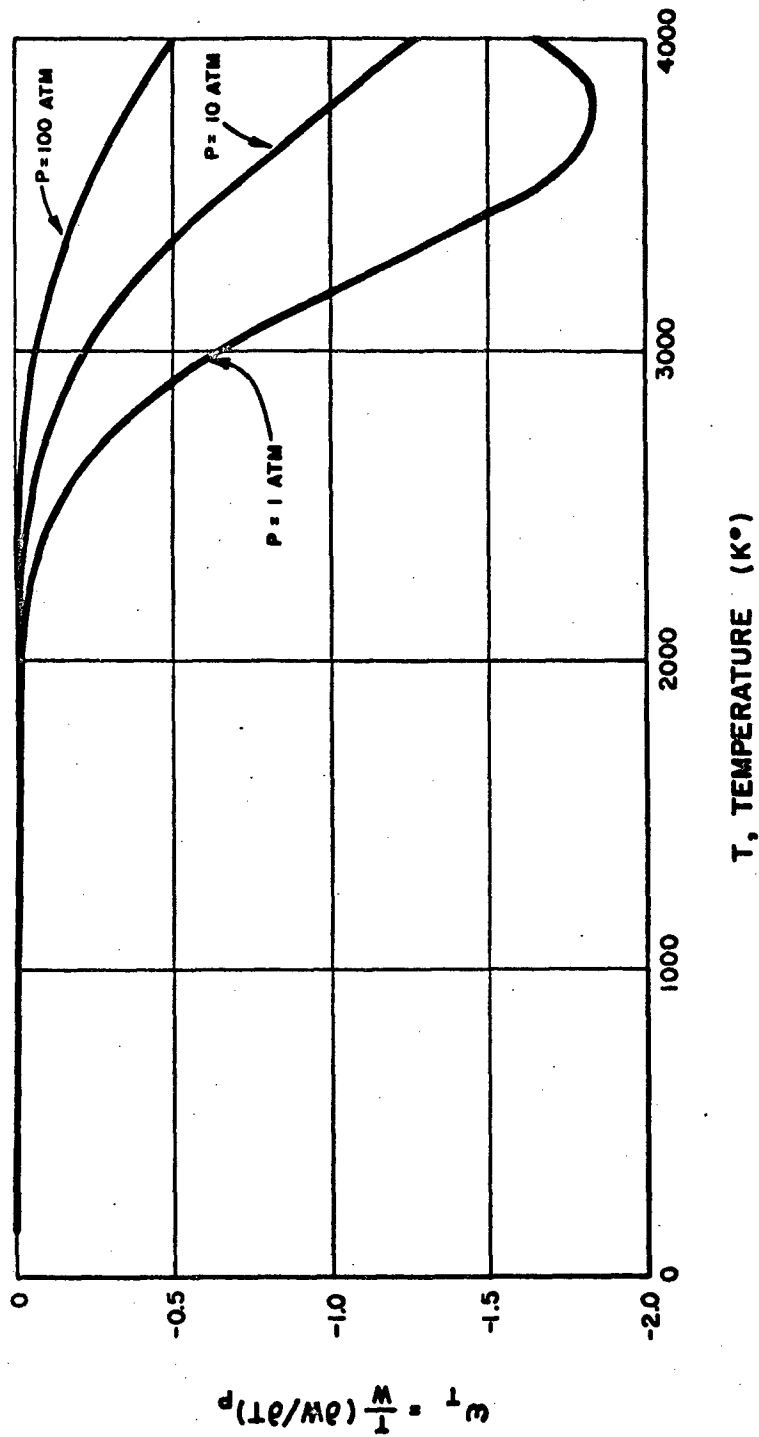


FIG. A-10: ω_T FOR NORMAL HYDROGEN ASSUMING EQUILIBRIUM COMPOSITION
FOR TEMPERATURES FROM 150° TO 4000° K

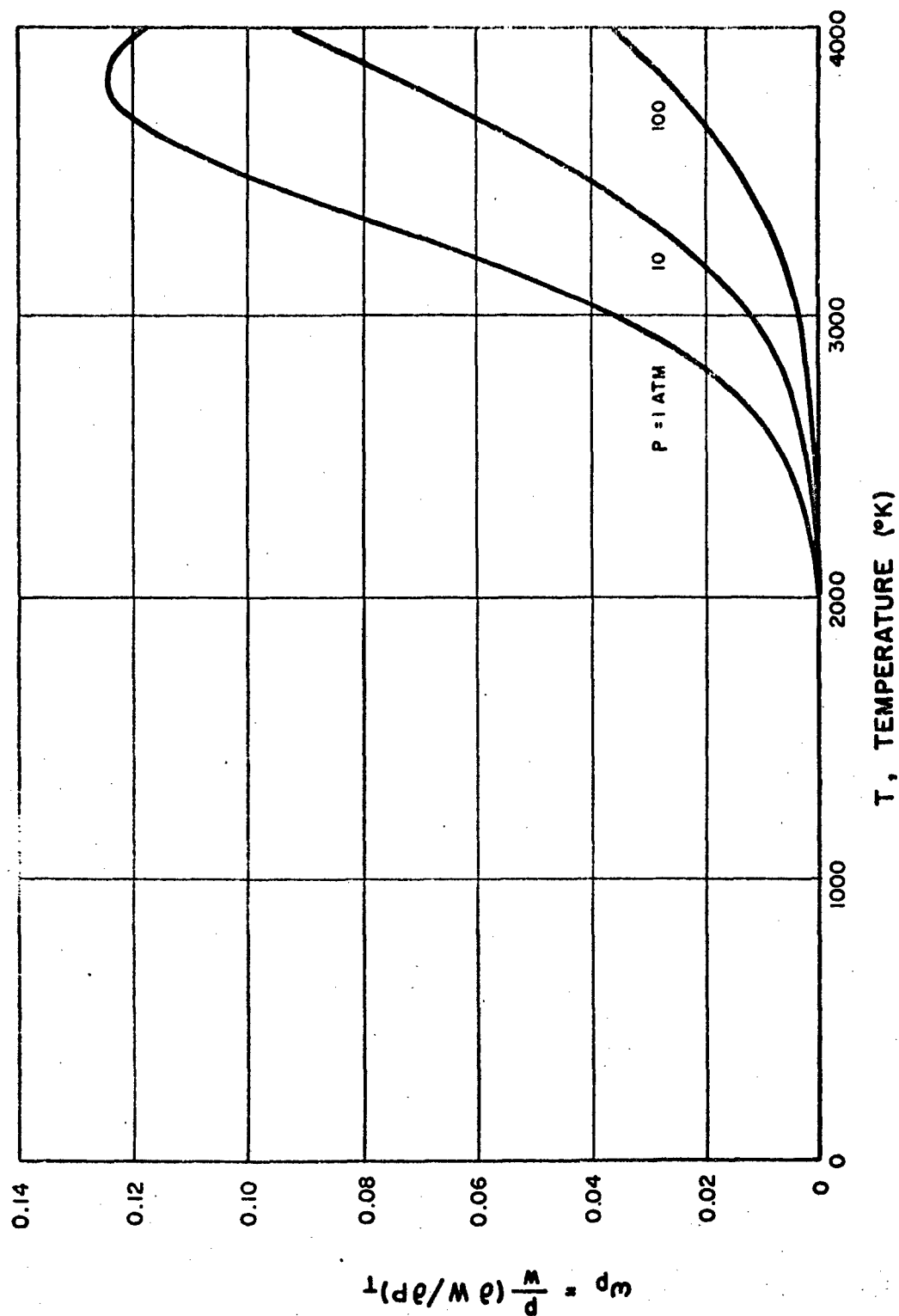


FIG. A-II: ω_p FOR NORMAL HYDROGEN ASSUMING EQUILIBRIUM COMPOSITION FOR TEMPERATURES FROM 150° TO 4000° K

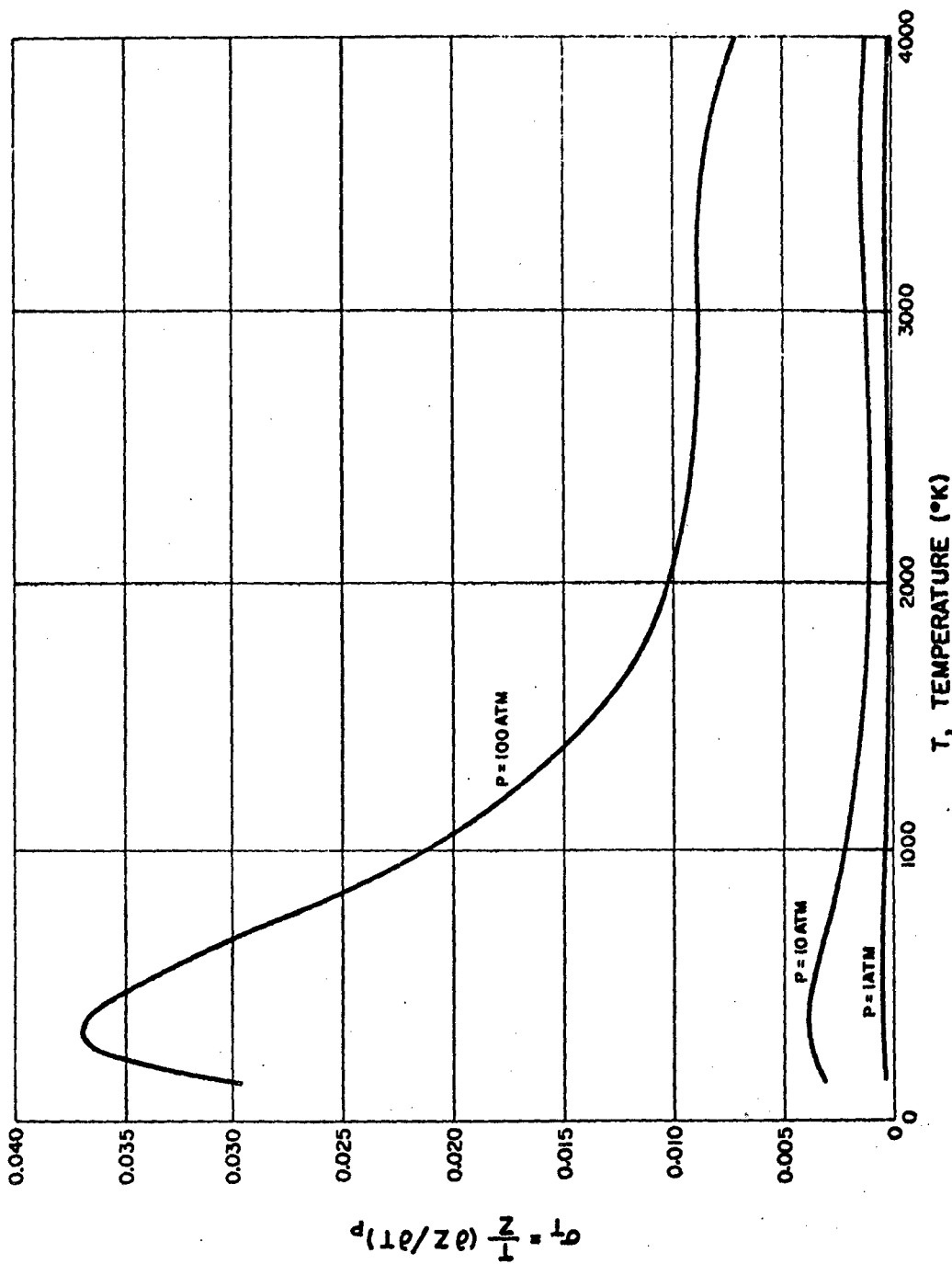


FIG. A-12: σ_T FOR NORMAL HYDROGEN ASSUMING EQUILIBRIUM COMPOSITION FOR TEMPERATURES FROM 150° TO 4000°K

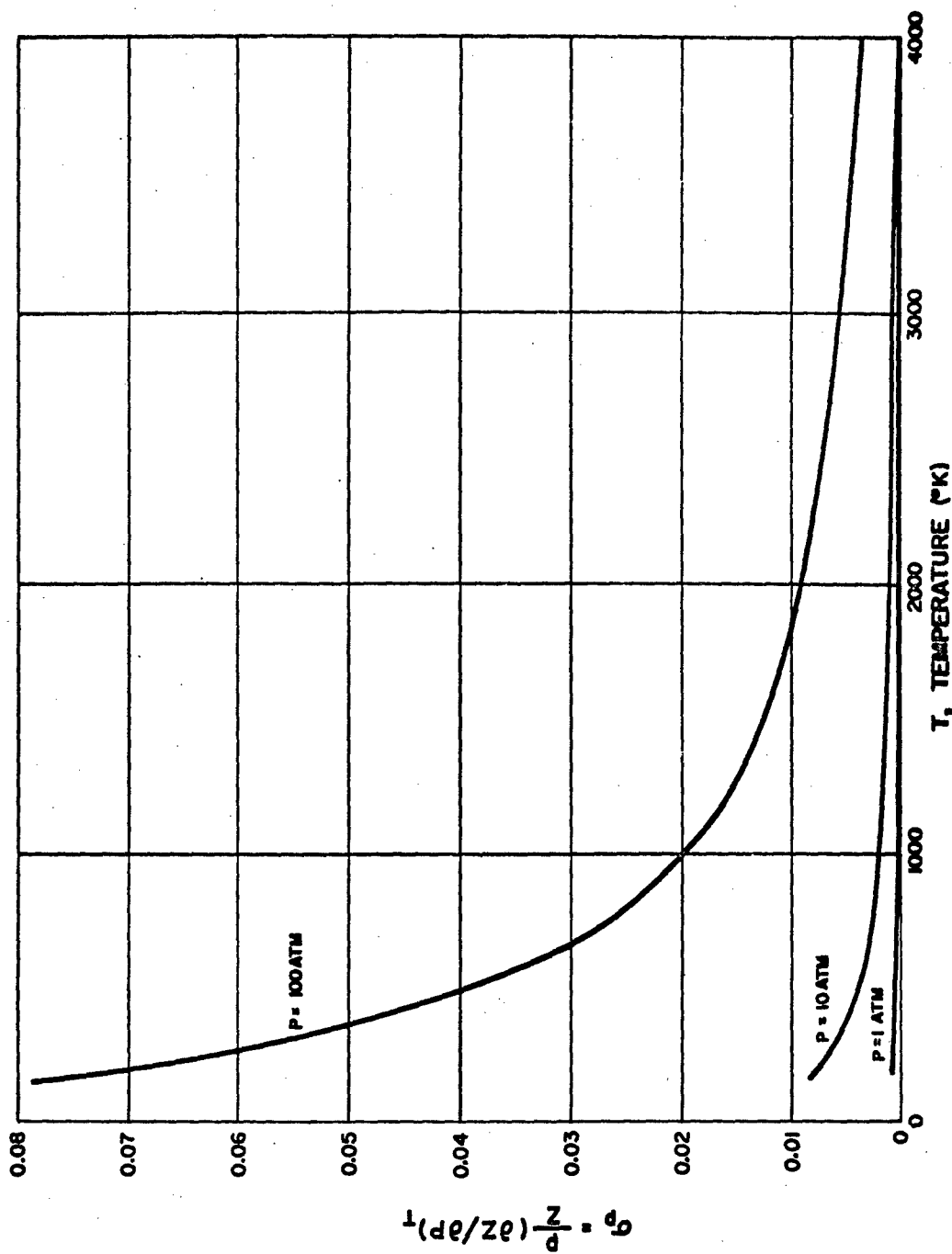


FIG. A-13: σ_p FOR NORMAL HYDROGEN ASSUMING EQUILIBRIUM COMPOSITION FOR TEMPERATURES FROM 150° TO 4000°K

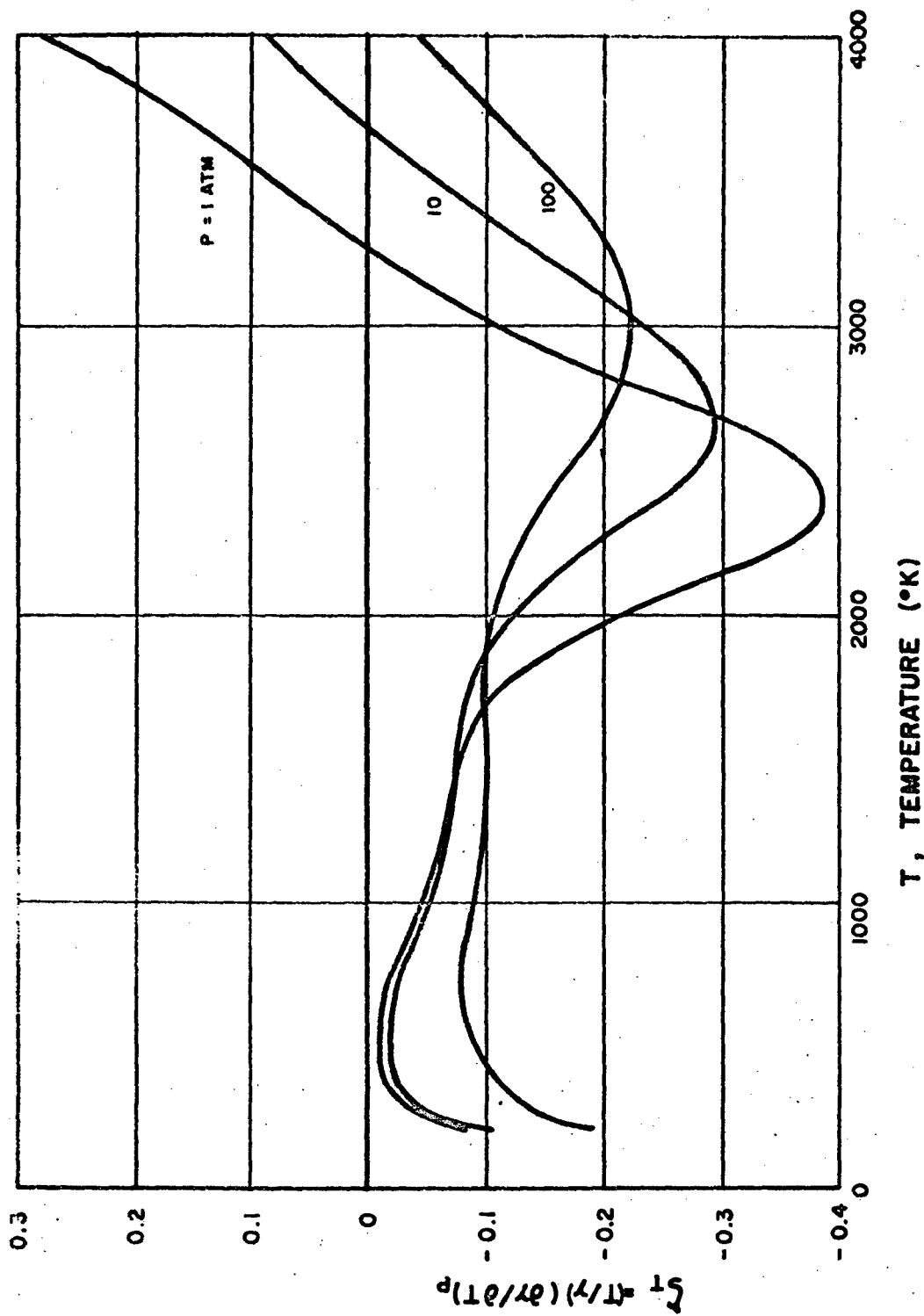


FIG. A-14: ζ_T FOR NORMAL HYDROGEN ASSUMING EQUILIBRIUM COMPOSITION FOR TEMPERATURES FROM 150° TO 4000° K

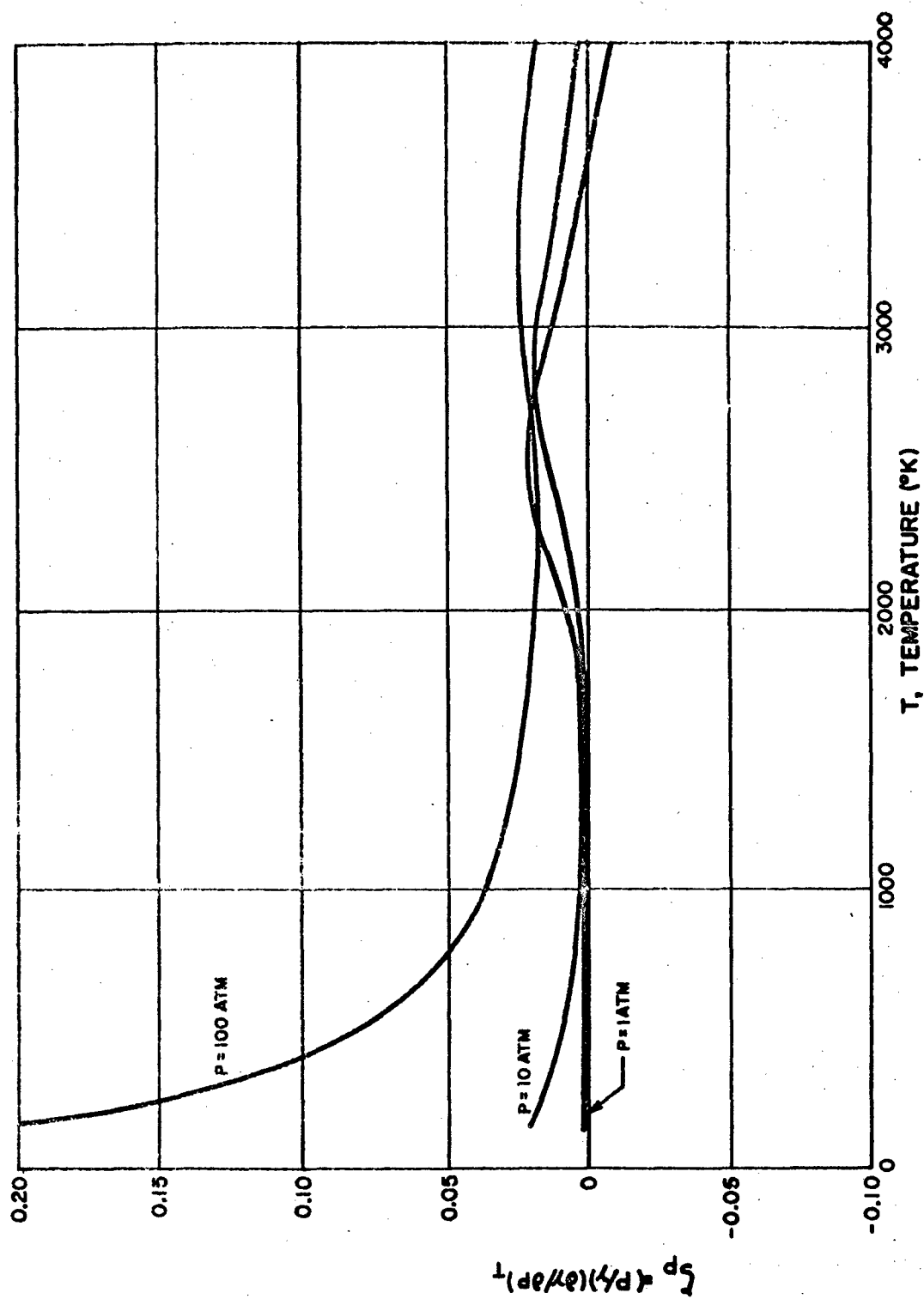


FIG. A-15: ΔG°_f FOR NORMAL HYDROGEN ASSUMING EQUILIBRIUM COMPOSITION FOR TEMPERATURES FROM 150° TO 4000°K

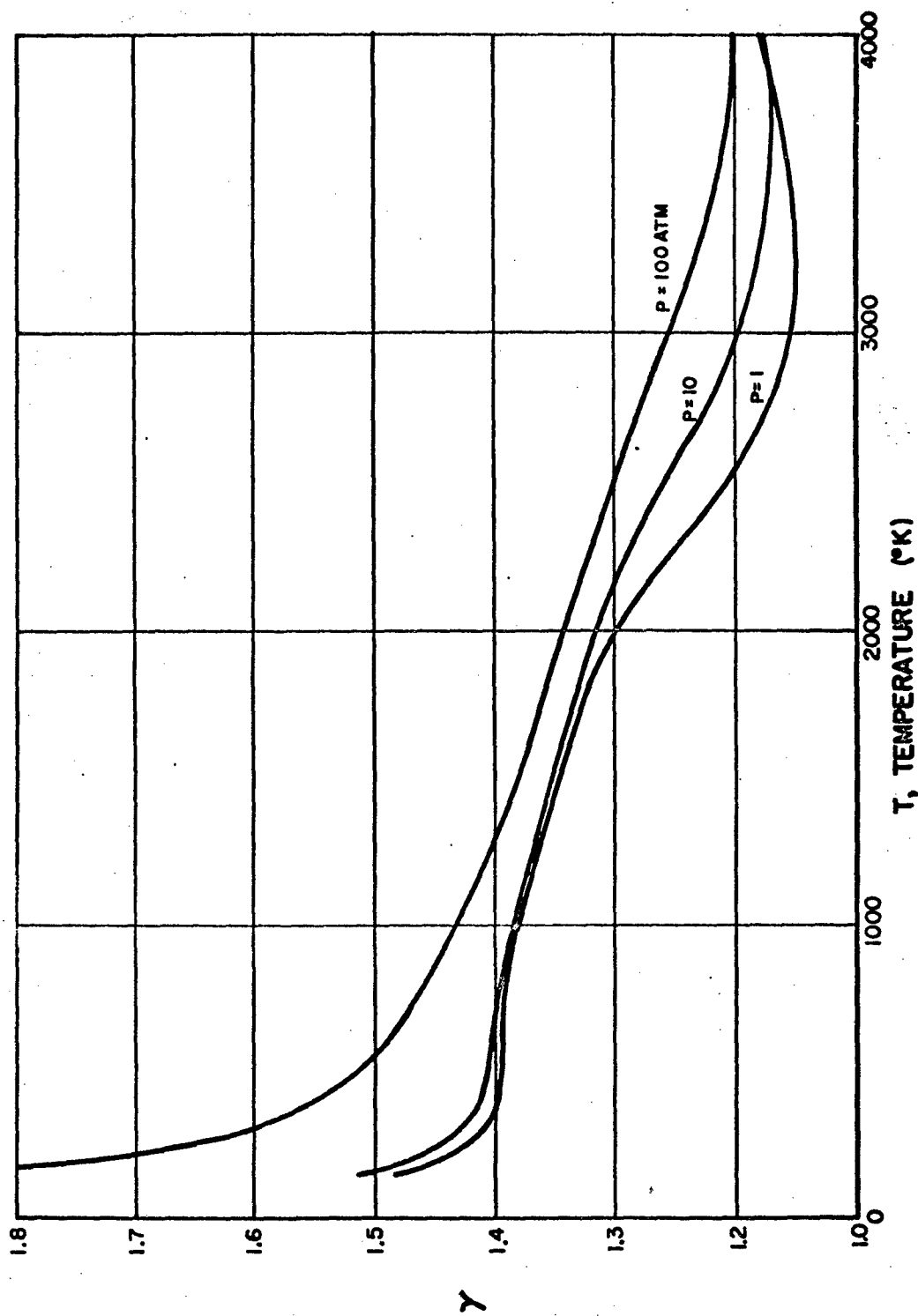


FIG. A-16: γ FOR NORMAL HYDROGEN ASSUMING EQUILIBRIUM COMPOSITION FOR TEMPERATURES FROM 150° TO 4000°K

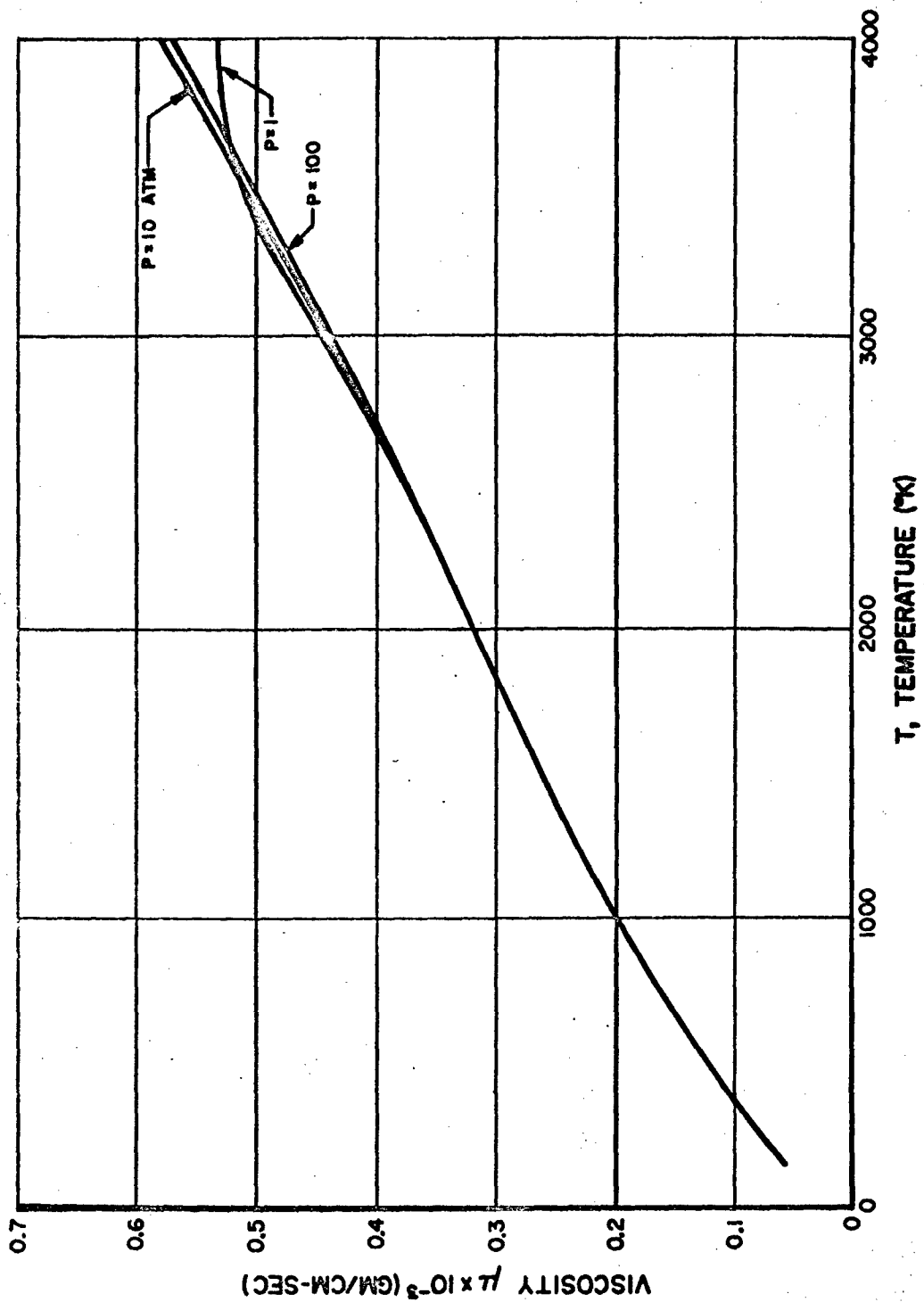


FIG. A-17: VISCOSITY OF NORMAL HYDROGEN ASSUMING EQUILIBRIUM COMPOSITION FOR TEMPERATURES FROM 150° TO 4000°K

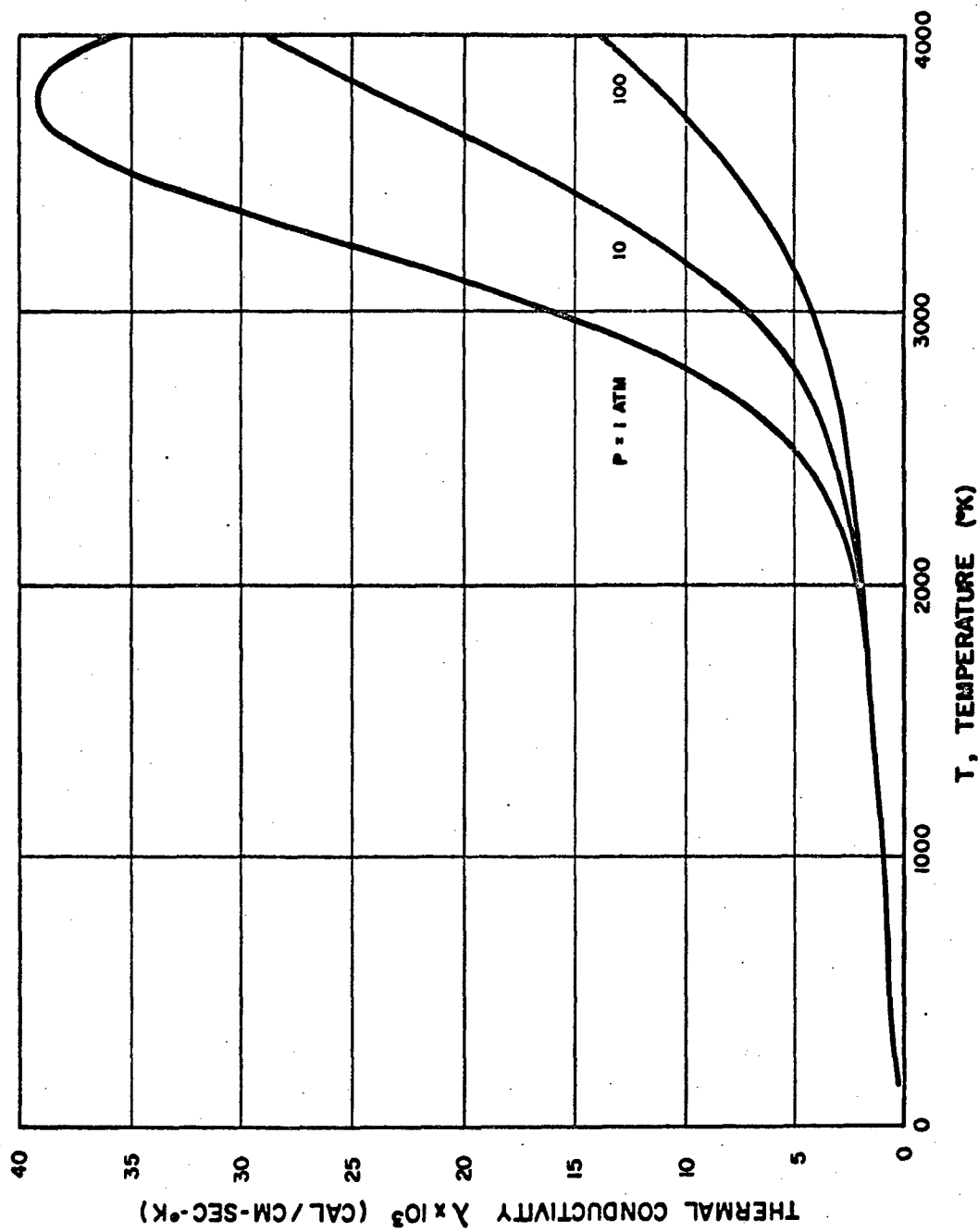


FIG. A-18: THERMAL CONDUCTIVITY OF NORMAL HYDROGEN ASSUMING EQUILIBRIUM COMPOSITION FOR TEMPERATURES FROM 150° TO 4000° K

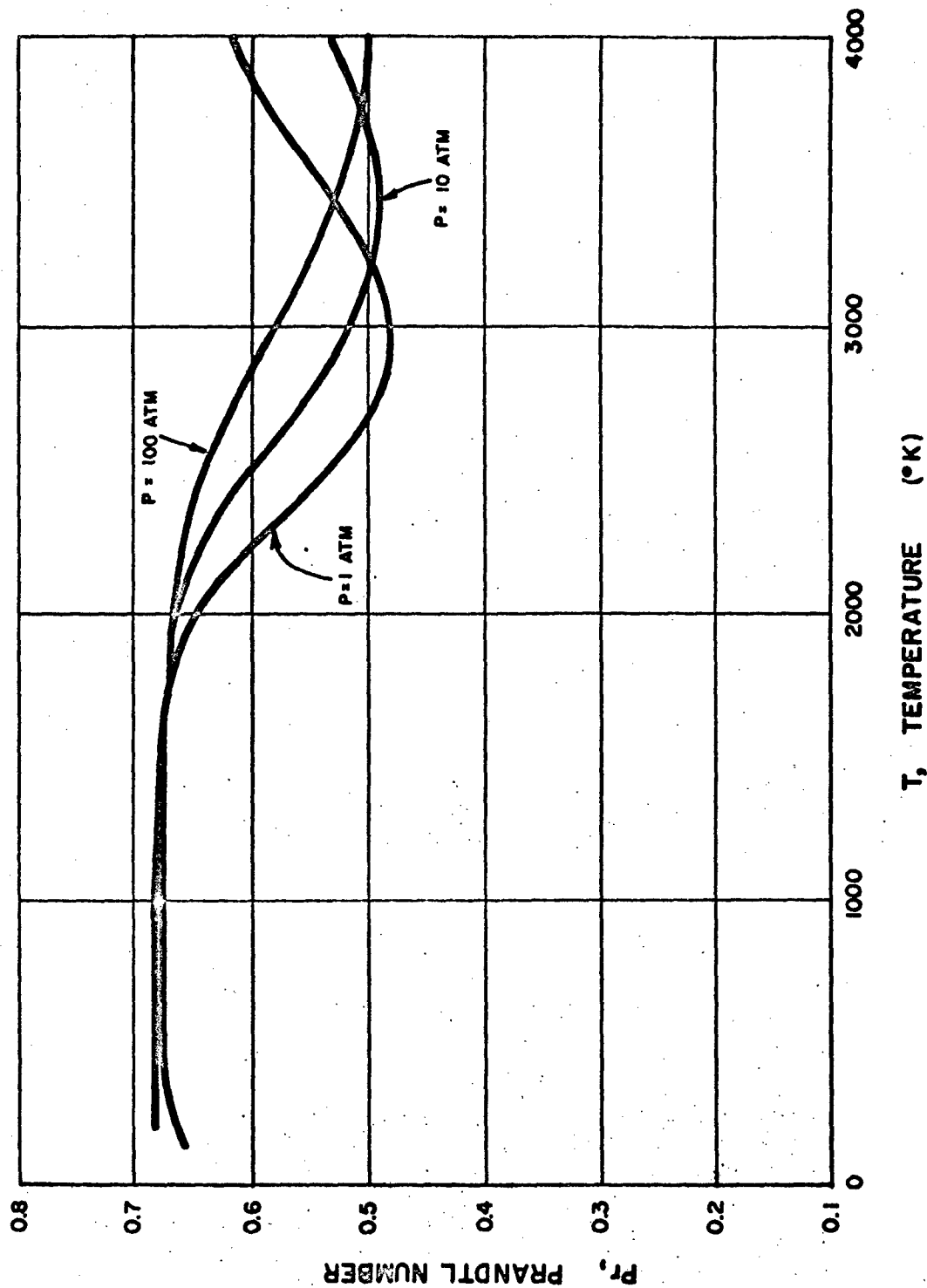


FIG. A-19: PRANDTL NUMBER FOR NORMAL HYDROGEN ASSUMING EQUILIBRIUM COMPOSITION FOR TEMPERATURES FROM 150° TO 4000 °K

7. Description of Computer Subroutine

The equations listed in previous sections have been written in Fortran language and included in a subroutine which was written for use on an IBM 709 or 7090. The Fortran listing of this subprogram is presented in this section. A description of the input, output and method of calling is given below.

Hydrogen Properties Subroutine

Purpose: To calculate the thermodynamic properties, the partial derivatives of the thermodynamic properties with respect to temperature and pressure, and the transport properties of normal hydrogen in cgs units.

Input: Temperature (T) -- ($^{\circ}\text{K}$) --- Range -- 150 - 4000
Pressure (P) -- (PSIA) - Range -- 0.1 - 1469
A - 6 x 40 matrix of coefficients for molecular hydrogen equations
B - 6 x 40 matrix of coefficients for atomic hydrogen equations
MARIE - integer variable determining which properties are to be calculated
JULIE - integer variable determining which type of properties are to be calculated

Output:

1. For (MARIE) negative - thermodynamic properties only

Molecular weight (W) - gm/gm-mole

Compressibility factor (Z) - dimensionless

Density (RHO) - gm/cm³

Enthalpy (H) - cal/gm

Entropy (S) - cal/gm-°K

Specific heat (CP) - cal/gm-°K

Isentropic exponent (GAM) - dimensionless

2. For (MARIE) positive one (+1) - thermodynamic properties listed in case 1 (MARIE negative) plus the following thermodynamic property derivatives:

$(\partial H / \partial P)_T$ - (DHP) - cal/gm-psia

$(\partial S / \partial T)_P$ - (DST) - cal/gm-°K²

$(\partial S / \partial P)_T$ - (DSP) - cal/gm-°K-psia

$(T/W)(\partial W / \partial T)_P$ - (OMEGT) - dimensionless

$(P/W)(\partial W / \partial P)_T$ - (OMEGP) - dimensionless

$(T/Z)(\partial Z / \partial T)_P$ - (SIGT) - dimensionless

$(P/Z)(\partial Z / \partial P)_T$ - (SIGP) - dimensionless

$(T/\gamma)(\partial \gamma / \partial T)_P$ - (ZETAT) - dimensionless

$(P/\gamma)(\partial \gamma / \partial P)_T$ - (ZETAP) - dimensionless

3. For (MARIE) zero (0) - thermodynamic properties listed in case 1 (MARIE negative) plus the following transport properties:

Viscosity - (EMU) - gm/cm-sec

Thermal conductivity - (CLAM) - cal/cm-sec-°K

Prandtl number - (PR) - dimensionless

4. For (MARIE) positive two (+2) - all the properties listed in cases 1, 2, and 3.
5. Effect of the value of JULIE
 - a. For (JULIE) positive two (+2) - properties include effects of compressibility ($Z \neq 1.0$) and effects of dissociation.
 - b. For (JULIE) positive one (+1) - properties include effects of compressibility ($Z \neq 1.0$) but do not include effects of dissociation (molecular hydrogen only).
 - c. For (JULIE) negative one (-1) - properties do not include effects of compressibility ($Z = 1.0$) or of dissociation (molecular hydrogen only).
 - d. For (JULIE) negative two (-2) - properties do not include effects of compressibility ($Z = 1.0$) but do include effects of dissociation.

ENTRANCE: CALL PROPS (T, P, A, B, MARIE, JULIE, W, Z, RHO, H, S, CP, GAM, DHP, DST, DSP, OMEGT, OMEGP, SIGT, SIGP, ZETAT, ZETAP, EMU, CLAM, PR)

Following the program listing is a listing of the matrices A and B. The elements of the matrices are arranged such that each row of the matrix takes up two lines of print. The elements of the first three columns being in the first line and the elements of the last three columns being in the second line.

LISTING OF HYDROGEN PROPERTIES SUBROUTINE

```

*      LIST
*      LABEL
C
C      HYDROGEN PROPERTIES
C
SUBROUTINE PROPS(T,P,A,B,MARIE,JULIE,W,Z,RHO,H,S,CP,GAM,DHP,DST,DS
1P,OMEGT,OMEGP,SIGT,SIGP,ZETAT,ZETAP,EMU,CLAM,PR)
DIMENSION A(6,40),B(6,40)
C
C      THERMODYNAMIC PROPERTIES
C
R=1.9859
RBAR=82.0618
PSI=14.6959
PA=P/PSI
RRP=R/(RBAR*PSI)
J=T/100.
HAL=((A(4,J)*T/4.+A(3,J)/3.)*T+A(2,J)/2.)*T+A(1,J)+A(5,J)/T
HBET=((B(4,J)*T/4.+B(3,J)/3.)*T+B(2,J)/2.)*T+B(1,J)+B(5,J)/T
SAL=((A(4,J)*T/3.+A(3,J)/2.)*T+A(2,J))*T+A(6,J)+A(1,J)*LOGF(T)
SBET=((B(4,J)*T/3.+B(3,J)/2.)*T+B(2,J))*T+B(6,J)+B(1,J)*LOGF(T)
CPAL=((A(4,J)*T+A(3,J))*T+A(2,J))*T+A(1,J)
CPBET=((B(4,J)*T+B(3,J))*T+B(2,J))*T+B(1,J)
SH=2.0*HBET-HAL
SCP=2.0*CPBET-CPAL
FE=SH-2.0*SBET+SAL
IF (XABSF(JULIE)-1) 540,400,390
390 IF (82.0-FE) 400,400,410
400 XB=0.0
GO TO 440
410 XB=(-1.0+SQRTF(1.0+4.0*PA*EXPF(FE)))/(2.0*PA*EXPF(FE))
440 XA=1.0-XB
W=1.00813*(2.0-XB)
RW=R/W
B0=2.0637415
B1=0.28729449
B2=-0.13125412E-01
B3=0.32781166E-03
B4=-0.31587838E-05
TR=T/100.0
YP=((B4*TR+B3)*TR+B2)*TR+B1)*TR+B0
DYPT=0.01*((B4*TR*4.0+B3*3.0)*TR+B2*2.0)*TR+B1)
D2YPT=0.0001*((B4*TR*12.0+B3*6.0)*TR+B2*2.0)
D3YPT=0.000001*(B4*TR*24.0+B3*6.0)
IF (JULIE) 442,540,444
442 BP=0.0
GO TO 448
444 BP=0.01*(EXPF(-YP))
448 DBPT=-BP*DYPT
D2BPT=BP*((DYPT**2)-D2YPT)
D3BPT=BP*(-(DYPT**3)+3.0*DYPT*D2YPT-D3YPT)
PAA=PA*XA
ZA=1.0+BP*PAA
Z=ZA/(XA+ZA*XB)
RHO=PA*W/(RBAR*T*Z)

```

```

HALR=HAL-T*PAA*DBPT
H=RW*T*(XA*HALR+XB*HBET)
SWRA=SAL-LOGF(PAA)
SWRAR=SWRA-PAA*(BP+T*DBPT)
IF (XB) 450,450,460
450 S=RW*XA*SWRAR
GO TO 490
460 SWRB=SBET-LOGF(PA*XB)
S=RW*(XA*SWRAR+XB*SWRB)
490 OMEGP=XB*XA/(2.0-XB)**2.
OMEGT=-SH*OMEGP
CPALR=CPAL-T*PAA*(2.0*DBPT+T*D2BPT)
CP=RW*(XA*CPALR+XB*CPBET-OMEGT*SH)
V=1.0/RHO
DXBT=-(2.0-XB)*OMEGT/T
DXBP=-(2.0-XB)*OMEGP/P
DZAT=PA*(XA*DBPT-BP*DXBT)
DZAP=PA*BP*(XA/P-DXBP)
SIGT=T*((1.0-Z*XB)*DZAT-Z*(ZA-1.0)*DXBT)/ZA
SIGP=P*((1.0-Z*XB)*DZAP-Z*(ZA-1.0)*DXBP)/ZA
DVT=V*(1.0-OMEGT+SIGT)/T
DVP=-V*(1.0+OMEGP-SIGP)/P
GAM=-(V**2.0)/(RW*T*(DVP/RRP+T*(DVT**2.0)/CP))
C
IF (MARIE) 540,510,500
C
C
C
THERMODYNAMIC PROPERTY DERIVATIVES
500 DCPAL=(3.*A(4,J)*T+2.0*A(3,J))*T+A(2,J)
DCPBET=(3.*B(4,J)*T+2.0*B(3,J))*T+B(2,J)
DCPART=DCPAL-DXBT*(CPALR-CPAL)/XA-PAA*(2.0*DBPT+4.0*T*D2BPT+(T**2.
10)*D3BPT)
DHP=V*(OMEGT-SIGT)*RRP
DST=CP/T
DSP=(DHP-V*RRP)/T
PXAXB=1.0/XB-1.0/XA+1.0/(2.0-XB)
D2XBT=DXBT*(SCP/(T*SH)-2.0/T+DXBT*PXAXB)
D2XBP=DXBP*(-1.0/P+DXBP*PXAXB)
D2XBTP=DXBP*DXBT*PXAXB
D2ZAT=PA*(XA*D2BPT-2.0*DBPT*DXBT-BP*D2XBT)
D2ZAP=-PA*BP*(2.0*DXBP/P+D2XBP)
D2ZATP=DZAT/P-PA*(DBPT*DXBP+BP*D2XBTP)
D2ZT=Z*(-2.0*Z*SIGT*(XB*DZAT+(ZA-1.0)*DXBT)/T+(1.0-Z*XB)*D2ZAT-Z*(
12.0*DZAT*DXBT+(ZA-1.0)*D2XBT))/ZA
D2ZP=Z*(-2.0*Z*SIGP*(XB*DZAP+(ZA-1.0)*DXBP)/P+(1.0-Z*XB)*D2ZAP-Z*(
12.0*DZAP*DXBP+(ZA-1.0)*D2XBP))/ZA
D2ZTP=Z*SIGP*(SIGT/T-Z*(XB*DZAT+(ZA-1.0)*DXBT)/ZA)/P-DZAP*(Z*SIGT/
1T+(Z**2.0)*DXBT)/ZA+Z*((1.0-Z*XB)*D2ZATP-Z*(DZAT*DXBP+(ZA-1.0)*D2X
2BTP))/ZA
DOMPP=-OMEGP*(2.0-3.0*XB)/(P*(2.0-XB)**2.0)
DOMTP=DOMPP*OMEGT/OMEGP
DOMPT=DOMTP*P/T
DOMTT=-SH*DOMPT-(OMEGT+OMEGP*SCP)/T
D2VT=DVT*(DVT/V-1.0/T)+V*(SIGT*(1.0-SIGT)/T+T*D2ZT/Z-DOMTT)/T
D2VP=+DVP*(DVP/V-1.0/P)+V*(SIGP*(1.0-SIGP)/P+P*D2ZP/Z-DOMPP)/P
D2VTP=DVT*DVP/V+V*(T*D2ZTP/Z-SIGT*SIGP/P-DOMTP)/T
DCPT=-CP*OMEGT/T+RW*(XA*DCPART+XB*DCPBET+(CPBET-CPALR)*DXBT-OMEGT*
1(2.0*CPBET-CPAL-SH)/T-SH*DOMTT)
DCPP=-T*D2VT*RRP

```

GZET=DVP+T*(DVT**2.0)*RRP/CP
 ZETAT=-1.0+OMEGT+2.0*T*DVT/V-T*(D2VTP+DVT*(DVT*(1.0-T*DCPT/CP)+2.0
 1*T*D2VT)*RRP/CP)/GZET
 ZETAP=OMEGP+2.0*P*DVP/V-P*(D2VP+T*DVT*(2.0*D2VTP-DVT*DCPP/CP)*RRP/
 1CP)/GZET

C IF (MARIE-1) 540,540,510

C
 C TRANSPORT PROPERTIES

510 BROX=PAA*(BP+ZA*(T*DBPT+BP))
 REMU=(((-0.405*BROX+0.7557)*BROX+0.175)*BROX+1.0
 RCLAM=(((-0.204*BROX+0.5017)*BROX+0.575)*BROX+1.0

C IF (T-1000.0) 530,520,520

C FOR T GREATER THAN 1000 K

520 TB=T/1000.0
 OM11AA=((0.14623574E-01*TB-0.18489490)*TB+0.91980880)*TB-2.557394
 19)*TB+7.0094541
 OM22AA=((0.95071874E-02*TB-0.10429573)*TB+0.45828106)*TB-1.480823
 11)*TB+7.1123388
 OM22BB=((0.16937599E-01*TB-0.23119789)*TB+1.2626982)*TB-3.6380257
 1)*TB+8.5409494
 OM11AB=((0.11138559E-01*TB-0.15841870)*TB+0.88615205)*TB-2.606318
 16)*TB+6.0232023
 ASTAR=(((-0.19584008E-03*TB+0.27802096E-02)*TB-0.15400604E-01)*TB+
 10.48876025E-01)*TB+1.1989301
 BSTAR=(((-0.10633974E-03*TB+0.16747451E-02)*TB-0.10818140E-01)*TB+
 10.44253705E-01)*TB+1.1649620
 GMU=0.026693*SQRTF(1.00813*T)
 EMUA=1.414214*GMU/OM22AA
 EMUB=GMU/OM22BB
 CLAMOA=3.69353*EMUA
 CLAMOB=7.38706*EMUB
 EMUA=EMUA*REMU
 DAAPA=0.002628*T*SQRTF(T/2.01626)/OM11AA
 DABPA=0.001314*T*SQRTF(3.0*T/1.00813)/OM11AB
 GH=164.1236*XA*XB*T/(3.02439*DABPA)
 HAA=1000.0*XA**2/EMUA+GH*(1.0+0.3*ASTAR)
 HBB=1000.0*XB**2/EMUB+GH*(1.0+1.2*ASTAR)
 HAB=-GH*(1.0-0.6*ASTAR)
 EMU=(XA**2/HAA+XB**2/HBB-(2.0*XA*XB*HAB)/(HAA*HBB))/(1.0-HAB**2/(
 1HAA*HBB))
 CLAMOA=CLAMOA*RCLAM
 GL=2.93846*XA*XB*T/DABPA
 GLAA=-4000.0*XA**2/CLAMOA-GL*(36.25-3.0*BSTAR+8.0*ASTAR)
 GLBB=-4000.0*XB**2/CLAMOB-GL*(32.5-12.0*BSTAR+8.0*ASTAR)
 GLAB=2.0*GL*(13.75-3.0*BSTAR-4.0*ASTAR)
 CLAMO=-4.0*(XA**2/GLAA+XB**2/GLBB-(2.0*XA*XB*GLAB)/(GLAA*GLBB))/
 1(1.0-GLAB**2/(GLAA*GLBB))
 CLAMIA=(0.0242*DAAPA/T)*(CPAL-2.5)
 CLAMIA=CLAMIA*RCLAM
 CLAMI=CLAMIA/(1.0+(XB*DAAPA)/(XA*DABPA))
 CLAMR=(0.0242*DABPA*SH**2/T)*(XA*XB/(2.0-XB)**2)
 CLAM=CLAMO+CLAMI+CLAMR
 PR=CP*EMU/CLAM
 GO TO 540

C
C
C

FOR T LESS THAN 1000 K

```

530 TSTAR=T/37.3
    Z11AA=((((-0.12178327E-06)*TSTAR+0.16290869E-04)*TSTAR-0.87840901E
    1-03)*TSTAR+0.27400643E-01)*TSTAR+0.80725122
    Z22AA=((((-0.18129117E-06)*TSTAR+0.23528693E-04)*TSTAR-0.12243225E
    1-02)*TSTAR+0.36848743E-01)*TSTAR+0.86982968
    ZMU3=((((-0.36862452E-05)*TSTAR+0.35797475E-03)*TSTAR-0.12028333E-0
    11)*TSTAR+0.16174087)*TSTAR-0.30542749E-01)*0.01+1.0
    ZLAM3=((((-0.57255974E-05)*TSTAR+0.55820177E-03)*TSTAR-0.18850735E-
    101)*TSTAR+0.25493221)*TSTAR-0.62684613E-01)*0.01+1.0
    ZD3=((((-0.29190797E-05)*TSTAR+0.28996069E-03)*TSTAR-0.10050974E-01
    1)*TSTAR+0.14094140)*TSTAR+0.17788263E-01)*0.01+1.0
    GDMU=((0.57142857*TSTAR)**(1.0/3.0))/11.135569
    EMUA=0.026693*SQRTF(2.01626*T)*GDMU*ZMU3/Z22AA
    CLAMO=0.369353E-02*EMUA*ZLAM3/ZMU3
    EMUA=EMUA*REMU
    CLAMO=CLAMO*RCLAM
    DAAPA=0.002628*T*SQRTF(T/2.01626)*GDMU*ZD3/Z11AA
    CLAMI=(0.0242*DAAPA/T)*(CPAL-2.5)
    CLAMI=CLAMI*RCLAM
    CLAM=CLAMO+CLAMI
    EMU=EMUA/1000.0
    PR=CP*EMU/CLAM
540 RETURN
    END

```

MATRIX A

+0.29892484E+01	-0.41034770E-02	+0.44077218E-04
-0.83561287E-07	+0.34011138E+05	-0.13244021E+01
+0.29892484E+01	-0.41034770E-02	+0.44077218E-04
-0.83561287E-07	+0.34011138E+05	-0.13244021E+01
+0.33832407E+01	-0.43245294E-03	+0.39127728E-05
-0.50612747E-08	+0.33930261E+05	-0.35720562E+01
+0.33832407E+01	-0.43245294E-03	+0.39127728E-05
-0.50612747E-08	+0.33930261E+05	-0.35720562E+01
+0.34590074E+01	-0.16560656E-03	+0.91534690E-06
-0.73994236E-09	+0.33916394E+05	-0.39817170E+01
+0.34590074E+01	-0.16560656E-03	+0.91534690E-06
-0.73994236E-09	+0.33916394E+05	-0.39817170E+01
+0.34807949E+01	-0.80579160E-04	+0.23165682E-06
-0.28805124E-12	+0.33914081E+05	-0.41010320E+01
+0.34807949E+01	-0.80579160E-04	+0.23165682E-06
-0.28805124E-12	+0.33914081E+05	-0.41010320E+01
+0.34807949E+01	-0.80579160E-04	+0.23165682E-06
-0.28805124E-12	+0.33914081E+05	-0.41010320E+01
+0.34719964E+01	-0.18114833E-03	+0.40466752E-06
-0.63931054E-10	+0.33931405E+05	-0.40049763E+01
+0.34719964E+01	-0.18114833E-03	+0.40466752E-06
-0.63931054E-10	+0.33931405E+05	-0.40049763E+01
+0.34719964E+01	-0.18114833E-03	+0.40466752E-06
-0.63931054E-10	+0.33931405E+05	-0.40049763E+01
+0.34789902E+01	-0.31594629E-03	+0.61678657E-06
-0.15052076E-09	+0.33942702E+05	-0.39957133E+01
+0.34789902E+01	-0.31594629E-03	+0.61678657E-06
-0.15052076E-09	+0.33942702E+05	-0.39957133E+01
+0.34789902E+01	-0.31594629E-03	+0.61678657E-06
-0.15052076E-09	+0.33942702E+05	-0.39957133E+01
+0.34789902E+01	-0.31594629E-03	+0.61678657E-06
-0.15052076E-09	+0.33942702E+05	-0.39957133E+01
+0.35844555E+01	-0.34525690E-03	+0.53527626E-06
-0.11389801E-09	+0.33862783E+05	-0.46725704E+01
+0.35844555E+01	-0.34525690E-03	+0.53527626E-06
-0.11389801E-09	+0.33862783E+05	-0.46725704E+01
+0.35844555E+01	-0.34525690E-03	+0.53527626E-06
-0.11389801E-09	+0.33862783E+05	-0.46725704E+01
+0.35844555E+01	-0.34525690E-03	+0.53527626E-06
-0.11389801E-09	+0.33862783E+05	-0.46725704E+01
+0.37594391E+01	-0.28808338E-03	+0.36483990E-06
-0.64597043E-10	+0.33655684E+05	-0.59075858E+01
+0.37594391E+01	-0.28808338E-03	+0.36483990E-06
-0.64597043E-10	+0.33655684E+05	-0.59075858E+01
+0.37594391E+01	-0.28808338E-03	+0.36483990E-06
-0.64597043E-10	+0.33655684E+05	-0.59075858E+01

MATRIX A CONT.

+0.37594391E+01	-0.28808338E-03	+0.36483990E-06
-0.64597043E-10	+0.33655684E+05	-0.59075858E+01
+0.37594391E+01	-0.28808338E-03	+0.36483990E-06
-0.64597043E-10	+0.33655684E+05	-0.59075858E+01
+0.3954861E+01	-0.22140298E-03	+0.22523788E-06
-0.31637688E-10	+0.33374923E+05	-0.73044520E+01
+0.39504861E+01	-0.22140298E-03	+0.22523788E-06
-0.31637688E-10	+0.33374923E+05	-0.73044520E+01
+0.39504861E+01	-0.22140298E-03	+0.22523788E-06
-0.31637688E-10	+0.33374923E+05	-0.73044520E+01
+0.39504861E+01	-0.22140298E-03	+0.22523788E-06
-0.31637688E-10	+0.33374923E+05	-0.73044520E+01
+0.39504861E+01	-0.22140298E-03	+0.22523788E-06
-0.31637688E-10	+0.33374923E+05	-0.73044520E+01
+0.40151762E+01	-0.24731652E-03	+0.21223369E-06
-0.27017443E-10	+0.33321516E+05	-0.77275210E+01
+0.40151762E+01	-0.24731652E-03	+0.21223369E-06
-0.27017443E-10	+0.33321516E+05	-0.77275210E+01
+0.40151762E+01	-0.24731652E-03	+0.21223369E-06
-0.27017443E-10	+0.33321516E+05	-0.77275210E+01
+0.40151762E+01	-0.24731652E-03	+0.21223369E-06
-0.27017443E-10	+0.33321516E+05	-0.77275210E+01
+0.40151762E+01	-0.24731652E-03	+0.21223369E-06
-0.27017443E-10	+0.33321516E+05	-0.77275210E+01
+0.42539189E+01	-0.15427069E-03	+0.10657981E-06
-0.10008309E-10	+0.32788324E+05	-0.95972790E+01
+0.42539189E+01	-0.15427069E-03	+0.10657981E-06
-0.10008309E-10	+0.32788324E+05	-0.95972790E+01
+0.42539189E+01	-0.15427069E-03	+0.10657981E-06
-0.10008309E-10	+0.32788324E+05	-0.95972790E+01

MATRIX H

+0.25003116E+01	+0.48528250E-05	-0.62114920E-07
+0.14158863E-09	+0.42945264E+05	-0.46096828E 00
+0.25003116E+01	+0.48528250E-05	-0.62114920E-07
+0.14158863E-09	+0.42945264E+05	-0.46096828E 00
+0.24996710E+01	-0.23852015E-05	+0.20472396E-07
-0.29554273E-10	+0.42945386E+05	-0.45731922E 00
+0.24996710E+01	-0.23852015E-05	+0.20472396E-07
-0.29554273E-10	+0.42945386E+05	-0.45731922E 00
+0.24990717E+01	-0.34323430E-05	+0.18960083E-07
-0.17546524E-10	+0.42945692E+05	-0.45338129E 00
+0.24990717E+01	-0.34323430E-05	+0.18960083E-07
-0.17546524E-10	+0.42945692E+05	-0.45338129E 00
+0.24995465E+01	-0.12618040E-05	+0.47722317E-08
-0.30921566E-11	+0.42945582E+05	-0.45618786E 00
+0.24995465E+01	-0.12618040E-05	+0.47722317E-08
-0.30921566E-11	+0.42945582E+05	-0.45618786E 00
+0.24995465E+01	-0.12618040E-05	+0.47722317E-08
-0.30921566E-11	+0.42945582E+05	-0.45618786E 00
+0.24989933E+01	-0.20950920E-05	+0.60151654E-08
-0.29485802E-11	+0.42946101E+05	-0.45220179E 00
+0.24989933E+01	-0.20950920E-05	+0.60151654E-08
-0.29485802E-11	+0.42946101E+05	-0.45220179E 00
+0.24989933E+01	-0.20950920E-05	+0.60151654E-08
-0.29485802E-11	+0.42946101E+05	-0.45220179E 00
+0.24999803E+01	-0.11020773E-06	+0.64889065E-10
+0.48341707E-14	+0.42945389E+05	-0.45899392E 00
+0.24999803E+01	-0.11020773E-06	+0.64889065E-10
+0.48341707E-14	+0.42945389E+05	-0.45899392E 00
+0.24999803E+01	-0.11020773E-06	+0.64889065E-10
+0.48341707E-14	+0.42945389E+05	-0.45899392E 00
+0.24999803E+01	-0.11020773E-06	+0.64889065E-10
+0.48341707E-14	+0.42945389E+05	-0.45899392E 00
+0.24992764E+01	-0.10212900E-05	+0.17426965E-08
-0.52359488E-12	+0.42946258E+05	-0.45376904E 00
+0.24992764E+01	-0.10212900E-05	+0.17426965E-08
-0.52359488E-12	+0.42946258E+05	-0.45376904E 00
+0.24992764E+01	-0.10212900E-05	+0.17426965E-08
-0.52359488E-12	+0.42946258E+05	-0.45376904E 00
+0.24992764E+01	-0.10212900E-05	+0.17426965E-08
-0.52359488E-12	+0.42946258E+05	-0.45376904E 00
+0.24999862E+01	-0.48149770E-07	+0.28523330E-11
+0.75962533E-14	+0.42945410E+05	-0.45904575E 00
+0.24999862E+01	-0.48149770E-07	+0.28523330E-11
+0.75962533E-14	+0.42945410E+05	-0.45904575E 00
+0.24999862E+01	-0.48149770E-07	+0.28523330E-11
+0.75962533E-14	+0.42945410E+05	-0.45904575E 00

MATRIX B CONT.

+0.24999862E+01	-0.48149770E-07	+0.28523330E-11
+0.75962533E-14	+0.42945410E+05	-0.45904575E 00
+0.24999862E+01	-0.48149770E-07	+0.28523330E-11
+0.75962533E-14	+0.42945410E+05	-0.45904575E 00
+0.25003308E+01	+0.16827689E-06	-0.23105728E-09
+0.45942012E-13	+0.42944715E+05	-0.46175197E 00
+0.25003308E+01	+0.16827689E-06	-0.23105728E-09
+0.45942012E-13	+0.42944715E+05	-0.46175197E 00
+0.25003308E+01	+0.16827689E-06	-0.23105728E-09
+0.45942012E-13	+0.42944715E+05	-0.46175197E 00
+0.25003308E+01	+0.16827689E-06	-0.23105728E-09
+0.45942012E-13	+0.42944715E+05	-0.46175197E 00
+0.25003308E+01	+0.16827689E-06	-0.23105728E-09
+0.45942012E-13	+0.42944715E+05	-0.46175197E 00
+0.25002231E+01	+0.68714240E-07	-0.89401590E-10
+0.14683878E-13	+0.42944842E+05	-0.46094814E 00
+0.25002231E+01	+0.68714240E-07	-0.89401590E-10
+0.14683878E-13	+0.42944842E+05	-0.46094814E 00
+0.25002231E+01	+0.68714240E-07	-0.89401590E-10
+0.14683878E-13	+0.42944842E+05	-0.46094814E 00
+0.25002231E+01	+0.68714240E-07	-0.89401590E-10
+0.14683878E-13	+0.42944842E+05	-0.46094814E 00
+0.25002231E+01	+0.68714240E-07	-0.89401590E-10
+0.14683878E-13	+0.42944842E+05	-0.46094814E 00
+0.24996156E+01	-0.27703100E-06	+0.20942038E-09
-0.28939034E-13	+0.42946455E+05	-0.45598696E 00
+0.24996156E+01	-0.27703100E-06	+0.20942038E-09
-0.28939034E-13	+0.42946455E+05	-0.45598696E 00
+0.24996156E+01	-0.27703100E-06	+0.20942038E-09
-0.28939034E-13	+0.42946455E+05	-0.45598696E 00

APPENDIX B

HEAT TRANSFER AND PRESSURE - DROP CHARACTERISTICS FOR THE FLOW OF A COMPRESSIBLE GAS IN A CONSTANT AREA CHANNEL

1. Summary

A procedure and computer program for calculating the heat transfer and pressure-drop characteristics for the flow of a real compressible gas in a constant area channel are developed. The particular problem for which the program was developed is that of determining the heat transfer characteristics of a gas cooled solid-core reactor such as would be used in a nuclear rocket. Consequently the prescribed conditions on the calculations are oriented to this particular case.

The method used to calculate the heat-transfer and friction characteristics for the flow is patterned after the method of influence coefficients developed by Shapiro and Hawthorne (24) for generalized compressible flow. The equations are developed here for a fluid which is not a perfect gas and reduced so that only one variable is used for the stepwise calculation along the axis of the channel.

2. Development of Fluid Flow Equations

The phenomena taken into consideration in the development of the fluid flow equations are:

1. Heat addition to the gas
2. Wall shear stress (friction)
3. Gas dissociation and its effects on molecular weight and thermodynamic properties

The following assumptions are made:

1. The flow is one-dimensional and steady
2. Changes in stream properties are continuous
3. Cross sectional area for flow is constant
4. Mass flow rate is constant
5. The fluid obeys the equation of state given in Eq. B-1.

The basic relations needed to develop the equations for changes in the stream properties along the axis of the channel are listed below.

The equation of state is:

$$p = \frac{ZpRT}{W} \quad (B-1)$$

The continuity equation is:

$$w = \rho V A_f \quad (B-2)$$

The definition of the Mach number is:

$$M^2 = \frac{V^2}{c^2} \quad (B-3)$$

The expression for the speed of sound is:

$$c^2 = \left(\frac{\partial p}{\partial \rho} \right)_s = \frac{\gamma RT}{W} \quad (B-4)$$

The energy equation is

$$wdQ - wdW_x = w \left(dH + d\frac{V^2}{2} \right) \quad (B-5)$$

The momentum equation is:

$$-A_f dp - \tau_w dA_s = wdV \quad (B-6)$$

Three other equations for the total differentials of three fluid properties are also used. Considering the molecular weight W , the compressibility factor Z , and the isentropic exponent γ as functions of temperature and pressure then:

$$dW = \left(\frac{\partial W}{\partial T} \right)_p dT + \left(\frac{\partial W}{\partial p} \right)_T dp \quad (B-7)$$

$$dZ = \left(\frac{\partial Z}{\partial T} \right)_p dT + \left(\frac{\partial Z}{\partial p} \right)_T dp \quad (B-8)$$

$$d\gamma = \left(\frac{\partial \gamma}{\partial T} \right)_p dT + \left(\frac{\partial \gamma}{\partial p} \right)_T dp \quad (B-9)$$

The logarithms of the terms of Eq. B-1 are:

$$\ln p = \ln Z + \ln p + \ln R + \ln T - \ln W \quad (B-10)$$

Then taking differentials:

$$\frac{dp}{p} = \frac{dZ}{Z} + \frac{dp}{\rho} + \frac{dT}{T} - \frac{dW}{w} \quad (B-11)$$

Similar operations on Eq. B-2 result in:

$$0 = \frac{dp}{\rho} + \frac{dV}{V} \quad (B-12)$$

or

$$\frac{dp}{\rho} = - \frac{1}{2} \frac{dV^2}{V^2} \quad (B-13)$$

Combining Eqs. B-3 and B-4 and performing the above operations yields

$$\frac{dM^2}{M^2} = \frac{dV^2}{V^2} + \frac{dw}{w} - \frac{d\gamma}{\gamma} - \frac{dT}{T} \quad (B-14)$$

Defining:

$$\omega_T = \frac{T}{W} \left(\frac{\partial W}{\partial p} \right)_p \quad (B-15)$$

$$\omega_p = \frac{p}{W} \left(\frac{\partial W}{\partial p} \right)_T \quad (B-16)$$

$$\sigma_T = \frac{T}{Z} \left(\frac{\partial Z}{\partial T} \right)_p \quad (B-17)$$

$$\sigma_p = \frac{p}{Z} \left(\frac{\partial Z}{\partial p} \right)_T \quad (B-18)$$

$$\zeta_T = \frac{T}{\gamma} \left(\frac{\partial \gamma}{\partial T} \right)_p \quad (B-19)$$

$$\zeta_p = \frac{p}{\gamma} \left(\frac{\partial \gamma}{\partial p} \right)_T \quad (B-20)$$

Eqs. B-7 through B-9 can then be written:

$$\frac{dW}{W} = \omega_T \frac{dT}{T} + \omega_p \frac{dp}{p} \quad (B-21)$$

$$\frac{dZ}{Z} = \sigma_T \frac{dT}{T} + \sigma_p \frac{dp}{p} \quad (B-22)$$

$$\frac{d\gamma}{\gamma} = \zeta_T \frac{dT}{T} + \zeta_p \frac{dp}{p} \quad (B-23)$$

The total differential of the enthalpy can be written as:

$$dH = \left(\frac{\partial H}{\partial T} \right)_p dT + \left(\frac{\partial H}{\partial p} \right)_T dp \quad (B-24)$$

By definition:

$$c_p \equiv \left(\frac{\partial H}{\partial T} \right)_p \quad (B-25)$$

and from thermodynamic relations and the equation of state,

Eq. B-1, it can be shown that:

$$\left(\frac{\partial H}{\partial p} \right)_T = v \left[1 - \frac{T}{v} \left(\frac{\partial v}{\partial T} \right)_p \right] \quad (B-26)$$

or

$$\left(\frac{\partial H}{\partial p} \right)_T = \frac{ZRT}{p} (\omega_T - \sigma_T) \quad (B-27)$$

Using Eqs. B-24, B-25, and B-27 and noting that the shaft work

W_x is zero the energy equation can be written:

$$dQ = c_p dT + \frac{ZRT}{pW} (\omega_T - \sigma_T) dp + d\frac{v^2}{2} \quad (B-28)$$

Dividing by $c_p T$ gives:

$$\frac{dQ}{c_p T} = \frac{dT}{T} + \frac{ZR}{Wc_p} (\omega_T - \sigma_T) \frac{dp}{p} + \frac{v^2}{2c_p T} \frac{dv^2}{v^2} \quad (B-29)$$

The coefficient of dv^2/v^2 can be rewritten as:

$$\frac{v^2}{2c_p T} = \frac{1}{2} \frac{M^2(\gamma RT/W)}{c_p T} = \frac{1}{2} \gamma M^2 \frac{R}{Wc_p} \quad (B-30)$$

Defining:

$$\eta = \frac{R}{Wc_p} \quad (B-31)$$

The energy equation can now be written:

$$\frac{dQ}{c_p T} = \frac{dT}{T} + Z\eta (\omega_T - \sigma_T) \frac{dp}{p} + \eta \frac{\gamma M^2}{2} \frac{dv^2}{v^2} \quad (B-32)$$

The wall shear stress in the momentum equation can be written in terms of the friction factor:

$$\tau_w = f \frac{v^2}{2} \quad (B-33)$$

The hydraulic diameter of the coolant channel is:

$$d = \frac{4A_c}{P} = \frac{4A_c}{(dA_s/dx)} \quad (B-34)$$

Using Eqs. B-33 and B-34 the momentum equation can be written:

$$- dp - f \frac{\rho V^2}{2} \frac{4dx}{d} = \rho V dV \quad (B-35)$$

Noting that:

$$\rho V^2 = \frac{pW}{ZRT} \frac{M^2 \gamma RT}{W} = \frac{p \gamma M^2}{Z} \quad (B-36)$$

Then Eq. B-35 can be put in the following form:

$$\frac{dp}{p} + \frac{\gamma M^2}{2Z} \frac{4fdx}{d} + \frac{\gamma M^2}{2Z} \frac{dV^2}{V^2} = 0 \quad (B-37)$$

Eqs. B-11, B-13, B-14, B-21, B-22, B-23, B-32 and B-37 are eight relations between ten variables, namely $\frac{dp}{p}$, $\frac{d\rho}{\rho}$, $\frac{dT}{T}$, $\frac{dW}{W}$, $\frac{dZ}{Z}$, $\frac{dM^2}{M^2}$, $\frac{dV^2}{V^2}$, $\frac{d\gamma}{\gamma}$, $\frac{dQ}{c_p T}$, and $\frac{4fdx}{d}$. Eight of the variables can be taken

as dependent and two as independent. For the case at hand the two variables taken as being independent are $\frac{dQ}{c_p T}$ and $\frac{4fdx}{d}$.

The eight equations are linear algebraic relations and can be solved simply in principal although the amount of manipulation is large. As the Mach number is included in the coefficients of the variables it is desirable to solve for the change in M^2 first. The result is:

$$\frac{dM^2}{M^2} = J \frac{dQ}{c_p T} + \frac{1}{2D} \left[-B + (1 + \eta \gamma M^2 D) J \right] \frac{4fdx}{d} \quad (B-38)$$

where:

$$A = (1 - \omega_T) (1 + \xi_p) + \xi_T (1 + \omega_p) - \sigma_T (\omega_p - \xi_p) - \sigma_p (1 - \omega_T + \xi_T) \quad (B-39)$$

$$B = 1 - \omega_T - \zeta_T + 2\sigma_T \quad (B-40)$$

$$D = 1 - \omega_T + \sigma_T \quad (B-41)$$

$$E = 1 + \omega_P - \sigma_P \quad (B-42)$$

$$F = 2 + \omega_P + \zeta_P - 2\sigma_P \quad (B-43)$$

$$C = 1 - \gamma M^2 \left(\frac{E}{Z} - \eta D^2 \right) \quad (B-44)$$

$$J = \frac{B + \gamma M^2 A}{C} \quad (B-45)$$

The expressions for the changes in the other variables are less complex. For the static pressure and temperature they are

$$\frac{dp}{p} = \frac{D \frac{dM^2}{M^2} + \frac{B}{Z} \frac{4fdx}{d}}{-A - \frac{BZ}{\gamma M^2}} \quad (B-46)$$

and

$$\frac{dT}{T} = \frac{\frac{dM^2}{M^2} + F \frac{dp}{p}}{B} \quad (B-47)$$

By obtaining another independent relation between $\frac{dQ}{c_p T}$ and $\frac{4fdx}{d}$ the number of independent variables can be reduced to one and consequently all the other changes in the stream

properties will be dependent variables. The heat transfer correlation and the correlation for the friction factor provide a basis for relating $\frac{dQ}{c_p T}$ and $\frac{4fdx}{d}$.

For these calculations the local heat transfer coefficient is calculated from an empirical correlation due to Taylor and Kirchgessner (14). This particular correlation was obtained for high ratios of the wall temperature to bulk fluid temperature. It is based on a film temperature which is defined as

$$T_f = \frac{T_B + T_W}{2} \quad (B-48)$$

The correlation itself is of the form

$$Nu_f = 0.021 Re_f^{0.8} Pr_f^{0.4} \quad (B-49)$$

where

$$Nu_f = \frac{hd}{k_f} \quad (B-50)$$

$$Re_f = \frac{\rho_f V d}{\mu_f} \quad (B-51)$$

$$Pr_f = \frac{c_{pf} \mu_f}{k_f} \quad (B-52)$$

The correlation for friction factor is

$$f = 0.046 \operatorname{Re}_B^{-0.2} \quad (\text{B-53})$$

where

$$\operatorname{Re}_B = \frac{\rho_{AV} V d}{\mu_B} = \frac{w}{A_f} \frac{d}{\mu_B} \quad (\text{B-54})$$

The heat transfer rate per unit cross sectional area is

$$\frac{dq}{A_f} = \frac{h d A_s}{A_f} (T_W - T_{AW}) = h \frac{4 dx}{d} (T_W - T_{AW}) \quad (\text{B-55})$$

In this expression T_{AW} is the adiabatic wall temperature which is related to the static temperature by

$$\frac{T_{AW}}{T} = 1 + R \frac{\gamma-1}{2} M^2 \quad (\text{B-56})$$

For turbulent flow the recovery factor is approximately

$$R = \sqrt[3]{\operatorname{Pr}} \quad (\text{B-57})$$

and for hydrogen the Prandtl number is 0.6 or larger. For a Mach number of 0.5 the ratio of T_{AW} to T_S is (assuming $\gamma = 1.3$)

$$\frac{T_{AW}}{T_S} = \frac{1 + R \frac{\gamma-1}{2} M^2}{1 + \frac{\gamma-1}{2} M^2} = 0.995 \quad (\text{B-58})$$

For these calculations representing a reactor core channel the above numbers are representative of the worst case as the gas is hydrogen and the flow is always subsonic with the exit Mach number generally less than 0.5. Consequently, the approximation made by substituting T_s for T_{AW} in the expression for the heat flux causes very little error in this case.

The heat transfer rate in Eq. B-55 must be equal to the amount of heat added to the fluid which can be written

$$\frac{w dQ}{A_f} = \frac{dq}{A_f} \quad (B-59)$$

Combining Eqs. B-49, B-55 and B-56 with the use of the definitions of Eqs. B-50, B-51, and B-52 results in:

$$dQ = \frac{4dx}{d} \left(\frac{T_w - T_{AW}}{w/A_f} \right) \frac{k_f}{d} 0.021 \left(\frac{\rho_f v d}{\mu_f} \right)^{0.8} \left(\frac{c_{pf} \mu_f}{k_f} \right)^{0.4} \quad (B-60)$$

By noting that

$$\frac{w}{A_f} = \rho_{AV} V \quad (B-61)$$

where ρ_{AV} is evaluated at the average static temperature T_{AV} along the element of length in question and using Eq. B-53 for

f, it can be shown that

$$\frac{dQ}{c_p T_{av}} = \frac{4fdx}{d} \frac{0.021}{0.046} \left(\frac{T_W - T_{AW}}{T_{AV}} \right) \left(\frac{\rho_f}{\rho_{AV}} \frac{\mu_B}{\mu_f} \right)^{0.8} \left(\frac{k_f}{c_{pAV} \mu_B} \right) \left(\frac{c_{pf} \mu_f}{k_f} \right)^{0.4} \quad (B-62)$$

or

$$\frac{4fdx}{d} = \frac{0.046}{0.021} \left(\frac{T_{AV}}{T_W - T_{AW}} \right) \left(\frac{\rho_{AV}}{\rho_f} \right)^{0.8} \left(\frac{\mu_B}{\mu_f} \right)^{0.2} \left(\frac{c_{pAV}}{c_{pf}} \right) (Pr_f)^{0.6} \left(\frac{dQ}{c_p T_{AV}} \right) \quad (B-63)$$

To determine $\frac{4fdx}{d}$ from the above expression the wall temperature must be known. In the event that the wall temperature is not specified as constant along the channel then some additional quantity must be specified. If either the wall temperature or the heat flux distribution is given as a function of non-dimensional length along with a value of $\frac{4fL}{d}$ or $\frac{L}{d^{1.2}}$ then the value of $\frac{4fdx}{d}$ can be determined. The latter case is straightforward for the calculation of $\frac{4fdx}{d}$ although the calculation of T_W is a trial and error process. The other case with T_W given as a function of x/L results in a trial and error calculation for $\frac{4fdx}{d}$. To date only the cases of

constant wall temperature and known heat flux distribution have been formulated and solved. The third case has been of no interest and consequently has not been set up.

The simplest case is obviously that when the wall temperature is constant. Then no trial and error calculation is involved for the determination of $\frac{4fdx}{d}$.

When the heat flux distribution is given, the non-dimensional length $\frac{x}{L}$ and consequently $\frac{dx}{L}$, the change from the last position, are obtained for a given value of Q/Q_{TOT}

Then

$$4f \frac{dx}{d} = 4f \frac{L}{d} \left(\frac{dx}{L} \right) = 4 (.043) \left(\frac{\mu}{\rho V} \right)^{0.2} \left(\frac{L}{d^{1.2}} \right) \left(\frac{dx}{L} \right) \quad (B-64)$$

The wall temperature is then determined by assuming a trial value, calculating the film temperature and all the film properties and then solving Eq. B-63 for T_w . If the calculated value of T_w does not agree with the assumed value a correction is made and the process is repeated.

3. Choice of Initial Independent Variables

To determine all the fluid properties at a particular location it is necessary to know two independent thermodynamic properties and one property describing the flow, such as velocity, Mach number, or flow per unit area. Consequently, three

pieces of data must be given at the channel end where the calculations are started. The calculations can be performed going either in the same direction as the flow or in the opposite direction. Some condition must be imposed on the channel length and diameter or on the fluid properties at the channel end where the calculations are to be stopped.

The present program has been written so that the stagnation temperature, stagnation pressure, and flow rate per unit area are to be specified at the channel end where calculations are started. The stagnation temperature is used as the index in the stepwise procedure and is also used as the quantity to determine where the calculations are to be stopped.

4. Starting Procedure

For a given initial stagnation temperature, stagnation pressure, and flow rate per unit area it is necessary to calculate the initial Mach number and static fluid properties. This is done in a trial and error calculation in the following manner. Initial estimates of the static temperature and pressure are made, the flow rate per unit area and entropy corresponding to these values are calculated. The differences between these calculated quantities and the given flow rate per unit area and stagnation entropy are determined and corrections are made to the values of static temperature and pressure. This process

is repeated until the corrections in static temperature and pressure are less than some prescribed limit. The initial estimates for static temperature and pressure are obtained from relationships for a perfect gas or empirical approximations. For a perfect gas the flow rate per unit area can be expressed as follows

$$\frac{w}{A_f} = \sqrt{\frac{\gamma W}{R}} \frac{P_S}{\sqrt{T_S}} \left[1 + \frac{\gamma-1}{2} M^2 \right]^{-\frac{\gamma+1}{2(\gamma-1)}} \quad (B-65)$$

If the flow rate per unit area, stagnation temperature, and stagnation pressure are known the Mach number is the only unknown quantity in the above equation.

By plotting

$$\frac{w}{A_f} \sqrt{\frac{T_S R}{\gamma W}} \frac{1}{P_S} \left(\frac{\gamma+1}{2} \right)^{\frac{\gamma+1}{2(\gamma-1)}} = \frac{A^*}{A} \quad (B-66)$$

versus Mach number where a value of 1.3 is assumed for γ and then approximating the curve by two straight lines, the following expressions were obtained

$$M = 0.625 \frac{A^*}{A} \quad \text{for} \quad \frac{A^*}{A} \leq 0.8 \quad (B-67)$$

$$M = -1.5 + 2.5 \frac{A^*}{A} \quad \text{for} \quad \frac{A^*}{A} > 0.8 \quad (B-68)$$

The approximations for static temperature and pressure are then obtained from the perfect gas relations

$$\frac{T_S}{T} = 1 + \frac{\gamma-1}{2} M^2 \quad (B-69)$$

$$\frac{P_S}{P} = \left(1 + \frac{\gamma-1}{2} M^2\right)^{\frac{\gamma}{\gamma-1}} \quad (B-70)$$

The flow rate per unit area is then calculated from

$$\frac{w}{A_f} = \rho V = \frac{pW}{ZRT} \sqrt{2(H_o - H)} \quad (B-71)$$

where the properties Z , W , and H are evaluated at the static conditions.

Here and throughout the description of the calculation procedure it is assumed that the thermodynamic and transport properties and certain derivatives of these properties are determined when the pressure and temperature are known. Actually these properties are all calculated from equations using pressure and temperature as the independent variables. The development and presentation of these equations is shown in Appendix A.

The values of corrections to static temperature and pressure are obtained from the expressions for the two total derivatives

$$d \frac{w}{A_f} = \left(\frac{\partial \frac{w}{A_f}}{\partial T} \right)_p dT + \left(\frac{\partial \frac{w}{A_f}}{\partial P} \right)_T dp \quad (B-72)$$

$$dS = \left(\frac{\partial S}{\partial T} \right)_p dT + \left(\frac{\partial S}{\partial P} \right)_T dp \quad (B-73)$$

The resulting expressions are

$$dT = \frac{\left(\frac{\partial \frac{w}{A_f}}{\partial P} \right)_T dS - \left(\frac{\partial S}{\partial P} \right)_T d \frac{w}{A_f}}{\left(\frac{\partial \frac{w}{A_f}}{\partial P} \right)_T \left(\frac{\partial S}{\partial T} \right)_p - \left(\frac{\partial \frac{w}{A_f}}{\partial T} \right)_p \left(\frac{\partial S}{\partial P} \right)_T} \quad (B-74)$$

and

$$dp = \frac{dS - \left(\frac{\partial S}{\partial T} \right)_p dT}{\left(\frac{\partial S}{\partial P} \right)_T} \quad (B-75)$$

where in terms of finite rather than infinitesimal differences

$$\Delta S = S_o - S \quad (B-76)$$

and

$$\Delta \frac{w}{A_f} = \left(\frac{w}{A_f} \right)_{\text{given}} - \left(\frac{w}{A_f} \right)_{\text{calc}} \quad (B-77)$$

The derivatives of w/A_f are obtained by differentiating Eq. B-2.

The results are:

$$\left(\frac{\partial \frac{w}{A_f}}{\partial T} \right)_p = \frac{w}{A_f} \left[\frac{\omega_T - \sigma_T - 1}{T} - \frac{c_p}{2(H_o - H)} \right] \quad (B-78)$$

$$\left(\frac{\partial \frac{w}{A_f}}{\partial p} \right)_T = \frac{w}{A_f} \left[\frac{\omega_p - \sigma_p + 1}{T} - \frac{(\frac{\partial H}{\partial p})_T}{2(H_o - H)} \right] \quad (B-79)$$

Once the correct static properties at the starting condition are determined the trial and error procedure using the influence coefficients can be started.

In the event that the Mach number was specified rather than the flow rate per unit area the correction for static temperature and pressure would be similar to Eqs. B-74 and B-75 with the derivatives of w/A replaced with the derivatives of M .

5. Stepwise Trial and Error Procedure

The procedure for calculating one step along the coolant channel involves the solution of Eq. B-38 written in terms of finite differences. The solution is a trial and error process because the coefficients in the equations for the changes in

Mach number, temperature, and pressure are dependent on the temperature and pressure. Consequently, trial values are assumed for the change in fluid temperature and pressure, the changes in these and other properties are calculated, and if the calculated values do not agree with the assumed values the procedure is repeated. The procedure is the same whether the wall temperature or the heat flux distribution is given although the calculation of $\frac{4fdx}{d}$ is different for the two cases as has been shown.

6. Calculation of the Fluid Stagnation Properties from the Static Properties and Fluid Velocity.

In the stepwise procedure the values of the stagnation properties must be calculated from the static properties and the velocity or Mach number which are obtained from Eqs. B-38, B-46, and B-47. The stagnation properties can be determined because the entropy is the same as the static entropy and the stagnation and static enthalpies are simply related to the velocity.

$$H_o = H + \frac{V^2}{2} \quad (B-80)$$

Initial guesses for the stagnation temperature and pressure are obtained from Eqs. B-69 and B-70. The enthalpy and entropy

are then calculated using these values. Corrections can then be made to the temperature and pressure if necessary. The expressions for the total derivatives of enthalpy and entropy can be solved to give:

$$\Delta T = \frac{\left(\frac{\partial S}{\partial p}\right)_T \Delta H - \left(\frac{\partial H}{\partial p}\right)_T \Delta S}{c_p \left(\frac{\partial S}{\partial p}\right)_T - \left(\frac{\partial H}{\partial p}\right)_T \left(\frac{\partial S}{\partial T}\right)_p} \quad (\text{B-81})$$

and

$$\Delta p = \frac{\Delta S - \left(\frac{\partial S}{\partial T}\right)_p \Delta T}{\left(\frac{\partial S}{\partial p}\right)_T} \quad (\text{B-82})$$

where

$$\Delta S = S_S - S_{\text{calc}} \quad (\text{B-83})$$

$$\Delta h = h_S - h_{\text{calc}} \quad (\text{B-84})$$

If ΔT and Δp are close enough to zero the trial and error process is halted but if either one is larger than some prescribed value the correction is added to the last value and the process is repeated.

7. Pressure and Temperature Corrections for the Stepwise Trial and Error Procedure

After the stagnation properties have been calculated from the static conditions they are checked against the values assumed at the beginning of the step. If the differences between the calculated and assumed values are not close enough to zero, the calculated values are used as the new assumed properties and the whole step is recalculated. This simple procedure converged for all cases that were calculated and in the runs which were checked the number of steps required was quite small.

APPENDIX C

STRESS CALCULATIONS

1. General

The model used to determine when the reactor is stress limited is an annular element with the same inside diameter as a coolant channel in the core and the same void fraction as the reactor. The general thermal stress equations of an annular element in plane strain are (33):

$$\sigma_r = -\frac{\alpha E}{1-\nu} \frac{1}{r^2} \int_{r_i}^r \theta \, r \, dr + \frac{E}{1-\nu} \left(\frac{C_1}{1-2\nu} - \frac{C_2}{r^2} \right) \quad (C-1)$$

$$\sigma_\theta = \frac{\alpha E}{1-\nu} \frac{1}{r^2} \int_{r_i}^r \theta \, r \, dr - \frac{\alpha E \theta}{1-\nu} + \frac{E}{1+\nu} \left(\frac{C_1}{1-2\nu} + \frac{C_2}{r^2} \right) \quad (C-2)$$

$$\sigma_z = -\frac{\alpha E \theta}{1-\nu} + \frac{2\nu E C_1}{(1+\nu)(1-2\nu)} + C_3 \quad (C-3)$$

The temperature is assumed to be symmetrical about the axis and variations in the axial direction are neglected in calculating the local stresses. The constant C_3 would be zero for the true plane strain case but is chosen to be finite here so the resultant force on the ends of the element is zero. This does not affect the radial or tangential stresses and gives

rise only to local effects at the ends. The boundary conditions on the stresses provide the information required to evaluate the constants in stress equations. Two different sets of boundary conditions are considered in the following sections.

In order to evaluate the stresses it is necessary to know the temperature distribution in the solid material. The heat generation rate is assumed to be uniform in the annular element and the outside boundary is taken to be adiabatic as the annulus is supposed to represent a unit cell of the reactor.

The heat conduction equation for an axisymmetric body with uniform heat generation and negligible temperature gradients in the axial direction is

$$k \left(\frac{d^2 T}{dr^2} + \frac{1}{r} \frac{dT}{dr} \right) + W_i = 0 \quad (C-4)$$

or

$$\frac{1}{r} \frac{d}{dr} \left(r \frac{dT}{dr} \right) = - \frac{W_i}{k} \quad (C-5)$$

The double integration of Eq. C-5 yields

$$T = - \frac{W_i}{4k} r^2 + C_1 \ln r + C_2 \quad (C-6)$$

The boundary conditions that $T = T_W$ at $r = r_i$ and $\frac{dT}{dr} = 0$

at $r = r_o$ are sufficient for the evaluation of C_1 and C_2 .

The resulting expression for the temperature difference θ is

$$\theta = T - T_W = \frac{W_i}{2k} \left(r_o^2 \ln \frac{r}{r_i} - \frac{r^2 - r_i^2}{2} \right) \quad (C-7)$$

For the evaluation of the local stresses the integral of $\theta r dr$ evaluated at different radii is required. Straightforward integration of Eq. C-7 multiplied by r results in

$$\int_{r_i}^r \theta r dr = \frac{W_i}{2k} \left[r_o^2 \left(\frac{r^2}{2} \ln \frac{r}{r_i} - \frac{r^2}{4} \right) - \left(\frac{r^4}{8} - \frac{r_i^2 r^2}{4} \right) \right]_{r_i}^r \quad (C-8)$$

After evaluating the limits and simplifying

$$\int_{r_i}^r \theta r dr = \frac{W_i}{4k} \left[r_o^2 \left(r^2 \ln \frac{r}{r_i} - \frac{r^2 - r_i^2}{2} \right) - \left(\frac{r^2 - r_i^2}{2} \right)^2 \right] \quad (C-9)$$

If the integral is evaluated between r_i and r_o rather than r_i and r , the result is

$$\int_{r_i}^{r_o} \theta r dr = \frac{W_i r_o^2}{4k} \left\{ \ln \frac{r_o}{r_i} - \frac{1 - \left(\frac{r_i}{r_o} \right)^2}{2} - \left[\frac{1 - \left(\frac{r_i}{r_o} \right)^2}{2} \right]^2 \right\} \quad (C-10)$$

The two sets of boundary conditions on the stress that were investigated are different at the outer boundary of the annulus. For the first case the radial stress at the outer

boundary is assumed to be zero while for the second case the gradient of the radial stress is set equal to zero. For both cases the radial stress at the inner boundary is equal to the negative value of the local fluid pressure.

2. Stress Equations when $\sigma_r = 0$ at $r = r_o$

The boundary conditions for the stresses in this case are

$$\sigma_r = -p \text{ at } r = r_i \quad (C-11)$$

$$\sigma_r = 0 \text{ at } r = r_o \quad (C-12)$$

Applying these boundary conditions to Eq. C-1 results in the following two equations for C_1 and C_2

$$-p = \frac{E}{1+\nu} \left(\frac{C_1}{1-2\nu} - \frac{C_2}{r_i^2} \right) \quad (C-13)$$

$$0 = \frac{-\alpha E}{1-\nu} \frac{1}{r_o^2} \int_{r_i}^{r_o} \theta r dr + \frac{E}{1+\nu} \left(\frac{C_1}{1-2\nu} - \frac{C_2}{r_o^2} \right) \quad (C-14)$$

Solving for C_1 and C_2

$$C_2 = \frac{1+\nu}{E} \frac{r_i^2 r_o^2}{r_o^2 - r_i^2} \left[p + \frac{\alpha E}{1-\nu} \frac{1}{r_o^2} \int_{r_i}^{r_o} \theta r dr \right] \quad (C-15)$$

and

$$C_1 = \frac{(1-2\nu)(1+\nu)}{E} \left[\frac{r_o^2}{r_o^2 - r_i^2} \left(p + \frac{\alpha E}{1-\nu} \frac{1}{r_o^2} \int_{r_i}^{r_o} \epsilon r dr \right) - p \right] \quad (C-16)$$

When these expressions are inserted in Eqs. C-1 and C-2 and the resulting equations are simplified, the results are:

$$\sigma_r = - \frac{r_i^2}{r^2} \left(\frac{r_o^2 - r^2}{r_o^2 - r_i^2} \right) p + \frac{\alpha E}{1-\nu} \frac{1}{r^2} \left[\frac{r^2 - r_i^2}{r_o^2 - r_i^2} \int_{r_i}^{r_o} \epsilon r dr - \int_{r_i}^{r_o} \epsilon r dr \right] \quad (C-17)$$

$$\sigma_\theta = \frac{r_i^2}{r_o^2} \left(\frac{r_o^2 + r_i^2}{r_o^2 - r_i^2} \right) p + \frac{\alpha E}{1-\nu} \frac{1}{r^2} \left[\frac{r^2 + r_i^2}{r_o^2 - r_i^2} \int_{r_i}^{r_o} \epsilon r dr + \int_{r_i}^r \epsilon r dr - \epsilon r^2 \right] \quad (C-18)$$

The resultant force on the ends of the element is to be zero. For this case the constant C_3 and consequently σ_z can be found in the following manner. The integral of the stress over area of the annulus must be zero.

$$\int_{r_i}^{r_o} \sigma_z r dr = 0 \quad (C-19)$$

Inserting Eq. C-3 and integrating yields

$$-\frac{\alpha E}{1-\nu} \int_{r_i}^{r_o} \theta r dr + \left[\frac{2\nu E C_1}{(1+\nu)(1-2\nu)} + C_3 \right] \left(\frac{r_o^2}{2} - \frac{r_i^2}{2} \right) = 0 \quad (C-20)$$

The term in the square bracket is just $\sigma_z + \frac{\alpha E \theta}{1-\nu}$ as can be seen from Eq. C-3. When this is inserted in Eq. C-20, an expression can be obtained for σ_z directly without solving for C_3 . The result is

$$\sigma_z = \frac{\alpha E}{1-\nu} \left[-\theta + \frac{2}{r_o^2 - r_i^2} \int_{r_i}^{r_o} \theta r dr \right] \quad (C-21)$$

Eqs. C-17, C-18, and C-21 are the three equations for the local stresses. Using Eqs. C-7, C-9, and C-10 to eliminate the temperature and the integrals and noting that the void fraction is

$$\nu = \left(\frac{r_i}{r_o} \right)^2 \quad (C-22)$$

the equations for the stresses can be rewritten. After a considerable amount of algebraic manipulation the results are

$$\sigma_r = -\frac{\nu}{\left(\frac{r}{r_o}\right)^2} \left[\frac{1 - \left(\frac{r}{r_o}\right)^2}{1-\nu} \right] p + \frac{\alpha E}{1-\nu} \frac{W_i}{4k} \frac{r_i^2}{\nu} \left\{ \left[\frac{\left(\frac{r}{r_o}\right)^2 - \nu}{1-\nu} \right] \frac{1}{\left(\frac{r}{r_o}\right)^2} \ln \sqrt{\frac{1}{\nu}} - \right.$$

$$\ln \frac{r}{r_o} \sqrt{\frac{1}{v}} \left] - \frac{\left(\frac{r}{r_o}\right)^2 - v}{4\left(\frac{r}{r_o}\right)^2} \left[1 - \left(\frac{r}{r_o}\right)^2 \right] \right\} \quad (C-23)$$

$$\sigma_\theta = \frac{v \left[1 + \left(\frac{r}{r_o}\right)^2 \right]}{\left(\frac{r}{r_o}\right)^2 (1-v)} p + \frac{\alpha E}{1-v} \frac{W_i}{4k} \frac{r_i^2}{v} \left\{ \frac{\left(\frac{r}{r_o}\right)^2 + v}{1-v} \frac{1}{\left(\frac{r}{r_o}\right)^2} \ln \frac{1}{\sqrt{v}} - \ln \left[\frac{r}{r_o} \sqrt{\frac{1}{v}} \right] \right\} + \frac{1}{4\left(\frac{r}{r_o}\right)^2} \left\{ \left(\frac{r}{r_o}\right)^2 \left[3\left(\frac{r}{r_o}\right)^2 - v \right] - \left[5\left(\frac{r}{r_o}\right)^2 + v \right] \right\} \quad (C-24)$$

$$\sigma_z = \frac{\alpha E}{1-v} \frac{W_i}{4k} \frac{r_i^2}{v} \left\{ 2 \left[\frac{1}{1-v} \ln \frac{1}{\sqrt{v}} - \ln \frac{r}{r_o} \sqrt{\frac{1}{v}} \right] - \frac{3-v}{2} + \left[\left(\frac{r}{r_o}\right)^2 - v \right] \right\} \quad (C-25)$$

The worst stresses in the annular element occur at the inner radius as was shown in Fig. 4-11. If Eqs. C-23 through C-25 are evaluated at the inside radius the expressions can be simplified to the following:

$$\sigma_r = -p \quad (C-26)$$

$$\sigma_\theta = \frac{1+v}{1-v} p + \frac{\alpha E}{1-v} \frac{W_i}{4k} \frac{r_i^2}{v} \left[\frac{2}{1-v} \ln \frac{1}{\sqrt{v}} - \frac{3-v}{2} \right] \quad (C-27)$$

$$\sigma_z = \frac{\alpha E}{1-v} \frac{W_i}{4k} \frac{r_i^2}{v} \left[\frac{2}{1-v} \ln \frac{1}{\sqrt{v}} - \frac{3-v}{2} \right] \quad (C-28)$$

3. Stress Equations when $\frac{d\sigma_r}{dr} = 0$ at $r = r_o$

The boundary conditions for this case are:

$$\frac{d\sigma_r}{dr} = 0 \quad \text{at} \quad r = r_o \quad (C-29)$$

$$\sigma_r = -p \quad \text{at} \quad r = r_i \quad (C-30)$$

Applying these boundary conditions to Eq. C-1 results in the following two equations for the constants.

$$-p = \frac{E}{1+\nu} \left(\frac{C_1}{1-2\nu} - \frac{C_2}{r_i^2} \right) \quad (C-31)$$

$$0 = \left[\frac{2\alpha E}{(1-\nu)r^3} \int_{r_i}^r \theta r dr - \frac{\alpha E}{1-\nu} \frac{\theta}{r} + \frac{E}{1+\nu} \left(\frac{2C_2}{r^3} \right) \right]_{r=r_o} \quad (C-32)$$

If Eq. C-32 is solved for C_2 , the result is

$$C_2 = \frac{1+\nu}{1-\nu} \alpha \left[\frac{r_o^2}{2} \theta_{r=r_o} - \int_{r_i}^{r_o} \theta r dr \right] \quad (C-33)$$

Then

$$C_1 = (1+\nu) (1-2\nu) \left[-\frac{p}{E} + \frac{\alpha}{(1-\nu)r_i^2} \left(\frac{r_o^2}{2} \theta_{r=r_o} - \int_{r_i}^{r_o} \theta r dr \right) \right] \quad (C-34)$$

When these expressions for the constants are inserted in Eqs. C-1 and C-2 and the resulting equations are simplified, the results are

$$\sigma_r = -p + \frac{\alpha E}{1-\nu} \left[\left(\frac{1}{r_i^2} - \frac{1}{r^2} \right) \left(\frac{r_o^2}{2} \theta_{r=r_o} - \int_{r_i}^{r_o} \theta r dr \right) - \frac{1}{r^2} \int_{r_i}^r \theta r dr \right] \quad (C-35)$$

$$\sigma_\theta = -p + \frac{\alpha E}{1-\nu} \left[\left(\frac{1}{r_i^2} + \frac{1}{r^2} \right) \left(\frac{r_o^2}{2} \theta_{r=r_o} - \int_{r_i}^{r_o} \theta r dr \right) - \frac{1}{r^2} \int_{r_i}^r \theta r dr - \theta \right] \quad (C-36)$$

The expression for σ_z is obtained in exactly the same manner as in the previous case and the result is the same. Using Eqs. C-7, C-9, and C-10 to eliminate the temperature and inserting the void fraction, given by Eq. C-22, the expressions for σ_r and σ_θ can be rewritten. The results, after some simplification, are

$$\sigma_r = -p + \frac{\alpha E}{1-\nu} \frac{W_i}{4k} \frac{r_i^2}{\nu} \left\{ -\ln \frac{r}{r_o} \sqrt{\frac{1}{\nu}} + \frac{\left(\frac{r}{r_o} \right)^{2-\nu}}{4} \left[\frac{1}{\left(\frac{r}{r_o} \right)^{2\nu}} + 1 \right] \right\} \quad (C-37)$$

$$\sigma_\theta = -p - \frac{\alpha E}{1-\nu} \frac{W_i}{4k} \frac{r_i^2}{\nu} \left\{ \ln \frac{r}{r_o} \sqrt{\frac{1}{\nu}} + \frac{\left[\left(\frac{r}{r_o} \right)^2 + \nu \right] \left[1-\nu \right]^2}{4 \left(\frac{r}{r_o} \right)^{2\nu}} + \right.$$

$$\frac{\left(\frac{r}{r_o}\right)^2 - \nu}{4\left(\frac{r}{r_o}\right)^2} \left[2 - 3\left(\frac{r}{r_o}\right)^2 + \nu \right] \quad (C-38)$$

The expression for σ_z is given by Eq. C-25 as it was for the other set of boundary conditions.

If the stresses are evaluated at the inside radius of the annulus the expressions for σ_r and σ_θ reduce to

$$\sigma_r = -p \quad (C-39)$$

$$\sigma_\theta = -p + \frac{\alpha E}{1-\nu} \frac{W_i}{4k} \frac{r_i^2}{v} \frac{(1-\nu)^2}{2} \quad (C-40)$$

The expression for σ_z is still given by Eq. C-28.

4. Failure Criteria

The different failure criteria that were considered for calculating the limiting stresses are the maximum principal stress, maximum strain, maximum shear, strain energy, and distortion energy theories. The expressions relating the yield point stress in pure tension to the principal stresses in the material for the different theories are presented here. For all the expressions, the magnitudes of the principal stresses are such that

$$\sigma_1 \geq \sigma_2 \geq \sigma_3 \quad (C-41)$$

The different theories and the corresponding expressions are:

maximum principal stress theory

$$\sigma_{YP} = \sigma_1 \quad (C-42)$$

maximum strain theory

$$\sigma_{YP} = \sigma_1 - \nu (\sigma_2 + \sigma_3) \quad (C-43)$$

maximum shear theory

$$\sigma_{YP} = 2 (\sigma_{SH})_{YP} = \sigma_1 - \sigma_3 \quad (C-44)$$

strain energy theory

$$\sigma_{YP}^2 = \sigma_1^2 + \sigma_2^2 + \sigma_3^2 - 2\nu (\sigma_1\sigma_2 + \sigma_2\sigma_3 + \sigma_1\sigma_3) \quad (C-45)$$

distortion energy theory

$$\sigma_{YP}^2 = \frac{1+\nu}{3} \left[(\sigma_1 - \sigma_2)^2 + (\sigma_1 - \sigma_3)^2 + (\sigma_2 - \sigma_3)^2 \right] \quad (C-46)$$

For both sets of boundary conditions considered in the previous sections the annular element is loaded such that it is a case of plain strain. Consequently, the principal stresses are in the directions of the principal axes. At each axial position the stresses can be compared to determine the correspondence between σ_r , σ_θ , σ_z , and σ_1 , σ_2 , σ_3 .

For an ideal brittle material (which is assumed to act elastically until fracture occurs) the maximum principal stress theory should apply (32). For actual brittle materials the failure is related to the flaws in the material and none of these criteria are exactly correct. Other failure theories for

brittle materials have been developed by Griffith and Weibull
(29) but they are not easily applied to engineering problems.

APPENDIX D
COMPUTER PROGRAM AND SAMPLE SOLUTION

1. Description of Program

The Fortran program presented in this appendix was written for use on an IBM 709 or 7090. The calculations for the different components and the input/output functions are in general performed with the use of separate subroutines. Consequently the main program is quite short although some of the subroutines are quite long. Almost all of the important variables are stored in COMMON storage so they can be transmitted implicitly, rather than explicitly, from the main program to the subroutines. This use of COMMON storage simplifies the call statements for the different subroutines and enables the storage area in the machine to be shared between the subprograms. There are some differences in the variables appearing in COMMON storage in the different subroutines. Dummy variables had to be used in some cases due to the duplication of variable names for different variables. Also more variables are inserted in COMMON storage in some subroutines than in others.

The calculations for most of the components are carried out using engineering units. The heat transfer and pressure drop characteristics of the flow through the reactor are not

because they were set up to be compatible with the hydrogen properties subroutine. Consequently the variables are transformed at both the beginning and the end of this subprogram. The units of the input and output variables are presented in the following sections.

The use of separate subroutines for different component calculations makes the program quite flexible. If it is desirable or necessary to change the method of calculation for a particular quantity or component only one subroutine, and not the complete program, must be modified and recompiled. In the process of debugging the program this proved to be quite helpful. The purpose of the separate subroutines and a brief description of each one is presented below.

NRSYS

This is the main program used to unify the separate subroutines. The data required for the calculation of the hydrogen properties is read from cards before any of the subroutines are called.

READD

This subroutine is for reading the data required for a single run with the exception of any data required to specify the shape of the power distribution. Nine data cards containing

values for 31 variables are read each time this subroutine is called.

PRNTD

The data which were read with with READD are printed and possibly punched on cards to provide a check on the values of the data in the event that the program halts before the execution of the complete problem is completed.

HT

The heat transfer and pressure drop characteristics for the flow of hydrogen through the reactor are calculated in this subroutine.

In addition to the characteristics of the hydrogen flow, a number of other quantities are computed. The local power density in the reactor core, the local surface temperature of the coolant channel, and the maximum temperature in the solid part of the core are among the quantities determined as a functions of the nondimensional length of the reactor. Any number of steps less than 200 can be used for the iterative calculations. The hydrogen properties subroutine PRØPS presented in appendix A and the next five subroutines described below are required by HT for different computations.

QØFX

When the shape of the power distribution for the heat transfer calculations cannot be specified by an analytic function, it is necessary to use tabular values. The purpose of this subroutine is to read in the tabular values of heat flux or power density along with the corresponding axial position. The data do not have to be given at uniform intervals of axial position or heat flux. After the data have been read from cards both the heat flux and the length are nondimensionalized for use in further computations. Two different forms of this subroutine are listed for two possible ways of having the tabular data presented as a function of axial position. The position of the data on the cards is not restricted to any set of columns as the format statements in the subroutines are variable.

QDIST

The purpose of this subroutine is to obtain the value of nondimensional reactor length that corresponds to a particular fraction of the total heat addition to the gas for a given shape of power distribution in the reactor. Two different subroutines are presented in the listing of the program. The first one is for a chopped sine power distribution where an analytic function is used to relate the length to the relative heat flux.

The second routine is to be used in conjunction with QØFX when tabular data is used to specify the shape of the power distribution.

PTC

This routine is used to make corrections in the initial estimates of the static properties of the gas for the principal trial and error loop in the stepwise heat transfer calculations. This procedure has remained a separate subroutine since the loop was tested for convergence, although there no longer is any reason for it.

GØFV

This routine is used to calculate a function of the void fraction used in HT to determine the solid temperature and the power density. It was made a separate subroutine so different spacings and geometries of the coolant channels could be considered without changing the heat transfer subroutine. Only one form of the subroutine for the location of coolant channels on the vertices of equilateral triangles is presented.

SIMP

This subroutine is used for calculating the specific impulse that can be obtained by expanding the gas from a given stagnation condition to a given nozzle exhaust pressure.

PRHT

The results which are obtained in HT are printed using this subroutine. If it is desired, the results can also be punched on cards.

ST

The stress calculations for the model considered to be a unit cell of the reactor are performed using the equations presented in this subroutine. Both the principal stresses and their relation to the different failure criteria are determined.

PRST

The results calculated in ST are printed and possibly punched on cards with the use of this subroutine.

RCSW

The critical size and weight of the reactor are determined using this subroutine. For the particular form of the routine which is listed the reactor dimensions are assumed to be known and only the weights of the core and reflector are calculated. Other routines where the critical dimensions are determined from reactor physics calculations can be inserted in place of the simpler one.

PRRCSW

The dimensions of the reactor core and reflectors along with the corresponding weights determined with the use of RCSW

are printed and possibly punched on cards using this subroutine.

PRSH

The weight and thickness of the pressure shell around the reactor are determined with the equations in this subroutine.

TP

The purpose of this subroutine is to obtain values for the weight of the turbopump, the power required to run the pump, and the bleed rate required to run the turbine.

NØZ

The nozzle size required for the expansion of the given flow rate of gas from specified stagnation conditions is determined using this subroutine. The size and weight of the convergent and divergent sections are calculated separately after the throat and exhaust areas are determined from fluid flow computations.

RMIS

This subroutine is used to determine the burning time and ratio of gross to empty weight of a rocket when the mission and the powerplant characteristics are specified. Additional characteristics of the rocket, such as the weights of fuel, tankage, structure and payload, are also computed.

PRSYS

A summary of the more important results of the complete program along with the results from the last three subroutines is printed with the use of this subroutine. It is also possible to have these results punched on cards.

2. Description of Input and Output Variables

The Fortran names of the important input and output variables along with the corresponding symbols used in the test and/or brief descriptions of the variables are presented in this section. The dimensions of the input variables are listed in this section while the dimensions of the output variables are given with the results of the sample problem. The variables are listed in order of their appearance in the input and output routines.

Input:

TITLE - descriptive title of calculated run containing up to 72 Holerith characters, the identifying number should be in columns 43 to 48.

NPR - control variable for printing, if the value is zero or negative the printing of some results is suppressed

NPÜ - control variable for punching, if the value is negative or zero different amounts of punching are suppressed

NGR - control variable for scope no longer used in program

JULIE - control variable for PROPS identified in Appendix A

N - number of computational steps to be performed in HT

TSE - T_{SE} ($^{\circ}R$)

PSE - p_{SE} (psia)

WA - w/A_f (lb/sec - in²)

TSRI - T_{SRI} ($^{\circ}R$)

PSRI - p_{SRI} , initial guess at reactor inlet pressure used for estimating total heat flux to gas (psia)

TWM - control variable for shape of power distribution, if TWM is negative the power distribution is to read from punched cards in QOFX, if TWM is zero the power distribution is specified by an analytic function in QDIST, and if TWM is positive the wall temperature is constant and its magnitude in $^{\circ}R$ is equal to TWM

CL - L (in)

V - v (dimensionless)

D - d (in)

RAD - R (in)

PNE - nozzle exhaust pressure used for specific impulse calculations (psia)

$VP - V_p$ (ft/sec)
 $HP - h_p$ (ft)
 $ALPHA - \alpha$ (1/ $^{\circ}R$)
 $E - E$ (psi)
 $PNU - \nu$ (dimensionless)
 $TK - k$ (Btu/in-sec- $^{\circ}R$)
 $TR - t_R$ (in)
 $TE - t_E$ (in)
 $SR - s_R$ (dimensionless)
 $SE - s_E$ (dimensionless)
 $RH\emptyset PS$ - density of material used in pressure shell (lb/ft³)
 $SIGPS$ - strength of material used in pressure shell (psi)
 $RH\emptyset N$ - density of material used in nozzle (lb/ft³)
 $SIGMAN$ - strength of material used in nozzle (psi)
 $CQ1 - CQ_1$, constant for chopped sine power distribution (dimensionless)

Output:

CI - specific impulse calculated from TSE, PSE, and PNE
 $CIMAX$ - specific impulse calculated from TSE, PSM, and PNE
 CME - Mach number at exit of reactor

CFA - thrust developed per unit flow area of reactor
 CFAPS - CFA / PS(M)
 PS(M) - maximum fluid stagnation pressure in the reactor
 DELPSC - stagnation pressure drop across the core
 PE - fluid static pressure at the reactor exit
 P(M) - maximum fluid static pressure in the reactor
 DELPC - static pressure drop across the core
 T(1) - fluid static temperature at the reactor exit
 T(M) - fluid static temperature at the reactor entrance
 FEXD(M) - fL/d evaluated at reactor exit
 FMLD - fL/d evaluated at reactor entrance
 XD12 - $L/d^{1.2}$
 REBD(M) - Re/d evaluated at reactor entrance
 REBD(1) - Re/d evaluated at reactor exit
 Q(M) - total heat added to unit mass of fluid
 QT - initial estimate of Q(M) based on initial estimate of PSRI
 CM(M) - Mach number at reactor entrance
 CIØIM - $CI/CIMAX$
 ETATS - $(TSE-TSRI) / (TWMAX-TSRI)$
 PSEØI - PSE / PSRI

PDAV - average power density in reactor
 TCWAV - average value of $(T_C - T_W)$
 TWMAX - maximum coolant channel surface temperature in core
 TCMAX - maximum solid temperature in reactor core
 GWT - web thickness between coolant channels
 CLD - L/d
 ACC - flow area per coolant channel
 WPC - flow rate per coolant channel
 FPC - thrust developed per coolant channel
 GV - function of void fraction computed in GØFV
 XL - non-dimensional length measured from reactor exit
 CM - fluid Mach number
 TS - fluid stagnation temperature
 T - fluid static temperature
 PS - fluid stagnation pressure
 P - fluid static pressure
 RHØ - fluid mass density
 XPL - non-dimensional length measured from reactor exit

$$(XPL(I) = (XL(I) + XL(I-1)) / 2.0)$$

DQQDXL - ratio of local to average heat flux

TW - coolant channel surface temperature

TC - maximum solid temperature in reactor core at a given axial position

PD - local power density in reactor

YL - non-dimensional length measured from reactor inlet

FIYD - fx/d measured at position XL in reactor

FEXD - fx/d measured at reactor exit for fraction of reactor length XL

YD12 - $y/d^{1.2}$ measured at YL

QY - heat addition per unit mass of fluid from reactor inlet to position YL

Q - heat addition per unit mass of fluid from reactor exit to position XL

REBD - Re/d at XL

SIGØ - σ_{θ}

SIGZ - σ_z

SIGR - σ_r

SIGST - maximum tensile stress for maximum strain failure theory

SIGSTP - maximum compressive stress for maximum strain failure theory

SIGSH - maximum shear stress times two $2\sigma_{SH}$ for maximum shear failure criterion

SIGSE - maximum stress for strain energy failure criterion

SIGDE - maximum stress for distortion energy failure criterion

AC - flow area of reactor core

EWTC - weight of end reflected reactor core

EWTR - weight of radial reflector around end reflected reactor core

EWTE - weight of end reflector on core

EWTT - total weight of reflectors and end reflected core

TPS - thickness of pressure shell

WPS - weight of pressure shell

RLD - length to diameter ratio of reactor core

SIGSHM - maximum value of SIGSH

SIGDEM - maximum value of SIGDE

DT - diameter of nozzle throat

DE - diameter of nozzle exit plane

AE - area of nozzle exit plane

AET - ratio of exit to throat area of nozzle

CNL - length of convergent section of the nozzle

DNL - length of the divergent section of the nozzle

WNC - weight of the convergent section of the nozzle

WND - weight of the divergent section of the nozzle

WN - total weight of the nozzle

PNEX - design exit pressure for the nozzle

CIEX - specific impulse calculated for expansion to PNEX

THRUST - thrust developed by the powerplant

WTP - weight of turbopump

PTP - pressure at exit of turbopump

WP - total mass flow through system

WBL - mass flow rate of bleed flow

YW - fraction of mass flow required to run turbopump

HPP - horsepower required by pump

CHN - number of coolant channels in reactor core

Q₀NAAV - average heat flux per unit surface area of reactor core

W₀WP - weight of powerplant divided by mass flow rate of coolant

WSØF - weight of powerplant divided by the total thrust developed

PØWSYS - ratio of power developed to weight of the powerplant

WPLØWG - ratio of payload to gross weight of rocket system

WSYS - weight of powerplant

WH2 - weight of hydrogen propellant

WTANK - weight of hydrogen propellant tank

WS - structure weight

WE - empty weight of rocket system

WG - gross weight of rocket system

WDL - dead load weight of rocket system

WPL - payload weight of rocket system

CBAR - exhaust velocity of gas from the nozzle

CISP - specific impulse corrected for bleed flow rate

PTANK - storage pressure of liquid hydrogen in the propellant
tank

FØWG - ratio of thrust to gross weight of rocket system

RLAM - ratio of gross to empty weight of rocket

TP - burning time required for mission

RZET - ratio of propellant to gross weight

PØWER - net power developed by the powerplant

PØWERT - total power developed without correcting for bleed flow
rate

PØEWTT - PØWER/EWTT

PTEWTT - PØWERT/EWTT

PØAC - PØWER/AC

PTAC - PØWERT/AC

3. Fortran Listing of the Computer Program

A listing of the Fortran source program and all the required subroutines, with the exception of the hydrogen properties subroutine given in Appendix A, is presented on the following pages. Where two subroutines with the same name are given only one should be used for a particular problem.

The input-output functions are performed off line automatically at the M.I.T. Computation Center where this program was used. Consequently, some modifications in the input-output may be required if a different monitor system is used.

LISTING OF NUCLEAR ROCKET SYSTEM PROGRAM

* LIST
* LABEL

CNRSYS2

```
COMMON A,B,TS,PS,T,P,CM,TITLE,NPR,NPU,NGR,TSE,PSE,WA,
1TSRI,PSRI,TWM,CL,V,D,JULIE,N,PNE,PD,ALPHA,E,PNU,TK,M,
2SIGR,SIGO,SIGZ,BO,TR,TE,SR,SE,RAD,AC,EWTC,EWTR,EWTE,EWT,
3RHOPS,SIGPS,PSMAX,DELTA,DELPA,WP,RHON,SIGMAN,CI,CIMAX,
4WAG,CME,CFAP,CFAPS,DELPSC,PE,DELP,FECD,FMLD,XD12,REBD,
5Q,QT,CIOIM,ETATS,PSEOI,PDV,TCWAV,TWMAX,TCMAX,GWT,CLD,ACC,
6WPC,FPC,GV,XL,RHOI,XPL,DQQDXL,TW,TC,YL,FIYD,FECD,YD12,QY,
7RAD,AC,WPS,TPS,DT,WNC,WND,WN,AE,DE,CNL,DNL,WTP,PTP,SIGST,
8SIGSTP,SIGSH,SIGSE,SIGDE,PNE,PEN,WSYS,QBAR,XBAR
9,CONDK,CONDR,CFA,RLD,SIGSHM,SIGDEM,PNEX,CIEX,THRUST,WBL,YW,HPP
COMMON VP,HP,PTANK,RLAM,UU,WH2,WTANK,WE,WG,FOWG,WS,WDL,WPL
```

1,CBAR,CISP

```
DIMENSION A(6,40),B(6,40),TS(200),PS(200),T(200),P(200),
1CM(200),TITLE(12),PD(200),SIGR(200),SIGO(200),SIGZ(200),
2FECD(200),XD12(200),REBD(200),Q(200),XL(200),
3RHOI(200),XPL(200),DQQDXL(200),TW(200),TC(200),YL(200),
4FIYD(200),YD12(200),QY(200)
5,SIGST(200),SIGSTP(200),SIGSH(200),SIGSE(200),SIGDE(200)
6,QBAR(100),XBAR(100)
```

```
READ 4000, ((A(I,J),I=1,6),J=1,40), ((B(I,J),I=1,6),J=1,40)
```

4000 FORMAT(3E20.8)

10 CALL READD

CALL PRNTD

CALL HT

CALL PRHT

CALL ST

CALL PRST

CALL RCSW

CALL PRRCSW

WP=WA*AC*144.0

CALL PRSH

CALL TP

CALL NOZ

RLD=CL/(2.0*RAD)

THRUST=CFAP*AC*(1.0-YW)

WSYS=EWT+WP+WN+WTP

CALL RMIS

CALL PRNTD

CALL PRSYS

40 GO TO 10

END


```

*      LIST
*      LABEL
CREADD1
C
C      READING OF DATA EXCEPT FOR QOFX AND QDIST
C
C      TEMPERATURES(DEGREES R), PRESSURES(PSIA), W/A(LB/IN2-SEC),
C      CL AND D(IN.), ALPHA(1/DEGREES R), E(PSI),TK(BTU/IN-SEC-R),
C      TR AND TE(IN.), BO(1/CM2), RHOPS AND RHON(LB-FT3),
C      SIGS AND SIGMAN(PSI)
C
      SUBROUTINE READD
      COMMON A,B,TS,PS,T,P,CM,TITLE,NPR,NPU,NGR,TSE,PSE,WA,
1TSRI,PSRI,TWM,CL,V,D,JULIE,N,PNE,PD,ALPHA,E,PNU,TK,M,
2SIGR,SIGO,SIGZ,BO,TR,TE,SR,SE,RAD,AC,EWTC,EWTR,EWTE,EWTT,
3RHOPS,SIGPS,PSMAX,DELTA,DELPA,WP,RHON,SIGMAN,CI,CIMAX,
4WAG,CME,CFAP,CFAPS,DELPSC,PE,DELP,CFEXD,FMLD,XD12,REBD,
5Q,QT,CIOIM,ETATS,PSEOI,PD,AV,TCWAV,TWMAX,TCMAX,GWT,CLD,ACC,
6WPC,FPC,GV,XL,RHOI,XPL,DQDQXL,TW,TC,YL,FIYD,FEXD,YD12,QY,
7RAD,AC,WPS,TPS,DT,WNC,WND,WN,AE,DE,CNL,DNL,WTP,PTP,SIGST,
8SIGSTP,SIGSH,SIGSE,SIGDE,PNE,PEN,WSYS,QBAR,XBAR
9,CONDK,CONDR,CFA,RLD,SIGSHM,SIGDEM,PNEX,CIEX,THRUST,WBL,YW,HPP
      COMMON VP,HP,PTANK,RLAM,TP,WH2,WTANK,WE,WG,FOWG,WS,WDL,WPL
1,CBAR,CISP
      DIMENSION A(6,40),B(6,40),TS(200),PS(200),T(200),P(200),
1CM(200),TITLE(12),PD(200),SIGR(200),SIGO(200),SIGZ(200),
2FEXD(200),XD12(200),REBD(200),Q(200),XL(200),
3RHOI(200),XPL(200),DQDQXL(200),TW(200),TC(200),YL(200),
4FIYD(200),YD12(200),QY(200)
5,SIGST(200),SIGSTP(200),SIGSH(200),SIGSE(200),SIGDE(200)
6,QBAR(100),XBAR(100)
      READ 4001, (TITLE(I),I=1,12)
      READ 4002, NPR,NPU,NGR,JULIE,N
      READ 4010, TSE,PSE,WA,TSRI,PSRI,TWM
      READ 4020, CL,V,D,RAD
      READ 4030, PNE,VP,HP
      READ 4040, ALPHA,E,PNU,TK
      READ 4050, TR,TE,SR,SE
      READ 4060, RHOPS,SIGPS
      READ 4060, RHON,SIGMAN
4001 FORMAT(1H1A5,11A6)
4002 FORMAT(5I10,24X,A6)
4010 FORMAT(6F10.3,24X,A6)
4020 FORMAT(4F10.3,34X,A6)
4030 FORMAT(F10.4,2F10.1,44X,A6)
4040 FORMAT(4E15.5,14X,A6)
4050 FORMAT(4F10.3,34X,A6)
4060 FORMAT(2E15.5,44X,A6)
      RETURN
      END

```

```
* LIST
* LABEL
CPRNTD1
```

```
C
C
C
```

PRINTING OF DATA EXCEPT FOR QOFX AND QDIST

SUBROUTINE PRNTD

```
COMMON A,B,TS,PS,T,P,CM,TITLE,NPR,NPU,NGR,TSE,PSE,WA,
1TSRI,PSRI,TWM,CL,V,D,JULIE,N,PNE,PD,ALPHA,E,PNU,TK,M,
2SIGR,SIGO,SIGZ,BO,TR,TE,SR,SE,RAD,AC,EWTC,EWTR,EWTE,EWTT,
3RHOPS,SIGPS,PSMAX,DELTA,DELPA,WP,RHON,SIGMAN,CI,CIMAX,
4WAG,CME,CFAP,CFAPS,DELPSC,PE,DELPC,FEXD,FMLD,XD12,REBD,
5Q,QT,CIOIM,ETATS,PSEOI,PDAV,TCWAV,TWMAX,TCMAX,GWT,CLD,ACC,
6WPC,FPC,GV,XL,RHOI,XPL,DQDQXL,TW,TC,YL,FIYD,FEXD,YD12,QY,
7RAD,AC,WPS,TPS,DT,WNC,WND,WN,AE,DE,CNL,DNL,WTP,PTP,SIGST,
8SIGSTP,SIGSH,SIGSE,SIGDE,PNE,PEN,WSYS,QBAR,XBAR
9,CONDK,CONDR,CFA,RLD,SIGSHM,SIGDEM,PNEX,CIEX,THRUST,WBL,YW,HPP
COMMON VP,HP,PTANK,RLAM,TP,WH2,WTANK,WE,WG,FOWG,WS,WDL,WPL
```

```
1,CBAR,CISP
```

```
DIMENSION A(6,40),B(6,40),TS(200),PS(200),T(200),P(200),
1CM(200),TITLE(12),PD(200),SIGR(200),SIGO(200),SIGZ(200),
2FEXD(200),XD12(200),REBD(200),Q(200),XL(200),
3RHOI(200),XPL(200),DQDQXL(200),TW(200),TC(200),YL(200),
4FIYD(200),YD12(200),QY(200)
5,SIGST(200),SIGSTP(200),SIGSH(200),SIGSE(200),SIGDE(200)
6,QBAR(100),XBAR(100)
```

```
PRINT 4001, (TITLE(I),I=1,12)
```

```
PRINT 4003
```

```
PRINT 4002, NPR,NPU,NGR,JULIE,N
```

```
PRINT 4008
```

```
PRINT 4009
```

```
PRINT 4010, TSE,PSE,WA,TSRI,PSRI,TWM
```

```
PRINT 4018
```

```
PRINT 4019
```

```
PRINT 4020, CL,V,D,RAD
```

```
PRINT 4028
```

```
PRINT 4029
```

```
PRINT 4030, PNE,VP,HP
```

```
PRINT 4038
```

```
PRINT 4039
```

```
PRINT 4040, ALPHA,E,PNU,TK
```

```
PRINT 4048
```

```
PRINT 4049
```

```
PRINT 4050, TR,TE,SR,SE
```

```
PRINT 4058
```

```
PRINT 4059
```

```
PRINT 4060, RHOPS,SIGPS,RHON,SIGMAN
```

```
IF (XABSF(NPU)) 20,20,5
```

```
5 IF (NPRD) 15,15,10
```

```
10 PUNCH 4003
```

```
PUNCH 4002, NPR,NPU,NGR,JULIE,N,TI1
```

```
PUNCH 4008
```

```
PUNCH 4009
```

```
PUNCH 4010, TSE,PSE,WA,TSRI,PSRI,TWM,TI1
```

```
PUNCH 4018
```

```
PUNCH 4019
```

```
PUNCH 4020, CL,V,D,RAD,TI1
```

```
PUNCH 4028
```

```
PUNCH 4029
```

```

PUNCH 4030, PNE,VP,HP,TI1
PUNCH 4038
PUNCH 4039
PUNCH 4040, ALPHA,E,PNU,TK,TI1
PUNCH 4048
PUNCH 4049
PUNCH 4050, TR,TE,SR,SE,TI1
PUNCH 4058
PUNCH 4059
PUNCH 4060, RHOPS,SIGPS,RHON,SIGMAN,TI1
NPRD=0
GO TO 20
15 NPRD=1
PUNCH 4001, (TITLE(I),I=1,12)
TI1=TITLE(8)
20 RETURN
4001 FORMAT(1H1A5,11A6)
4002 FORMAT(5I10,24X,A6)
4003 FORMAT(50H0      NPR      NPU      NGR      JULIE      NI
4008 FORMAT(58H0      TSE      PSE      WA      TSRI      PSRI      T
1WM)
4009 FORMAT(59H      DEG R      PSIA LB/IN2-SEC      DEG R      PSIA      DE
1G R)
4010 FORMAT(6F10.3,14X,A6)
4018 FORMAT(38H0      CL      V      D      RAD)
4019 FORMAT(38H      IN.      IN.      IN.)
4020 FORMAT(4F10.3,34X,A6)
4028 FORMAT(28H0      PNE      VP      HP)
4029 FORMAT(28H      PSIA      FT      FT)
4030 FORMAT(F10.4,2F10.1,44X,A6)
4038 FORMAT(58H0      ALPHA      E      PNU
1 K)
4039 FORMAT(60H      1/DEG R      PSI      BTU/IN-S
1EC-R)
4040 FORMAT(4E15.5,14X,A6)
4048 FORMAT(38H0      TR      TE      SR      SE)
4049 FORMAT(18H      IN.      IN.)
4050 FORMAT(4F10.3,34X,A6)
4058 FORMAT(58H0      RHOPS      SIGPS      RHON      SIGM
1AN)
4059 FORMAT(58H      LB/FT3      PSI      LB/FT3      P
1SI)
4060 FORMAT(4E15.5,14X,A6)
END

```

```

* LIST
* LABEL
CHT1
C
C
C
HEAT TRANSFER CALCULATIONS

SUBROUTINE HT
COMMON A,B,TS,PS,T,P,CM,TITLE,NPR,NPU,NGR,TSE,PSE,WA,
1TSRI,PSRI,TWM,CL,V,D,JULIE,N,PNE,PD,ALPHA,E,PNU,TK,M,
2SIGR,SIGO,SIGZ,BO,TR,ZZ,SR,YY,RAD,AC,EWTC,EWTR,EWTE,EWTT,
3RHOPS,SIGPS,PSMAX,DELTA,DELPA,WP,RHON,SIGMAN,CI,CIMAX,
4WAG,CME,CFAP,CFAPS,DELPSC,PE,DELPC,FEXD,FMLD,XD12,REBD,
5Q,QT,CIOIM,ETATS,PSEOI,PDVAV,TCWAV,TWMAX,TCMAX,GWT,CLD,ACC,
6WPC,FPC,GV,XL,RHOI,XPL,DQQDXL,TW,TC,YL,FIYD,FEXD,YD12,QY,
7RAD,AC,WPS,TPS,DT,WNC,WND,WN,AE,DE,CNL,DNL,WTP,PTP,SIGST,
8SIGSTP,SIGSH,SIGSE,SIGDE,PNE,PEN,WSYS,QBAR,XBAR
9,CONDK,CONDR,CFA,RLD,SIGSHM,SIGDEM,PNEX,CIEX,THRUST,WBL,YW,HPP
DIMENSION A(6,40),B(6,40),TS(200),PS(200),T(200),P(200),
1CM(200),TITLE(12),PD(200),SIGR(200),SIGO(200),SIGZ(200),
2FEXD(200),XD12(200),REBD(200),Q(200),XL(200),
3RHOI(200),XPL(200),DQQDXL(200),TW(200),TC(200),YL(200),
4FIYD(200),YD12(200),QY(200)
5,SIGST(200),SIGSTP(200),SIGSH(200),SIGSE(200),SIGDE(200)
6,QBAR(100),XBAR(100)
DIMENSION HS(200),DELQ(200),FEDXD(200),DELXL(200),YPL(200)
FREQUENCY 1352(1,0,0),1690(0,0,1),1711(0,0,1),1931(0,0,1),
11971(1,0,0),2030(1,0,0),2050(0,1,1),2191(1,0,0),2210(0,0,1)
M=N+1
CONDR=12.0*3600.0*TK
CONDK=CONDR/241.9
TN=N
DELTS=(TSRI-TSE)/TN
DELTA=0.5
DELPA=0.1
DELMA=0.00001
DELTWG=20.0
DELTWE=2.0
NCM=40
CTAVC1=1.00017
CPAVC1=0.9998
CPSIC1=1.0
CCMIC=1.01
CDELMC=0.8
1060 TSE=TSE/1.8
TSRI=TSRI/1.8
TWM=TWM/1.8
DELTS=DELTS/1.8
DELTWG=DELTWG/1.8
DELTWE=DELTWE/1.8
WA=WA*453.5924/(2.54**2.0)
CL=2.54*CL
D=2.54*D
1131 CD12=2.54**0.2
1140 R=1.9859
RBAR=82.0618
PSI=14.6959
GGCS=980.665
GCM=1033.23
WAG=WA

```

```

CALL PROPS(TSE,PSE,A,B,-1,JULIE,WSE,Z,RHO,HSE,SSE,CP,GAMSE,DHP,
1DST,DSP,OMEGT,OMEGP,SIGT,SIGP,ZETAT,ZETAP,EMU,CLAM,PR)
CALL PROPS(TSRI,PSRI,A,B,-1,JULIE,W,Z,RHO,HSRI,S,CP,GAM,DHP,DST,
1DSP,OMEGT,OMEGP,SIGT,SIGP,ZETAT,ZETAP,EMU,CLAM,PR)
QT=HSRI-HSE
AOAS=(PSE/(PSI*WA))*SQRTF(GGCS*GCM*WSE*GAMSE/(RBAR*TSE))*(2.0/
1(GAMSE+1.0))*((GAMSE+1.0)/(2.0*(GAMSE-1.0)))
IF (AOAS-1.25) 1203,1204,1204
1203 CME=-1.5+2.5/AOAS
GO TO 1205
1204 CME=0.625/AOAS
1205 GME=1.0+((GAMSE-1.0)/2.0)*CME**2
TE=TSE/GME
PE=PSE/GME**((GAMSE/(GAMSE-1.0)))
IF (NCM) 1241,1245,1245
1241 PRINT 4001, (TITLE(I),I=1,12)
PRINT 4050
PRINT 4010, TSE,PSE,WA,TSRI,PSRI,TWM
PRINT 4051
PRINT 4011, CL,V,D,CONDK,CONDR
PRINT 4060
PRINT 4020, JULIE,N,DELTS,DELTWG,DELTWE,DELMA,PNE
PRINT 4150
1245 N1=1
1250 CALL PROPS(TE,PE,A,B,+1,JULIE,WE,Z,RHOE,HE,SE,CPE,GAME,DHPE,DSTE,
1DSPE,OMEGTE,OMEGPE,SIGTE,SIGPE,ZETATE,ZETAPE,EMU,CLAM,PR)
CM2=2.0*WE*(HSE-HE)/(GAME*R*TE)
1290 CME=SQRTF(CM2)
VE=CME*SQRTF(GAME*RBAR*TE*GGCS*GCM/WE)
DELWA=WA-RHOE*VE
DELS=SSE-SE
DWADT=WA*((OMEGTE-SIGTE-1.0)/TE-CPE/(2.0*(HSE-HE)))
DWADP=WA*((OMEGPE-SIGPE+1.0)/PE-DHPE/(2.0*(HSE-HE)))
DELT=(DWADP*DELS-DSPE*DELWA)/(DWADP*DSTE-DWADT*DSPE)
DELP=(DELS-DSTE*DELT)/DSPE
IF (NCM) 1312,1320,1320
1312 PRINT 4160, N1,TE,PE,GME,CM2,DELS,DWADT,DWADP,DELT,DELP
1320 IF (ABSF(DELT)-DELTA) 1330,1330,1340
1330 IF (ABSF(DELP)-DELP) 1370,1370,1340
1340 TE=TE+DELT
PE=PE+DELP
1352 IF (N1-XABSF(NCM)) 1355,1361,1361
1355 N1=N1+1
GO TO 1250
1361 IF (NCM) 2500,1365,1365
1365 NCM=-2*NCM
GO TO 1140
1370 CALL PROPS(TSE,PE,A,B,+0,JULIE,W,Z,RHO,H,S,CP,GAM,DHP,DST,DSP,
1OMEGT,OMEGP,SIGT,SIGP,ZETAT,ZETAP,EMUBE,CLAM,PR)
WAP=WA*(30.48**2)/453.5924
1400 REBDE=WA/EMUBE
CFE=(REBDE**0.2)/0.046
FELD=CL/(CFE*D**1.2)
1403 FELD=-FELD
1404 P(1)=PE
PS(1)=PSE
T(1)=TE
TS(1)=TSE
HS(1)=HSE

```

```

      CM(1)=CME
      Q(1)=0.0
      FEXD(1)=0.0
1500  XL(1)=0.0
      DELQ(1)=0.0
      QY(1)=-QT
      FEDXD(1)=0.0
      XD12(1)=0.0
      REBD(1)=REBDE
      DELXL(1)=0.0
      XPL(1)=0.0
      DQQDXL(1)=0.0
      YL(1)=1.0
1600  YPL(1)=1.0
      RHOI(1)=RHOE
      PD(1)=0.0
      TC(1)=0.0
      CDX=0.046/(4.0*0.021)
      TCMAX=0.0
      IF (TWM) 1620,1643,1660
1620  CALL QOFX
1643  TW(1)=TSE
      GO TO 1670
1660  TW(1)=ABSF(TWM)
1670  DO 2240 I=2,M
1671  N2=1
      TS(I)=TS(I-1)+DELTS
1690  IF (TS(I)-TSR1) 1700,1710,1710
1700  TS(I)=TSR1
1710  TB=(TS(I)+TS(I-1))/2.0
      TAV=CTAVC1*TB*T(I-1)/TS(I-1)
1711  IF (I-2) 1712,1712,1713
1712  TIC=T(I-1)
      PIO=P(I-1)
      PSIO=PS(I-1)
      GO TO 1714
1713  TIO=T(I-2)
      PIO=P(I-2)
      PSIO=PS(I-2)
1714  PAV=P(I-1)+CPAVC1*(P(I-1)-PIO)/2.0
      PS(I)=PS(I-1)+CPSIC1*(PS(I-1)-PSIO)
      TAV1=TAV
      PAV1=PAV
      PS1=PS(I)
1720  CALL PROPS(TS(I),PS(I),A,B,-1,JULIE,W,Z,RHO,HS(I),S,CP,GAM,DHP,DST
1,DSP,OMEGT,OMEGP,SIGT,SIGP,ZETAT,ZETAP,EMU,CLAM,PR)
1721  TIG=2.0*TAV-T(I-1)
1722  PIG=2.0*PAV-P(I-1)
      PSN2=PS(I)
      CALL PROPS(TB,PAV,A,B,+0,JULIE,W,Z,RHO,H,S,CPB,GAM,DHP,DST,DSP,
1,OMEGT,OMEGP,SIGT,SIGP,ZETAT,ZETAP,EMUB,CLAM,PR)
      RMU02=(EMUBE/EMUB)**0.2
      CALL PROPS(TAV,PAV,A,B,+1,JULIE,WAV,ZAV,RHOAV,H,S,CPAV,GAMAV,DHP,
1DST,DSP,OMEGTV,OMEGPV,SIGTV,SIGPV,ZETATV,ZETAPV,EMU,CLAM,PR)
      DELQ(I)=HS(I)-HS(I-1)
      Q(I)=Q(I-1)+DELQ(I)
      DQCPT=DELQ(I)/(CPAV*TAV)
1800  IF (TWM) 1870,1870,1810
1810  TW(I)=TWM

```

```

TFI=(TW(I)+TB)/2.0
CALL PROPS(TFI,PAV,A,B,+0,JULIE,W,Z,RHOI,H,S,CPFI,GAM,DHP,DST,DSP
1,OMEGT,OMEGP,SIGT,SIGP,ZETAT,ZETAP,EMUFI,CLAMFI,PRFI)
FBDXD=CDX*PRFI**0.6*(EMUB/EMUFI)**0.2*(RHOAV/RHOI)**0.8*DELQ(I)/
1(CPFI*(TW(I)-TB))
FEDXD(I)=FBDXD*RMU02
GO TO 1891
1870 CALL QDIST(Q(I),QT,XL(I))
DELXL(I)=XL(I)-XL(I-1)
FEDXD(I)=FELD*DELXL(I)
FBDXD=FEDXD(I)/RMU02
1891 IF (NCM) 1892,1895,1895
1892 PRINT 4170
PRINT 4160, N2,TIG,PIG,TAV,PAV,PS(I),HS(I),HS(I-1),DQCPT,FBDXD
PRINT 4180
1895 N3=1
IF (N2-1) 1900,1900,1910
1900 CM(I)=CCM1C*CM(I-1)*TS(I)/TS(I-1)
1901 CM1=CM(I)
1910 CMBAR=(CM(I)+CM(I-1))/2.0
CMBAR2=CMBAR**2
GM2D=1.0-OMEGTV+SIGTV
GM2E=1.0+OMEGPV-SIGPV
GM2F=GM2E+1.0+ZETAPV-SIGPV
GM2B=GM2D-ZETATV+SIGTV
GM2A=GM2D*GM2F-GM2B*GM2E
ETA=R/(WAV*CPAV)
GM2C=1.0-GAMAV*CMBAR2*((GM2E/ZAV)-ETA*GM2D**2)
GM2J=(GM2A*GAMAV*CMBAR2/ZAV+GM2B)/GM2C
DELM2=CMBAR2*(GM2J*DQCPT+(-GM2B+GM2J*(1.0+GAMAV*ETA*CMBAR2*GM2D)))*
1FBDXD*2.0/GM2D)
1931 IF (CM(I-1)**2+DELM2) 1932,1932,1934
1932 CMC=0.0
GO TO 1941
1934 IF (CM(I-1)**2+DELM2-1.0) 1940,1985,1985
1940 CMC=SQRTF(CM(I-1)**2+DELM2)
1941 IF (NCM) 1942,1950,1950
1942 PRINT 4160, N3,CM(I),CMBAR,GM2B,GM2D,GM2J,GAMAV,ETA,DELM2,CMC
1950 DELM=CMC-CM(I)
IF (CMC) 1970,1970,1952
1952 IF (ABSF(DELM)-DELM) 1990,1990,1970
1970 CM(I)=CM(I)+CDELMC*DELM
1971 IF (N3-XABSF(NCM)) 1972,1985,1985
1972 N3=N3+1
GO TO 1910
1985 IF (NCM) 1986,1988,1988
1986 M=I-1
NPR=1
NPU=0
NGR=0
GO TO 2242
1988 NCM=-2*NCM
GO TO 1892
1990 DELPOP=(GM2D*DELM2/CMBAR2+2.0*GM2B*FBDXD)/(-GM2A-GM2B*ZAV/(GAMAV*
1CMBAR2))
DELTOT=(DELM2/CMBAR2+GM2F*DELPPOP)/GM2B
P(I)=P(I-1)*(2.0+DELPPOP)/(2.0-DELPPOP)
T(I)=T(I-1)*(2.0+DELTOT)/(2.0-DELTOT)
CALL PROPS(T(I),P(I),A,B,-1,JULIE,WI,Z,RHOI(I),HI,SI,CP,GAMI,DHP,

```

```

1DST,DSP,OMEGT,OMEGP,SIGT,SIGP,ZETAT,ZETAP,EMU,CLAM,PR)
HSIC=HI+(CM(I)**2.0)*GAMI*R*T(I)/(2.0*WI)
2001 TSS=TS(I)
N4=1
IF (NCM) 2007,2010,2010
2007 PRINT 4190
PRINT 4160, N2,DELM,CMBAR2,GM2F,DELPPOP,DELTOT,P(I),T(I),HSIC,TSS
PRINT 4200
2010 CALL PROPS(TSS,PS(I),A,B,+1,JULIE,W,Z,RHO,HSSI,SSI,CPSI,GAM,DHPSI,
1DSTSI,DSPSI,OMEGT,OMEGP,SIGT,SIGP,ZETAT,ZETAP,EMU,CLAM,PR)
DELHS=HSIC-HSSI
DELS=SI-SSI
DELTSI=(DSPSI*DELHS-DHPSI*DELS)/(CPSI*DSPSI-DHPSI*DSTSI)
DELPPI=(DELS-DSTSI*DELTSI)/DSPSI
IF (NCM) 2016,2019,2019
2016 PRINT 4160, N4,HSSI,HSIC,DELHS,SSI,DELS,DELTSI,DELPPI,PS(I),TSS
2019 IF (ABSF(DELTSI)-DELTA) 2020,2020,2030
2020 IF (ABSF(DELPPI)-DELPA) 2040,2040,2030
2030 IF (N4-XABSF(NCM)) 2031,2036,2036
2031 PS(I)=PS(I)+DELPPI
TSS=TSS+DELTSI
N4=N4+1
GO TO 2010
2036 IF (NCM) 1986,2037,2037
2037 NCM=-2*NCM
PS(I)=PSN2
GO TO 2001
2040 CALL PTC(T(I),T(I-1),TAV,P(I),P(I-1),PAV,PS(I),PSN2,TS(I),TSS,
1DELTA,DELTA,DELPA,N2,NCM)
2050 IF (N2) 2055,2058,2051
2051 N2=N2+1
GO TO 1720
2055 IF (NCM) 1986,2056,2056
2056 NCM=-2*NCM
GO TO 1671
2058 CALL PROPS(TS(I),PS(I),A,B,+0,JULIE,W,Z,RHO,HS(I),S,CP,GAM,DHP,DST
1,DSP,OMEGT,OMEGP,SIGT,SIGP,ZETAT,ZETAP,EMUS,CLAM,PR)
FEXD(I)=FEXD(I-1)+FEDXD(I)
XD12(I)=CFE*ABSF(FEXD(I))
QY(I)=-QT+Q(I)
REBD(I)=WA/EMUS
IF (TWM) 2071,2071,2240
2071 N5=1
IF (NCM) 2075,2080,2080
2075 PRINT 4210
2080 CT=FBDXD/(CDX*DELQ(I)*EMUB**0.2*RHOAV**0.8)
TW(I)=TW(I-1)
2100 DELT=2.0*DELTWG
CGTW=0.0
2120 TFI=(TW(I)+TB)/2.0
CALL PROPS(TFI,PAV,A,B,+0,JULIE,W,Z,RHOFI,H,S,CPFI,GAM,DHP,DST,DSP
1,OMEGT,OMEGP,SIGT,SIGP,ZETAT,ZETAP,EMUFI,CLAMFI,PRFI)
GTW=CT*CLAMFI**0.6*(CPFI/EMUFI)**0.4-1.0/((TW(I)-TB)*RHOFI**0.8)
CTW=SIGNF(1.0,GTW)
IF (NCM) 2152,2160,2160
2152 PRINT 4160, N5,CT,TW(I-1),TW(I),DELT,CGTW,TB,TFI,GTW,CTW
2160 IF (CTW-CGTW) 2170,2190,2170
2170 IF (DELT-DELTA) 2240,2240,2180
2180 DELT=DELT/2.0

```



```

2190 CGTW=CTW
2191 IF (N5-XABSF(NCM)) 2198,2194,2194
2194 IF (NCM) 1986,2195,2195
2195 NCM=-2*NCM
      GO TO 2071
2198 N5=N5+1
2200 TW(I)=TW(I)-CGTW*DELT
2210 IF (TW(I)-TB) 2220,2220,2120
2220 TW(I)=TB+DELTWE
      GO TO 2120
2240 CONTINUE
2242 FIYD(1)=-FEXD(M)
      FMLD=FEXD(M)*(REBDE/REBD(M))**0.2
      YD12(1)=XD12(M)
      D=(CL/XD12(M))**(1.0/1.2)
      CALL GOFV(V,D,GV,GWT)
      PAVLV=1.16279E-09*3600.0*(30.48**3)*WA*ABSF(Q(M))
      GTCV=WA*ABSF(Q(M))/(16.0*XD12(M))
      GGTC=GV*D**0.8/CONDK
      GPD=V/CL
      TWMAX=TW(1)
2248 PAVLV=PAVLV/2.54
      CL=CL/2.54
      D=D/2.54
      GWT=GWT/2.54
      GPD=V/CL
2250 IF (TWM) 2251,2251,2256
2251 DO 2254 I=2,M
      IF (TWMAX-TW(I)) 2253,2254,2254
2253 TWMAX=TW(I)
2254 CONTINUE
      GO TO 2260
2256 DO 2258 I=2,M
      DELXL(I)=FEDXD(I)/FEXD(M)
2258 XL(I)=XL(I-1)+DELXL(I)
2260 DO 2320 I=2,M
      XPL(I)=XL(I-1)+0.5*DELXL(I)
      DQQDXL(I)=DELQ(I)/(QT*DELXL(I))
      YL(I)=1.0-XL(I)
      YPL(I)=1.0-XPL(I)
      FEYD=-FEXD(M)+FEXD(I)
      FIYD(I)=FEYD*(REBDE/REBD(I))**0.2
      YD12(I)=CFE*ABSF(FEYD)
      PD(I)=GPD*PAVLV*DQQDXL(I)
      TC(I)=TW(I)+GGTC*GTCV*DQQDXL(I)
      IF (TCMAX-TC(I)) 2319,2320,2320
2319 TCMAX=TC(I)
2320 CONTINUE
2336 TSMAX=TSE
      TSMIN=TS(M)
      PSMAX=PS(M)
      PSMIN=PSE
2340 CALL SIMP(TSMAX,PSMIN,PNE,CI)
      CALL SIMP(TWMAX,PSMAX,PNE,CIMAX)
2357 CFA=CI*WA
      CFAP=CI*WAP
      TCWAV=GGTC*GTCV
      PDAV=GPD*PAVLV
      ACC=3.14159*D**2/4.0

```

```

CLD=CL/D
WPC=WAP*ACC/144.0
FPC=CFAP*ACC/144.0
DELPSC=ABSF(PSE-PS(M))
DELPSC=ABSF(PE-P(M))
CFAPS=CFAP/(144.0*PSMAX)
PSEOI=PSMIN/PSMAX
CIOIM=CI/CIMAX
ETATS=(TSMAX-TSMIN)/(TWMAX-TSMIN)
2361 TSE=1.8*TSE
TSRI=1.8*TSRI
TWM=1.8*TWM
TWMAX=1.8*TWMAX
TCMAX=1.8*TCMAX
TCWAV=1.8*TCWAV
DELTS=1.8*DELTS
DELTA=1.8*DELTA
DELTWG=1.8*DELTWG
DELTWE=1.8*DELTWE
QT=1.8*QT
WA=WA*(2.54**2.0)/453.5924
GRHO=(2.54**3)/453.5924
DO 2460 I=1,M
TS(I)=1.8*TS(I)
T(I)=1.8*T(I)
TC(I)=1.8*TC(I)
2400 DELQ(I)=1.8*DELQ(I)
Q(I)=1.8*Q(I)
QY(I)=1.8*QY(I)
XD12(I)=CD12*XD12(I)
YD12(I)=CD12*YD12(I)
REBD(I)=2.54*REBD(I)
HS(I)=1.8*HS(I)
RHOI(I)=GRHO*RHOI(I)
2460 TW(I)=1.8*TW(I)
4001 FORMAT(1H1A5,11A6)
4010 FORMAT(6F10.3,14X,A6)
4011 FORMAT(5F10.3,24X,A6)
4020 FORMAT(2I10,3F10.3,F10.6,F10.4,4X,A6)
4050 FORMAT(58H0      TSE      PSE      WA      TSRI      PSRI      T
1WM)
4051 FORMAT(48H0      L      V      D      K      K)
4060 FORMAT(68H0      JULIE      N      DELTS      DELTWG      DELTWE      DEL
1MA      PNE)
4150 FORMAT(120H N1      TE      PE      GME      CM2
1      DELS      DWADT      DWADP      DELT      DELP)
4160 FORMAT(13,9E13.5)
4170 FORMAT(120HON2      TIG      PIG      TAV      PAV
1      PS(I)      HS(I-1)      DQCPT      FBDXD)
4180 FORMAT(120H N3      CM(I)      CMBAR      GM2B      GM2D
1      GM2J      GAMAV      ETA      GM2F      CMC)
4190 FORMAT(120H N2      DELM      CMBAR2      HSIC      DELPOP
1      DELTOT      P(I)      T(I)      HSIC      TSS)
4200 FORMAT(120H N4      HSSI      HSIC      DELHS      SS1
1      DELS      DELTSI      DELPSI      PS(I)      TSS)
4210 FORMAT(120H N5      CT      TW(I-1)      TW(I)      DELT
1      CGTW      TB      TFI      GTW      CTW)
2500 RETURN
END

```

```

*      LIST
*      LABEL
CQOFX1
C
C      NORMALIZED Q VS. X FOR QXP(I) AND NORMALIZED
C      Y(I)=1.0-X(I) GIVEN
C
      SUBROUTINE QOFX
      COMMON  A,B,TS,PS,T,P,CM,TITLE,NPR,NPU,NGR,TSE,PSE,WA,
1TSRI,PSRI,TWM,CL,V,D,JULIE,N,PNE,PD,ALPHA,E,PNU,TK,M,
2SIGR,SIGO,SIG7,B0,TR,TE,SR,SE,RAD,AC,EWTC,EWTR,EWTE,EWTI,
3RHOPS,SIGPS,PSMAX,DELTA,DELPA,WP,RHON,SIGMAN,CI,CIMAX,
4WAG,CME,CFAP,CFAPS,DELPSC,PE,DELP,FECD,FMLD,XD12,REBD,
5Q,QT,CIOIM,ETATS,PSEOI,PDAV,TCWAV,TWMAX,TCMAX,GWT,CLD,ACC,
6WPC,FPC,GV,XL,RHOI,XPL,DQDQXL,TW,TC,YL,FIYD,FECD,YD12,QY,
7RAD,AC,WPS,TPS,DT,WNC,WND,WN,AE,DE,CNL,DNL,WTP,PTP,SIGST,
8SIGSTP,SIGSH,SIGSE,SIGDE,PNE,PEN,WSYS,QBAR,XBAR
9,CONDK,CONDR,CFA
      DIMENSION  A(6,40),B(6,40),TS(200),PS(200),T(200),P(200),
1CM(200),TITLE(12),PD(200),SIGR(200),SIGO(200),SIGZ(200),
2FECD(200),XD12(200),REBD(200),Q(200),XL(200),
3RHOI(200),XPL(200),DQDQXL(200),TW(200),TC(200),YL(200),
4FIYD(200),YD12(200),QY(200)
5,SIGST(200),SIGSTP(200),SIGSH(200),SIGSE(200),SIGDE(200)
6,QBAR(100),XBAR(100)
      DIMENSION QQ(100),X(100),QSUM(100),FMT(12)
      READ  110, NQ
110  FORMAT(I10)
      READ  130, (FMT(I),I=1,12)
130  FORMAT(12A6)
      READ  FMT, (X(I),QQ(I),I=1,NQ)
      QSUM(1)=0.0
      DO 170 I=2,NQ
170  QSUM(I)=QSUM(I-1)+QQ(I)*(X(I-1)-X(I))
      DO 200 I=1,NQ
      QBAR(I)=QSUM(I)/QSUM(NQ)
200  XBAR(I)=1.0-X(I)
      RETURN
      END

```

```

*      LIST
*      LABEL
CQOFX2
C
C      NORMALIZED Q VS. X FOR Q(I) GIVEN AT X(I) AND X(1)=0.0
C
      SUBROUTINE QOFX
      COMMON A,B,TS,PS,T,P,CM,TITLE,NPR,NPJ,NGR,TSE,PSE,WA,
1TSRI,PSRI,TWM,CL,V,D,JULIE,N,PNE,PD,ALPHA,E,PNU,TK,M,
2SIGR,SIGO,SIGZ,PO,TR,TE,SR,SE,RAD,AC,EWTC,EWTR,EWTE,EWTT,
3RHOPS,SIGPS,PSMAX,DELTA,DELPA,WP,RHON,SIGMAN,CI,CIMAX,
4WAG,CME,CFAP,CFAPS,DELPSC,PE,DELPD,FEXD,FMLD,XD12,REBD,
5Q,QT,CIOIM,ETATS,PSEOI,PDAV,TCWAV,TWMAX,TCMAX,SWT,CLD,ACC,
6WPC,FPC,QV,XL,RHOI,XPL,DQQDXL,TW,TC,YL,FIYD,FEXD,YD12,QY,
7RAD,AC,WPS,TPS,DT,WNC,WND,WN,AE,DE,CNL,DNL,WTP,PTP,SIGST,
8SIGSTP,SIGSH,SIGSE,SIGDE,PNE,PEN,WSYS,QBAR,XBAR
9,CONDK,CONDR,CFA
      DIMENSION A(6,40),B(6,40),TS(200),PS(200),T(200),P(200),
1CM(200),TITLE(12),PD(200),SIGR(200),SIGO(200),SIGZ(200),
2FEXD(200),XD12(200),REBD(200),Q(200),XL(200),
3RHOI(200),XPL(200),DQQDXL(200),TW(200),TC(200),YL(200),
4FIYD(200),YD12(200),QY(200)
5,SIGST(200),SIGSTP(200),SIGSH(200),SIGSE(200),SIGDE(200)
6,QBAR(100),XBAR(100)
      DIMENSION QQ(100),X(100),QSUM(100),FMT(12)
      READ 110, NQ
110 FORMAT(I10)
      READ 130, (FMT(I),I=1,12)
130 FORMAT(12A6)
      READ FMT, (X(I),QQ(I),I=1,NQ)
      QSUM(1)=0.0
      DO 170 I=2,NQ
170 QSUM(I)=QSUM(I-1)+(QQ(I-1)+QQ(I))*(X(I)-X(I-1))/2.0
      DO 200 I=1,NQ
      QBAR(I)=QSUM(I)/QSUM(NQ)
200 XBAR(I)=X(I)/X(NQ)
      RETURN
      END

```

```

*      LIST
*      LABEL
CQDIST1
C
C      AXIAL DISTRIBUTION OF HEAT GENERATION
C      1 IS CHOPPED SIN FUNCTION
C
      SUBROUTINE QDIST (QDQ,QT,QDXL)
      COMMON  A,B,TS,PS,T,P,CM,TITLE,NPR,NPU,NGR,TSE,PSE,WA,
1TSRI,PSRI,TWM,CL,V,D,JULIE,N,PNE,PD,ALPHA,E,PNU,TK,M,
2SIGR,SIGO,SIGZ,BO,TR,TE,SR,SE,RAD,AC,EWTC,EWTR,EWTE,EWT,
3RHOPS,SIGPS,PSMAX,DELTA,DELPA,WP,RHON,SIGMAN,CI,CIMAX,
4WAG,CME,CFAP,CFAPS,DELPSC,PE,DELP,FECD,FMLD,XD12,REBD,
5Q,QT,CIOIM,ETATS,PSEOI,PDAV,TCWAV,TWMAX,TCMAX,GWT,CLD,ACC,
6WPC,FPC,GV,XL,RHOI,XPL,DQQDXL,TW,TC,YL,FIYD,FECD,YD12,QY,
7RAD,AC,WPS,TPS,DT,WNC,WND,WN,AE,DE,CNL,DNL,WTP,PTP,SIGST,
8SIGSTP,SIGSH,SIGSE,SIGDE,PNE,PEN,WSYS,QBAR,XBAR
9,CONDK,CONDR,CFA
      DIMENSION  A(6,40),B(6,40),TS(200),PS(200),T(200),P(200),
1CM(200),TITLE(12),PD(200),SIGR(200),SIGO(200),SIGZ(200),
2FECD(200),XD12(200),REBD(200),Q(200),XL(200),
3RHOI(200),XPL(200),DQQDXL(200),TW(200),TC(200),YL(200),
4FIYD(200),YD12(200),QY(200)
5,SIGST(200),SIGSTP(200),SIGSH(200),SIGSE(200),SIGDE(200)
6,QBAR(100),XBAR(100)
      IF (WSYS) 20,10,10
10 READ 1000, CQ1
      WSYS=-1.0
      T11=TITLE(8)
      PRINT 1010, CQ1
      IF (XABSF(NPU)) 20,20,15
15 PUNCH 1010,CQ1,T11
20 QDXL=ACOSF(1.0-(1.0-COSF(CQ1))*QDQ/QT)/CQ1
1000 FORMAT(F10.4)
1010 FORMAT(8H0 CQ1=F6.4,60X,A6)
      RETURN
      END

```

```

*      LIST
*      LABEL
CQDIST2

```

```

C
C      AXIAL DISTRIBUTION OF HEAT GENERATION- 2 IS TABULAR DATA
C

```

```

      SUBROUTINE QDIST (QDQ,QT,QDXL)
      COMMON  A,B,TS,PS,T,P,CM,TITLE,NPR,NPU,NGR,TSE,PSE,WA,
      1TSRI,PSRI,TWM,CL,V,D,JULIE,N,PNE,PD,ALPHA,E,PNU,TK,M,
      2SIGR,SIGO,SIGZ,BO,TR,IE,SR,SE,RAD,AC,EWTC,EWTR,EWTE,EWT,
      3RHOPS,SIGPS,PSMAX,DELTA,DELPA,WP,RHON,SIGMAN,CI,CIMAX,
      4WAG,CME,CFAP,CFAPS,DELPSC,PE,DELP,FECD,FMLD,XD12,REBD,
      5Q,QT,C10IM,ETATS,PSEOI,PD,AV,TCWAV,TWMAX,TCMAX,GWT,CLD,ACC,
      6WPC,FPC,GV,XL,RHOI,XPL,DQQDXL,TW,TC,YL,FIYD,FECD,YD12,QY,
      7RAD,AC,WPS,TPS,DT,WNC,WND,WN,AE,DE,CNL,DNL,WTP,PTP,SIGST,
      8SIGSTP,SIGSH,SIGSE,SIGDE,PNE,PEN,WSYS,QBAR,XBAR
      9,CONDK,CONDR,CFA
      DIMENSION  A(6,40),B(6,40),TS(200),PS(200),T(200),P(200),
      1CM(200),TITLE(12),PD(200),SIGR(200),SIGO(200),SIGZ(200),
      2FECD(200),XD12(200),REBD(200),Q(200),XL(200),
      3RHOI(200),XPL(200),DQQDXL(200),TW(200),TC(200),YL(200),
      4FIYD(200),YD12(200),QY(200)
      5,SIGST(200),SIGSTP(200),SIGSH(200),SIGSE(200),SIGDE(200)
      6,QBAR(100),XBAR(100)
      I=2
      RQ=QDQ/QT
      IF (1.0-RQ) 103,110,110
103  RQ=1.0
110  IF (QBAR(I)-RQ) 120,140,140
120  I=I+1
      GO TO 110
140  QDXL=XBAR(I-1)+(QDQ/QT-QBAR(I-1))*(XBAR(I)-XBAR(I-1))/
      1(QBAR(I)-QBAR(I-1))
      RETURN
      END

```

```

*      LIST
*      LABEL
CPTC201
C
C      PRESSURE AND TEMPERATURE CORRECTIONS FOR LOOP 2 IN JCHT1
C
      SUBROUTINE PTC (TI2,TI1,TAV,PI2,PI1,PAV,PSI2,PSN2I,TSI2,
1TSS,DEL TSA,DELTME,DELPME,N2,N2M)
100 TIG=2.0*TAV-TI1
110 PIG=2.0*PAV-PI1
120 PSIG=PSN2I
130 DTS=TSS-TSI2
140 IF (ABSF(DTS)-DEL TSA) 150,150,380
150 IF (ABSF(TI2-TIG)-DELTME) 160,160,380
160 IF (ABSF(PI2-PIG)-DELPME) 170,170,380
170 IF (ABSF(PSI2-PSIG)-DELPME) 460,460,380
380 IF (N2-XABSF(N2M)) 390,480,480
390 TIG=TI2
400 PIG=PI2
410 PSIG=PSI2
420 TAV=(TI1+TIG)/2.0
430 PAV=(PI1+PIG)/2.0
440 PSI2=PSIG
450 GO TO 490
460 N2=0
470 GO TO 490
480 N2=-N2
490 RETURN
      END

```

* LIST
* LABEL
CGOFV01

C
C
C

1 IS VOID FRACTION PARAMETER FOR EQUILATERAL HOLE SPACINGS

SUBROUTINE GOFV(V,D,GV,GWT)

C1=2.0*3.14159/3.0**1.5

GV=(V-LOGF(V)+LOGF(C1)-0.94148*C1)/(1.0-V)

GWT=D*((C1/V)**0.5-1.0)/2.0

RETURN

END

*
*
C
C
C

LIST
LABEL

SPECIFIC IMPULSE CALCULATION

```

SUBROUTINE SIMP (CITS,CIPS,CIPNE,CISP)
COMMON A,B,TS,PS,T,P,CM,TITLE,NPR,NPU,NGR,TSE,PSE,WA,
1TSRI,PSRI,TWM,CL,V,D,JULIE,N,PNE,PD,ALPHA,E,PNU,TK,M,
2SIGR,SIGO,SIGZ,BO,TR,TE,SR,SE,RAD,AC,EWTC,EWTR,EWTE,EWT,
3RHOPS,SIGPS,PSMAX,DELTA,DELPA,WP,RHON,SIGMAN,CI,CIMAX,
4WAG,CME,CFAP,CFAPS,DELPSC,PE,DELPC,FEXD,FMLD,XD12,REBD,
5Q,QT,CIOIM,ETATS,PSEOI,PDAV,TCWAV,TWMAX,TCMAX,GWT,CLD,ACC,
6WPC,FPC,GV,XL,RHOI,XPL,DQQDXL,TW,TC,YL,FIYD,FEXD,YD12,QY,
7RAD,AC,WPS,TPS,DT,WNC,WND,WN,AE,DE,CNL,DNL,WTP,PTP,SIGST,
8SIGSTP,SIGSH,SIGSE,SIGDE,PNE,PEN,WSYS,QBAR,XBAR
9,CONDK,CONDR,CFA
  DIMENSION A(6,40),B(6,40),TS(200),PS(200),T(200),P(200),
  1CM(200),TITLE(12),PD(200),SIGR(200),SIGO(200),SIGZ(200),
  2FEXD(200),XD12(200),REBD(200),Q(200),XL(200),
  3RHOI(200),XPL(200),DQQDXL(200),TW(200),TC(200),YL(200),
  4FIYD(200),YD12(200),QY(200)
  5,SIGST(200),SIGSTP(200),SIGSH(200),SIGSE(200),SIGDE(200)
  6,QBAR(100),XBAR(100)
  CALL PROPS(CITS,CIPS,A,B,-1,JULIE,W,Z,RHO,CIHS,SS,CP,GAMS,DHP,
  1DST,DSP,OMEGT,OMEGP,SIGT,SIGP,ZETAT,ZETAP,EMU,CLAM,PR)
  TNE=CITS*((CIPNE/CIPS)**((GAMS-1.0)/GAMS))
10 CALL PROPS(TNE,CIPNE,A,B,1,JULIE,W,Z,RHO,HNE,SNE,CP,GAM,DHP,DSTNE,
  1DSP,OMEGT,OMEGP,SIGT,SIGP,ZETAT,ZETAP,EMU,CLAM,PR)
  DELTAS=SS-SNE
  DELTAT=DELTAS/DSTNE
  IF (ABSF(DELTAT)-DELTA) 30,30,20
20 TNE=TNE+DELTAT
  GO TO 10
30 VNEC=SQRTF(2.0*(CIHS-HNE)*82.0168*980.665*1033.23/1.9859)
  CISP=VNEC/980.665
  RETURN
  END

```

```

PUNCH 4011, CL,V,D,CONDK,CONDR,TI1
PUNCH 4041
PUNCH 4042
PUNCH 4043, C1,CIMAX,WAG,CME,CFA,CFAP,CFAPS,TI1
PUNCH 4044
PUNCH 4045,PS(M),DELPSC,PE,P(M),DELPC,T(1),T(M),TI1
PUNCH 4046
PUNCH 4047,FEXD(M),FMLD,XD12(M),REBD(M),REBD(1),Q(M),QT,TI1
PUNCH 4048
PUNCH 4049, CM(M),CIOIM,ETATS,PSEOI,PDAV,TCWAV,TWMAX,TI1
PUNCH 4055
PUNCH 4056, TCMAX,GWT,CLD,ACC,WPC,FPC,GV,TI1
PUNCH 4001, (TITLE(I),I=1,12)
PUNCH 4070
PUNCH 4080,(XL(I),CM(I),TS(I),T(I),PS(I),P(I),RHOI(I),I=1,M)
PUNCH 4001, (TITLE(I),I=1,12)
PUNCH 4090
PUNCH 4100,(XPL(I),DQQDXL(I),TW(I),TC(I),PD(I),I=1,M)
PUNCH 4001, (TITLE(I),I=1,12)
PUNCH 4110
PUNCH 4120,(YL(I),FIYD(I),FEXD(I),YD12(I),QY(I),Q(I),REBD(I),I=1,M)
1)
4001 FORMAT(1H1A5,11A6)
4010 FORMAT(6F10.3,14X,A6)
4011 FORMAT(5F10.3,24X,A6)
4030 FORMAT(69HODIMENSIONS OF VARIABLES-P(PSI), T(DEGREES R), Q(BTU/LB)
1, L AND D(IN))
4041 FORMAT(68H0    ISP    ISPMAX    W/A    CME    F/A    F
1/A    F/A-P01)
4042 FORMAT(60H LB-SEC/LB LB-SEC/LB GM/CM-SEC
1/FT2)
4043 FORMAT(3F10.3,F10.6,2F10.2,F10.6,4X,A6)
4044 FORMAT(69H0    PSM    DELPS    PE    PM    DELP
1 TE    TM)
4045 FORMAT(7F10.3,4X,A6)
4046 FORMAT(68H0    FEL/D    FML/D    L/D12    REBM/D    REBE/D
1 Q    QT)
4047 FORMAT(2F10.6,F10.3,2F10.0,2F10.2,4X,A6)
4048 FORMAT(68H0    CMM    I/IMAX    ETATS    PSE/PSI    PDAV    TCW
1AV    TWMAX)
4049 FORMAT(4F10.6,3F10.3,4X,A6)
4050 FORMAT(58H0    TSE    PSE    WA    TSRI    PSRI    T
1WM)
4051 FORMAT(48H0    L    V    D    K    K)
4055 FORMAT(68H0    TCMAX    GWT    L/D    ACC    WPC    F
1PC    GV)
4056 FORMAT(3F10.3,4F10.6,4X,A6)
4070 FORMAT(69H    X/L    M    TS    T    PS
1 P    1000 RHO)
4080 FORMAT(0P2F10.6,4F10.3,3PF10.6)
4090 FORMAT(48H    XP/L    DQQDXL    TW    TC    PD)
4100 FORMAT(2F10.6,3F10.3)
4110 FORMAT(68H    Y/L    FIY/D    FEX/D    Y/D12    QY
1 Q    REB/D)
4120 FORMAT(3F10.6,F10.3,2F10.2,F10.0)
3995 RETURN
END

```

```

* LIST
* LABEL
CST1
C
C CALCULATION OF STRESSES IN ANNULAR ELEMENT
C
C GRADIENT OF RADIAL STRESS EQUALS ZERO ON OUTER BOUNDARY
C
SUBROUTINE ST
COMMON A,B,TS,PS,T,P,CM,TITLE,NPR,NPU,NGR,TSE,PSE,WA,
1TSRI,PSRI,TWM,CL,V,D,JULIE,N,PNE,PD,ALPHA,E,PNU,TK,M,
2SIGR,SIGO,SIGZ,BO,TR,TE,SR,SE,RAD,AC,EWTC,EWTR,EWTE,EWTT,
3RHOPS,SIGPS,PSMAX,DELTA,DELPA,WP,RHON,SIGMAN,CI,CIMAX,
4WAG,CME,CFAP,CFAPS,DELPSC,PE,DELPC,FEXD,FMLD,XD12,REBD,
5Q,QT,CIOIM,ETATS,PSEOI,PDAV,TCWAV,TWMAX,TCMAX,GWT,CLD,ACC,
6WPC,FPC,GV,XL,RHOI,XPL,DQQDXL,TW,TC,YL,FIYD,FEXD,YD12,QY,
7RAD,AC,WPS,TPS,DT,WNC,WND,WN,AE,DE,CNL,DNL,WTP,PTP,SIGST,
8SIGSTP,SIGSH,SIGSE,SIGDE,PNE,PEN,WSYS,QBAR,XBAR
9,CONDK,CONDR,CFA,RLD,SIGSHM,SIGDEM,PNEX,CIEX,THRUST,WBL,YW,HPP
DIMENSION A(6,40),B(6,40),TS(200),PS(200),T(200),P(200),
1CM(200),TITLE(12),PD(200),SIGR(200),SIGO(200),SIGZ(200),
2FEXD(200),XD12(200),REBD(200),Q(200),XL(200),
3RHOI(200),XPL(200),DQQDXL(200),TW(200),TC(200),YL(200),
4FIYD(200),YD12(200),QY(200)
5,SIGST(200),SIGSTP(200),SIGSH(200),SIGSE(200),SIGDE(200)
6,QBAR(100),XBAR(100)
R=D/2.0
S=1.0-V
AB=SQRTF(V)
B=R/AB
RLV=-LOGF(AB)
ALPHAF=ALPHA
EPSI=E
TKBFT=TK*12.0
RB=AB
RB2=V
PDCF=10.0**6*3.41275/3600.0
AFT=R/12.0
GSIG2=ALPHAF*EPSI*PDCF*AFT**2/(4.0*(1.0-PNU)*TKBFT*V*S)
SIGSHM=0.0
SIGDEM=0.0
DO 500 I=1,M
GSIG1=GSIG2*PD(I)
SIGR(I)=-P(I)
SIGZ(I)=GSIG1*(2.0*RLV/S-(3.0-V)/2.0)
SIGO(I)=-P(I)+GSIG1*S**2/(2.0*V)
SIG3=SIGR(I)
IF (SIGO(I)-SIGZ(I)) 90,90,100
90 SIG1=SIGZ(I)
SIG2=SIGO(I)

```

```

GO TO 110
100 SIG1=SIG0(I)
   SIG2=SIGZ(I)
110 SIGST(I)=SIG1-PNU*(SIG2+SIG3)
   SIGSTP(I)=SIG3-PNU*(SIG1+SIG2)
   SIGSH(I)=SIG1-SIG3
   SIGSE(I)=SQRTF(SIG1**2+SIG2**2+SIG3**2-2.0*PNU*(SIG1*SIG2+
1 SIG2*SIG3+SIG1*SIG3))
   SIGDE(I)=SQRTF((1.0+PNU)*((SIG1-SIG2)**2+(SIG1-SIG3)**2
1 +(SIG2-SIG3)**2)/3.0)
   IF (SIGSH(I)-SIGSHM) 160,160,150
150 SIGSHM=SIGSH(I)
160 IF (SIGDE(I)-SIGDEM) 500,500,170
170 SIGDEM=SIGDE(I)
500 CONTINUE
   RETURN
   END

```

* LIST
* LABEL

CPRST1

C
C
C

PRINTING OF RESULTS FROM STRESS CALCULATIONS

SUBROUTINE PRST

```

COMMON A,B,TS,PS,T,P,CM,TITLE,NPR,NPU,NGR,TSE,PSE,WA,
1TSRI,PSRI,TWM,CL,V,D,JULIE,N,PNE,PD,ALPHA,E,PNU,TK,M,
2SIGR,SIGO,SIGZ,BO,TR,TE,SR,SE,RAD,AC,EWTC,EWTR,EWTE,EWT,
3RHOPS,SIGPS,PSMAX,DELTA,DELPA,WP,RHON,SIGMAN,CI,CIMAX,
4WAG,CME,CFAP,CFAPS,DELPSC,PE,DELPC,FEXD,FMLD,XD12,REBD,
5Q,QT,CIOIM,ETATS,PSEOI,PDAV,TCWAV,TWMAX,TCMAX,GWT,CLD,ACC,
6WPC,FPC,GV,XL,RHOI,XPL,DQQDXL,TW,TC,YL,FIYD,FEXD,YD12,QY,
7RAD,AC,WPS,TPS,DT,WNC,WND,WN,AE,DE,CNL,DNL,WTP,PTP,SIGST,
8SIGSTP,SIGSH,SIGSE,SIGDE,PNE,PEN,WSYS,QBAR,XBAR
9,CONDK,CONDR,CFA
  DIMENSION A(6,40),B(6,40),TS(200),PS(200),T(200),P(200),
1CM(200),TITLE(12),PD(200),SIGR(200),SIGO(200),SIGZ(200),
2FEXD(200),XD12(200),REBD(200),Q(200),XL(200),
3RHOI(200),XPL(200),DQQDXL(200),TW(200),TC(200),YL(200),
4FIYD(200),YD12(200),QY(200)
  5,SIGST(200),SIGSTP(200),SIGSH(200),SIGSE(200),SIGDE(200)
6,QBAR(100),XBAR(100)
  PRINT 4001, (TITLE(I),I=1,12)
  PRINT 1108
  PRINT 1109
  PRINT 1110, ALPHA,E,PNU,TK
  PRINT 1118
  PRINT 1119
  PRINT 1120, D,V
  PRINT 4001, (TITLE(I),I=1,12)
  PRINT 1150
  PRINT 1160
  PRINT 1170
  PRINT 1180, (XL(I),P(I),PD(I),SIGO(I),SIGZ(I),SIGR(I),I=1,M)
  PRINT 4001, (TITLE(I),I=1,12)
  PRINT 1190
  PRINT 1200
  PRINT 1210, (XL(I),SIGST(I),SIGSTP(I),SIGSH(I),SIGSE(I)
1,SIGDE(I),I=1,M)
  IF (NPU) 20,20,10
10 T11=TITLE(8)
  PUNCH 1108
  PUNCH 1109
  PUNCH 1110, ALPHA,E,PNU,TK,T11
  PUNCH 1118
  PUNCH 1119
  PUNCH 1120, D,V,T11
  PUNCH 1150
  PUNCH 1160
  PUNCH 1170
  PUNCH 1180, (XL(I),P(I),PD(I),SIGO(I),SIGZ(I),SIGR(I),I=1,M)
  PUNCH 1190
  PUNCH 1200
  PUNCH 1210, (XL(I),SIGST(I),SIGSTP(I),SIGSH(I),SIGSE(I)
1,SIGDE(I),I=1,M)
20 CONTINUE

```

```

1108 FORMAT(58H0      ALPHA      E      NU
1 K)
1109 FORMAT(58H      1/DEG F      PSI      BTU/IN-SEC
1-F)
1110 FORMAT(4E15.5,14X,A6)
1118 FORMAT(18H0      D      V)
1119 FORMAT(9H      IN.)
1120 FORMAT(2F10.3,54X,A6)
1150 FORMAT(52H0STRESS CALCULATIONS FOR ZERO STRESS GRADIENT AT R=8)
1160 FORMAT(58H0      XL      P      PD      SIGO      SIGZ      SI
1GR)
1170 FORMAT(59H      PSIA      MW/FT3      PSI      PSI
1PSI)
1180 FORMAT(F10.4,2F10.3,3F10.1)
1190 FORMAT(58H0      XL      SIGST      SIGSTP      SIGSH      SIGSE      SIG
1DE)
1200 FORMAT(59H      PSI      PSI      PSI      PSI
1PSI)
1210 FORMAT(F10.4,5F10.1)
4001 FORMAT(1H1A5,11A6)
      RETURN
      END

```

```
* LIST
* LABEL
```

```
CRC SW2
```

```
C
C
C
```

CALCULATION OF REACTOR CRITICAL SIZE AND WEIGHT

```
SUBROUTINE RCSW
```

```
COMMON A,B,TS,PS,T,P,CM,TITLE,NPR,NPU,NGR,TSE,PSE,WA,
1TSRI,PSRI,TWM,CL,V,D,JULIE,N,PNE,PD,ALPHA,E,PNU,TK,M,
2SIGR,SIGO,SIGZ,BO,TR,TE,SR,SE,RAD,AC,EWTC,EWTR,EWTE,EWTT,
3RHOPS,SIGPS,PSMAX,DELTA,DELPA,WP,RHON,SIGMAN,CI,CIMAX,
4WAG,CME,CFAP,CFAPS,DELPSC,PE,DELPC,FEXD,FMLD,XD12,REBD,
5Q,QT,CIOIM,ETATS,PSEOI,PDAV,TCWAV,TWMAX,TCMAX,GWT,CLD,ACC,
6WPC,FPC,GV,XL,RHOI,XPL,DQQDXL,TW,TC,YL,FIYD,FEXD,YD12,QY,
7RAD,AC,WPS,TPS,DT,WNC,WND,WN,AE,DE,CNL,DNL,WTP,PTP,SIGST,
8SIGSTP,SIGSH,SIGSE,SIGDE,PNE,PEN,WSYS,QBAR,XBAR
9,CONDK,CONDR,CFA
```

```
DIMENSION A(6,40),B(6,40),TS(200),PS(200),T(200),P(200),
1CM(200),TITLE(12),PD(200),SIGR(200),SIGO(200),SIGZ(200),
2FEXD(200),XD12(200),REBD(200),Q(200),XL(200),
3RHOI(200),XPL(200),DQQDXL(200),TW(200),TC(200),YL(200),
4FIYD(200),YD12(200),QY(200)
5,SIGST(200),SIGSTP(200),SIGSH(200),SIGSE(200),SIGDE(200)
6,QBAR(100),XBAR(100)
```

```
HE=2.54*CL
```

```
R=2.54*RAD
```

```
TR=2.54*TR
```

```
TE=2.54*TE
```

```
DENC=1.659
```

```
DENR=1.85
```

```
DENE=DENR
```

```
SC=1.0-V
```

```
1100 ACOR=3.1416*R**2
```

```
AC=ACOR*(1.0-SC)*0.0001
```

```
EWTC=ACOR*HE*SC*DENC*0.001
```

```
EWTR=(3.1416*(R+TR)**2-ACOR)*(HE+TE)*DENR*SR*0.001
```

```
EWTE=ACOR*TE*SE*DENE*0.001
```

```
EWTT=EWTC+EWTR+EWTE
```

```
RAD=R/2.54
```

```
TE=TE/2.54
```

```
TR=TR/2.54
```

```
AC=10000.0*AC/(144.0*2.54**2)
```

```
EWTC=2.2*EWTC
```

```
EWTR=2.2*EWTR
```

```
EWTE=2.2*EWTE
```

```
EWTT=2.2*EWTT
```

```
RETURN
```

```
END
```

```
* LIST
* LABEL
CPRRSW1
```

```
C
C
C
```

PRINTING OF RESULTS FROM REACTOR SIZE AND WEIGHT CALCULATIONS

```

SUBROUTINE PRRCSW
COMMON A,B,TS,PS,T,P,CM,TITLE,NPR,NPU,NGR,TSE,PST,WA,
1TSRI,PSRI,TWM,CL,V,D,JULIE,N,PNE,PD,ALPHA,E,PNU,TK,1,
2SIGR,SIGO,SIGZ,BO,TR,TE,SR,SE,RAD,AC,EWTC,EWTR,EWTE,EWT,
3RHOPS,SIGPS,PSMAX,DELTA,DELPA,WP,RHON,SIGMAN,CI,CIMAX,
4WAG,CME,CFAP,CFAPS,DELPSC,PE,DELP,CFEXD,FMLD,XD12,REBD,
5Q,QT,CIOIM,ETATS,PSEOI,PDAV,TCWAV,TWMAX,TCMAX,GWT,CLD,ACC,
6WPC,FPC,GV,XL,RHOI,XPL,DQQDXL,TW,TC,YL,FIYD,FEXD,YD12,QY,
7RAD,AC,WPS,TPS,DT,WNC,WND,WN,AE,DE,CNL,DNL,WTP,PTP,SIGST,
8SIGSTP,SIGSH,SIGSE,SIGDE,PNE,PEN,WSYS,QBAR,XBAR
9,CONDK,CONDR,CFA
DIMENSION A(6,40),B(6,40),TS(200),PS(200),T(200),P(200),
1CM(200),TITLE(12),PD(200),SIGR(200),SIGO(200),SIGZ(200),
2FEXD(200),XD12(200),REBD(200),Q(200),XL(200),
3RHOI(200),XPL(200),DQQDXL(200),TW(200),TC(200),YL(200),
4FIYD(200),YD12(200),QY(200)
5,SIGST(200),SIGSTP(200),SIGSH(200),SIGSE(200),SIGDE(200)
6,QBAR(100),XBAR(100)
PRINT 4001, (TITLE(I),I=1,12)
PRINT 2005
PRINT 2006
PRINT 2007, CL,TE,TR,SR,SE,BO
PRINT 2008
PRINT 2009
PRINT 2010, RAD,AC,EWTC,EWTR,EWTE,EWT
IF (NPU) 20,20,10
10 T11=TITLE(8)
PUNCH 2005
PUNCH 2006
PUNCH 2007, CL,TE,TR,SR,SE,BO,T11
PUNCH 2008
PUNCH 2009
PUNCH 2010, RAD,AC,EWTC,EWTR,EWTE,EWT,T11
20 CONTINUE
2005 FORMAT(58H0      L      TE      TR      SR      SE
1BO)
2006 FORMAT(59H      IN.      IN.      IN.      1/
1CM2)
2007 FORMAT(5F10.3,F12.8,12X,A6)
2008 FORMAT(58H0      RAD      AC      EWTC      EWTR      EWTE      EW
1TT)
2009 FORMAT(59H      IN.      FT2      LB      LB      LB
1 LB)
2010 FORMAT(6F10.2,14X,A6)
4001 FORMAT(1H1A5,11A6)
RETURN
END

```


* LIST
* LABEL

CPRSH1

C
C
C
C
C
C

CALCULATION OF PRESSURE SHELL WEIGHT

RHOPS IS IN LB/FT3

DR AND CLR IN FEET, WPS IN POUNDS

SUBROUTINE PRSH

```
COMMON A,B,TS,PS,T,P,CM,TITLE,NPR,NPU,NGR,TSE,PSE,WA,
1TSRI,PSRI,TWM,CL,V,D,JULIE,N,PNE,PD,ALPHA,E,PNU,TK,M,
2SIGR,SIGO,SIGZ,BO,TR,TE,SR,SE,RAD,AC,EWTC,EWTR,EWTE,EWT,
3RHOPS,SIGPS,PSMAX,DELTA,DELPA,WP,RHON,SIGMAN,CI,CIMAX,
4WAG,CME,CFAP,CFAPS,DELPSC,PE,DELPC,FEXD,FMLD,XD12,REBD,
5Q,QT,CIOIM,ETATS,PSEOI,PDAV,TCWAV,TWMAX,TCMAX,GWT,CLD,ACC,
6WPC,FPC,GV,XL,RHOI,XPL,DQQDXL,TW,TC,YL,FIYD,FEXD,YD12,QY,
7RAD,AC,WPS,TPS,DT,WNC,WND,WN,AE,DE,CNL,DNL,WTP,PTP,SIGST,
8SIGSTP,SIGSH,SIGSE,SIGDE,PNE,PEN,WSYS,QBAR,XBAR
9,CONDK,CONDR,CFA,RLD,SIGSHM,SIGDEM,PNEX,CIEX,THRUST,WBL,YW,HPP
  DIMENSION A(6,40),B(6,40),TS(200),PS(200),T(200),P(200),
1CM(200),TITLE(12),PD(200),SIGR(200),SIGO(200),SIGZ(200),
2FEXD(200),XD12(200),REBD(200),Q(200),XL(200),
3RHOI(200),XPL(200),DQQDXL(200),TW(200),TC(200),YL(200),
4FIYD(200),YD12(200),QY(200)
5,SIGST(200),SIGSTP(200),SIGSH(200),SIGSE(200),SIGDE(200)
6,QBAR(100),XBAR(100)
  DR=2.0*(RAD+TR)/12.0
  CLR=(CL+TE)/12.0
  WPS=3.14159*RHOPS*DR**2*CLR*PSMAX*(1.0+DR/(4.0*CLR))/(2.0*SIGPS)
  TPS=12.0*PSMAX*DR/(2.0*SIGPS)
  RETURN
  END
```

* LIST
* LABEL

CTP1

C

C

C

C

C

CALCULATION OF TURBOPUMP WEIGHT

PTP IS IN PSIA AND WP IS IN LB/SEC

SUBROUTINE TP

```
COMMON A,B,TS,PS,T,P,CM,TITLE,NPR,NPU,NGR,TSE,PSE,WA,  
1TSRI,PSRI,TWM,CL,V,D,JULIE,N,PNE,PD,ALPHA,E,PNU,TK,M,  
2SIGR,SIGO,SIGZ,BO,TR,TE,SR,SE,RAD,AC,EWTC,EWTR,EWTE,EWTT,  
3RHOPS,SIGPS,PSMAX,DELTA,DELPA,WP,RHON,SIGMAN,CI,CIMAX,  
4WAG,CME,CFAP,CFAPS,DELPSC,PE,DELP,FECD,FMLD,XD12,REBD,  
5Q,QT,CIOIM,ETATS,PSEOI,PDAV,TCWAV,TWMAX,TCMAX,GWT,CLD,ACC,  
6WPC,FPC,GV,XL,RHOI,XPL,DQQDXL,TW,TC,YL,FIYD,FECD,YD12,QY,  
7RAD,AC,WPS,TPS,DT,WNC,WND,WN,AE,DE,CNL,DNL,WTP,PTP,SIGST,  
8SIGSTP,SIGSH,SIGSE,SIGDE,PNE,PEN,WSYS,QBAR,XBAR  
9,CONDK,CONDR,CFA,RLD,SIGSHM,SIGDEM,PNEX,CIEX,THRUST,WBL,YW,HPP  
DIMENSION A(6,40),B(6,40),TS(200),PS(200),T(200),P(200),  
1CM(200),TITLE(12),PD(200),SIGR(200),SIGO(200),SIGZ(200),  
2FECD(200),XD12(200),REBD(200),Q(200),XL(200),  
3RHOI(200),XPL(200),DQQDXL(200),TW(200),TC(200),YL(200),  
4FIYD(200),YD12(200),QY(200)  
5,SIGST(200),SIGSTP(200),SIGSH(200),SIGSE(200),SIGDE(200)  
6,QBAR(100),XBAR(100)  
PTANK=20.0  
EFFTP=0.50  
EFFP=SQRTF(EFFTP)  
DELHT=1775.0  
RHOLH=4.4  
PTP=1.33*PSMAX  
YW=144.0*(PTP-PTANK)/(778.0*EFFTP*RHOLH*DELHT)  
HPP=144.0*WP*(PTP-PTANK)/(550.0*EFFP*RHOLH)  
WBL=YW*WP  
WTP=0.00251*PTP*WP  
RETURN  
END
```

* LIST
* LABEL

CNOZ1

C
C
C
C
C
C
C

CALCULATION OF NOZZLE SIZE AND WEIGHT

RHON IS IN LB/FT3, DR AND DT ARE IN FT
HALF ANGLE OF CONVERGENT SECTION IS 30 DEGREES
HALF ANGLE OF DIVERGENT SECTION IS 15 DEGREES

SUBROUTINE NOZ

```
COMMON A,B,TS,PS,T,P,CM,TITLE,NPR,NPU,NGR,TSE,PSE,XX,
1TSRI,PSRI,TWM,CL,V,D,JULIE,N,PNE,PD,ALPHA,E,PNU,TK,M,
2SIGR,SIGO,SIGZ,BO,TR,ZZ,SR,YY,RAD,AC,EWTC,EWTR,EWTE,EWTT,
3RHOPS,SIGPS,PSMAX,DELTA,DELPA,WP,RHON,SIGMAN,CI,CIMAX,
4WAG,ZZZ,CFAP,CFAPS,DELPSC,WW,DELP,FECD,FMLD,XD12,REBD,
5Q,QT,CIOIM,ETATS,PSEOI,PDVAV,TCWAV,TWMAX,TCMAX,GWT,CLD,ACC,
6WPC,FPC,GV,XL,RHOI,XPL,DQQDXL,TW,TC,YL,FIYD,FECD,YD12,QY,
7RAD,AC,WPS,TPS,DT,WNC,WND,WN,AE,DE,CNL,DNL,WTP,PTP,SIGST,
8SIGSTP,SIGSH,SIGSE,SIGDE,PNE,PEN,WSYS,QBAR,XBAR
9,CONDK,CONDR,CFA,RLD,SIGSHM,SIGDEM,PNEX,CIEX,THRUST,WBL,YW,HPP
DIMENSION A(6,40),B(6,40),TS(200),PS(200),T(200),P(200),
1CM(200),TITLE(12),PD(200),SIGR(200),SIGO(200),SIGZ(200),
2FECD(200),XD12(200),REBD(200),Q(200),XL(200),
3RHOI(200),XPL(200),DQQDXL(200),TW(200),TC(200),YL(200),
4FIYD(200),YD12(200),QY(200)
5,SIGST(200),SIGSTP(200),SIGSH(200),SIGSE(200),SIGDE(200)
6,QBAR(100),XBAR(100)
R=1.9859
RBAR=82.0618
GGCS=980.665
GCM=1033.23
TSE=TSE/1.8
DELTA=DELTA/1.8
CALL PROPS (TSE,PSE,A,B,-1,JULIE,W,Z,RHO,HSE,SSE,CP,GAMSE,
1DHP,DST,DSP,OMEGT,OMEGP,SIGT,SIGP,ZETAT,ZETAP,EMU,CLAM,PR)
GME=1.0+((GAMSE-1.0)/2.0)
10 TT=TSE/GME
PT=PSE/GME*(GAMSE/(GAMSE-1.0))
20 CALL PROPS (TT,PT,A,B,+1,JULIE,WT,Z,RHOT,HT,ST,CPT,GAMT,DHPT,
1DSTT,DSPT,OMEGTT,OMEGPT,SIGTT,SIGPT,ZETATT,ZETAPT,EMU,CLAM,PR)
CM2=2.0*WT*((HSE-HT)/(GAMT*R*TT))
CMT=SQRTF(CM2)
DELM2=1.0-CM2
DELS=SSE-ST
DM2DT=-CM2*(1.0-OMEGTT+ZETATT+CPT*TT/(HSE-HT))/TT
DM2DP=CM2*(OMEGPT-ZETAPT-PT*DHPT/(HSE-HT))/PT
DELT=(DM2DP*DELS-DSPT*DELM2)/(DM2DP*DSTT-DM2DT*DSPT)
DELP=(DELS-DSTT*DELT)/DSPT
IF (ABSF(DELT)-DELTA) 50,50,60
50 IF (ABSF(DELP)-DELPA) 80,80,60
60 TT=TT+DELT
PT=PT+DELP
GO TO 20
80 VT=SQRTF(GAMT*RBAR*TT*GGCS*GCM/WT)
WA=RHOT*VT
WAP=WAP*(30.48**2)/453.5924
AT=(1.0-YW)*WP/WAP
DT=SQRTF(4.0*AT/3.14159)
```

```

DR=2.0*(RAD+TR)/12.0
WNC=1.5*3.14159*RHON*DR*PSE*(DR**2-DT**2)/(8.0*
1SINF(3.14159/6.0)*SIGMAN)
C1=0.147
C2=0.000268
C3=0.0000117
PSEF=144.0*PSE
AET=50.0
WND=C1*DT**2*PSEF**((1.0/3.0)*(AET-1.0)+C2*PSEF*DT**3*
1(AET**((1.0/6.0)-1.0)+C3*PSEF*DT**3
WN=WNC+WND
WANE=WA/AET
CME=5.0
GME=1.0+((GAMSE-1.0)/2.0)*CME**2
TE=TSE/GME
PE=PSE/GME**((GAMSE/(GAMSE-1.0)))
1250 CALL PROPS(TE,PE,A,B,+1,JULIE,WE,Z,RHOE,HE,SE,CPE,GAME,DHPE,DSTE,
1DSPE,OMEGTE,OMEGPE,SIGTE,SIGPE,ZETATE,ZETAPE,EMU,CLAM,PR)
CM2=2.0*WE*(HSE-HE)/(GAME*R*TE)
CME=SQRTF(CM2)
VE=CME*SQRTF(GAME*RBAR*TE*GGCS*GCM/WE)
DELWA=WANE-RHOE*VT
DELS=SSE-SE
DWADT=WA*((OMEGTE-SIGTE-1.0)/TE-CPE/(2.0*(HSE-HE)))
DWADP=WA*((OMEGPE-SIGPE+1.0)/PE-DHPE/(2.0*(HSE-HE)))
DELT=(DWADP*DELS-DSPE*DELWA)/(DWADP*DSTE-DWADT*DSPE)
DELP=(DELS-DSTE*DELT)/DSPE
1320 IF (ABSF(DELT)-DELTA) 1330,1330,1340
1330 IF (ABSF(DELP)-DELP) 1370,1370,1340
1340 TE=TE+DELT
PE=PE+DELP
GO TO 1250
1370 PNEX=PE
CALL SIMP(TSE,PSE,PNEX,CIEX)
AE=AET*3.1416*DT**2/4.0
CNL=12.0*(DR-DT)/(2.0*TANF(3.14159/6.0))
DT=12.0*DT
DE=DT*SQRTF(AET)
DNL=(DE-DT)/(2.0*TANF(3.14159/12.0))
TSE=1.8*TSE
DELTA=1.8*DELTA
PEN=AET
RETURN
END

```

```
* LIST
* LABEL
CRMIS1
```

```
C
C MISSION CALCULATIONS
C
```

```

SUBROUTINE RMIS
COMMON A,B,TS,PS,T,P,CM,TITLE,NPR,NPU,NGR,TSE,PSE,WA,
1TSRI,PSRI,TWM,CL,V,D,JULIE,N,PNE,PD,ALPHA,E,PNU,TK,M,
2SIGR,SIGO,SIGZ,BO,TR,TE,SR,SE,RAD,AC,EWTC,EWTR,EWTE,EWTT,
3RHOPS,SIGPS,PSMAX,DELTA,DELPA,WP,RHON,SIGMAN,CI,CIMAX,
4WAG,CME,CFAP,CFAPS,DELPSC,PE,DELPC,FEXD,FMLD,XD12,REBD,
5Q,QT,CIOIM,ETATS,PSEOI,PDAV,TCWAV,TWMAX,TCMAX,GWT,CLD,ACC,
6WPC,FPC,GV,XL,RHOI,XPL,DQQDXL,TW,TC,YL,FIYD,FEXD,YD12,QY,
7RAD,AC,WPS,TPS,DT,WNC,WND,WN,AE,DE,CNL,DNL,WTP,PTP,SIGST,
8SIGSTP,SIGSH,SIGSE,SIGDE,PNE,PEN,WSYS,QBAR,XBAR
9,CONDK,CONDR,CFA,RLD,SIGSHM,SIGDEM,PNEX,CIEX,THRUST,WBL,YW,HPP
COMMON VP,HP,PTANK,RLAM,TP,WH2,WTANK,WE,WG,FOWG,WS,WDL,WPL
1,CBAR,CISP
DIMENSION A(5,40),B(5,40),TS(200),PS(200),T(200),P(200),
1CM(200),TITLE(12),PD(200),SIGR(200),SIGO(200),SIGZ(200),
2FEXD(200),XD12(200),REBD(200),Q(200),XL(200),
3RHOI(200),XPL(200),DQQDXL(200),TW(200),TC(200),YL(200),
4FIYD(200),YD12(200),QY(200)
5,SIGST(200),SIGSTP(200),SIGSH(200),SIGSE(200),SIGDE(200)
6,QBAR(100),XBAR(100)
G=32.174
PTANK=20.0
CISP=CI*(1.0-YW)
CBAR=32.174*CISP
TPA=0.1
TP=0.0
TPP=0.0
ATP=G/(2.0*CBAR)
DTP=HP/CBAR
10 RLNLAM=(VP+G*TP)/CBAR
RLAM=EXP(-RLNLAM)
BLAM=1.0-RLNLAM/(RLAM-1.0)
IF (BLAM**2-4.0*ATP*DTP) 15,15,17
15 TP=TP+10.0
GO TO 20
17 TP=(BLAM-SQRT(BLAM**2-4.0*ATP*DTP))/(2.0*ATP)
IF (ABS(TP-TPP)-TPA) 30,30,20
20 TPP=TP
GO TO 10
30 WH2=WP*TP
WTANK=6.88E+07*(1.131E-11*WH2*PTANK**3+0.00407)/(PTANK**2)
WE=WH2/(RLAM-1.0)
WG=WE+WH2
FOWG=THRUST/WG
WS=0.02*WG
WDL=WE-WTANK-WSYS
WPL=WDL-WS
RETURN
END
```

* LIST
* LABEL

CPRSYS1

C
C
C

PRINTING OF RESULTS FOR NUCLEAR ROCKET SYSTEM

SUBROUTINE PRSYS

```

COMMON A,B,TS,PS,T,P,CM,TITLE,NPR,NPU,NGR,TSE,PSE,WA,
1TSRI,PSRI,TWM,CL,V,D,JULIE,N,PNE,PD,ALPHA,E,PNU,TK,M,
2SIGR,SIGO,SIGZ,BO,TR,TE,SR,SE,RAD,AC,EWTC,EWTR,EWTE,EWTT,
3RHOPS,SIGPS,PSMAX,DELTA,DELPA,WP,RHON,SIGMAN,CI,CIMAX,
4WAG,CME,CFAP,CFAPS,DELPSC,PE,DELPC,FEXD,FMLD,XD12,REBD,
5Q,QT,CIOIM,ETATS,PSEOI,PDAV,TCWAV,TWMAX,TCMAX,GWT,CLD,ACC,
6WPC,FPC,GV,XL,RHOI,XPL,DQQDXL,TW,TC,YL,FIYD,FEXD,YD12,QY,
7RAD,AC,WPS,TPS,DT,WNC,WND,WN,AE,DE,CNL,DNL,WTP,PTP,SIGST,
8SIGSTP,SIGSH,SIGSE,SIGDE,PNE,PEN,WSYS,QBAR,XBAR
9,CONDK,CONDR,CFA,RLD,SIGSHM,SIGDEM,PNEX,CIEX,THRUST,WBL,YW,HPP
COMMON VP,HP,PTANK,RLAM,TP,WH2,WTANK,WE,WG,FOWG,WS,WDL,WPL
1,CBAR,CISP
DIMENSION A(6,40),B(6,40),TS(200),PS(200),T(200),P(200),
1CM(200),TITLE(12),PD(200),SIGR(200),SIGO(200),SIGZ(200),
2FEXD(200),XD12(200),REBD(200),Q(200),XL(200),
3RHOI(200),XPL(200),DQQDXL(200),TW(200),TC(200),YL(200),
4FIYD(200),YD12(200),QY(200)
5,SIGST(200),SIGSTP(200),SIGSH(200),SIGSE(200),SIGDE(200)
6,QBAR(100),XBAR(100)
AET=PEN
CHN=WP/WPC
QONAAV=1000000.0*PDAV*RAD**2/(3.41275*12.0*D*CHN)
WSOWP=WSYS/WP
WSOF=WSYS/THRUST
RZET=1.0-1.0/RLAM
POWSYS=-0.001055*Q(M)*(1.0-YW)/WSOWP
WPLWG=WPL/WG
POWER=POWSYS*WSYS
POWER=POWER/(1.0-YW)
POEWT=POWER/EWTT
PTEWT=POWER/EWTT
POAC=POWER/AC
PTAC=POWER/AC
PRINT 4001, (TITLE(I),I=1,12)
PRINT 4041
PRINT 4042
PRINT 4043, CI,CIMAX,WAG,CME,CFA,CFAP,CFAPS
PRINT 4044
PRINT 4050
PRINT 4045,PS(M),DELPSC,PE,P(M),DELPC,T(1),T(M)
PRINT 4046
PRINT 4051
PRINT 4047,FEXD(M),FMLD,XD12(M),REBD(M),REBD(1),Q(M),QT
PRINT 4048
PRINT 4052
PRINT 4049, CM(M),CIOIM,ETATS,PSEOI,PDAV,TCWAV,TWMAX
PRINT 4055
PRINT 4053
PRINT 4056, TCMAX,GWT,CLD,ACC,WPC,FPC,GV
PRINT 2008
PRINT 2009
PRINT 2010, RAD,AC,EWTC,EWTR,EWTE,EWTT

```

```

PRINT 1000
PRINT 1010
PRINT 1020, TPS,WPS,RLD,SIGSHM,SIGDEM
PRINT 1030
PRINT 1040
PRINT 1050, DT,DE,AE,AET,CNL,DNL
PRINT 1060
PRINT 1070
PRINT 1080, WNC,WND,WN,PNEX,CIEX,THRUST
PRINT 1090
PRINT 1100
PRINT 1110, WTP,PTP,WP,WBL,YW,HPP
PRINT 1111
PRINT 1112
PRINT 1113, CHN,QONAAV,WSOWP,WSOF,POWSYS,WPLOWG
PRINT 1120
PRINT 1130
PRINT 1140, EWT, WPS,WN,WTP,WSYS
PRINT 1150
PRINT 1160
PRINT 1170, WH2,WTANK,WS,WE,WG,WDL,WPL
PRINT 1180
PRINT 1190
PRINT 1200, CBAR,CISP,PTANK,FOWG,RLAM,TP,RZET
PRINT 1210
PRINT 1220
PRINT 1230, POWER,POWER,POEWT,PTWT,POAC,PTAC
IF (XABSF(NPU)) 20,20,10
10 T11=TITLE(8)
PUNCH 4041
PUNCH 4042
PUNCH 4043, CI,CIMAX,WAG,CME,CFA,CFAP,CFAPS,T11
PUNCH 4044
PUNCH 4050
PUNCH 4045,PS(M),DELPSC,PE,P(M),DELP,CT(1),T(M),T11
PUNCH 4046
PUNCH 4051
PUNCH 4047,FEXD(M),FMLD,XD12(M),REBD(M),REBD(1),Q(M),QT,T11
PUNCH 4048
PUNCH 4052
PUNCH 4049, CM(M),CIOIM,ETATS,PSEOI,PDAV,TCWAV,TWMAX,T11
PUNCH 4055
PUNCH 4053
PUNCH 4056, TCMAX,GWT,CLD,ACC,WPC,FPC,GV,T11
PUNCH 2008
PUNCH 2009
PUNCH 2010, RAD,AC,EWTC,EWTR,EWTE,EWT,T11
PUNCH 1000
PUNCH 1010
PUNCH 1020, TPS,WPS,RLD,SIGSHM,SIGDEM,T11
PUNCH 1030
PUNCH 1040
PUNCH 1050, DT,DE,AE,AET,CNL,DNL,T11
PUNCH 1060
PUNCH 1070
PUNCH 1080, WNC,WND,WN,PNEX,CIEX,THRUST,T11
PUNCH 1090
PUNCH 1100
PUNCH 1110, WTP,PTP,WP,WBL,YW,HPP,T11

```

PUNCH 1111
 PUNCH 1112
 PUNCH 1113, CHN,QONAAV,WSOWP,WSOF,POWSYS,WPLWG,T11
 PUNCH 1120
 PUNCH 1130
 PUNCH 1140, EWTT,WPS,WN,WTP,WSYS,T11
 PUNCH 1150
 PUNCH 1160
 PUNCH 1170, WH2,WTANK,WS,WE,WG,WDL,WPL,T11
 PUNCH 1180
 PUNCH 1190
 PUNCH 1200, CBAR,CISP,PTANK,FOWG,RLAM,TP,RZET,T11
 PUNCH 1210
 PUNCH 1220
 PUNCH 1230, POWER,POWER,POEWT,PTWT,POAC,PTAC,T11
 PUNCH 4057
 1000 FORMAT(48H0 TP5 WPS L/D SIGSHM SIGDEM)
 1010 FORMAT(48H IN. LB PSI PSI)
 1020 FORMAT(5F10.3,24X,A6)
 1030 FORMAT(58H0 DT DE AE AE/AT CNL D
 1NL)
 1040 FORMAT(58H IN. IN. FT2 IN. I
 1N.)
 1050 FORMAT(6F10.3,14X,A6)
 1060 FORMAT(58H0 WNC WND WN PNEX CIEX THRU
 1ST)
 1070 FORMAT(58H LB LB LB PSIA LB-SEC/LB
 1LB)
 1080 FORMAT(5F10.3,F10.1,14X,A6)
 1090 FORMAT(58H0 WTP PTP WP WBL YW H
 1PP)
 1100 FORMAT(58H LB PSIA LB/SEC LB/SEC
 1HP)
 1110 FORMAT(5F10.3,F10.1,14X,A6)
 1111 FORMAT(58H0 CHN QAV/A WS'S/WP WSYS/F P/WSYS WPL/
 1WG)
 1112 FORMAT(48H BTU/HR-FT2 LB-SEC/LB MW/LB)
 1113 FORMAT(2F10.1,4F10.4,14X,A6)
 1120 FORMAT(48H0 EWTT WPS WN WTP WSYS)
 1130 FORMAT(49H LB LB LB LB)
 1140 FORMAT(5F10.2,24X,A6)
 1150 FORMAT(68H0 WH2 WTANK WS WE WG W
 1DL WPL)
 1160 FORMAT(68H LB LB LB LB LB
 1LB LB)
 1170 FORMAT(7F10.1,4X,A6)
 1180 FORMAT(68H0 CBAR CISP PTANK F/WG RLAM
 1TP RZET)
 1190 FORMAT(58H FT/SEC LB-SEC/LB PSIA S
 1EC)
 1200 FORMAT(2F10.1,5F10.3,4X,A6)
 1210 FORMAT(58H0 POWER POWER P/EWTT PT/EWTT P/AC PT/
 1AC)
 1220 FORMAT(58H MW MW MW/LB MW/LB MW/FT2 MW/F
 1T2)
 1230 FORMAT(2F10.1,2F10.3,2F10.1,14X,A6)
 2008 FORMAT(58H0 RAD AC EWTC EWTR EWTE EW
 1TT)
 2009 FORMAT(59H IN. FT2 LB LB LB


```

1 LB)
2010 FORMAT(6F10.2,14X,A6)
4001 FORMAT(1H1A5,11A6)
4030 FORMAT(69HODIMENSIONS OF VARIABLES-P(PSI), T(DEGREES R), Q(BTU/LB)
1, L AND D(IN))
4041 FORMAT(68H0    ISP    ISPMAX    W/A    CME    F/A    F
1/A    F/A-P01)
4042 FORMAT(60H LB-SEC/LB LB-SEC/LB GM/CM-SEC    GM/CM2    LB
1/FT2)
4043 FORMAT(3F10.3,F10.6,2F10.2,F10.6,4X,A6)
4044 FORMAT(69H0    PSM    DELPS    PE    PM    DELP
1 TE    TM)
4045 FORMAT(7F10.3,4X,A6)
4046 FORMAT(68H0 FEL/D    FML/D    L/D12    REBM/D    REBE/D
1 Q    QT)
4047 FORMAT(2F10.6,F10.3,2F10.0,2F10.2,4X,A6)
4048 FORMAT(68H0    CMM    I/IMAX    ETATS    PSE/PSI    PDAV    TCW
1AV    TWMAX)
4049 FORMAT(4F10.6,3F10.3,4X,A6)
4050 FORMAT(69H    PSIA    PSIA    PSIA    PSIA    PSIA    DE
1G R    DEG R)
4051 FORMAT(68H    1/IN.2    1/IN    1/IN    BTU/
1LB    BTU/LB)
4052 FORMAT(68H    MW/FT3    DEG
1 R    DEG R)
4053 FORMAT(68H    DEG R    IN.    IN2    LB/SEC
1LB    )
4055 FORMAT(68H0 TCMAX    GWT    L/D    ACC    WPC    F
1PC    GV)
4056 FORMAT(3F10.3,4F10.6,4X,A6)
4057 FORMAT(9H    END)
20 RETURN
END

```

4. Sample Problem

The data and results for a typical run are presented in this section. The power distribution is a chopped sine function which is specified analytically. The number of iterative steps used to obtain the heat transfer characteristics in the reactor is 50. The time required to do these calculations on an IBM 7090 is approximately 0.5 minutes.

DATA FOR SAMPLE PROBLEM

```

1ROCKET SYSTEM CALC.-QOFX FOR CHOPPED SIN RSS001    05/11/64
      +1      +1      0      +2      50
4668.000    800.000    0.858    400.000    1200.000    0.000
49.620      0.300      0.100      31.300
14.6959    26000.0    1584000.0
0.28000E-05    0.14000E+07    0.33000E+00    0.70000E-03
3.150      1.181      0.900      0.900
0.48400E+03    0.60000E+05
0.48400E+03    0.60000E+05
2.5000
  
```

RESULTS FOR SAMPLE PROBLEM

ROCKET SYSTEM CALC.-QOFX FOR CHOPPED SIN RSS001 05/11/64

CQ1=2.5000

ROCKET SYSTEM CALC.-QOFX FOR CHOPPED SIN RSS001 05/11/64

DIMENSIONS OF VARIABLES-P(P(SI)), T(DEGREES R), Q(BTU/LB), L AND D(IN)

TSE 4668.000	PSE 800.000	WA .858	TSRI 400.000	PSRI 1200.000	TWM 0.	
L 49.620	V .300	D .100	K .125	K 30.240		
ISP LB-SEC/LB 758.380	ISPMAX LB-SEC/LB 789.135	W/A GM/CM-SEC 60.323	CME .338291	F/A GM/CM2 45748.06	F/A LB/FT2 93699.41	F/A-P01 .568759
PSM 1144.053	DELPS 344.053	PE 743.975	PM 1140.802	DELP 396.827	TE 4597.190	TM 399.765
FEL/D -2.750610	FML/D -1.976105	L/D12 786.456	REBM/D 2056414	REBE/D 393564	Q -16464.71	QT -16464.16
CMM .060907	I/IMAX .961027	ETATS .969890	PSE/PSI .699268	PDAV 155.685	TCWAV 201.699	TWMAX 4800.499
TCMAX 4926.613	GWT .050	L/D 496.217	ACC .007853	WPC .006738	FPC 5.110162	GV .793563

ROCKET SYSTEM CALC.-GOFX FOR CHOPPED SIN RSS001						05/11/64	
X/L	M	TS	T	PS	P	1000 RHO	
0.	.338291	4668.000	4597.190	800.000	743.975	.017494	
.121043	.302167	4582.640	4525.755	874.193	824.736	.019699	
.170300	.288257	4497.280	4445.468	902.013	855.259	.020799	
.208014	.277815	4411.920	4363.856	922.340	877.700	.021745	
.239794	.269140	4326.560	4281.591	938.831	895.970	.022625	
.267817	.261569	4241.200	4198.925	952.858	911.585	.023473	
.293206	.254765	4155.840	4115.984	965.150	925.326	.024306	
.316629	.248531	4070.480	4032.837	976.133	937.654	.025136	
.338525	.242737	3985.120	3949.531	986.088	948.870	.025971	
.359198	.237294	3899.760	3866.093	995.204	959.184	.026817	
.378870	.232137	3814.400	3782.544	1003.624	968.747	.027679	
.397708	.227212	3729.040	3698.895	1011.453	977.671	.028561	
.415842	.222480	3643.680	3615.157	1018.773	986.045	.029468	
.433372	.217919	3558.320	3531.337	1025.643	993.937	.030403	
.450381	.213496	3472.960	3447.445	1032.117	1001.402	.031371	
.466938	.209191	3387.600	3363.484	1038.238	1008.486	.032375	
.483099	.204987	3302.240	3279.461	1044.036	1015.225	.033419	
.498912	.200871	3216.880	3195.379	1049.544	1021.652	.034507	
.514418	.196829	3131.520	3111.242	1054.784	1027.792	.035644	
.529654	.192852	3046.160	3027.053	1059.778	1033.669	.036835	
.544652	.188930	2960.799	2942.816	1064.545	1039.302	.038085	
.559439	.185059	2875.440	2858.532	1069.103	1044.708	.039400	
.574039	.181220	2790.079	2774.202	1073.462	1049.904	.040787	
.588474	.177412	2704.719	2689.829	1077.636	1054.900	.042252	
.602766	.173621	2619.359	2605.416	1081.631	1059.710	.043804	
.616932	.169845	2533.999	2520.964	1085.463	1064.343	.045452	
.630991	.166088	2448.639	2436.474	1089.136	1068.809	.047206	
.644961	.162340	2363.279	2351.949	1092.661	1073.116	.049077	
.658859	.158590	2277.919	2267.389	1096.045	1077.273	.051080	
.672700	.154842	2192.559	2182.795	1099.295	1081.286	.053230	
.686503	.151092	2107.199	2098.171	1102.413	1085.162	.055544	
.700288	.147334	2021.839	2013.516	1105.412	1088.908	.058043	
.714075	.143563	1936.479	1928.833	1108.291	1092.529	.060752	
.727883	.139773	1851.119	1844.119	1111.059	1096.031	.063700	
.741735	.135956	1765.759	1759.371	1113.717	1099.419	.066921	
.755661	.132126	1680.399	1674.602	1116.274	1102.700	.070456	
.769686	.128256	1595.039	1589.805	1118.831	1105.875	.074355	
.783837	.124336	1509.679	1504.977	1121.096	1108.948	.078680	
.798142	.120358	1424.319	1420.127	1123.361	1111.923	.083504	
.812633	.116319	1338.959	1335.248	1125.626	1114.803	.088923	
.827344	.112199	1253.599	1250.330	1127.634	1117.591	.095058	
.842336	.108031	1168.239	1165.400	1129.643	1120.291	.102061	
.857661	.103728	1082.879	1080.437	1131.651	1122.904	.110136	
.873358	.099275	997.519	995.433	1133.413	1125.434	.119556	
.889478	.094653	912.159	910.406	1135.174	1127.878	.130691	
.906118	.089934	826.799	825.364	1136.936	1130.241	.144064	
.923383	.084916	741.439	740.281	1138.469	1132.524	.160445	
.941322	.079582	656.079	655.172	1140.002	1134.724	.180992	
.960018	.073895	570.719	570.023	1141.431	1136.839	.207563	
.979611	.067867	485.359	484.898	1142.859	1138.868	.243284	
1.000041	.060907	400.000	399.765	1144.053	1140.802	.293981	

ROCKET SYSTEM CALC.--QOFX FOR CHOPPED SIM RSS001

05/11/64

XP/L	DQGDXL	TW	TC	PD
0.	0.	4668.000	0.	0.
.160522	.208410	4733.030	4775.035	32.446
.145671	.494080	4800.499	4900.154	76.921
.189157	.631952	4796.749	4924.213	98.385
.223904	.736814	4777.999	4926.613	114.711
.253805	.822622	4751.748	4917.670	128.070
.280511	.895385	4719.248	4899.846	139.398
.304918	.958395	4683.623	4876.930	149.208
.327577	1.013710	4644.248	4848.712	157.819
.348862	1.062698	4602.372	4816.717	165.446
.369034	1.106358	4557.997	4781.148	172.243
.388289	1.145409	4511.747	4742.775	178.323
.406775	1.180402	4462.997	4701.082	183.771
.424607	1.211768	4412.995	4657.409	188.654
.441877	1.239848	4361.121	4611.197	193.026
.458660	1.264925	4307.996	4563.130	196.930
.475019	1.287225	4252.996	4512.628	200.402
.491006	1.306938	4196.121	4459.728	203.471
.506665	1.324224	4138.620	4405.715	206.162
.522036	1.339218	4079.870	4349.989	208.496
.537153	1.352035	4019.870	4292.574	210.492
.552045	1.362772	3958.620	4233.489	212.163
.566739	1.371516	3896.744	4173.377	213.524
.581257	1.378337	3833.619	4111.628	214.586
.595620	1.383298	3769.869	4048.878	215.359
.609849	1.386455	3704.869	3984.515	215.850
.623961	1.387852	3639.869	3919.797	216.068
.637976	1.387531	3574.243	3854.107	216.018
.651910	1.385523	3507.368	3786.827	215.705
.665779	1.381856	3440.493	3719.212	215.134
.679602	1.376547	3373.618	3651.266	214.308
.693396	1.369611	3306.118	3582.367	213.228
.707182	1.361051	3238.618	3513.140	211.895
.720979	1.350866	3170.492	3442.960	210.309
.734809	1.339042	3102.367	3372.450	208.469
.748698	1.325558	3034.242	3301.605	206.369
.762673	1.310376	2966.117	3230.418	204.006
.776761	1.293452	2898.617	3159.504	201.371
.790989	1.274733	2830.492	3087.604	198.457
.805387	1.254148	2762.366	3015.327	195.252
.819988	1.231615	2694.866	2943.281	191.744
.834840	1.207010	2627.991	2871.444	187.913
.849998	1.180183	2561.741	2799.782	183.737
.865509	1.150975	2491.741	2723.891	179.190
.881418	1.119221	2427.366	2653.111	174.246
.897798	1.084675	2365.490	2584.268	168.868
.914751	1.047006	2309.240	2520.420	163.003
.932353	1.005916	2259.240	2462.132	156.606
.950670	.961075	2222.365	2416.213	149.625
.969814	.912064	2206.115	2390.077	141.995
.989826	.858603	2227.990	2401.169	133.672

ROCKET SYSTEM CALC.-QOFX FOR CHOPPED SIN RSS001						05/11/64	REB/D
Y/L	FIY/D	FEX/D	Y/D12	QY	Q		
1.000000	2.750610	0.	786.456	16464.16	0.	393564	
.878957	2.410644	-.332930	691.264	16048.82	-415.34	399342	
.829700	2.268871	-.468409	652.528	15648.14	-816.02	405262	
.791986	2.159310	-.572143	622.868	15255.74	-1208.42	411335	
.760206	2.066444	-.659552	597.876	14870.22	-1593.94	417568	
.732183	1.984225	-.736630	575.838	14490.68	-1973.47	423972	
.706794	1.909529	-.806462	555.872	14116.41	-2347.75	430558	
.683371	1.840491	-.870889	537.451	13746.80	-2717.36	437335	
.661475	1.775889	-.931113	520.231	13381.36	-3082.80	444317	
.640802	1.714872	-.987974	503.974	13019.66	-3444.50	451514	
.621130	1.656816	-1.042081	488.504	12661.34	-3802.82	458941	
.602292	1.601252	-1.093895	473.689	12306.08	-4158.08	466611	
.584158	1.547821	-1.143772	459.428	11953.66	-4510.49	474541	
.566628	1.496235	-1.191989	445.642	11603.92	-4860.24	482746	
.549618	1.446266	-1.238774	432.265	11256.70	-5207.45	491245	
.533062	1.397723	-1.284313	419.244	10911.89	-5552.27	500057	
.516901	1.350447	-1.328764	406.535	10569.40	-5894.76	509203	
.501088	1.304305	-1.372257	394.099	10229.14	-6235.02	518707	
.485582	1.259183	-1.414907	381.905	9891.07	-6573.09	528593	
.470346	1.214981	-1.456813	369.923	9555.13	-6909.02	538889	
.455348	1.171611	-1.498064	358.129	9221.29	-7242.87	549625	
.440561	1.129000	-1.538735	346.500	8889.51	-7574.64	560835	
.425961	1.087083	-1.578893	335.018	8559.83	-7904.33	572554	
.411526	1.045801	-1.618598	323.665	8232.24	-8231.92	584824	
.397234	1.005103	-1.657906	312.426	7906.76	-8557.40	597688	
.383068	.964940	-1.696870	301.286	7583.39	-8880.77	611198	
.369009	.925266	-1.735540	290.229	7262.14	-9202.02	625408	
.355039	.886037	-1.773965	279.243	6942.99	-9521.16	640382	
.341141	.847216	-1.812191	268.313	6625.97	-9838.19	656189	
.327300	.808766	-1.850260	257.428	6311.07	-10153.09	672910	
.313497	.770645	-1.888226	246.573	5998.24	-10465.92	690633	
.299712	.732809	-1.926142	235.732	5687.39	-10776.77	709463	
.285925	.695219	-1.964062	224.890	5378.45	-11085.70	729517	
.272117	.657832	-2.002041	214.031	5071.35	-11392.81	750932	
.258265	.621294	-2.040141	203.138	4765.96	-11698.19	769584	
.244339	.583902	-2.078443	192.186	4462.05	-12002.11	795610	
.230314	.546559	-2.117019	181.157	4159.47	-12304.69	823905	
.216163	.509221	-2.155942	170.028	3858.12	-12606.04	854789	
.201858	.471848	-2.195288	158.778	3557.89	-12906.27	888648	
.187367	.434394	-2.235145	147.382	3258.68	-13205.48	925962	
.172656	.396811	-2.275608	135.813	2960.37	-13503.79	967328	
.157664	.359000	-2.316844	124.023	2662.44	-13801.72	1013504	
.142339	.320889	-2.358994	111.971	2364.67	-14099.49	1065472	
.126642	.282447	-2.402170	99.626	2067.20	-14396.95	1124531	
.110522	.243633	-2.446508	86.949	1770.16	-14693.99	1192432	
.093882	.204321	-2.492276	73.863	1473.00	-14991.16	1271614	
.076617	.164401	-2.539765	60.285	1175.38	-15288.78	1365581	
.058678	.123926	-2.589105	46.178	878.28	-15585.87	1479558	
.039982	.082933	-2.640527	31.475	582.46	-15881.70	1621741	
.020389	.041433	-2.694418	16.067	288.25	-16175.91	1805787	
-.000041	0.	-2.750610	0.	-.56	-16464.71	2056414	

ROCKET SYSTEM CALC.-QOFX FOR CHOPPED SIN R55001

05/11/64

ALPHA	E	NU	K
1/DEG F	PSI		BTU/IN-SEC-F
.28000E-05	.14000E 07	.33000E 00	.70000E-03

D	V
IN.	
.100	.300

STRESS CALCULATIONS FOR ZERO STRESS GRADIENT AT R=B

XL	P PSIA	PD MW/FT3	SIGO PSI	SIGZ PSI	SIGR PSI
0.	743.975	0.	-744.0	0.	-744.0
.1210	824.736	32.446	-463.1	163.8	-824.7
.1703	855.259	76.921	2.0	388.3	-855.3
.2080	877.700	98.385	218.7	496.7	-877.7
.2398	895.970	114.711	382.4	579.1	-896.0
.2678	911.585	128.070	515.6	646.6	-911.6
.2932	925.326	139.398	628.1	703.7	-925.3
.3166	937.654	149.208	725.1	753.3	-937.7
.3385	948.870	157.819	809.9	796.7	-948.9
.3592	959.184	165.446	884.6	835.2	-959.2
.3789	968.747	172.243	950.8	869.6	-968.7
.3977	977.671	178.323	1009.6	900.3	-977.7
.4158	986.045	183.771	1061.9	927.8	-986.0
.4334	993.937	188.654	1108.5	952.4	-993.9
.4504	1001.402	193.026	1149.7	974.5	-1001.4
.4669	1008.486	196.930	1186.1	994.2	-1008.5
.4831	1015.225	200.402	1218.1	1011.7	-1015.2
.4989	1021.652	203.471	1245.9	1027.2	-1021.7
.5144	1027.792	206.162	1269.7	1040.8	-1027.8
.5297	1033.669	208.496	1289.8	1052.6	-1033.7
.5447	1039.302	210.492	1306.5	1062.7	-1039.3
.5594	1044.708	212.163	1319.7	1071.1	-1044.7
.5740	1049.904	213.524	1329.6	1078.0	-1049.9
.5885	1054.900	214.586	1336.5	1083.3	-1054.9
.6028	1059.710	215.359	1340.3	1087.2	-1059.7
.6169	1064.343	215.850	1341.1	1089.7	-1064.3
.6310	1068.809	216.068	1339.1	1090.8	-1068.8
.6450	1073.116	216.018	1334.2	1090.6	-1073.1
.6589	1077.273	215.705	1326.6	1089.0	-1077.3
.6727	1081.286	215.134	1316.2	1086.1	-1081.3
.6865	1085.162	214.308	1303.1	1081.9	-1085.2
.7003	1088.908	213.228	1287.3	1076.5	-1088.9
.7141	1092.529	211.895	1268.9	1069.7	-1092.5
.7279	1096.031	210.309	1247.7	1061.7	-1096.0
.7417	1099.419	208.469	1223.8	1052.4	-1099.4
.7557	1102.700	206.369	1197.1	1041.8	-1102.7
.7697	1105.875	204.006	1167.6	1029.9	-1105.9
.7838	1108.948	201.371	1135.2	1016.6	-1108.9
.7981	1111.923	198.457	1099.7	1001.9	-1111.9
.8126	1114.803	195.252	1061.1	985.7	-1114.8
.8273	1117.591	191.744	1019.2	968.0	-1117.6
.8423	1120.291	187.913	973.8	948.7	-1120.3
.8577	1122.904	183.737	924.7	927.6	-1122.9
.8734	1125.434	179.190	871.5	904.6	-1125.4
.8895	1127.878	174.246	813.9	879.7	-1127.9
.9061	1130.241	168.868	751.6	852.5	-1130.2
.9234	1132.524	163.003	684.0	822.9	-1132.5
.9413	1134.724	156.606	610.5	790.6	-1134.7
.9600	1136.839	149.625	530.6	755.4	-1136.8
.9796	1138.868	141.995	443.5	716.9	-1138.9
1.0000	1140.802	133.672	348.9	674.8	-1140.8

ROCKET SYSTEM CALC.-QOFX FOR CHOPPED SIN RSS001

05/11/64

XL	SIGST PSI	SIGSTP PSI	SIGSH PSI	SIGSE PSI	SIGDE PSI
0.	491.0	-498.5	744.0	861.2	700.5
.1210	588.8	-726.0	988.5	899.3	815.8
.1703	669.9	-984.1	1243.6	1049.8	1038.1
.2080	714.2	-1113.8	1374.4	1186.4	1185.2
.2398	748.6	-1213.3	1475.1	1306.4	1306.2
.2678	777.2	-1295.1	1558.1	1412.1	1409.6
.2932	801.8	-1364.9	1629.1	1505.9	1499.7
.3166	823.4	-1425.5	1690.9	1589.6	1579.1
.3385	860.1	-1479.1	1758.8	1664.7	1649.9
.3592	925.5	-1526.7	1843.8	1732.4	1713.4
.3789	983.5	-1569.5	1919.5	1793.5	1770.5
.3977	1035.1	-1607.9	1987.3	1848.8	1822.0
.4158	1081.2	-1642.6	2048.0	1898.8	1868.5
.4334	1122.2	-1674.0	2102.4	1943.9	1910.5
.4504	1158.6	-1702.4	2151.1	1984.6	1948.3
.4669	1190.9	-1728.0	2194.6	2021.2	1982.3
.4831	1219.2	-1751.1	2233.3	2053.9	2012.8
.4989	1244.0	-1771.8	2267.5	2083.1	2040.0
.5144	1265.4	-1790.3	2297.5	2108.8	2064.1
.5297	1283.6	-1806.7	2323.5	2131.2	2085.2
.5447	1298.7	-1821.1	2345.8	2150.6	2103.5
.5594	1311.0	-1833.7	2364.4	2167.0	2119.1
.5740	1320.4	-1844.4	2379.6	2180.5	2132.1
.5885	1327.1	-1853.4	2391.4	2191.3	2142.6
.6028	1331.2	-1860.8	2400.0	2199.4	2150.7
.6169	1332.8	-1866.5	2405.5	2205.0	2156.5
.6310	1331.8	-1870.7	2407.9	2208.0	2160.0
.6450	1328.5	-1873.3	2407.3	2208.6	2161.3
.6589	1322.7	-1874.4	2403.9	2206.9	2160.4
.6727	1314.6	-1874.0	2397.5	2202.7	2157.4
.6865	1304.2	-1872.2	2388.3	2196.3	2152.3
.7003	1291.4	-1869.0	2376.2	2187.7	2145.2
.7141	1276.4	-1864.3	2361.4	2176.8	2136.0
.7279	1259.0	-1858.1	2343.7	2163.7	2124.8
.7417	1239.3	-1850.6	2323.2	2148.4	2111.6
.7557	1217.2	-1841.6	2299.8	2130.9	2096.3
.7697	1192.7	-1831.1	2273.5	2111.2	2079.0
.7838	1165.6	-1819.0	2244.1	2089.3	2059.6
.7981	1136.0	-1805.5	2211.6	2065.1	2038.1
.8126	1103.7	-1790.3	2175.9	2038.6	2014.4
.8273	1068.6	-1773.4	2136.8	2009.9	1988.4
.8423	1030.5	-1754.7	2094.1	1978.7	1960.2
.8577	993.0	-1734.2	2050.5	1945.0	1929.4
.8734	988.4	-1711.6	2030.1	1908.8	1896.2
.8895	983.3	-1686.8	2007.6	1869.9	1860.2
.9061	977.5	-1659.6	1982.8	1828.4	1821.4
.9234	970.9	-1629.8	1955.4	1784.0	1779.5
.9413	963.6	-1597.1	1925.3	1736.7	1734.4
.9600	955.4	-1561.2	1892.2	1686.7	1685.9
.9796	946.3	-1521.8	1855.7	1634.0	1634.0
1.0000	936.2	-1478.6	1815.6	1579.2	1578.7

ROCKET SYSTEM CALC.-QOFX FOR CHOPPED SIN RSS001 05/11/64

L IN. 49.620	TE IN. 1.181	TR IN. 3.150	SR .900	SE .900	BO 1/CM2 0.
RAD IN. 31.30	AC FT2 6.41	EWTC LB 6393.88	EWTR LB 1984.12	EWTE LB 218.19	EWTT LB 8596.18

ROCKET SYSTEM CALC.-GOFX FOR CHOPPED SIN RSS001 05/11/64

NPR 1	NPU 1	NGR 0	JULIE 2	N 50		
TSE DEG R 4668.000	PSE PSIA LB/IN2-SEC 800.000	WA LB/IN2-SEC .858	TSRI DEG R 400.000	PSRI PSIA 1200.000	TWM DEG R 0.	
CL IN. 49.620	V .300	D IN. .100	RAD IN. 31.300			
PNE PSIA 14.6959	VP FT 26000.0	HP FT 1584000.0				
ALPHA 1/DEG R .28000E-05	E PSI .14000E 07	PNU .33000E 00	K BTU/IN-SEC-R .70000E-03			
TR IN. 3.150	TE IN. 1.181	SR .900	SE .900			
RHOPS LB/FT3 .48400E 03	SIGPS PSI .60000E 05	RHON LB/FT3 .48400E 03	SIGMAN PSI .60000E 05			
ISP LB-SEC/LB 758.380	ISPMAX LB-SEC/LB 789.135	W/A GM/CM-SEC 60.323	CME .338291	F/A GM/CM2 45748.06	F/A LB/FT2 93699.41	F/A-P01 .568759
PSM PSIA 1144.053	DELPS PSIA 344.053	PE PSIA 743.975	PM PSIA 1140.802	DELP PSIA 396.827	TE DEG R 4597.190	TM DEG R 399.765
FEL/D -2.750610	FML/D -1.976105	L/D12 1/IN.2 786.456	REBM/D 1/IN 2056414	REBE/D 1/IN 393564	Q BTU/LB -16464.71	QT BTU/LB -16464.16
CMM .060907	I/IMAX .961027	ETATS .969890	PSE/PSI .699268	PDAV MW/FT3 155.685	TCWAV DEG R 201.699	TWMAX DEG R 4800.499
TCMAX DEG R 4926.613	GWT IN. .050	L/D 496.217	ACC IN2 .007853	WPC LB/SEC .006738	FPC LB 5.110162	GV .793563
RAD IN. 31.30	AC FT2 6.41	EWTC LB 6393.88	EWTR LB 1984.12	EWTE LB 218.19	EWTT LB 8596.18	
TPS IN. .657	WPS LB 2709.128	L/D .793	SIGSHM PSI 2407.896	SIGDEM PSI 2161.255		

DT IN. 24.268	DE IN. 171.599	AE FT2 160.605	AE/AT 50.000	CNL IN. 38.653	DNL IN. 274.925
WNC LB 1260.534	WND LB 1679.300	WN LB 2939.834	PNEX PSIA LB-SEC/LB 1.796	CIEX 839.801	THRUST LB 558046.2
WTP LB 3025.657	PTP PSIA 1521.591	WP LB/SEC 792.224	WBL LB/SEC 56.385	YW .071	HPP HP 100106.4
CHN 117571.1	GAV/A BTU/HR-FT2 316784.4	WSYS/WP LB-SEC/LB 21.8004	WSYS/F .0309	P/WSYS MW/LB .7401	WPL/WG .1170
EWTT LB 8596.18	WPS LB 2709.13	WN LB 2939.83	WTP LB 3025.66	WSYS LB 17270.80	
WH2 LB 132205.7	WTANK LB 2757.5	WS LB 3528.1	WE LB 44199.4	WG LB 176405.1	WDL LB 24171.1
CBAR FT/SEC LB-SEC/LB 22663.5	CISP 704.4	PTANK PSIA 20.000	F/WG 3.163	RLAM 3.991	TP SEC 166.879
POWER MW 12781.7 END	POWER MW 13761.1	P/EWTT MW/LB 1.487	PT/EWTT MW/LB 1.601	P/AC MW/FT2 1993.4	PT/AC MW/FT2 2146.1
					WPL LB 20643.0 RZET .749

BIOGRAPHICAL NOTE

The author, John Donald Christie, was born in Greensburg, Pennsylvania on April 20, 1937. He received his elementary and secondary-school training in the public schools of Greensburg, Pennsylvania. He entered the Massachusetts Institute of Technology in 1955 and received a Bachelor of Science degree in Mechanical Engineering from the Institute in June, 1959. He continued his education at the Massachusetts Institute of Technology and received a Master of Science degree in Mechanical Engineering in June, 1960 and the professional degree of Mechanical Engineer in January, 1963. He has been registered as a doctoral student at the Institute since January, 1963.

REPORT DOCUMENTATION PAGE				<i>Form Approved</i> <i>OMB No. 0704-0188</i>	
<p>The public reporting burden for this collection of information is estimated to average 1 hour per response, including the time for reviewing instructions, searching existing data sources, gathering and maintaining the data needed, and completing and reviewing the collection of information. Send comments regarding this burden estimate or any other aspect of this collection of information, including suggestions for reducing the burden, to Department of Defense, Washington Headquarters Services, Directorate for Information Operations and Reports (0704-0188), 1215 Jefferson Davis Highway, Suite 1204, Arlington, VA 22202-4302. Respondents should be aware that notwithstanding any other provision of law, no person shall be subject to any penalty for failing to comply with a collection of information if it does not display a currently valid OMB control number.</p> <p>PLEASE DO NOT RETURN YOUR FORM TO THE ABOVE ADDRESS.</p>					
1. REPORT DATE (DD-MM-YYYY) May 1964		2. REPORT TYPE Final - Thesis		3. DATES COVERED (From - To) 1964	
4. TITLE AND SUBTITLE Large payload nuclear rockets				5a. CONTRACT NUMBER	
				5b. GRANT NUMBER	
				5c. PROGRAM ELEMENT NUMBER	
6. AUTHOR(S) Christie, John D.				5d. PROJECT NUMBER	
				5e. TASK NUMBER	
				5f. WORK UNIT NUMBER	
7. PERFORMING ORGANIZATION NAME(S) AND ADDRESS(ES) Massachusetts Institute of Technology Cambridge MA				8. PERFORMING ORGANIZATION REPORT NUMBER	
9. SPONSORING/MONITORING AGENCY NAME(S) AND ADDRESS(ES)				10. SPONSOR/MONITOR'S ACRONYM(S)	
				11. SPONSOR/MONITOR'S REPORT NUMBER(S)	
12. DISTRIBUTION/AVAILABILITY STATEMENT A: Approved for Public Release. Distribution unlimited.					
13. SUPPLEMENTARY NOTES Also available from MIT Libraries. Works published before 1978 are governed by previous Copyright Law. Under that law, if a work was published without the required copyright notice, all copyright protection for that work was lost in the United States.					
14. ABSTRACT					
15. SUBJECT TERMS					
16. SECURITY CLASSIFICATION OF:			17. LIMITATION OF ABSTRACT	18. NUMBER OF PAGES	19a. NAME OF RESPONSIBLE PERSON
a. REPORT	b. ABSTRACT	c. THIS PAGE			19b. TELEPHONE NUMBER (Include area code)